Plant Hormone Signalling Pathways and Resistance to Plant Parasitic Nematodes

Chhoa Mondal

Submitted in accordance with the requirements for the degree of Doctor of Philosophy

The University of Leeds

School of Biology

Faculty of Biological Sciences

August 2025

The candidate confirms that the work submitted is their own and that appropriate credit has been given where reference has been made to the work of others.

Acknowledgements

I would like to express my profound gratitude to my respected supervisor Professor Peter Urwin for his endless support and supervision throughout the project. His encouragement and pastoral support have motivated me to complete my research successfully.

I would like to convey my sincere thankfulness to Dr. Catherine Lilley for the time and dedication she has devoted both to me and to this project. Her invaluable guidance and steadfast support have been influential, and this work would not have been possible without her.

I would like to thank my co-supervisor, Dr. Yoselin Benitez-Alfonso, for her encouragement and motivational support throughout my research journey.

A heartfelt thank you to both past and present members of the Plant Nematology Laboratory for their valuable assistance and for contributing to such a positive and collaborative atmosphere. The friendships I have made have greatly enriched my experience.

Finally, I would like to thank to my husband, family and friends for their unwavering support throughout my research journey.

This project is funded by Science and Technology Fellowship Trust, People's Republic of Bangladesh. I am deeply grateful for their consistent financial assistance, without which the successful completion of this work would not have been possible. I also wish to extend my sincere appreciation to all the staff members of the Science and Technology Fellowship Trust for their continued cooperation, encouragement, and administrative support throughout the entire duration of my doctoral research.

Abstract

Some of the most harmful plant-parasitic nematodes are those endoparasites that invade the roots of their host and induce the formation of distinctive and metabolically active "feeding sites". Many changes in root gene expression are required for establishment of a feeding site. Different reporters have been used to monitor these molecular changes during nematode infection, but they are either destructive or require specialized microscopy and are therefore not suitable for real-time monitoring of gene expression on a whole root-system scale. Hence, we wanted to evaluate a non-destructive method for assessing nematode infection that would be easily visible in soil grown plants. The RUBY betalain reporter (He *et al.,* 2020) was evaluated in both Arabidopsis and potato plants infected with root-knot and cyst nematodes. Arabidopsis lines carrying the CaMV35S-RUBY construct exhibited gene silencing when constitutive overexpression was detrimental, whereas in potato, the same construct drove stable RUBY expression throughout the plant's lifespan. Notably, RUBY expression in giant cells and syncytia was maintained during nematode development in both Arabidopsis and potato. This contrasts with previous studies using GUS and GFP reporters that showed apparent silencing of the CaMV35S promoter expression in syncytia.

To minimize side effects of constitutive expression, we also employed RUBY under root-expressed, nematode-inducible promoters. By integrating two candidate promoter sequences upstream of the RUBY gene, two constructs (pBI:PG1-RUBY and pBI:PG2-RUBY) were generated, enabling visualization of transcriptional activation in roots of transgenic potato plants. These newly developed RUBY constructs demonstrated clear root-specificity in transgenic lines, confirming their utility as targeted visual markers. Together, these findings establish RUBY as a reliable visual marker for studying plant-nematode interactions.

Another aim of our study was to identify one or more sources of resistance to potato cyst nematodes in a panel of *Solanum americanum* accessions. To that end, segregating F_2 generations arising from crosses between susceptible and resistant parents were tested, allowing identification of resistant individuals and analysis of inheritance patterns. To optimise screening of F_2 populations and identify effective infection conditions, the susceptible parent was tested across soil types and inoculum levels, revealing that compost and sand-loam with high nematode inoculum and root exudates significantly enhanced *G. pallida* populations for robust resistance screening. Segregation patterns indicated one accession with a single dominant resistance locus and a second accession with two or more unlinked dominant genes conferring strong resistance. Characterisation of resistant Solanum accessions revealed both early and late oxidative bursts, highlighting dynamic defence signalling. These results confirm the heritability of resistance traits and underscore the genetic diversity within Solanum populations.

Table of Contents

List of Tables

List of Figures

List of Abbreviations

AMF	Arbuscular Mycorrhizal Fungi
ANOVA	Analysis of Variance
APX	Ascorbate Peroxidase
ATG	Autophagy-related Gene
Bcp	Blue Copper Protein
BLAST	Basic Local Alignment Search Tool
CaMV35S	Cauliflower Mosaic Virus 35S Promoter
CAT	Catalase
cDNA	Complementary Deoxyribonucleic Acid
CN	Cyst Nematode
CTAB	Cetyl Trimethyl Ammonium Bromide
DAB	3,3'-Diaminobenzidine
DAI	Days After Inoculation/ Infection
dATP	Deoxyadenosine Triphosphate
DNA	Deoxyribonucleic Acid
DPI	Days Post Infection
EcoRI	Restriction Enzyme EcoRI
EDTA	Ethylenediaminetetraacetic Acid
ELGA	Purified water
ET	Ethylene
FT	FLOWERING LOCUS T
GAL4	Transcription factor in the yeast
gDNA	Genomic DNA
GFP	Green Fluorescent Protein
GUS	β-Glucuronidase
HR	Hypersensitive Response
J2s	Second Stage Juveniles
JA	Jasmonic acid
Lac	Lactose Operon
lacZα	LacZ Alpha Fragment
LB	Luria-Bertani
LE DNA	Linearized DNA
LS	Linsmaier and Skoog

LOX	Lipoxygenase
LUC	Luciferase
MES	2-(N-morpholino) ethanesulfonic Acid
MS	Murashige and Skoog
NAA	Naphthalene Acetic Acid
NEB	New England Biolabs
NFS	Nematode Feeding Site
pBI	Plant Binary Vector
PCN	Potato Cyst Nematode
PCR	Polymerase Chain Reaction
Pdf2.1	Plant defensin promoter genes
PG	Potato Promoter Gene
pGEM-T	Plasmid Vector pGEM-T
PT/PHT	Phosphate Transporter
PPM	Plant Preservative Mixture
PTGS	Post-transcriptional Gene Silencing
RFP	Red Fluorescent Protein
RNA	Ribonucleic Acid
RNN	Root Knot Nematode
ROS	Reactive Oxygen Species
RPM	Revolutions Per Minute
RT	Reverse Transcriptase
SA	Salicylic acid
SacI	Restriction Enzyme SacI
SAR	Systemic Acquired Resistance
SIM	Shoot Induction Media
SOC	Super Optimal Broth with Catabolite Repression
TAE	Tris-Acetate-EDTA Buffer
T-DNA	Transfer DNA
TobRB7	Giant cell specific tobacco promoter
UAS	Upstream activation sequences
UV	Ultraviolet
VAC-RFP	Red Fluorescent Protein Expressed in Vacuole
VP16/64	Herpes simplex virus protein

VSP2	Vegetative stage protein 2
XbaI	Restriction Enzyme XbaI
X-gal	5-Bromo-4-Chloro-3-Indolyl-β-D-Galactopyranoside
YFP	Yellow Fluorescent Protein

Chapter 1

General Introduction

1.1 Nematoda

Nematodes are wormlike, microscopic, unsegmented, pseudocoelomate, colorless multicellular animals (Hasan, 2019). They are a diverse group of organisms, classified under the Phylum Nematoda (Hodda, 2022). Recently nematodes have been recognized as among the most ancient animals on Earth (Shatilovich et al., 2023). They are ecologically and economically important organisms, with 28537 species described to date and have been identified in nearly every habitat on the earth (Barker et al. 1994, Lambshead, 1993 and 2004, Hodda et al., 2009; Yeates et al., 2009, Hodda, 2022; Hodda and Khudhir, 2022). Most soil-inhabiting nematodes are classified as beneficial nematodes or free living and parasitic nematodes. Beneficial groups play key roles in the soil system by feeding exclusively on microorganisms, fungi, algae, protozoa, and other nematodes (Wilschut and Geisen, 2021; Ronn et al., 2012) and maintaining carbon equilibrium in the soil (Zhang et al., 2021) as well as the wider ecosystem (Oriol et al., 2017). In contrast, parasitic nematodes represent a significant threat to the health of humans, animals, and plants (Jones et al., 2013; Jasmer et al., 2003). When the nematodes survive by feeding on plant parts or tissues, they are categorized as plant parasitic nematodes (PPN) (Yeates et al., 1993).

1.2 Plant parasitic nematodes

Plant-Parasitic Nematodes (PPNs) are a group of nematodes that infect and feed on a wide range of plants in horticulture, agriculture, and forestry (Kumar et al., 2020). So far, more than 4100 species of plant parasitic nematodes have been reported (Decraemer and Hunt, 2006, Singh et al., 2025) and many of these are regarded as major agro-economic pests. Hence, 12.3% crop losses are estimated due to nematode infection (Singh et al., 2015) which accounts for an annual loss of 173 billion USD (Singh et al., 2025). Whereas the most serious insect pests damage only 70 billion USD annually (Bradshaw et al., 2016).

Most of the soil-borne plant-parasitic nematodes generally consume plant roots although they can also attack other parts of plants like stems, leaves, flowers and seeds. Plant-parasitic

nematodes are classified according to their feeding modes as ectoparasitic and endoparasitic nematodes (Figure 1.1). The endoparasites are further categorized as migratory nematodes and sedentary nematodes as per their motility in the host tissue during feeding (Kaloshian and Teixeira, 2019). Migratory endoparasites (e.g. *Pratylenchus spp*., *Radopholus spp*., *Hirschmanniella spp*., and *Bursaphelenchus spp.*) trigger huge destruction while migrating through the host tissues and hence generate necrotic symptoms. This has led to *Pratylenchus spp.* being commonly known as lesion nematodes (Fosu-Nyarko and Jones, 2016). On the contrary, sedentary endoparasitic nematodes establish intricate host-parasitic relationships by penetrating the host and initiating a single feeding site from which they subsequently feed throughout their whole life cycle. Root knot nematodes of *Meloidogyne* genus and cyst nematodes of *Heterodera* and *Globodera* genera are the most remarkable groups of this category of nematode. Contrastingly, ectoparasitic nematodes (e.g. *Trichodorous* spp.) remain entirely in the soil throughout their life cycle, feeding by puncturing plant roots only when needed to extract nutrients (Jones et al., 2013).

Most of the plant parasitic nematodes possess a similar odontostyle stylet despite having discrepancies in their parasitic mechanism. This stylet facilitates the uptake of host nutrients during their feeding (Smant et al., 2018) and is also used to inject effectors into the host that are produced in their pharyngeal glands to initiate host parasitism (Rehman et al., 2016; Vieira and Gleason, 2019).

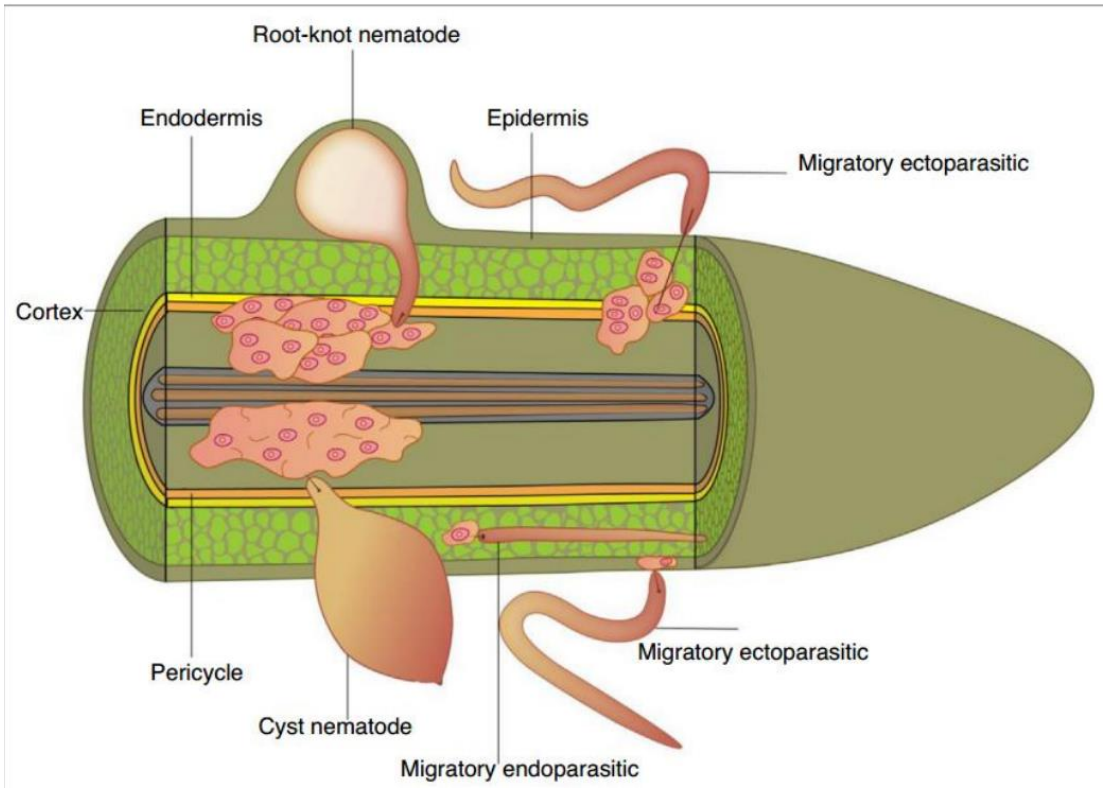

Figure 1.1. Key feeding approaches adopted by plant-parasitic nematodes (Siddique and Grundler, 2018).

1.3 Root Knot-Nematodes

Root-knot nematodes of the *Meloidogyne* genus comprise over 101 species (Kaur et al., 2024). Among this genus, *Meloidogyne incognita* and *Meloidogyne javanica* are the most rapidly expanding plant pathogens among all the pests and pathogens in the world (Bebber et al., 2014). The species which have extensive geological distribution are tremendously polyphagous (Moens et al., 2009). *Meloidogyne arenaria*, *M. incognita*, *M. javanica* and *M. hapla* can infect various important agricultural crops for instance wheat, rice, tobacco and tomato. Meloidogyne species exhibit overlapping but distinct host preferences. *M. arenaria* and *M. hapla* can infect groundnut, tomato, and pepper, while *M. incognita* infects cotton, potato, tomato, and watermelon but not groundnut. *M. javanica* infects cotton and tomato but does not infect pepper, highlighting species-specific differences in host compatibility. (Sasser, 1980; Moens et al., 2009). However, there are a few species which are host specific, for instance, *M. baetica* attacks only wild olive (Castillo et al., 2003).

1.3.1 Life cycle of root knot nematodes

1.3.1.1 Pre-invasion

The eggs of *Meloidogyne* genus remain enclosed in a gelatinous egg mass which protects the egg from the soil environment. Hatching of the eggs is usually stimulated by temperature related signals instead of host-specific factors (Goodell and Ferris, 1989), although root exudates can also accelerate hatching. Second-stage juveniles (J2s) of *M. chitwoodi* hatched in a temperature-dependent way during the early growing season of the plant, whereas unhatched J2s inside egg masses at the end of the growing season of plant could be stimulated to hatch by host root diffusates (Wesemael et al., 2006).

The second stage juvenile (J2) is the infective stage; after hatching, it is attracted to plant roots and invades the root just behind the elongation zone of the root tip (Figure 1.2). CO_2 and amino acids released by growing roots serve as general attractants, creating gradients in the soil that act to navigate the J2s. Specifically, CO_2 has been shown to attract J2s of *M. incognita* and *M. javanica* (Rasmann et al., 2012) while soil pH levels ranging from 4.5 to 5.4 have also been considered as favourable cues (Wang et al., 2009).

1.3.1.2 Invasion and induction of giant cells

The infective J2 employs its anterior, needle-like stylet both to penetrate the root epidermis and to insert secretions from its pharyngeal gland cells. These secretions include cell wall degrading enzymes that assist separation of cells and migration through the root. After successful invasion, the J2 nematodes migrate intercellularly through the cortex towards the root-tip until they reach the apex of the meristematic zone and then turn round and migrate back towards differentiating vascular tissue. Then the nematodes stop moving and initiate the formation of the feeding sites by reprogramming development of host cells (Palomares-Rius et al., 2017; Matuszkiewicz and Sobczak, 2023).

The J2 starts feeding from a few cells by inserting the stylet and introducing gland secretions, generating multi-nucleate giant cells (Figure 1.2). Giant cells are generated from single cells. Initially, binucleated cells are formed due to improper cell plate formation between two daughter nuclei, leading to karyokinesis without cytokinesis (Caillaud et al., 2008). This process continues until formation of cells with more than 100 nuclei, and finally resulting in hypertrophied, expanded, multinucleate structures. Giant cell production involves substantial transcriptional alterations. Genes which are associated with secondary metabolism or chiefly related to defence mechanisms are suppressed in the early-medium phases of infection. On the other hand, as soon as metabolism of the giant cells actively becomes engaged in nematode feeding, other induced stress regulated genes might act as molecular chaperones to inhibit accumulation of highly synthesized protein (Barcala et al., 2008; Barcala et al., 2010). The most important regulated gene groups are associated with hormone regulation pathways (exclusively related to auxin-cytokinin balance e.g LOB-domain protein gene LBD16) that are necessary for the development of the gall or giant cells and are also often common to lateral root development (Cabrera et al., 2015); the AUXIN1 and LIKE AUXIN (LAX3) influx proteins are essential in the generation of both giant cells and syncytia (Kyndt et al., 2016) and chorismate mutase may affect hormone balances (suppressing auxin formation) within the cell (Doyle and Lambert, 2003). Therefore, nematodes establish feeding sites by recruiting specific plant developmental pathways, involving hormonal cross talk. At the same time, nematodes need to suppress plant defence and its interacting hormone pathways. This interface between development and defence results in a complex pattern in which it is difficult to unravel the specific roles of different plant hormones (Gheysen and Mitchum, 2019).

Juveniles undergo their first moult from J1 to J2 within the egg and hatch into the soil as pre-parasitic J2s. Once a feeding site is established, the second stage juvenile becomes sedentary, starts feeding from the giant cells moving only the head to use the stylet to feed from one giant cell after another (Sijmons et al., 1991). The nematodes feed only from these giant cells as they develop and grow into adults (Kumar et al., 2021; Kumar and Miyara, 2022). These cells act as the harbour of nutrients throughout their life span. Within the host, Meloidogyne species go through a further two moults through the J3 and J4 stages before the final moulting to adults (Figure 1.3).

The majority of adults in a parthenogenetic species such as *M. incognita* are females, which exhibit a saccate (sac-like) body shape. They remain inside the host to feed from the giant cells. Sexual dimorphism is correlated with the sedentary lifestyle of saccate female nematodes and the motile vermiform males. The female remains always sedentary, while the male nematode becomes vermiform and motile again during the third stage of moulting, and eventually leaves the root (Papadopoulou and Triantaphyllou, 1982). As the life cycle comes to an end, the female nematode produces eggs and releases these in a gelatinous matrix on the root surface. Most *Meloidogyne* species (*M. incognita, M. arenaria, M. javanica* and some populations of *M. hapla*) reproduce by obligate mitotic parthenogenesis. In these species, while males may be present, they do not play active role in nematode reproduction.

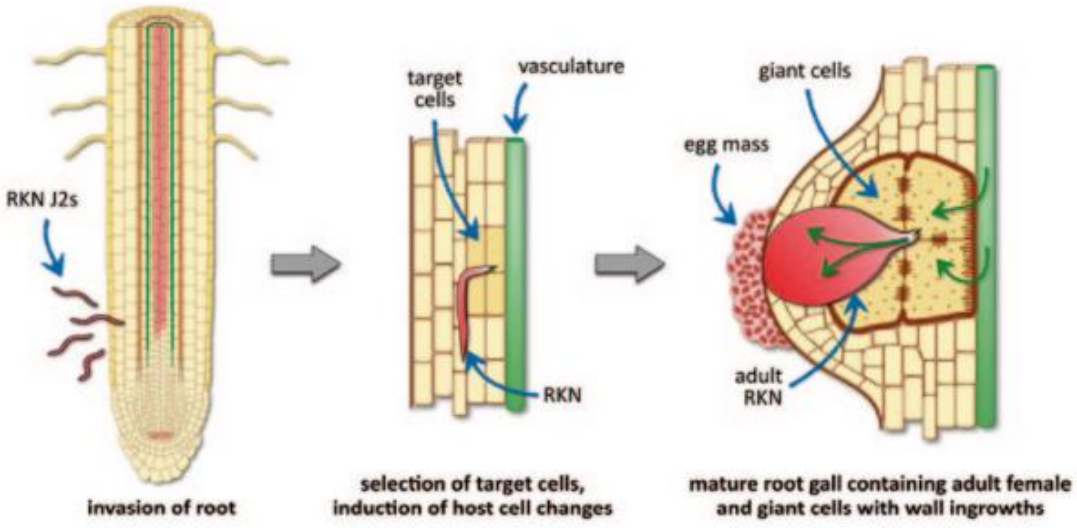

Figure 1.2. Invasion of J2s and formation of giant cells induced by *Meloidogyne* (Jones et al., 2011)

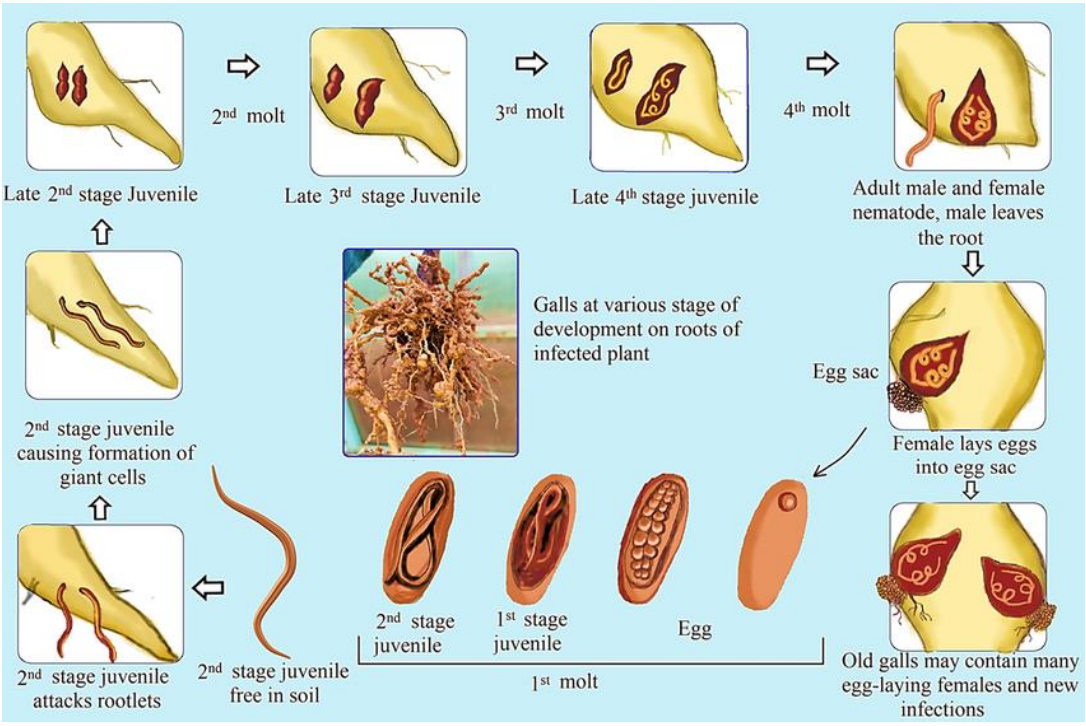

Figure 1.3. Schematic presentation of life cycle of root-knot nematodes (*Meloidogyne* genus) (Pradhan et al., 2023)

1.4 Cyst Nematodes

The most economically destructive species of cyst nematodes include cereal cyst nematodes (*Heterodera avenae; H. filipjevi*), soybean cyst nematodes (*Heterodera glycines*) and potato cyst nematodes (*Globodera pallida* and *G. rostochiensis*) (Jones et al., 2013). Generally, each cyst nematode species has a narrower host range than that of root knot nematodes and each species can infect only a small range of crops. *G. pallida* and *G. rostochiensis* can infect exclusively members of the Solanaceae family (tomato, potato, and eggplant) while *H. avenae* and *H. filipjevi* attack wheat, maize, barley, and oats. Whereas *H. glycines* can infect soybean, other legume crops, as well as certain non-leguminous weeds. However, *H. schachtii* has a wider host range and reproduced on chickpea, broccoli, and spinach as well as its main host, sugar beet (Price et al., 2021). The pea cyst nematode (*Heterodera goettingiana*) solely infects peas (*Pisum sativum*) (Di Vito and Greco, 1986).

1.4.1 The life cycle of cyst nematodes

The first stage juvenile (J1) of *Heterodera* or *Globodera* spp. develops and moults to the J2 within the eggshell (Figure 1.4). Eggs are contained in the protective cyst that is formed by the body wall of the fertilised female. After stimulation by host root exudate, the infective J2 hatches into the soil then locates towards a host (Sijmons, 1993). J2s of cyst nematode invade generally behind the root tip and migrate intracellularly to the developing vascular cylinder. The J2s use stylet thrusts in order to cut through the cell wall and disrupt the cells as well as using secreted cell wall degrading enzymes to weaken the cell walls. The J2 initiates a feeding site called a syncytium after selecting an appropriate host cell in the root. This J2 stage cannot be differentiated sexually and several factors e.g. environmental conditions, availability of nutrients influence the determination of sex (Grundler et al., 1991). The formation of male nematodes is most likely the result of poorer nutrient conditions within the syncytium (Sobczak et al., 1997). The first indication of differentiation in sex can be detected at the end of the second juvenile stage (J2) and just before the moulting to the third juvenile stage (J3) (Wyss and Grundler, 1992). During this J3 stage, nematodes continue their feeding from the syncytium and become fusiform. At the end of this stage, the nematode moults to develop the male or female nematode. The male moults into a fourth-stage juvenile (J4) male that stops feeding and then becomes an adult male, reverting to a vermiform shape. The adult male leaves the root to fertilise female nematodes. Cyst nematodes are amphimictic, therefore, prior to development of the egg, females require

fertilisation (Triantaphyllou and Riggs, 1979). The female J3 moults into the J4 stage, when the nematode continues feeding and then becomes saccate. Therefore, an adult female is formed following the final moulting. Once the female has been fertilised, eggs are produced in the body of a female nematode. Then the female nematode dies, and her cuticle becomes tanned which later forms a cyst, in which the eggs remain protected until external cues (e.g. host root exudates) stimulate hatching (Sijmons, 1993).

1.4.2 Syncytium formation

The cyst nematode feeding site, called a syncytium, is formed by degradation of adjacent cell walls and protoplast fusion, leading to cells becoming connected thus creating a multinucleated syncytium. A syncytial cell can be up to 200 times larger than surrounding cells and the hypertrophy of its elements further enlarges the feeding site, ensuring a continuous nutrient supply for the nematode (Golinowski et al., 1996). Despite the ultrastructural similarities in male and female induced syncytia, the female induced syncytium is notably larger than its male counterpart (Sobczak et al, 1997, Goverse et al, 2000, Ali et al., 2016). The induction and regulation of these structures is controlled by the secretion of effectors that aid host penetration, migration as well as establishment of parasitism. The nematode secretes effector molecules from gland cells through an anterior stylet (Jones et al, 2013, Chen et al., 2022), which activate numerous modifications in gene expression for facilitating formation of the syncytium. During nematode parasitism, the syncytium displays distinct physiological and morphological features including enhanced cytoplasmic density, cytoskeletal element restructuring and altered vacuole structures (Yusuf and Bello, 2025). Several host genes for instance expansins (Wieczorek et al., 2006) as well as endo-β-1,4-glucanases become upregulated in syncytia and are necessary for not only successful infection but also for cell expansion (Karczmarek et al., 2008). Effectors also have a role in suppressing host defence responses. The Hs4F01 gene of *H. schachtii* is involved in pathogen susceptibility, interacting with an Arabidopsis oxygenase (Patel et al., 2010). Similarly, a chorismate mutase gene associated with *G. pallida* also has a role in decreasing the defence response or altering auxin levels of the host plant (Jones et al., 2003). More putative effectors have also been detected in *G. pallida*, however, the function of the most of these effectors is still unknown. GFP fusions have been used to show that they localize to various compartments of plant cells including the cytoplasm and nucleus (Thorpe et al., 2014). Regulation of host genes and the precise localization of nematode effectors underscore the complex molecular interplay between nematodes and their host plants.

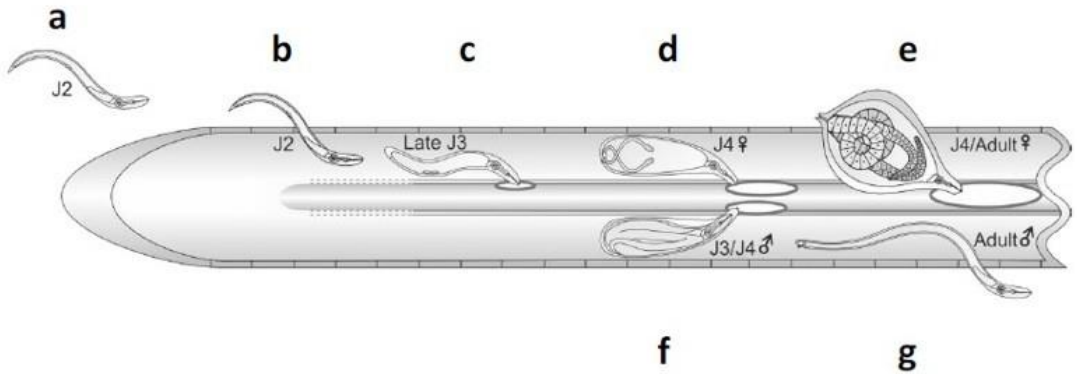

Figure 1.4. Schematic representation of the life cycle of cyst nematodes (Lilley et al., 2005).

Life cycle of a cyst nematode (*G. pallida*). a) Eggs hatch in the soil as migratory second-stage juveniles (J2). Hatching triggered by host-derived cues under favourable conditions. b) The J2s penetrate the root and migrate intracellularly toward the vascular cylinder, where a feeding site is initiated, and sex determination occurs late in this stage. c) The J2s then moult into J3s, during which a syncytium is formed, and the nematode begins feeding and swelling. d) The final moult to the J4 stage occurs, and female ovaries begin to develop. e) Within the female body, eggs are formed, and the cyst wall is tanned by phenol oxidases to create a durable structure. f) Males develop into vermiform forms within the J4 cuticle. g) Adult males finally exit the root to fertilise the females.

1.5 Potato Cyst Nematodes

Potato is regarded as the world's third most and the UK's second most important staple crop (Campbell, 2024). Although potatoes grow best in temperate climates, they are cultivated in more than 150 countries (FAO, 2022). Like other agricultural crops, potatoes are threatened by a variety of pests and diseases. Potato cyst nematodes (PCNs) are one of the most detrimental pests to the potato industry (Orlando and Boa, 2023; Subbotin et al., 2020). Two cyst nematode species (*Globodera pallida and Globodera rostochiensis*) are considered as the most economically important species of potato cyst nematode in the world (Bohlmann and Sobczak, 2014, Jones et al., 2013). Although they have a narrow host range and are limited to crops of the Solanaceae family, however, globally 9% crop losses occur due to these diseases (Perry et al., 2018). Another potato cyst nematode species, *G. ellingtonae* was identified in potato fields in the USA during 2008 (Handoo et al., 2012). Still the pathogenicity of this species to potato is not consistent (Zasada et al., 2019).

At present, PCNs have been prevalent in 80 countries, with three countries affected by *G. pallida* alone, 27 countries infested by *G. rostochiensis* alone, and 50 countries facing invasions of both species (CABI, 2022a, 2022b; EPPO, 2024; Orlando and Boa, 2023). Potato cyst nematode (PCN) is the most significant pest of potato in the UK, with infestations capable of reducing tuber yields by more than 80%, costing the industry an estimated £50 million annually. The greatest damage occurs when juvenile nematodes hatch from cysts and invade potato roots, leading to wilting, stunted growth, and other symptoms associated with root damage and stress. In England and Wales, around 65% of land used for ware potato production is infested with PCN (ADAS, 2020). Planning an efficient control strategy of PCN requires a deep comprehension of their life cycle (**Section 1.3.1**, Figure 1.4). *G. rostochiensis* and *G. pallida* are notable for having similar life cycle characteristics, which offers a useful foundation for comparative research and focused interventions (Price et al., 2021). Their early cyst colour prior to tanning provides a simple method for distinguishing between these PCN species, with *G. pallida* having cream or white coloured mature females and *G. rostochiensis* forming golden or yellow coloured untanned cysts (Evans and Stone, 1977). Hundreds of J2 nematodes develop from J1s inside eggs in the cyst, where they wait for a signal to hatch. Without a host crop, these eggs can remain dormant in the soil for 20 years or longer (Turner, 1996). The prolonged host-free survival period of PCNs presents a significant difficulty for growers, as it demands long-term effective management strategies (Spychalla and De Jong, 2024).

1.6 Need for Exploring Resistance to Potato Cyst Nematode

Infection with potato cyst nematodes causes serious crop losses because of the damage caused by the prolonged feeding of the parasitic nematodes as well as the earlier intracellular migration of the J2s. The infected plants generally contain reduced levels of nitrogen, potassium and phosphorus in their foliage. The plants also become more susceptible to the attack of other pathogens therefore reveal wilting symptoms. Yield loss due to the infection is related to reduced light interference owing to the reduction of leaf area. It has been suggested that a hormonal imbalance during nematode infection is one of the causes of this reduction, moreover, nutrient deficiency due to nematode feeding may also interfere with the rate of photosynthesis (De Ruijter and Haverkort, 1999).

Given the global significance of potato as one of the major crops, there is an urgent need for the development of sustainable management strategies against potato cyst nematodes. An array of effective control methods has been used to manage potato cyst nematodes including trap crops, soil managements and use of nematicides (Back et al., 2018; Sasanelli et al., 2021). The chemical control strategy is limited as well as not accepted widely due to concerns about its effects on the environment. Since the early 2000s, the ban on soil-applied pesticides has shifted cyst nematode management toward more sustainable approaches. Current control strategies primarily rely on crop rotation and the deployment of a limited range of resistance genes in crop cultivars (Hillocks, 2012). However, the natural enemy sources for nematodes are limited and crop rotation can cause yield reduction due to the forced utilization of suboptimal farmland. Therefore, several research programmes have focused on the development of natural resistance against potato cyst nematode worldwide (Koropacka, 2010).

Using resistant varieties has become a key eco-friendly and efficient component of the integrated management strategies. Various wild relatives as well as landraces of cultivated potato crop have been considered for providing a source of resistance genes against potato cyst nematode which have been used successfully in breeding programmes. These strategies exhibit varying levels of effectiveness, but they can significantly contribute to reducing PCN populations when used individually or in combination with the deployment of resistant varieties, forming an integral part of integrated pest management approaches (Spychalla and De Jong, 2024).

However, producing such resistant varieties requires intensive efforts over many years to gain commercial acceptance. Recent advancement in the genomics of potato have been providing tools to map resistance genes rapidly as well as to develop molecular markers for facilitating selection during breeding (Gartner et al., 2021).

PCN resistance screening began many decades ago (Castelli et al., 2003; Ellenby, 1952) and continues still to date. So far, more than fifty tuber forming Solanum species have been found that confer resistance to *G. pallida* and/or *G. rostochiensis* in the case of at least one pathotype and one accession. Initial approaches to identify potato cyst nematode resistance sources in potato screened almost 1,200 wild accessions from the Commonwealth Potato Collection and this led to the first identification of the resistance locus H1 against potato cyst nematode from *S. tuberosum ssp. andigena*. This locus provided almost complete resistance against *G. rostochiensis* (pathotypes Ro1 and Ro4) (Ellenby, 1952) and has been widely deployed around the world including in European cultivars (Faggian et al., 2012; Galek et al., 2011; Schultz et al., 2012). The incorporation of the H1 gene, which provides resistance to *G. rostochiensis*, together with genes conferring resistance to *G. pallida*, did not diminish the effectiveness of the *G. pallida* resistance, indicating that stacking these resistance sources can be achieved without negative interactions (Price et al. 2024). However, extensive use of potato cultivars containing the H1 locus, such as Maris Piper, has led to the selection of *G. pallida* that has now become the dominant species in the UK. Recently, it was shown that potato genotypes carrying the resistance locus (H1) also resist *G. ellingtonae* (Whitworth et al., 2018; Zasada et al., 2019).

Subsequently, the broad spectrum nematode resistance gene Hero was detected from wild tomato species, conferring resistance to all pathotypes of *G. rostochiensis* (Ellis and Maxon-Smith, 1971; Ganal et al., 1995). The Hero A gene, cloned via map-based cloning and complementation, is a member of a multigene family within the coiled-coil nucleotide-binding site (NBS) leucine-rich repeat (LRR) class of resistance genes (Ernst et al., 2002). Expression of Hero A in transgenic PCN susceptible tomato lines conferred resistance to all pathotypes of *G. rostochiensis* and partial resistance to *G. pallida* pathotype Pa2/3 (Sobczak et al., 2005). To date, over 20 loci conferring resistance to potato cyst nematodes (PCN) have been identified in potato and its close relative, tomato, of which three genes such as *Gpa2*, *Hero*, and *Gro1-4* (Gartner, 2024) and *Rhg1* in soybean (Concibido et al., 2004) have been cloned and characterized.

According to the “gene-for-gene” hypothesis (Flor, 1971), PCN quantitative resistance might be conferred by the products of dominant resistance genes (*R*). These *R* genes recognise effector proteins produced by the pathogen in infected host cells (encoded by *Avr* genes) triggering defence responses that may include a hypersensitive reaction (Davies and Elling, 2015; Van der Biezen and Jones, 1998). Over the course of time, cell death occurs thus nematodes are deprived of an adequate food source, finally leading to resistance. Although almost all the characterised genomic loci providing resistance to *G. pallida* or *G. rostochiensis* are *R* genes of the nucleotide-binding site-leucine-rich repeat (NB-LRR) family, other classes of gene are also important in conferring resistance to potato cyst as well as other cyst nematodes. For instance, the Cf-2 gene that confers resistance to both the *Cladosporium fulvum* fungus and *G. rostochiensis* encodes an extracellular receptor-like protein containing a LRR domain (Lozano-Torres et al., 2012).

Potato cyst nematode resistance genes are a valuable commodity. However, there are inadequate numbers of resistance genes that are responsive to introgression, and which will likely make a significant effect in future *G. pallida* management strategies. Therefore, there is an urgent requirement for the new resistant cultivars against *G. pallida* which will meet the commercial requirements, hence, more effort will be required to ensure durable and effective resistance (Gartner et al., 2021).

1.7 *Solanum spp*. as a Potential Source of Resistance to Potato Cyst Nematode

Nematode resistance was not primarily found in *Solanum tuberosum ssp. tuberosum*. Therefore, nematode resistance breeding is based on the identification of resistance in alternative Solanum species (Dalamu et al., 2012). Resistance to *G. pallida* and *G. rostochiensis* from *S. tuberosum ssp. andigena* and *Solanum vernei* has been combined into breeding programmes (Rousselle-Bourgeois and Mugniery, 1995). The dominant *Gpa2* gene for example, related to *G. pallida* resistance (pathotype Pa2) was identified in *S. tuberosum ssp. andigena* (van der Voort et al., 1999). The dominant H2 gene was detected in *S. multidissectum*, which provided resistance to *G. pallida* (pathotype Pa1) (Strachan et al., 2019). However, there is a continuous need for exploring other sources. Numerous wild species of Solanum could be effective sources of resistance to nematodes (Milczarek et al., 2020). A range of Solanum species with resistance has been explored from *S. gourlayi*, *S. sparsipilum*, *S. kurtzianum* and *S. acaule* (Castelli et al., 2003). *S. gourlayi* was one source of

resistance against *G. pallida* that was detected among accessions of wild species of Solanum (Ruiz de Galarreta et al., 1998; Castelli et al., 2005). *G. pallida* resistance gene Gpa VI^{1}_{spg} was also derived from wild potato species *S. spegazzinii* recently (Gartner et al., 2024).

Recent studies highlighted interactions between potato cyst nematode and *S. sisymbriifolium* (Wixom et al., 2020; Varandas et al., 2024). *S. sisymbriifolium* is used as an efficient trap crop for potato cyst nematode as it confers high resistance against *G. pallida*. Root exudates of this plant stimulate nematode hatching in a high number; however, the nematodes cannot complete their lifecycle (Scholte and Vos, 2000). Moreover, non-tuber forming wild relatives of potato, belonging to the genus Solanum, have the potential to act as a key source of novel *G. pallida* resistance (*R*) genes which could then be used in the development of new, resistant potato cultivars via transgenesis rather than traditional breeding. One such wild relative is the American Black Nightshade *Solanum americanum*. Recent work by Witek et al. (2021) demonstrated that *S. americanum* could also act as a source of *R* genes for another devastating potato pathogen, *Phytophthora infestans*. Using integrated genomic and phenotypic data, three NLR-encoding genes designated *Rpi-amr4*, R02860, and R04373 recognizing the *P. infestans* RXLR effectors PITG_22825 (AVRamr4), PITG_02860, and PITG_04373 respectively, were successfully cloned. These genomic resources and methodologies provide a strong foundation for engineering potatoes with durable resistance to late blight and hold potential for application in combating diseases in other crops (Lin et al., 2023). Therefore, this finding raises the possibility that the *S. americanum* genome may harbour unexploited resistance genes that could be utilised to develop effective control strategies against *G. pallida*. The systematic identification and characterization of these resistance traits will provide a strong foundation for the mapping of resistance loci and the discovery of novel R-genes. Ultimately, such insights will be invaluable for the development of durable nematode-resistant potato cultivars, contributing to sustainable crop protection and reducing reliance on chemical nematicides.

1.8 Cellular mechanism of Potato Cyst Nematode resistance

Cyst nematodes move intracellularly during their early stage of infection to cause root damage, leading to the release of either Damage-Associated Molecular Patterns (DAMPs) or Nematode-Associated Molecular Patterns (NAMPs). These compounds are recognized by extracellular Pattern Recognition Receptors (PRRs), which in turn activate basal immune responses, a defence mechanism commonly referred to as Pathogen-Associated Molecular

Pattern (PAMP)-Triggered Immunity (PTI) (Choi and Klessig, 2016) (Figure 1.5). In the ongoing evolutionary arms race between plants and pathogens, plants have developed a second line of defence in which effector proteins secreted by pathogens are recognized by nucleotide-binding leucine-rich repeat (NB-LRR or NLR) proteins, leading to effector-triggered immunity (ETI). Leucine-rich repeat receptors are also stated as resistance proteins (R-proteins). ETI represents a robust and amplified defence response, often culminating in a localised programmed cell death known as the hypersensitive response (HR) (Lolle et al., 2020). At the biochemical level, ETI is characterized by a biphasic accumulation of apoplastic reactive oxygen species (ROS), although the amount and intensity of ROS production vary with each plant-pathogen interaction (Wu et al., 2023). Typically, NLR-triggered HR produces an initial low-amplitude, transient ROS burst followed by a prolonged, higher-intensity phase, while PTI is generally confined to only the transient first phase (Torres et al., 2006).

Within the first few days following inoculation with cyst nematodes or root-knot nematodes, a burst of ROS can be observed in the roots of infected plants (Holbein et al., 2014; Melillo et al., 2006; Siddique et al., 2014; Singh et al., 2020). To prevent oxidative damage to plant cells and biomolecules, a robust ROS-scavenging system is activated, comprising nonenzymatic antioxidants like anthocyanins, ascorbic acid (vitamin C), and glutathione, along with enzymatic defences including catalases, superoxide dismutases, thioredoxins, and peroxidases (Smirnoff, 2018). Recent studies examined the interaction between the potato cyst nematode (*G. pallida*) and its immune host, *Solanum sisymbriifolium* (Kooliyottil et al., 2019; Wixom et al., 2020). This plant provides high resistance to *G. pallida* and is widely used as an effective trap crop (Dandurand and Knudsen, 2016), as it induced extensive hatching of nematodes but prevented them from completing their life cycle within its roots (Timmermans et al., 2006). The defence response of *S. sisymbriifolium* appears to be strongly associated with reactive oxygen species (ROS) production and the hypersensitive response (HR) (Timmermans, 2005; Wixom et al., 2020). In many plant species, resistance to nematodes is commonly linked to a characteristic hypersensitive response (HR) in root cells, triggered by nematode invasion. A key factor in this defence mechanism is the precise timing of hydrogen peroxide (H_2O_2) production, which plays a crucial role in preventing the nematodes from successfully developing. These insights into ROS dynamics and hypersensitive responses not only deepen our understanding of plant-nematode interactions but also provide a valuable framework for screening and characterising resistance traits against potato cyst nematodes.

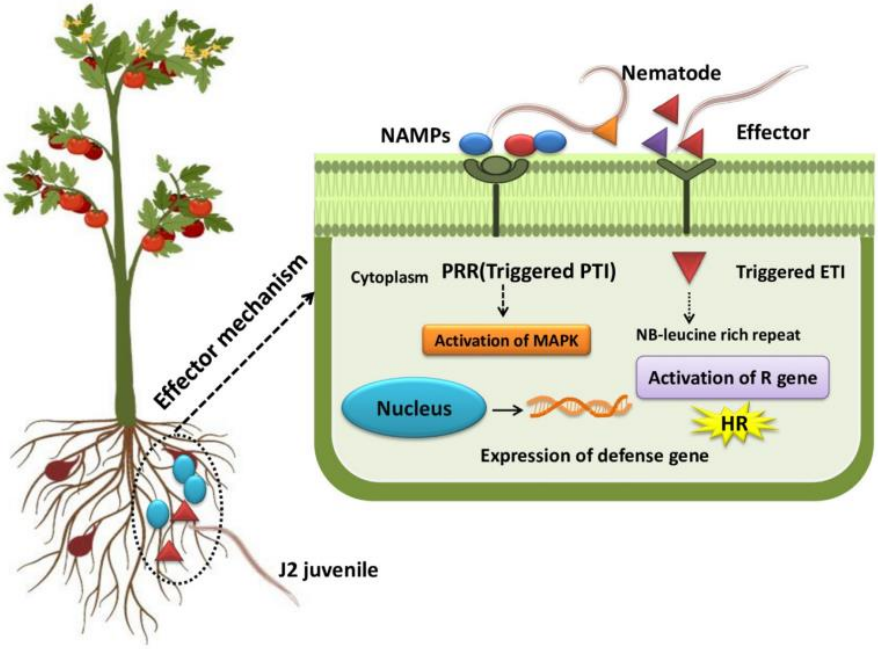

Figure 1.5. The interaction between plant immune receptors and defence signalling components (Gupta et al., 2023)

The interaction begins when nematode-associated molecular patterns (NAMPs) are recognized by membrane-bound pattern recognition receptors (PRRs), triggering PAMP-triggered immunity (PTI). In response, certain nematode effector proteins can be detected by intracellular receptors, activating effector-triggered immunity (ETI) and initiating a hypersensitive response (HR) to limit nematode infection.

1.9 Reporter genes as powerful tools for monitoring gene expression

1.9.1 Overview

A reporter gene is a heterologous coding region of a gene engineered to produce a detectable and quantifiable phenotype, by clearly distinguishing the reporter signal from the background of endogenous proteins (Alam and Cook, 1990). It is typically fused to a transcriptional regulatory sequence and introduced into cells or organisms to monitor the activity of promoters or enhancers in cells, tissues and the entire organism (Wood, 1995, Ghim et al., 2010, Sharifova et al., 2025). Reporters are designed so they are not naturally expressed in the cells or organisms being studied. When the reporter is expressed, it can be measured, either by detecting the enzyme activity it produces or by observing the protein directly under a microscope or other imaging method (Sharifova et al., 2025). Diverse genetically encoded reporters have been developed and optimised to monitor gene expression and transgenic events (He et al., 2020, Hu et al., 2025).

Since bacterial β-galactosidase (*LacZ gene*) was first demonstrated as an enzymatic reporter in 1980 (Casadaban et al., 1980), additional enzymatic reporters such as β-glucuronidase (GUS gene) (Jefferson et al., 1986), and firefly luciferase (Luc gene) from bioluminescent species have also been developed (Ow et al., 1986). The invention of green fluorescent protein (GFP) from the Pacific jellyfish (*Aequorea victoria*) in 1994 marked the first use of a fluorescent reporter for gene expression studies (Chalfie, 1995). This progression led to the generation of diverse fluorescent protein reporters, such as cyan (CFP), red (RFP) and yellow (YFP) as well as mCherry and other fluorescent proteins from various organisms (Rodriguez et al., 2017, Wang, et al., 2023). Although the fluorescent proteins were primarily intended solely as markers for gene expression, fluorescent reporters have since been adapted to qualitatively and quantitatively track and visualize a wide range of cellular and physiological activities (Rodriguez et al., 2017, Wang, et al., 2023).

Among the various types of reporter genes, uidA or gusA is one of the most widely used for assessing the gene expression and hormonal signalling pathways in plants. This gene encodes the GUS enzyme, which cleaves the chromogenic substrate X-gluc (5-bromo-4-chloro-3-indolyl β-D-glucuronic acid), producing an insoluble blue colour in plant cells exhibiting GUS activity (Karcher, 2002). The GUS assay is highly visible, reliable and requires no expensive equipment (Jefferson et al., 1989). However, GUS staining is invasive, requires a costly substrate and necessitates the sacrifice of plants (He et al., 2020). Another reporter, LUC

gene (encodes luciferase enzyme), is employed extensively in animals and plants (Contag and Bachmann, 2002, Khakhar et al., 2020). It enables non-invasive monitoring but requires a special camera and application of an expensive substrate. Fluorescent proteins are observed using either fluorescence or confocal microscopy and can be used with live samples, but these reporters are less useful in evaluating naturally growing plants in glasshouse or field conditions. Furthermore, autofluorescence and stress-induced fluorogenic compounds in plant cells can interfere with fluorescent reporters, necessitating strategies to improve the signal-to-noise ratio (Sadoine et al., 2021). Although these reporter assays offer significant advantages, they also provide practical difficulties in monitoring transformants and gene-targeted mutants (He et al., 2020; Yang et al., 2023). Hence, developing non-invasive cost-effective reporter systems capable of continuously monitoring cellular activities is essential for the efficient selection of transformants (Ge et al., 2022; Lee et al., 2023).

Due to these and other limitations, a new betalain-based (RUBY) reporter has recently been developed since 2020, that is visible to the naked eye and allows non-invasive, continuous, and cost-effective monitoring of cellular activities in a wide range of plants and in animals, including silkworms (He et al., 2020; Yang et al., 2023; Sharifova et al., 2025). The RUBY reporter gene cassette has been shown to stably express in both monocots and dicots, including *Arabidopsis*, tobacco, rice, tomato, and maize, confirming its functional stability and broad applicability (He et al., 2020; Lee et al. 2023; Wang et al., 2023a). RUBY has been adapted for biomolecular studies, serving as an inducible system for protein-protein interaction analysis via the yeast GAL4 transcription factor (Chen et al., 2023), combining with eYGFPuv (a UV-visible green fluorescent protein) for dual-visible transcription factor-DNA interaction assays (Sun et al., 2023), and enabling quantitative betalain measurement through spectrophotometry and pixel analysis (Chen et al., 2023), offering substantial variability for explicating molecule-interactions.

1.9.2 Use of reporter genes in studies of nematode parasitism

Studies of plant host gene responses to nematode infection have often relied on targeted analyses of a small number of known sequences using promoter–reporter constructs (Escobar et al., 1999; Goddijn et al., 1993; Niebel et al., 1993; Mazarei et al., 2003). Among the most commonly used reporters, β-glucuronidase (GUS) and green fluorescent protein (GFP), provided distinct advantages for studying host-pathogen interactions.

The GUS reporter gene system has proven to be an invaluable tool for studying plant responses during nematode parasitism. By linking GUS to specific promoters, researchers can visualize and quantify gene expression within nematode-induced feeding sites, providing detailed insights into host-nematode interactions at the molecular level. This reporter system has been widely used to study nematode parasitism, with promoters like *Arabidopsis thaliana AtGRP* (Glycine-Rich Protein), *RD29A* (a gene responsive to desiccation, cold and salinity) and synthetic promoters (Soybean Cyst Nematode-inducible) showing strong, specific expression in nematode-induced feeding sites, and genes such as *LBD16* (LATERAL ORGAN BOUNDARIES-DOMAIN 16) being upregulated in root galls, highlighting both spatial and functional insights into host-nematode interactions (Yamaguchi-Shinozaki and Shinozaki, 1993; Huang et al., 2003; Sultana et al., 2022; Zhang et al., 2023; Singh et al., 2025). The GFP reporter was first expressed in *E. coli* and the nematode *C. elegans* (Chalfie et al., 1994). Previous findings demonstrated GFP as an efficient and reliable marker for studying gene expression in entomopathogenic nematodes (Hashmi et al., 1997).

The RUBY (betalain-based) reporter is an emerging and versatile tool for evaluating both abiotic and biotic stresses, offering a clear, visible display that facilitates rapid and non-destructive monitoring of plant responses. Promoters from defence-related genes such as *PR1* and *WRKY70* have been fused to the RUBY cassette to visibly track spatial and temporal activation patterns during infection by pathogens like *Pseudomonas syringae* (Baral et al., 2024). Similarly, mycorrhiza-responsive promoters in the MycoRed system have been used to drive betalain accumulation in roots, enabling real-time visualisation of arbuscular mycorrhizal colonisation alongside pathogen-response studies (Timoneda et al., 2021). The RUBY reporter has not yet been explored in the context of nematode infections, offering an exciting opportunity to pioneer its use with nematode-responsive promoters for visible and non-destructive monitoring of plant responses.

1.10 Role of promoters in monitoring gene expression

Promoters are regulatory DNA sequences located upstream of coding regions that function as molecular switches, controlling the initiation and level of gene transcription. They contain cis-acting elements, which serve as binding sites for transcription factors (TFs) and other proteins that recruit RNA polymerase and regulate downstream gene expression (Smale and Kadonaga, 2003; Hernandez-Garcia and Finer, 2014). Acting as molecular biological clocks, promoters determine the timing and specificity of gene activity (Potenza et al., 2004).

Promoters of protein-coding genes are generally organized into core, proximal, and distal regions. The core promoter provides the minimal sequences required for transcription initiation, whereas the proximal and distal regions contain regulatory elements such as enhancers, silencers, insulators, and other cis-elements. These elements contribute to the fine-tuning of transcriptional regulation, ensuring accurate spatial and temporal control of gene expression (Hernandez-Garcia and Finer, 2014). In plant genes, promoters typically contain a TATA box and an initiator (Inr) element, along with a well-defined transcription start site (TSS) located approximately 20–30 base pairs downstream of the TATA element.

In the upstream regions of plant gene promoters, several positive and negative regulatory elements have been identified, many of which function as enhancers or silencers (Timko et al., 1985; Tyagi, 2001). To study their function, a minimal promoter commonly a 46 bp derivative of the CaMV 35S promoter or its 90 bp version is often fused at its 5′ end to heterologous promoter sequences and at its 3′ end to a reporter gene such as *GUS*, *LUC*, or *CAT*. These promoter–reporter constructs are then introduced into plant cells using Agrobacterium-mediated transformation, electroporation, or biolistics, and are subsequently analysed for transient expression or for expression in stable transgenic systems. The expression patterns driven by heterologous promoter sequences have proven highly informative in characterising the functional properties of both developmental and inducible regulatory promoters (Tyagi et al., 1999; Tyagi, 2001).

Promoters can be strategically selected for the development of transgenic plants depending on the desired trait and the specific target tissue to be regulated (Bilas et al., 2016). Based on their recognition by RNA polymerases, promoters are primarily classified into RNA polymerase II (Pol II) (Figure 1.6) and RNA polymerase III (Pol III) promoters. Pol II promoters can be further classified into constitutive, tissue-specific, stress-inducible, and synthetic promoters (Bilas et al., 2016). In contrast, Pol III promoters are mostly corresponding to the U3 small nucleolar RNA and U6 small nuclear RNA promoters (Marshallsay et al., 1992).

The Cauliflower mosaic virus 35S (CaMV35S or 35S) constitutive promoter is one of the most widely used promoters for gene expression in transgenic plants and in basic functional genomics studies (Porto et al., 2014). Cauliflower mosaic virus (CaMV) is an aphid transmitted plant pathogenic virus that infects Brassica species such as cauliflower, cabbage, turnip and oilseed (Amack et al., 2020). CaMV infection was first documented in the scientific literature in the United States during the 1920s (Goldstein, 1927). Notably, CaMV was also the first plant pathogen to be characterized as a double-stranded DNA virus (Shepherd et al.,

1968). During its infection cycle, the virus generates an abundant transcript known as the 35S RNA (Amack et al., 2020), which serves as the primary template for producing both viral proteins and sub-genomic RNAs. Odell et al. (1985) first isolated and characterised the promoter, showing that it drives strong gene expression in tobacco and that it alone is sufficient to direct transcription in plant cells without requiring additional viral factors. Because of this broad and robust activity, the CaMV35S promoter has become one of the most commonly used constitutive promoters in plant biotechnology and functional genomics.

While constitutive promoters like 35S drive continuous expression in most tissues, specific or inducible promoters offer the advantage of increased gene expression in target tissues or at defined developmental stages. Such promoters provide more precise and predictable control over gene expression, often minimizing any negative impact on plant growth or final yield. Recent advances in the discovery of proteins with programmable DNA-binding specificities have opened up numerous applications in synthetic biology, including transcriptional regulation, genome editing, and epigenetic modifications. These developments enable the design of synthetic promoters and regulatory systems with enhanced precision and versatility, expanding the toolkit for targeted gene expression in plants (Figure 1.7) (Ali and Kim, 2019).

Due to the importance of the CaMV35S promoter in plant biotechnology and its relevance to understanding how sedentary nematodes manipulate host gene expression, it represents a valuable tool for developing targeted strategies to enhance plant resistance. Although the 35S promoter drives strong constitutive expression of anti-nematode genes, its broad activity across all tissues can lead to inefficiencies and potential off-target effects, highlighting the need for infection- or tissue-specific promoters for precise and energy-efficient resistance responses (Dutta et al., 2023).

In contrast to constitutive promoter, nematode-responsive promoters enable tissue-specific gene expression that is activated upon nematode infestation. This targeted strategy enhances resistance precisely at the site of infection while minimizing unintended effects in other tissues, providing a more efficient, eco-friendly, and cost-effective approach for managing plant-parasitic nematodes (Kakrana et al., 2017; Singh et al., 2017; Joshi et al., 2022; Thorat et al., 2024). Numerous nematode-responsive promoters have been recognized and successfully exploited in resistance approaches. GUS and GFP are the most extensively used reporter gene assays for quantifying the activity of promoters. The tobacco root-

specific (TobRB7) promoter was expressed in *M. incognita*-induced giant cells (Opperman et al., 1994), while the wound-inducible (wun1) promoter revealed strong GUS activity in roots infected with *G. pallida* and *M. javanica* (Hansen et al., 1996). Similarly, the *Parasponia andersonii* haemoglobin, Arabidopsis *atao1*, tomato LEMMI9, Auxin-responsive GH3, chalcone synthase (CHS), and sunflower *Hahsp17.7G4* promoters were activated in giant cells during gall initiation and development induced by *Meloidogyne spp*. (Ehsanpour and Jones, 1996; Møller et al., 1998; Escobar et al., 1999; Hutangura et al., 1999; Escobar et al., 2003). In cyst nematodes, nematode-inducible promoters (Pyk20, ARM1, 728, 25, LEMMI9, *Atgrp*, and *AtSUC2)* were upregulated in feeding sites (Puzio et al., 2000; Van Poucke et al., 2001; Karimi et al., 2002). Whereas constitutive promoters such as CaMV35S, nos, RolC, and RolD were found to be downregulated at different time points during nematode infection (Van Poucke et al., 2001), interestingly, CaMV35S also drove GFP expression in feeding sites of *H. schachtii* and *M. incognita*, displaying contrasting expression dynamics between the two nematodes (Urwin et al., 1997a).

Recently developed non-invasive RUBY reporter also demonstrated the potentiality of using it under the control of CaMV35S promoter as well as tissue-specific and species-adapted promoters. Arabidopsis Maize UBIQUITIN promoter, Arabidopsis seed-specific At2S3 promoter and YUC4 promoter (encodes auxin biosynthesis enzyme), DR5 promoter (auxin responsive) (He et al., 2020) and cassava vein mosaic virus promoter (CsVMV) in soybean roots (Mejias et al., 2025) have demonstrated significantly enhanced and more precise expression of target genes like RUBY in plant systems, minimizing off-target effects and improving functional outcomes. Although nematode-responsive promoters have not yet been explored using the RUBY reporter system, the betalain-based MycoRed system driven by blue copper protein and phosphate transporter promoters, has been successfully applied for fungal visualization in arbuscular mycorrhizal symbiosis, offering a promising model for future promoter-reporter studies in plant-microbe interactions (Timoneda et al., 2021). Therefore, the generation of novel RUBY construct regulated by a root-specific, nematode-responsive promoter will enable precise visualization of gene expression patterns during nematode infection, offering a powerful tool for exploring host-pathogen interactions.

Given these considerations, the present study was conducted to explore the potential utility of the RUBY (betalain based) reporter system for monitoring gene expression during nematode infection. We first used RUBY to resolve questions surrounding the stability of CaMV35S expression in syncytia of cyst nematodes. Subsequently, this RUBY construct with

a single constitutive promoter was used to generate a new construct into which we could insert novel potato promoters, which would be a valuable tool for investigating nematode-plant interactions, enabling the spatial and temporal tracking of gene expression during nematode invasion and in nematode feeding structures.

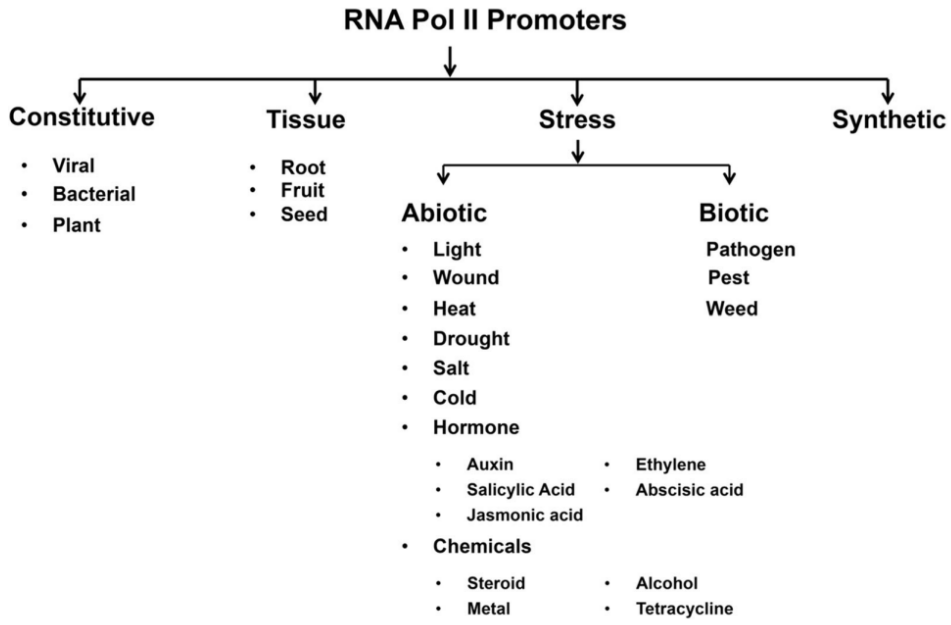

Figure 1.6. Flow chart illustrating the classification of RNA polymerase II (Pol II) promoters based on their expression patterns into four major types: constitutive, tissue-specific, stress-inducible, and synthetic promoters (Kummari et al., 2020).

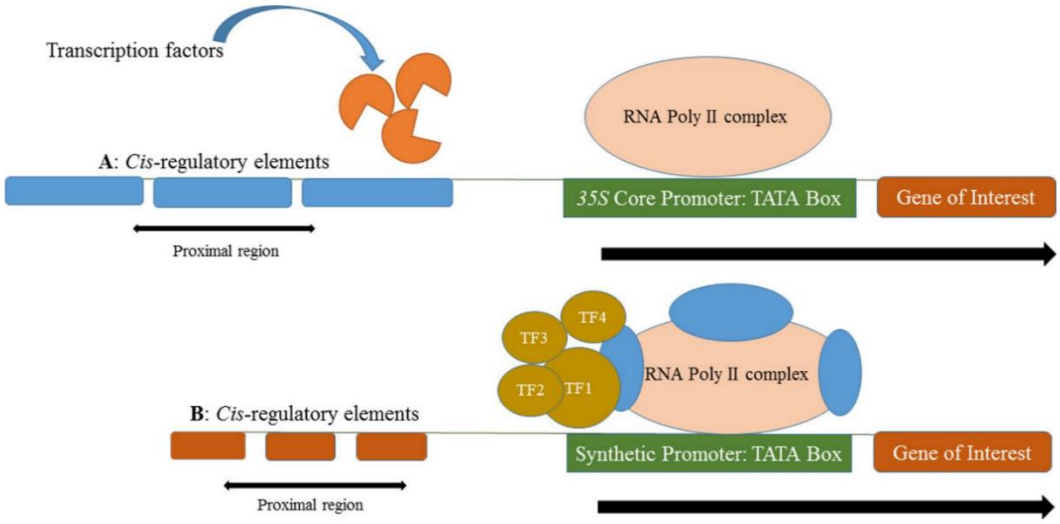

Figure 1.7. Schematic representation of promoter architectures controlling gene expression (Ali and Kim, 2019).

A) A long native (35S) promoter containing multiple copies of identical cis-regulatory elements regulates the expression of a gene of interest. Transcription factors, responsive to the cellular environment, bind to native cis-elements in the proximal region and recruit the RNA polymerase II complex to drive transcription.

B) A short and robust synthetic promoter in which multiple, diverse cis-regulatory elements from different origins collectively regulate the expression of the gene of interest.

1.11 Objectives of the project

- To generate CaMV35S:RUBY transgenic Arabidopsis and potato lines and investigate RUBY expression during nematode infection.
- To resolve the spatial interaction between root knot nematode and arbuscular mycorrhizal fungi using the MycoRed reporter system.
- To develop novel RUBY constructs driven by nematode-responsive promoters, enabling the evaluation of transgene expression and plant responses to nematode infection.
- To screen and characterise *Solanum americanum* accessions for resistance against *G. pallida*, with the goal of identifying and mapping resistance loci for future breeding and genetic studies.

Chapter 2

General Materials and Methods

2.1 Biological material

2.1.1 Plant maintenance

Wild type potato plants (*Solanum tuberosum* 'Désirée') were multiplied in sterile culture on Murashige and Skoog medium (pH 5.8) with 30g/L sucrose (MS30), solidified with 5.5g/L plant agar (Melford) in a controlled growth room environment at 20℃ with 16 hours supplementary light per day. *Arabidopsis thaliana* (wild type, Col-0) plants were grown from seeds on ½-strength MS10 medium (pH 5.8) in the same conditions in either a growth room or plant growth cabinet (Sanyo). Prior to sowing, seeds were sterilised by incubation in 20% bleach for 20 mins with rotation, followed by 5-6 washes with sterile deionised water. Sterilised seeds were then stratified at 4 °C for 24-48 hours prior to sowing to aid synchronisation of germination. For growth in the glasshouse, Arabidopsis was sown in potting compost (No.2 Potting Supreme; Petersfield Growing Mediums) then transplanted as seedlings to individual pots of the same medium for transformation or phenotype analysis. Growth conditions were 20-22 °C with 16 hours photoperiod. Tomato (*Solanum lycopersicum*, 'Ailsa craig') plants were grown from seeds in potting compost in glasshouse conditions (23-25 °C temperature, ambient relative humidity with 16 hours day length.

Nicotiana benthamiana (Phosphate transporter (PT5b), and Blue copper protein (Bcp1) promoter-reporter lines that respond to AMF infection; Timoneda et al., 2021) seeds were sown in compost for *M. incognita* and AMF (arbuscular mycorrhiza fungus) infection in glasshouse conditions (22^{o}C, 16h day length) prior to subsequent use in experiments. *Solanum americanum* plants were sown in potting compost then transplanted into sand:loam (50:50) (silver sand:Norfolk Topsoil; both Bailey's of Norfolk) mixture in glasshouses at approximately 20 °C with ambient relative humidity and 16 hours of light per day.

2.1.2 Root exudate preparation

Root exudates for induction of potato cyst nematode hatch were prepared from tomato or potato plant roots. Firstly, four weeks old plants were removed from sand:loam and washed

thoroughly under tap water to remove the soil. The plants were then placed in a large beaker with the roots submerged in sterilized tap water overnight. The roots were blotted dry and weighed the following day then final volume of water was adjusted to achieve an exudate concentration of 80 g root/L. The exudates were filter sterilized using a 0.22 µm syringe filter and stored at 4°C until further use.

2.1.3 Nematode maintenance and extraction

2.1.3.1 Cyst nematodes (*Heterodera schachtii* and *Globodera pallida*)

Independent stocks for *G. pallida* were maintained by growing a susceptible potato cultivar (Désirée) in 18 cm diameter pots of 50:50 sand:loam soil infested with *G. pallida* cysts to provide approximately 300 eggs/g soil. *Heterodera schachtii* were maintained by planting 4 weeks-old cabbage plants (*Brassica oleracea var. Primo II*) in sand: loam (50:50 mix) containing *H. schachtii* cysts to provide approximately 20 eggs/g soil. In both cases plants were allowed to grow for 2-3 months. Damp soil containing cysts of *H. schachtii* and dry soil containing *G. pallida* cysts were then stored at 4^{o}C. Cysts were separated from soil using the Fenwick canning method (Fenwick, 1940), where soil containing cysts was washed into a Fenwick can through a wide meshed sieve. Heavy soil sank to the bottom whereas lighter cysts floated to the top, then those were washed over the edge of the can and collected on a fine-meshed sieve (250 µm). Debris on the sieve, including cysts, was then transferred in water to a sealed funnel containing a fast-flow filter paper. Cysts remained on the surface of the water and a drop of detergent was added to disrupt surface tension and encourage the cysts to move to the edges. The clamp sealing the funnel outlet was released and water flowed out of the funnel, leaving cysts (and other floating debris) on the filter paper at the previous water line. Then cysts were collected from the filter paper into a 1.5 ml Eppendorf tube observing under a stereo-binocular microscope.

Cysts were then surface sterilised using 0.1% chlorhexidine digluconate, 0.5 mg/ml CTAB solution for 30 minutes followed by three washes with sterile ELGA water containing 0.01% Tween-20. Cysts were transferred to 3 mM ZnCl2 solution (for *H. schachtii*) or potato root exudate (for *G. pallida*) in a small Petri dish for inducing hatching of J2s. Every 2-3 days hatched J2s were collected into a 15 ml polystyrene tube and stored at 11^{o}C, and fresh hatching solution added to the cysts.

2.1.3.2 Root Knot Nematode (*Meloidogyne incognita*)

Meloidogyne incognita population VW6 were cultured on tomato plants 'Ailsa craig' with a rolling stock renewed every two weeks. Four weeks old plants were transferred to 18 cm pots containing potting compost (Petersfield Growing Mediums W E Hewitt & Son Ltd, UK), which had been mixed with 3-4 lengths of chopped, infected roots from an 8-weeks post-infection plant that were well galled with egg masses on the surface. Newly infected plants were generally grown for a further eight weeks until used for collection of eggs/J2s for experiments or the roots used for infection of new stock plants.

J2s of *Meloidogyne incognita* were extracted from tomato roots that had been infected for a duration of eight weeks. The roots were severed from the above-ground parts of the plants, cleaned, and placed onto a nylon mesh covered with tissue paper, positioned above a funnel. This setup was placed inside a misting chamber where water was sprayed for five minutes every hour, which facilitated the hatching of nematodes and the migration of J2s out of the roots. The nematodes then moved down through the funnel into 50 ml collection tubes. Due to the slow water flow, the J2s settled at the bottom of the tubes. Nematodes were collected daily, rinsed with sterile tap water, and stored at 11°C until further use.

For collecting eggs or clean J2s for tissue culture infections, an alternate method was carried out. Infected tomato plant roots (after 8 weeks of infection) were washed, cleaned, and cut into small pieces (2-3 cm). Then the pieces were shaken for 2 minutes in 1% sodium hypochlorite solution with a view to dissolving the gelatinous egg mass matrix and releasing the eggs. The solution containing eggs was poured into nested sieves of 150, 65 and 25 µm pore size and thoroughly washed with tap water to remove the dirt. Finally, the eggs including any fine debris were washed from the 25 µm meshed sieve into a 50 ml tube. The tube was centrifuged at 3000 rpm for 10 minutes to obtain a pellet, which was then resuspended in 40% sucrose solution. Three to five mls of tap water were carefully layered on top of the sucrose solution. The solution was centrifuged again under the same conditions to pellet the debris and leave the eggs at the sucrose:water interface. The eggs were collected with a glass Pasteur pipette and immediately transferred into a large volume of water to dilute the sucrose solution. Finally, the eggs were transferred into a 15 ml polystyrene tube after washing and concentration on a 25 µm mesh sieve. Eggs were then surface sterilised using 0.1% chlorhexidine digluconate, 0.5 mg/ml CTAB solution and 0.01% Tween-20 solution for 30 minutes followed by three washes with sterile tap water. These eggs were either kept at 11°C for use in infection assays or placed on a 20 µm nylon mesh in

a sterilised hatching jar containing sterile ELGA water and incubated at 25 °C in darkness for collecting J2s.

2.2 Staining of nematode, AMF and plant material

2.2.1 Acid fuchsin staining of nematodes

The above ground plant tissues were cut off and the root system was washed to remove soil. Then roots were soaked in diluted sodium hypochlorite solution (1 % available chlorine) for 2 minutes. Roots were washed for approximately 5 minutes with 3 changes of tap water (this was done in beakers or Petri dishes depending on the size of the root system). Finally, roots were transferred to a beaker of boiling acid fuchsin stain. This should be just simmering and not boiling vigorously. When necessary, the Bunsen burner was turned off while the roots were in the beaker and then relit to get the stain back to boiling point for the next set of roots. 1x stain diluted from 10x stock was used (10x stock is 0.35 % acid fuchsin made up in 25 % glacial acetic acid). Roots were left in the hot stain for 2 minutes. Subsequently, roots were rinsed briefly (a few seconds) in tap water and placed in a petri dish containing acidified glycerol (1 drop of glacial acetic acid per 100 ml glycerol). To more easily visualise nematodes, roots were then incubated at 65^{o}C overnight to remove excess stain from the root tissue. Root lengths were examined using a Leica M165C stereo-binocular microscope and images were captured with a Q IMAGING camera and QCapture Pro 6.0 software.

2.2.2 Ink-vinegar staining of AMF

Roots were cut into short lengths of 1-1.5 cm and placed into embedding cassettes. The cassettes were transferred to 10% KOH (w/v) and moved into a 65°C oven for 30 minutes. before being removed from the KOH and rinsed in water three times. The cassettes were then submerged in ink + vinegar stain (5 % Pelikan Brilliant Black ink, 5 % acetic acid, 90 % d.H2O) (Vierheilig et al., 1998) and incubated at room temperature for approximately 20 minutes. After removing from the stain, cassettes were shaken to remove excess ink then immersed and shaken briefly in 1% acetic acid to rinse the excess stain out. The roots were kept in fresh 1% acetic acid overnight to allow stain to diffuse. The cassettes were removed from the acetic acid and shaken/blotted dry. All the roots were removed with forceps and placed into the middle of a cutting tile. A few drops of 50% glycerol were added followed by teasing the roots apart with forceps. Around 10-15 lengths of root were selected. Roots were dab dried and transferred to a microscope slide, aligning them straight on the slide. A few

drops of PVLG mounting medium (Distilled water:100 ml, Lactic acid: 100 ml, Glycerol: 10 ml and Polyvinyl alcohol: 16.6 g) were added and a coverslip was gently added for mounting. Then the slides were incubated at 65°C overnight. Finally, slides were observed using a microscope (ZEISS AX10) and images were taken using an Axiocam 305 colour camera and ZEN 2.6 (blue edition) software.

2.2.3 DAB staining

Nematode-infected (4 DAI and 7 DAI) plants were removed from media plates, the roots were separated from the plants, and placed into 12-well plates, with a single root system in each well. DAB (3,3'- diaminobenzidine tetrahydrochloride salt) solution (1mg/ml in water) was prepared by adding HCl to solubilize DAB (usually takes 4/5 hours) after dissolving, the pH was adjusted to 5.5. Then DAB solution was added to the each well to submerge the whole roots. The plates, without their lids, were quickly placed in a vacuum-infiltration chamber for 5 minutes. The lids were replaced and the plates incubated on an orbital shaker for 4 hours at room temperature after wrapping with aluminium foil. After incubation, the stained roots were repeatedly treated with a fresh bleaching solution (ethanol: acetic acid: glycerol = 3:1:1) by floating the plate in a 95°C water bath for 20 minutes. The roots were then either stored at 4°C or visualised immediately after transfer to fresh bleaching solution using a Leica M165C stereo-binocular microscope. Images were captured as described in **section 2.2.1**.

2.3 Media and antibiotics

Standard bacterial and plant growth media for culture maintenance were prepared as described below and autoclaved at 121°C for 20 minutes.

2.3.1 Luria-Bertani (LB) Growth Medium

LB broth was made by dissolving tryptone (10 g/l), NaCl (5 g/l), yeast extract (5 g/l) in ELGA water. 1 % bacteriological agar (w/v) was added to make solid media plates.

2.3.2 Murashige and Skoog (MS) Media

MS 30 media was prepared by dissolving 4.30 g of Murashige and Skoog medium with vitamins, 30 g of sucrose, 5.75 g of plant agar in 1 litre of ELGA water and the pH was adjusted

to 5.8 with KOH. For preparing MS20 and ½ MS10 media, the MS and sucrose were adjusted accordingly.

2.3.3 Antibiotic solutions

Antibiotic stock solutions were prepared, filter sterilized and stored at –20 °C for future use.

Table 2.1. List of antibiotics used

Antibiotic	Solvent	Stock solution	Working concentration
Spectinomycin	Deionised water	100 mg/ml	100 µg/ml
Rifampicin	Ethanol	10 mg/ml	50 µg/ml
Kanamycin	Deionised water	50 mg/ml	50 µg/ml
Hygromycin	Deionised water	50 mg/ml	20 µg/ml
Ampicillin	Deionised water	100 mg/ml	100 µg/ml
Cefotaxime	Deionised water	200 mg/ml	500 µg/ml

2.4 General molecular techniques

2.4.1 Plant DNA extraction

Leaf tissues from different plant samples (100 mg/sample) were collected in 1.5 ml microcentrifuge tubes, snap frozen in liquid nitrogen and stored at -80°C. Genomic DNA from plant leaves was extracted using the E.Z.N.A.® Plant DNA Kit- Short Protocol (Omega Bio-Tek, USA) following the manufacturer's instructions. Leaf tissues were ground using disposable pestles after dipping the tubes carefully in liquid nitrogen. The sample was thoroughly vortexed after adding P1 Buffer to disperse all the clumps. After an incubation period of 5 minutes at 65°C, P2 buffer was added, vortexed and centrifuged for 10 minutes to get a clear lysate solution. The lysate was then measured and one-half volume of P3 Buffer and one volume of ethanol (100%) was added and vortexed to obtain a homogenous solution. The sample was passed through a HiBind® DNA Mini Column to bind DNA to the surface of the membrane. Subsequently the DNA was washed twice using DNA wash buffer to remove the impurities. The first elution of DNA was done in 50 µl of Elution Buffer and second elution was done in 100 µl of Elution Buffer to maximize the recovery of DNA from column matrix. All the eluted DNA was stored at -20 °C for future use.

2.4.2 Total RNA extraction

RNA from plant leaves were extracted using E.Z.N.A.® Plant RNA Kit (Omega Bio-Tek, USA) according to the manufacturer's instructions. The stored leaf samples as described in section 2.4.1 were ground using disposable pestles after dipping the tubes carefully in liquid nitrogen. The samples were completely suspended in RB buffer mixed with 2-mercaptoethanol. The lysate was passed through a Homogenizer Mini Column to remove the debris. Cleared lysate was vortexed with 70% ethanol and passed through a HiBind® RNA Mini Column that bound RNA with the surface of the membrane. The RNA was then washed with RNA Wash Buffer I, followed by washing with RNA Wash Buffer II to remove the impurities. The RNA was eluted by adding 50 µl of Nuclease-free-Water and stored at -80 °C until further use.

2.4.3 cDNA synthesis

cDNA synthesis was carried out on extracted RNA using the iSCRIPT™ cDNA Synthesis Kit (Bio-Rad, United Kingdom) following the manufacturer's protocol. The reaction mixture was prepared in a final volume of 20 µl, comprising 4 µl of 5x iScript Reaction Mix, 1 µl iScript Reverse Transcriptase, 1 µg RNA template and total volume adjusted with nuclease–free water. The mixture was gently pipetted and centrifuged to ensure homogeneity. The reaction was subjected to 25°C for priming (5 minutes), 46°C for reverse transcription (20 minutes), 95°C for reverse transcriptase inactivation (1 minute) and final hold at 4°C.

2.4.4 Estimation of DNA/RNA concentration

A NanoDrop Lite Spectrophotometer (Thermoscientific™) was used to determine nucleic acid concentration of DNA or RNA, together with an assessment of purity via 260/280 nm and 260/230 nm absorbance ratios

2.4.5 Polymerase chain reaction (PCR)

cDNA, genomic DNA or plasmid DNA was used as a template to amplify the genes of interest throughout the experiments. Different types of DNA polymerase (listed in Table 2.2) were used based on the necessity and required fidelity of the experiments. PCRs were carried out following the conditions and guidelines of the manufacturers (Table 2.2).

Table 2.2. Lists of DNA polymerase and conditions of PCR cycles

DNA Polymerase	Step	Temperature	Time	Cycles
Phusion™ high-fidelity DNA polymerase (New England Biolabs)	Initial denaturation	98°C	30 s	1
	Denaturation	98°C	5-10 s	25-35
	Primer annealing	45-72°C (Primer specific)	10-30 s	
	Extension	72°C	15-30 s/kb	
	Final extension	72°C	5-10 min	1
	Hold	4-10°C	∞	∞
MyTaq™ RedMix (Meridian Bioscience, USA)	Initial denaturation	95°C	2 min	1
	Denaturation	95°C	15 s	25-35
	Primer annealing	55°C	15 s	
	Extension	72°C	10 s	
	Final extension	72°C	5-10 min	1
	Hold	4-10°C	∞	∞
OneTaq® (New England Biolabs)	Initial denaturation	94°C	30 s or 3 min for colony PCRs	1
	Denaturation	94°C	30 s	30
	Primer annealing	45-68°C (Primer specific)	30 s	
	Extension	68°C	1 min/kb	
	Final extension	68°C	5-10 min	1
	Hold	4-10°C	∞	∞

2.4.6 Agarose gel electrophoresis

DNA fragments were separated by electrophoresis to determine the specific size of the amplified or digested DNA. A 1% (w/v) agarose gel was prepared by dissolving agarose in 1x TAE buffer (40 mM Tris; 20 mM Acetate; 1 mM EDTA) by heating in a microwave oven. After the gel was cooled, 3 µl GelRed (1: 40,000) was added, and the solution was poured into a gel casting tray with a comb to solidify. Once the gel had set, the comb was carefully removed, and the gel was placed in an electrophoresis chamber filled with 1x TAE buffer. DNA samples were mixed with a loading dye and carefully pipetted into the wells alongside

1 kb DNA ladder (Bioline, UK). The gel was electrophoresed at 90V for approximately 45-60 minutes until the dye migrated an appropriate distance. Following electrophoresis, the gel was visualized on a UV transilluminator to assess DNA band patterns and fragment sizes.

2.4.7 Purification of PCR products

DNA fragments corresponding to the anticipated size of the target genes were isolated from the remaining portion of successfully amplified PCR reactions using a E.Z.N.A® Cycle Pure Kit (Omega Bio-Tek, USA) following the manufacturer's protocol. Firstly, CP buffer (4x reaction volume) was mixed with the PCR product, which was then passed through a HiBind® DNA Column to bind DNA. The bound DNA was washed with DNA wash buffer and finally, elution buffer (30-50 µl) was added to elute the purified DNA into a clean microcentrifuge tube.

If the amplified DNA was at low concentration, the E.Z.N.A® MicroElute Cycle Pure Kit (Omega Bio-Tek, USA) that allowed a final elution volume of 15 µl was used following the same protocol.

When non-specific DNA fragments were present alongside the amplification product of interest, gel extraction was conducted to purify the expected DNA fragment, following the guidelines of the E.Z.N.A® Gel Extraction Kit (Omega Bio-Tek, USA). The target DNA was cut from the gel with a scalpel and transferred to a clean microcentrifuge tube. It was then incubated with a similar volume of binding buffer (XP2) at 60°C until completely melted. After vortexing the solution was passed through a MicroElute® LE DNA Column to bind DNA. The DNA was eluted using 15 µl of elution buffer following washes with DNA wash buffer.

In all cases DNA was stored at -20°C until further use.

2.5 Molecular Cloning Techniques

2.5.1 Transformation of *Escherichia coli* (*E. coli*) competent cells

Escherichia coli competent cells (DH5α strain and Stellar HST08 strain) were transformed following the manufacturer's guidelines (Invitrogen™ One Shot™ Top 10, and Takara Bio Inc., respectively). For transformation, 1 µl of plasmid DNA was added to 100 µl of competent cells and placed on ice for 30 minutes followed by 30 seconds (for Stellar cells, 1 minute) incubation at 42°C in a water bath. Then the cells were put back on ice for 2 minutes. After that pre-warmed 1ml LB (90 µl SOC medium for Stellar cells) was added and the cells

incubated with shaking (225 rpm) at 37°C for 1 hour. Transformed cells were plated onto LB agar plates with selective antibiotic, then incubated overnight at 37°C.

2.5.2 Transformation of competent Agrobacterium cells

2.5.2.1 Preparation of competent Agrobacterium cells

A 5 ml culture of *Agrobacterium tumefaciens* (LBA4404 or GV3101:pMP90) inoculated from a single colony in LB medium containing rifampicin was grown at 28°C overnight, with shaking at 200 rpm. Then a 2 ml aliquot of the overnight culture was added to 50 ml LB medium + rifampicin in a 250 ml flask and growth continued at 28°C until the OD_{600} reached 0.5. The cells were then chilled on ice for 15 mins, pelleted at 4000 rpm at 4°C for 5 minutes after dividing between two centrifuge tubes (30 ml). The culture supernatant was discarded, and the cells gently resuspended in 5 ml (total) of ice cold 20 mM $CaCl_2$ then centrifuged as before. The supernatant was removed, and the pellet gently resuspended in 1.0 ml (total) of ice cold 20 mM $CaCl_2$. after Cells were divided into 100-200 µl aliquots, flash-frozen in liquid nitrogen and stored at -70°C until required.

2.5.2.2 Transformation of Agrobacterium competent cells

Plasmid DNAs were introduced into *Agrobacterium tumefaciens* strain GV3101, which harbours helper plasmid pBBR1MCS5-VIRG-N54D (encoding mutated *virG* gene, $virG^{N54D}$) (van der Fits et al., 2000). The freeze thaw method was used for transforming the Agrobacterium (Xu and Qingshun, 2008).

A 200 µl aliquot of frozen cells was placed on ice. 1-2 µl of plasmid DNA (eg. 35S: RUBY) was added to the cells as they started to thaw. The cells were allowed to thaw on ice for 5 mins, flicked gently to mix a couple of times then transferred to a 37°C water bath for 5 mins to allow for complete thawing and heat shock. The tube was flicked once or twice whilst it was in the water bath. 1 ml of LB medium was immediately added to the cells, which were transferred to a 50 ml tube and incubated at 28°C with shaking at 200 rpm for at least 4 hours. 150 µl cells and the remaining cells (spin at 3000 rpm for 4 mins, remove supernatant and resuspend cells, put all onto one plate) were transferred onto selective LB agar plates containing rifampicin and selective antibiotic, then incubated at 28°C for 48-72 hours. Individual colonies were then restreaked onto fresh selection plates with selective antibiotic and grown again at 28°C for 24-48 hrs. To confirm the presence of the introduced plasmid, colony PCR was performed (**described in 2.5.3**).

2.5.3 Colony PCRs

To screen for the presence of plasmids containing target genes in transformed *Agrobacterium* and *E. coli* cells, colony PCRs were performed by suspending a single colony in 100 or 50 µl of sterile ELGA water. The suspension was boiled at 95°C for 5 minutes to lyse the cells and release the DNA. 1or 2 µl of the suspension was used as DNA template in a PCR. An alternative method was also employed to achieve complete bacterial cell lysis, where PCR master mix and DNA template were incubated in a thermocycler at 99°C for 5 minutes after mixing, prior to initiating the PCR programme. For colony PCR, MyTaq™ RedMix (Meridian Bioscience, USA) or OneTaq® (New England Biolabs) was used as per the conditions described in section **2.4.5.**

2.5.4 DNA minipreps

Transformed *E. coli* (**described in 2.5.1**) harbouring the desired construct was used to isolate plasmid DNA (minipreps) according to the protocol of the E.Z.N.A.® Plasmid DNA Mini Kit (Omega Bio-Tek, USA). For this, 5 ml overnight culture was grown from a single colony in LB broth containing selective antibiotic at 37°C with continuous shaking (225 rpm). The bacterial cells were pelleted by centrifugation at 12200 rpm and then sequentially suspended in Solution I followed by Solution II and Solution III to facilitate cell lysis and precipitation of cellular components. The debris from the cells was pelleted by centrifuging at maximum speed and the resulting supernatant with plasmid DNA was loaded onto a HiBind® Mini Column. The column was washed a number of times with the provided wash buffers to remove impurities and finally DNA was eluted with 30 µl elution buffer and stored at -20 °C for subsequent use.

2.5.5 Preparative and qualitative restriction digests

Preparative restriction digests were performed before ligations to cut the plasmid DNA ready to accept an insert. Qualitative digests were performed to assess the correct restriction digestion pattern ensuring successful cloning of desired insert following plasmid DNA minipreps. Generally, a 20 µl digest reaction (unless stated) was prepared based on the specific requirements of the experiment. Different restriction enzymes were selected to achieve precise cleavage at the target sites, ensuring optimal fragment generation for subsequent analysis and applications. The specific composition of the reaction mixture,

including the choice of restriction enzyme and buffer conditions will be discussed in detail in Chapter 4.

Digest reactions were incubated at 37°C for 2 hours. The samples were then subjected to agarose gel (1%) electrophoresis (**section 2.4.6**) after adding 6x loading dye to assess digestion efficiency and verify fragment size.

2.5.6 Ligations

Ligation was conducted to join the digested DNA fragments using T4 DNA ligase. The ligation reaction mixture was prepared in a total volume of 10 µl with T4 DNA ligase (1 µl), 10x ligation buffer (1 µl) and an appropriate amount of DNA fragment and vector. The molar ratio of insert to vector was optimized to facilitate efficient ligation. The reaction was incubated at room temperature for 1 hour then kept at 4°C overnight. Appropriate amounts of ligation reaction were used to transform the *E. coli* competent cell as described in **section 2.5.1**.

2.5.7 Sanger Sequencing

The plasmid DNA minipreps that were judged from restriction digestion to contain the DNA of interest were subjected to Sanger sequencing for verification of successful cloning. The samples were prepared according to the guidelines and sent to Genewiz from Azenta Life Science for sequencing with M13 forward and reverse primers or using additional gene specific primers if a longer insert required complete sequencing.

2.5.8 Arabidopsis transformation by floral dip

Wild type Arabidopsis plants (Col-0) were grown in glass house conditions (22 °C with 16 hours photoperiod) until inflorescence development. The primary inflorescence was removed to encourage multiple secondary inflorescences to maximise the number of buds available for transformation. Transformation was carried out when the majority of the flowers were present as just-opening buds. A single colony of *A. tumefaciens* (GV3101) harbouring the construct of interest was grown in 20 ml LB media with selective antibiotics overnight at 28 °C with continuous shaking at 200 rpm. The 20 ml culture was then transferred to 200 ml LB media with selective antibiotic and grown in similar conditions for 4-5 hours until the OD_{600} reached 0.5-0.8. The cells were pelleted by centrifugation for 10 minutes at 2500 rpm and then resuspended with 200 ml of 5% sucrose solution containing 100 µl Silwet (Lehle Seeds, USA). Arabidopsis inflorescences were dipped into this solution

for 30 seconds with continuous agitation and the plant was laid on a bigger tray under a propagator lid for 24 hours. After that the plant was grown normally by keeping upright in glass house conditions until the collection of transformed seeds.

Chapter 3

Exploring the Potential Utility of the RUBY Reporter System in Plant-Nematode Research

3.1 Introduction

A reporter gene is a heterologous coding sequence engineered to produce a detectable and quantifiable signal, allowing clear distinction from the background of endogenous proteins (Alam and Cook, 1990). Typically, it is fused to a transcriptional regulatory element such as a promoter or enhancer and introduced into cells or organisms to monitor gene activity across specific tissues, developmental stages, or environmental conditions (Wood, 1995; Ghim et al., 2010; Sharifova et al., 2025). Reporters are important tools in plant-nematology research, they are used to investigate early host responses to invasion, nematode activities, identifying affected tissues, timing of cellular events and hormonal roles. They are valuable for understanding the interaction dynamics and for identifying promoters that can drive transgenic defences, either at the feeding site or during initial infection (Gheysen and Mitchum, 2019).

The complex physiological and morphological alterations during the formation of nematode feeding sites involve altered expression of genes in the infected root cell (Gheysen et al., 1996). To monitor these gene expression, cellular and hormonal changes, different types of genetically encoded reporters have been utilized (He et al., 2020). The β-glucuronidase (GUS) reporter has been widely applied in plants (Jefferson et al., 1987) and luciferase is used in both animals and plants (Contag and Bachmann, 2002). Both luciferase and GUS staining require the use of expensive luciferin and X-Gluc substrates, respectively. Moreover, GUS staining is not only invasive but also involves sacrifice of the respective plants whereas luciferase is non-invasive, but a special camera and spraying of the expensive substrate is required and is not feasible for field grown plants. The green fluorescent protein (GFP) and its derivatives such as red fluorescent protein (RFP), yellow fluorescent protein (YFP) and mCherry have been used as reporters for gene expression as well as fusion proteins for subcellular localization (Chalfie et al., 1994; Heim et al., 1995). Fluorescent proteins are

observed under a fluorescent microscope and can be used with live samples, but these reporters are less useful in evaluating naturally growing plants in glasshouse or field conditions. All the traditional reporters have limitations despite having usefulness (He et al., 2020). Therefore, non-invasive reporters that would be cost-effective as well would be tremendously useful for continuous monitoring of gene expression (Jogam et al., 2024).

Plants produce numerous colourful compounds that can also be used as reporters. For instance, anthocyanins show red-blue colours hence, anthocyanin-producing rice plants have been employed to create fascinating patterns. However, anthocyanin synthesis requires numerous enzymes and also varies considerably between different plants (Misyura et al., 2013; Li et al., 2016). Therefore, it is not easy to use anthocyanins as universal visible reporters. Another class of plant natural products, betalains, which are derived from the amino acid tyrosine (Xu et al., 2020; Strack et al., 2003) are responsible for accumulation of the bright red colour in beets, Swiss chard, dragon fruit and other plants. Betalain potentially can be used as a reporter to monitor gene expression and visualize transgenic events. Betalain biosynthesis has been well characterised and needs only three enzymatic reactions to convert tyrosine into betalain (Polturak and Aharoni, 2018). Hence, betalain would be more convenient than other reporters as it is visible to the naked eye without any requirement for special equipment, processing of samples is not necessary, it permits continuous monitoring throughout an organism's life cycle and it is suitable for large plants grown under field conditions. Therefore, a new reporter has been developed that uses three enzymes to convert tyrosine to betalain (He et al., 2020). This can be used to monitor gene expression non-invasively under sterile conditions in plants and was demonstrated to be an effective selection marker for transformation in both Arabidopsis and rice.

Two different approaches have been taken for expression of the multi-step pathway required for betalain synthesis in transgenic plants. Timoneda et al. (2021) developed a construct in which each of the three required genes was controlled by a separate promoter, whereas He et al. (2020) generated a synthetic construct in which the open reading frames of the three genes were joined as a translation fusion by cleavable linker sequences (Figure 3.1). In the second approach, termed 'RUBY', only a single promoter is required to drive betalain synthesis, resulting in a simpler cloning strategy. The multi-promoter approach was

used to generate *N. benthamiana* plants responsive to arbuscular mycorrhizal fungi (AMF) by using promoters for either a phosphate transporter, belonging to the phosphate transporter 1 (PHT1) subfamily (NbPT5b) or a member of the blue copper protein (BCP) family (NbBCP1b). Expression of both the NbPT5b and NbBCP1b genes is induced during symbiosis with AMF *R. irregularis*. When only one of the three genes had the AMF-responsive promoter and the other two had a constitutive promoter, developmental defects were noted in the plants. To avoid these all three betalain biosynthesis genes were subsequently expressed separately under the same AM symbiosis–specific promoter (Timoneda et al., 2021).

Conversely, when all three betalain biosynthesis genes were expressed at the same level from the constitutive CaMV35S promoter as a translational fusion in the RUBY construct, no developmental defects were reported (He et al., 2020). It is possible that the unbalanced expression of the three enzymes in the work of Timoneda et al. may have led to deleterious accumulation of some reaction products, or that the effects on the plant are species dependent.

GUS and GFP have traditionally been the most commonly used reporters in plant nematology research. These reporters have been used to assess the activity of promoters that may direct expression in feeding sites (Lilley et al., 2004; Barthels et al. 1997; Hashmi et al., 1997), or to monitor the plant response to nematode invasion (Guo et al., 2017; Ali and Abbas, 2016). The strong, constitutive cauliflower mosaic virus 35S (CaMV35S) promoter, which is used extensively in plant genetic engineering (Benfey and Chua, 1990), has also been analysed with GUS and GFP reporters. These previous studies revealed some inconsistencies in the apparent activity of the CaMV35S promoter in nematode feeding sites. The down-regulation of a GUS construct under control of CaMV35S promoter was reported in the syncytial feeding cells of cyst nematodes (*Heterodera schachtii*) parasitizing Arabidopsis roots (Goddijn et al., 1993). Significant reduction of GFP levels directed by the CaMV35S promoter was also observed in the syncytial structure of *H. schachtii* females that continued until the final moulting (Urwin et al., 1997a). However, it is not clear if this apparent down-regulation is a consequence of the syncytium becoming more opaque or less accessible to substrates, since transgenic defences that act through the syncytium are highly effective when controlled by

the CaMV35S promoter (Goverse et al., 1998; Ali and Abbas, 2016).

Considering the above aspects, these two contrasting betalain reporter constructs were evaluated in the context of plant-nematode interactions in a quest for an alternative reporter system that can widely be used to screen gene expression continuously and non-invasively as well as cost effectively. Such a system would be a useful tool for the plant nematode community and could facilitate research into plant-nematode interactions.

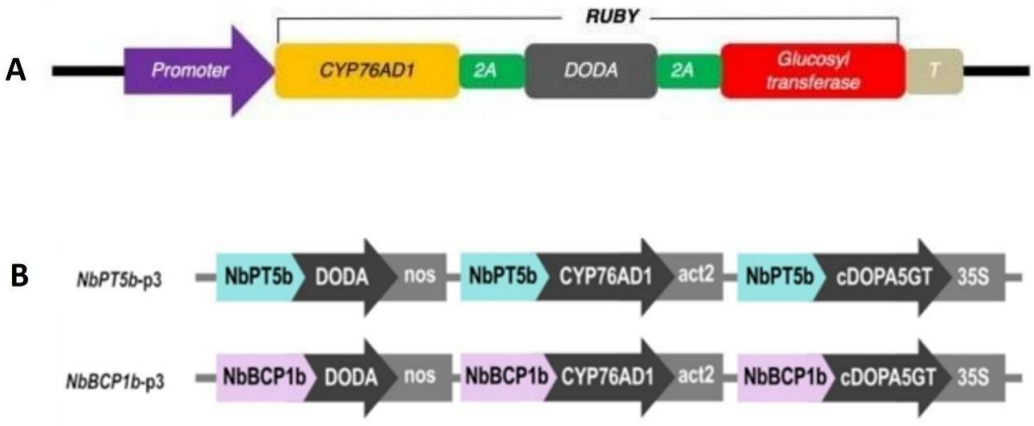

Figure 3.1. Two distinct betalain-based constructs used to express betalain biosynthesis enzymes.

A) RUBY construct developed by He et al. (2020) comprising single promoter to express betalain biosynthesis enzymes (CYP76AD1, DODA, and glucosyl transferase) linked via 2A peptides.

B) Three betalain biosynthesis enzymes have their own promoters to express betalain in the constructs developed by Timoneda et al. (2021).

3.2 Aims

- To generate and characterise Arabidopsis and potato lines transformed with a CaMV35S:RUBY construct.

- To evaluate expression of RUBY in cyst and root-knot nematode feeding sites of potato and Arabidopsis plants.

- To resolve the spatial interaction between root-knot nematode and arbuscular mycorrhizal fungi using the Myco-Red reporter system.

3.3 Materials and Methods

3.3.1 Generation and characterization of CaMV35S:RUBY transgenic Arabidopsis

A 35S:RUBY plasmid (He et al., 2020) was obtained from Addgene, introduced into *A. tumefaciens* GV3101 and used to transform *Arabidopsis thaliana* Col-0 by floral dipping (**section 2.5.8**). Red T1 seeds produced by the transformed plants were selected for characterisation and generation of T2 seeds. Plants grown both in the glasshouse and in tissue culture on ½ MS 10 media were phenotyped for betalain expression both visually and microscopically. The phenotype of tissue culture grown plants was monitored by taking photographs during growth and development using a Leica M165C microscope with Q IMAGING camera and QCapture Pro 6.0 software. The proportions of red and brown seeds produced in the T2 generation were quantified using the formula:

$$\text{Red seeds: Brown Seeds} = \frac{\text{Number of red seeds from 100 seeds}}{\text{Total (100) number of seeds}} : \frac{\text{Number of brown seeds from 100 seeds}}{\text{Total (100) number of seeds}}$$

3.3.2 Determination of silencing of the 35S:RUBY construct in Arabidopsis lines

The silencing of the 35S: RUBY construct in Arabidopsis plants was investigated by conducting reverse transcriptase (RT-) PCR. Genomic DNA and RNA from both green and red leaves from the same plant were extracted using the E.Z.N.A.® Plant DNA Kit and E.Z.N.A.® Plant RNA Kit, respectively (Omega Bio-Tek, USA) according to the manufacturer's instructions (details in **sections 2.4.1 and 2.4.2**), then cDNA synthesis was carried out on extracted RNA using the iSCRIPT™ cDNA Synthesis Kit (Bio-Rad, United Kingdom) following the manufacturer's protocol (described in **section 2.4.3**). PCR amplification of a region of the RUBY coding sequence was performed using MyTaq™ RedMix (Meridian Bioscience, USA) (Table 2.2), with specific primers (RUBY check F: 5'-ATCCTCGCGATCTGGTTCAT-3' and RUBY check R: 3'- GCCGGCTGTAACACTATTCG-5'). The PCR products were analyzed by 1% agarose gel electrophoresis, with a 1 kb DNA ladder (Bioline, UK) used to determine the size of the PCR product.

3.3.3 Generating transgenic potato lines and monitoring the phenotype

Agrobacterium tumefaciens (GV3101:pMP90 strain) culture containing the 35S:RUBY construct was used to transform the wild type potato variety 'Desiree' following the standard procedure for transformation using stem cuttings (**section 4.3.4.1**). Transgenic potato plants producing red pigment were rooted in Murashige and Skoog (MS) medium supplemented with 0.1 mg/L l-naphthalene acetic acid (NAA) before transfer to either compost or a growth pouch system. The phenotype of transgenic RUBY potato plants was monitored both in tissue culture and glasshouse conditions through photographic recording during growth and development. For glasshouse-grown plants, this continued until flowering, tuber production and plant senescence. Mature plant tissues including tubers, stolons, stems, and leaf petioles were detached, transected and images captured using a Leica M165C microscope with QIMAGING camera and QCapture Pro 6.0 software.

3.3.4 Monitoring of nematode-infected RUBY Arabidopsis and potato plants

J2s of *Globodera pallida, Heterodera schachtii* and *M. incognita* were hatched and sterilised following the protocol described in **section 2.1.3**.

3.3.4.1 Infection of RUBY Arabidopsis in tissue culture

A 30 µl aliquot containing approximately 30 sterilised *H. schachtii* J2s was applied to each Arabidopsis plant (2 weeks old) growing on ½ MS10 medium, distributed across multiple sites on the roots. The plates were left to dry before being sealed with micropore tape and placed vertically and grown at 22 °C under a 16-hour light cycle. In the time course of infection with cyst nematode, red plants of Arabidopsis 35S: RUBY-2 plant were visualized for the infection under a microscope without staining. Cyst nematode infection sites encompassing the syncytium were monitored regularly under the microscope during the course of infection and imaged using a Leica M165C microscope with QIMAGING camera and QCapture Pro 6.0 software.

3.3.4.2 Infection of RUBY potato in growth pouches

To evaluate the expression of the RUBY reporter in transgenic potato plants infected with

both root-knot and cyst nematodes, the plants were grown in CYG growth pouches (Mega International) (Figure 3.2). Potato plantlets grown in Magenta pots containing MS30 media at pH 5.7 and at the stage of developing roots were rinsed free of agar, and two plantlets were placed into each growth pouch. Once new root growth had been established after 5 to 7 days, around five root tips/plant were each inoculated with twenty-five J2s of either *M. incognita* or *G. pallida*, which were covered with a 1 cm^2 GF/A filter (Whatman, Maidstone, UK). The filters were subsequently removed after 24 hours. Root-knot nematode infection sites, encompassing galls and giant cells, and cyst nematode infection sites encompassing syncytia were monitored regularly under the microscope during the course of infection from 1 to 45 dpi and imaged using a Leica M165C microscope with QIMAGING camera and QCapture Pro 6.0 software. Transected galls and syncytial regions were mounted on microscope slides and observed under a ZEISS AX10 microscope then imaged using an Axiocam 305 colour camera and ZEN 2.6 (blue edition) software.

3.3.4.3 Monitoring of root-knot and cyst nematode development

The development of the root-knot nematode *M. incognita* and the cyst nematodes *G. pallida* and *H. schachtii* was tracked from the second-stage juvenile (J2) to the mature female stage. Mature females were carefully dissected from their feeding sites and subsequently analysed using a ZEISS AX10 microscope.

3.3.5 Assessment of root knot nematode and cyst nematode access to the vacuole

An Arabidopsis VAC-RFP marker line, expressing red fluorescent protein targeted to the vacuole, was used for investigating whether or not nematodes can access vacuolar contents and therefore ingest RFP. The seeds of the VAC-RFP line were sown in tissue culture (described in **section 3.3.1**). One week after germination the plants were transferred to either square plates containing ½ MS10 medium or growth pouches for *H. schachtii* and *M. incognita* infection respectively (**sections 3.3.4.1 and 3.3.4.2**). Infected plants were monitored regularly under a microscope during the course of infection from 1 to 45 dpi and excised roots and nematodes were imaged using a Zeiss confocal upright LSM 880 microscope with 561 nm excitation wavelength and ZEN 2.6 (blue edition) software.

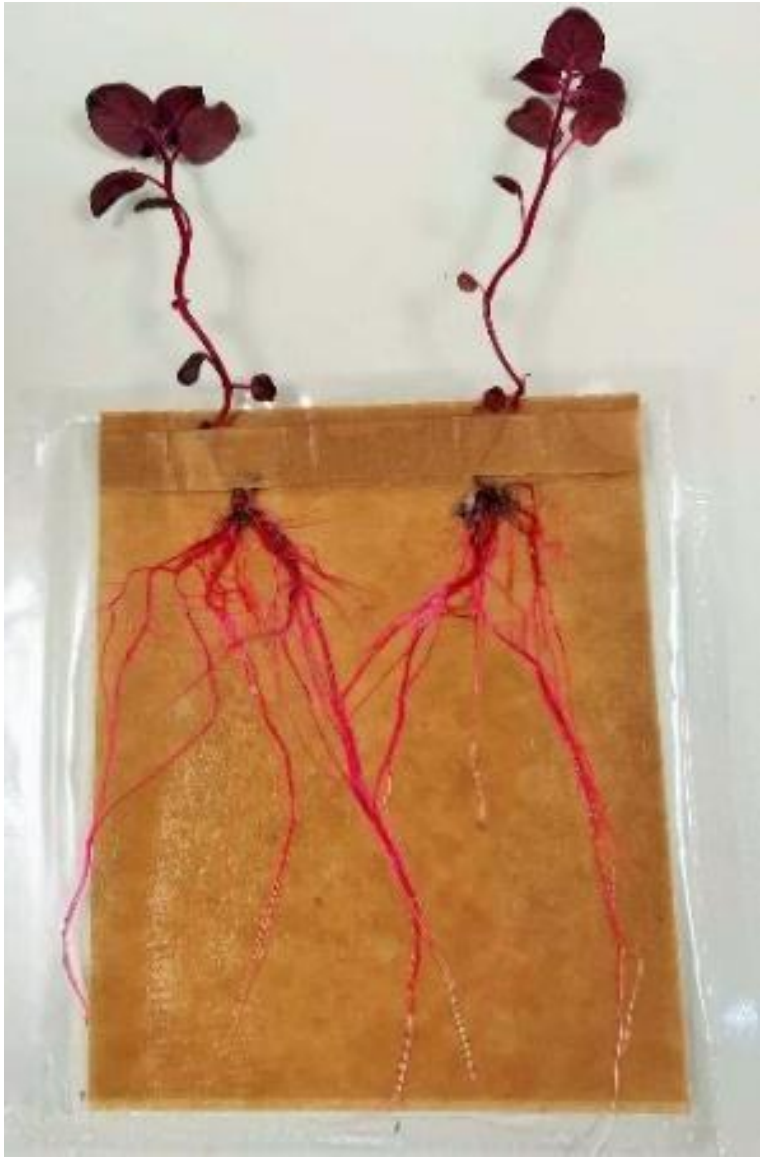

Figure 3.2. 35S:RUBY potato plants in a growth pouch for infection with root-knot and cyst nematodes.

3.3.6 Betalain visualisation and AMF colonisation in *Nicotiana benthamiana* transgenic lines

Seeds of *N. benthamiana* Phosphate transporter (NbPT5b) and Blue copper protein (NbBCP1b) MycoRed reporter lines responding to AMF infection were sown as described in **section 2.1.1.** Then the seedlings were assigned after four weeks to four different treatment combinations (Figure 3.3): A) Seedlings transplanted into 50:50 sand/loam soil inoculated with AMF *R. irregularis* (10 g/kg soil) (PlantWorks Ltd, Sittingbourne, UK), B) Seedlings transplanted into 50:50 sand/loam containing both AMF inoculum and *M. incognita* eggs at the rate of 80 eggs/g of soil, C) Seedlings transplanted into 50:50 sand/loam infected only with *M. incognita* eggs, D) Seedlings transplanted into 50:50 sand/loam containing AMF substrate only (considered as a control). Then 6-8 weeks after inoculation, each plant was collected for visualisation of betalain in the roots, galls produced by the nematode as well as colonization of AMF. Washed roots were examined visually for the presence of galls and red betalain pigment and then photographed. More precise localisation of betalain pigmentation was confirmed by sectioning of red roots, mounting on glass slides in 50% glycerol and capturing images using a ZEISS AX10 microscope, Axiocam 305 colour camera and ZEN 2.6 (blue edition) software. Where appropriate, the presence of nematodes and/or AMF was also confirmed by acid fuchsin and ink-vinegar staining, respectively, as described in **Chapter 2.**

3.3.7 Spatial interaction between AMF and root-knot nematode

Nicotiana benthamiana (BCP1 reporter line) roots infected with both root-knot nematode and AMF were selected for analysis of the spatial interactions of the two symbionts. A total of 20 galled root lengths per plant were randomly selected from three plants**,** considering each plant as a replication. Each segment was examined for the presence of red betalain pigmentation. Similarly, root segments without galls were randomly selected and assessed for red pigmentation. The proportion of root segments showing red pigmentation was then calculated separately for galled and ungalled roots and for those roots the percentage of red coverage was measured in both cases. Pairwise t-tests were performed using Analysis ToolPak, Microsoft Excel 365.

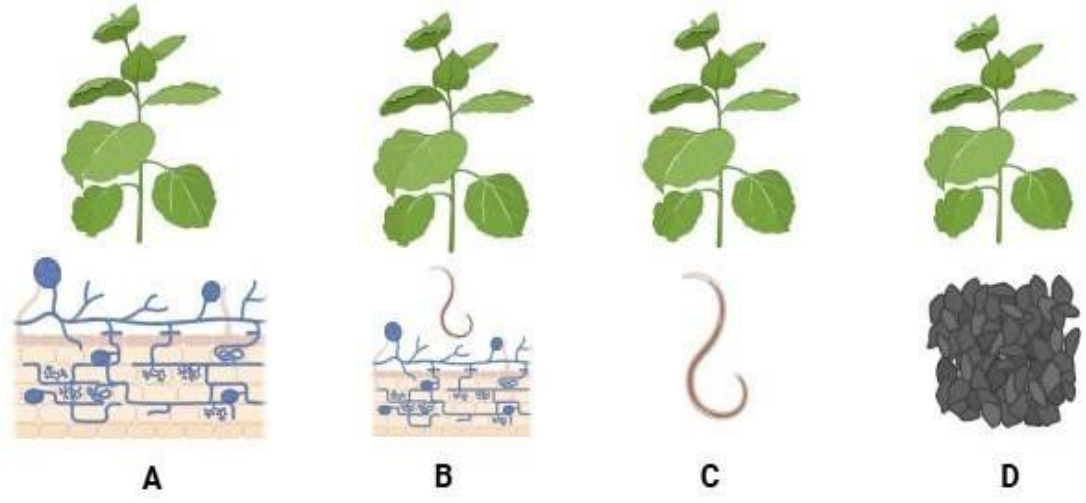

Figure 3.3. Treatment combinations of AMF and nematode infected tobacco lines.

A) Blue copper protein (NbBCP1b) or Phosphate transporter line (NbPT5b) colonised with AMF only;

B) BCP1 or PT5b lines infected with root-knot nematode + AMF;

C) BCP1 or PT5b lines infected with root-knot nematode only;

D) BCP1 or PT5b control plant (inoculated with AMF mock substrate).

3.4 Results

For the first evaluation, a RUBY reporter construct under control of the CaMV35S promoter was used to transform Arabidopsis and potato plants and then expression of the reporter in nematode-infected roots was determined, focusing on the feeding sites. Subsequently, previously characterised Myco-red tobacco (*N. benthamiana*) transgenic lines responding to AMF colonization were investigated to determine if either the NbPT5b promoter or the NbBCP1b respond to nematode infection. The same plants were also used to investigate the spatial interaction between AMF and root-knot nematodes hosted on the same root system.

3.4.1 Expression of CaMV35S:RUBY in transgenic Arabidopsis and potato

The CaMV35S:RUBY construct described by He et al. (2020) was used to transform both Arabidopsis and potato. Red seeds that were produced from the floral dip transformation of Arabidopsis were selected as transgenic T1 lines and were grown in compost to produce T2 seeds. The germination success of the T1 seeds was low and surprisingly, only a few plants that grew from the red F1 seeds had any red tissues. Most of the plants that grew from these red seeds were completely green, however some of the green plants subsequently produced a proportion of red seeds. Initially, we analysed the segregation of seed colour from plants with the different phenotypes. Firstly, we examined the T2 seeds of 35S:RUBY-1 Arabidopsis line where the T1 parent plant was green but produced a mix of brown and red seeds. After counting the seeds, we found the ratio of red : brown seeds was ~ 3:1. Among these red seeds, some darker red seeds were also found under close microscopic observation. Then the seeds were grown separately. Subsequently, after germination it was observed that T2 seeds of 35S:RUBY-1 produced green plants with white roots like wild type plants irrespective of the seed colour. A separate Arabidopsis line (35S:RUBY-2) where the T1 parent plant was red producing some red seeds, also produced both brown and red T2 seeds.

As expected, brown seeds of 35S:RUBY-2 produced green seedlings with white roots, however, red seeds produced two types of plants; green seedlings with white roots and red seedlings with red roots. During growth of the plants, we also noticed that some red seedlings lost red colour in some parts of the plant hence gradually developed a mixture of

red and green leaves and red and white roots as the plant developed (Figure 3.4). Our hypothesis was that the construct is silenced if the very high level of constitutive over-expression becomes detrimental to the plant. Reverse-transcriptase (RT-) PCR was used to determine if gene silencing occurred by testing red and green leaf tissue from the same plant. We found that the RUBY sequence could be amplified from gDNA extracted from both green and red leaves, indicating that the transgene was stably maintained. An identical product was amplified from cDNA prepared from red leaves, but not from cDNA of green leaves or wild type DNA, suggesting that expression was progressively silenced as the plants grew (Figure 3.5).

Three independent transgenic potato lines were produced using the same 35S:RUBY construct and, unlike Arabidopsis, these transformed plants expressed RUBY strongly in all tissues whilst maintained in *in vitro* culture (Figure 3.6). The betalain pigment was present from the earliest stages of callus formation, highlighting its potential use as a visual, antibiotic-free selection marker during the transformation of potato. We had noticed that the silencing of RUBY was more severe when Arabidopsis plants were grown in the glasshouse and so we monitored the phenotype of transformed RUBY potato lines under glasshouse conditions.

Transgenic potato plants of all three lines growing in the glasshouse expressed RUBY in all tissue types throughout the plants' lifecycle (Figure 3.7), maintaining strong betalain (RUBY) pigmentation from early stage to mature stage. This confirmed the constitutive expression of the CaMV35S promoter in mature tissues of glasshouse plants, something that is not easily monitored using a reporter such as GUS (Figure 3.8). Unlike Arabidopsis, no gene silencing was detected in RUBY potato plants.

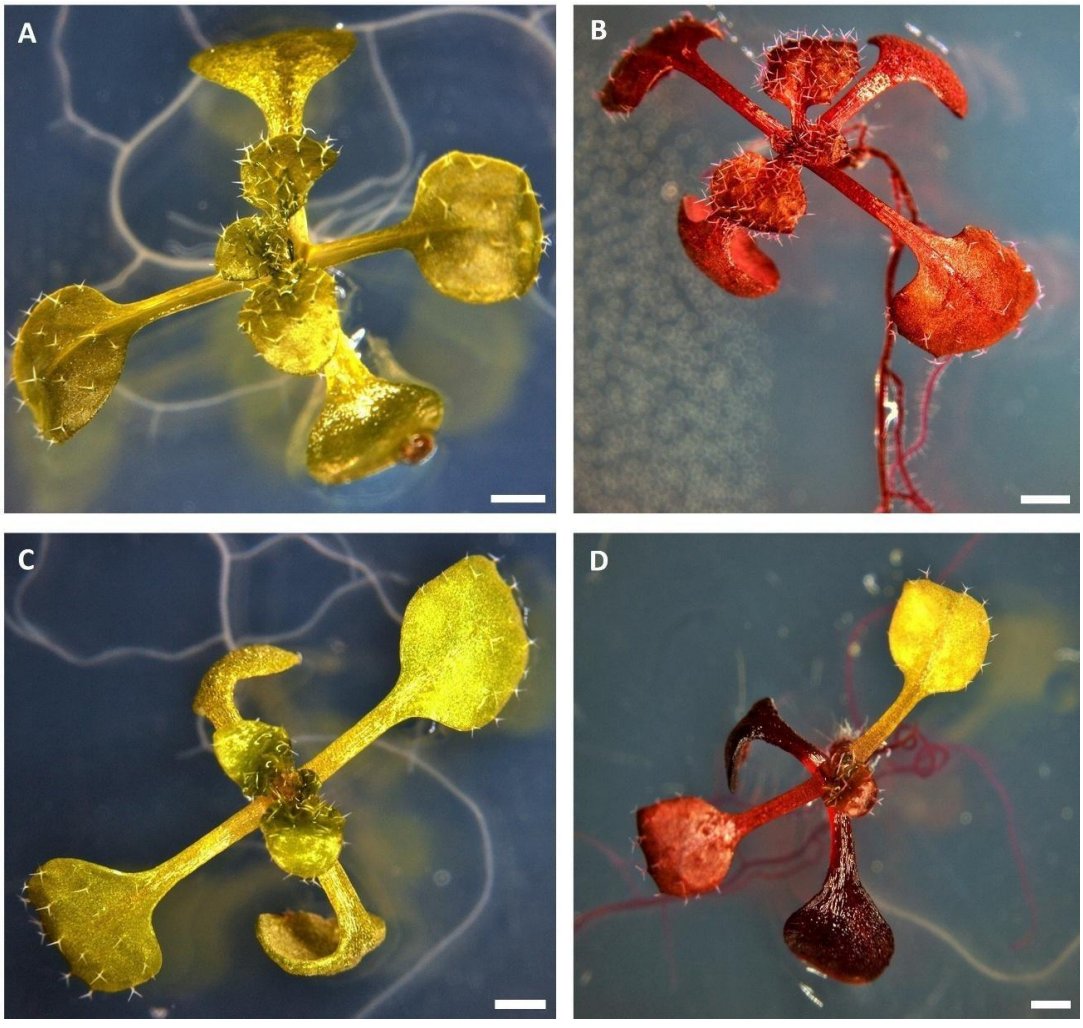

Figure 3.4. Phenotype of Arabidopsis plants produced from Arabidopsis 35S:RUBY-2 T2 seeds.

A) brown seeds of 35S:RUBY-2 produced green plants and white roots;

B) red seeds produced red plants with red roots;

C) red seeds produced green plants with white roots; and

D) red seeds produced partially red plants with the mixture of red and white roots. All the images are shown with a uniform scale bar of 1 mm.

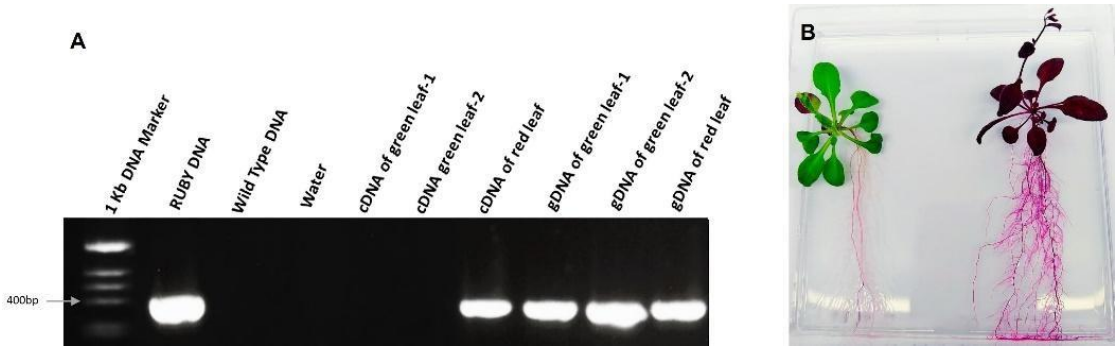

Figure 3.5. CaMV35S: RUBY-2 Arabidopsis plant exhibited progressive gene silencing during developmental growth.

A) RUBY sequence amplification from cDNA and gDNA of red and green leaf tissue from the same Arabidopsis plant (CaMV35S:RUBY 2) representing gene silencing. cDNA of red leaf, gDNA of green leaf-1, gDNA of green leaf-2 and gDNA of red leaf successfully amplified RUBY DNA; While wild type DNA, negative control (water), cDNA of green leaf-1 and cDNA of green leaf-2 did not amplify the RUBY DNA sequence.

B) Arabidopsis plant (left) exhibiting progressive silencing of RUBY expression as the plant grew. Arabidopsis plant (right) continued to exhibit RUBY expression throughout the development.

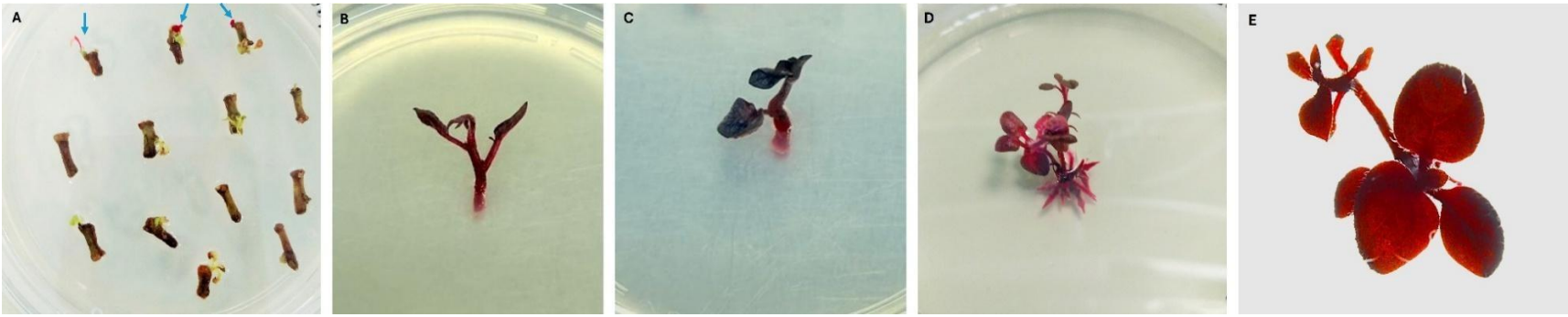

Figure 3.6. Transgenic RUBY potato producing betalain in tissue culture.

A) Red callus formation induced in transgenic RUBY potato, arrows indicate RUBY red callus of potato;

B) RUBY red potato explant on root induction media;

C) RUBY red potato explant developed gradually on root induction media;

D) Transgenic RUBY potato produced roots on root induction media;

E) Transgenic RUBY potato sustained RUBY expression throughout the growth of the plants.

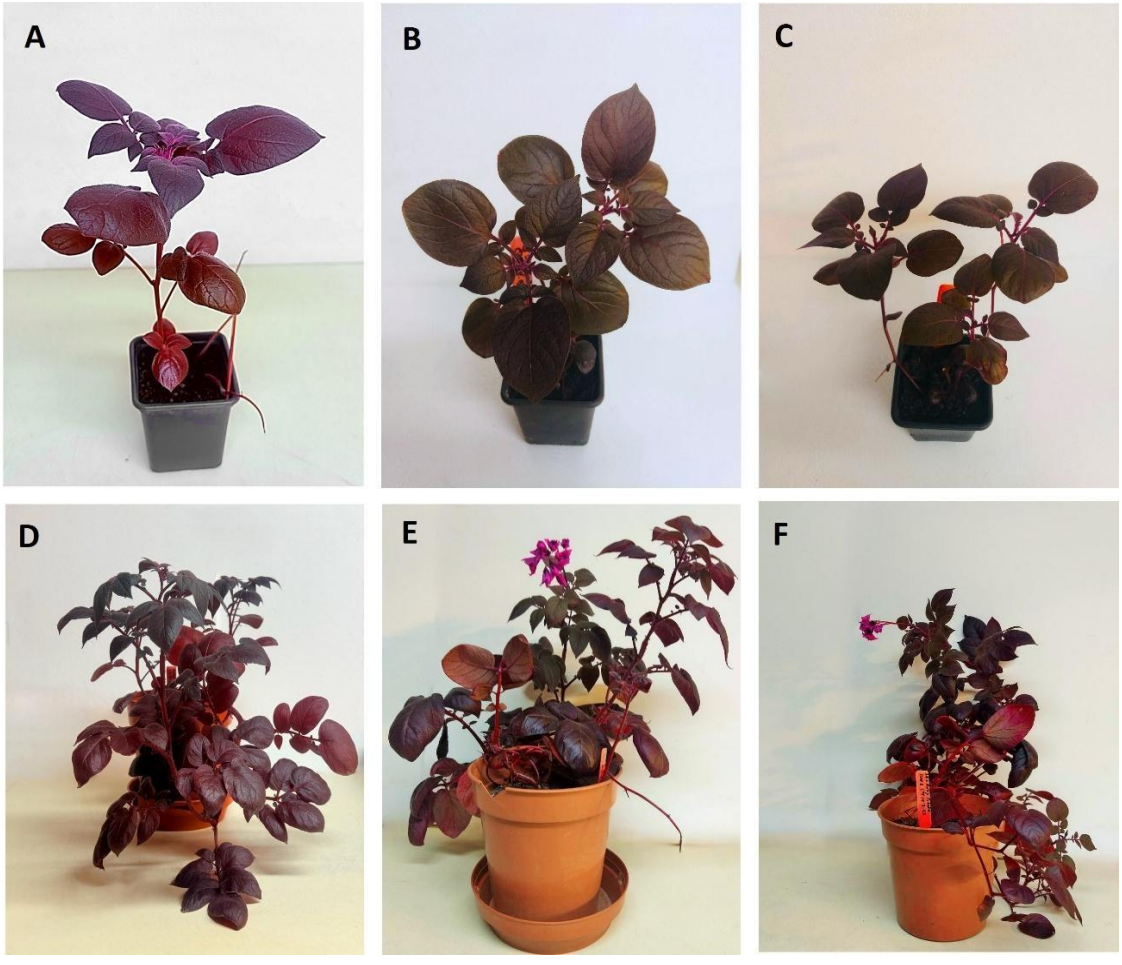

Figure 3.7. Transgenic RUBY potato producing betalain in glasshouse conditions.

A-C) Three potato lines expressed RUBY in glasshouse at early stage;

D-F) Three potato lines sustained RUBY in glasshouse during the mature stage of plant development.

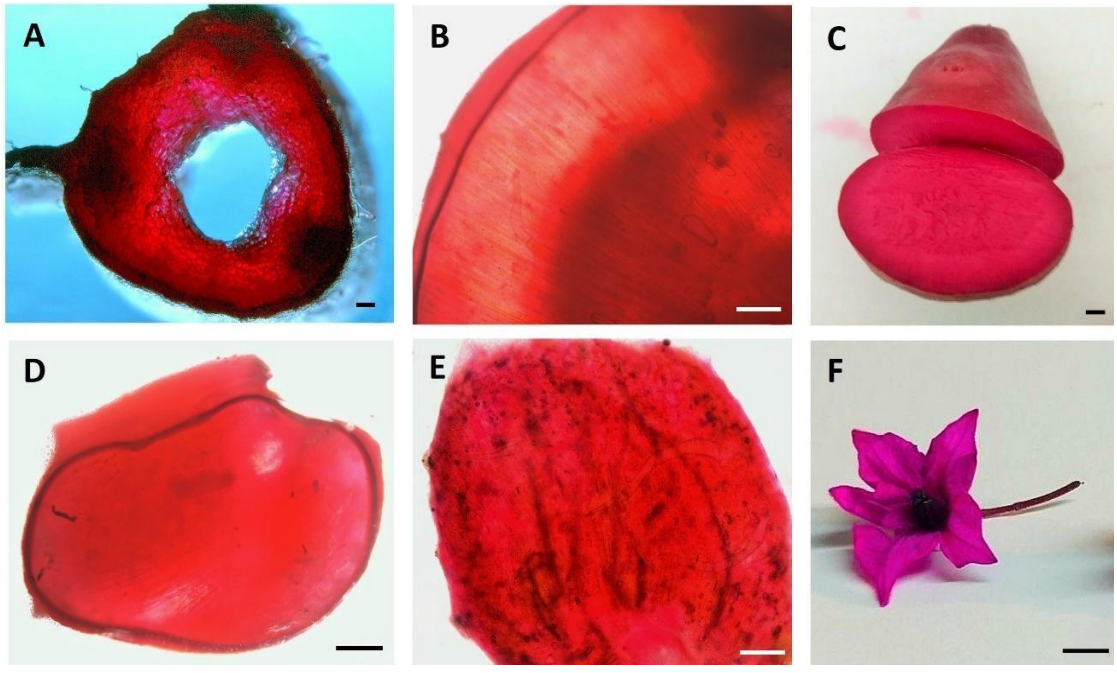

Figure 3.8. Different mature parts and tissues of transgenic potato plants expressed RUBY.

A) Transection of stem cutting; **B)** Transection of leaf petiole; **C)** Potato tuber; **D)** Transection of stolon; **E)** Transection of flower petiole; **F)** Flower of potato plant. Scale bar represents either 200 µm (A, B, D, E) or 1 mm (C, F).

3.4.2 RUBY expression in nematode-infected Arabidopsis and potato plants

Transgenic RUBY Arabidopsis and potato plants were infected with cyst and root-knot nematodes to investigate the RUBY expression in nematode feeding sites. The CaMV35S promoter is commonly used as a constitutive promoter, but its activity often appears reduced in nematode-induced feeding sites when using GUS/GFP reporters. Testing RUBY expression in Arabidopsis and potato could allow us to see whether CaMV35S remains active in these cells, which is critical for transgenic strategies against nematodes. 35S:RUBY-2 T2 Arabidopsis plants with consistent RUBY expression were monitored under the microscope after seven days of infection with *H. schachtii*. As the betalain pigment in the roots was an intense red, it was possible to observe the unstained J2s clearly against the red background without staining the plants. In the time course of infection, the development of J2s into J3 and male or female nematodes was also clearly visible because the red pigmentation did not disappear. Even in the nematode feeding site syncytium, the intense red colour was still apparent (Figure 3.9). We also observed the infected RUBY potato roots under the microscope at different time points of infection with cyst (*G. pallida*) and root-knot (*M. incognita*) nematodes. RUBY expression was again maintained in 35S:RUBY potato roots during the course of infection. Betalain was present in the syncytia during development of cyst nematodes as well as in the giant cells during development of root-knot nematodes (Figure 3.10).

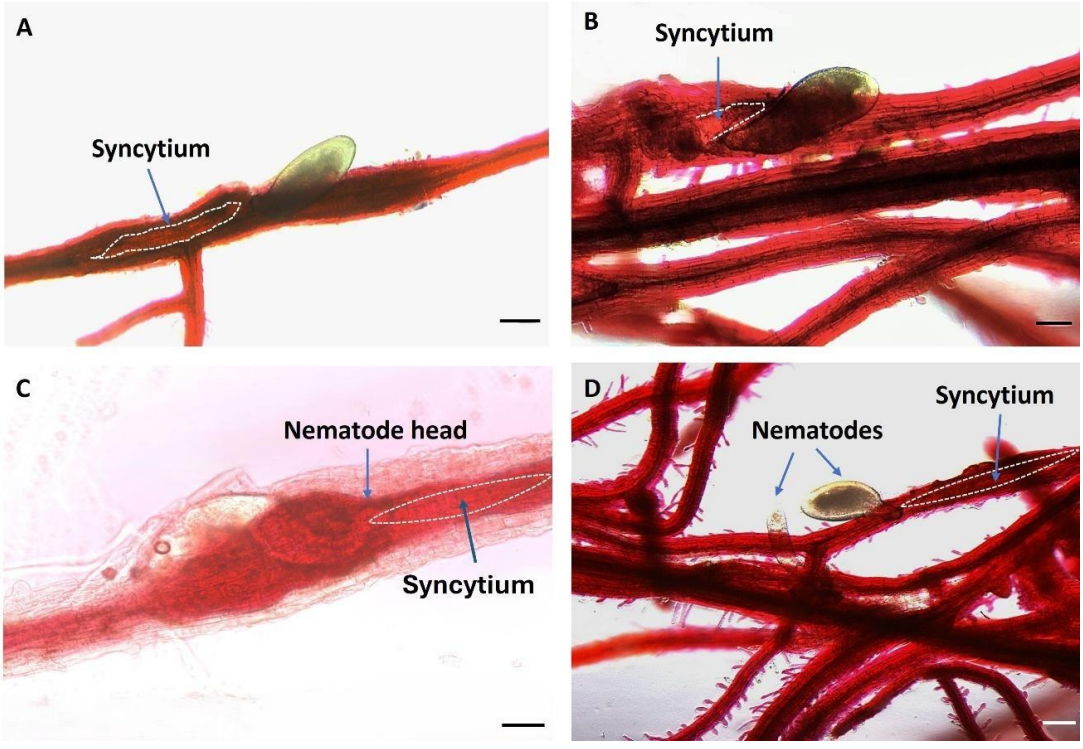

Figure 3.9. Expression of RUBY in cyst nematode (*H. schachtii*) infected Arabidopsis roots.

A-**D)** RUBY expression and betalain accumulation in *H. schachtii* syncytia.

The syncytia are highlighted by white dashed lines. Scale bar denotes 100 µm.

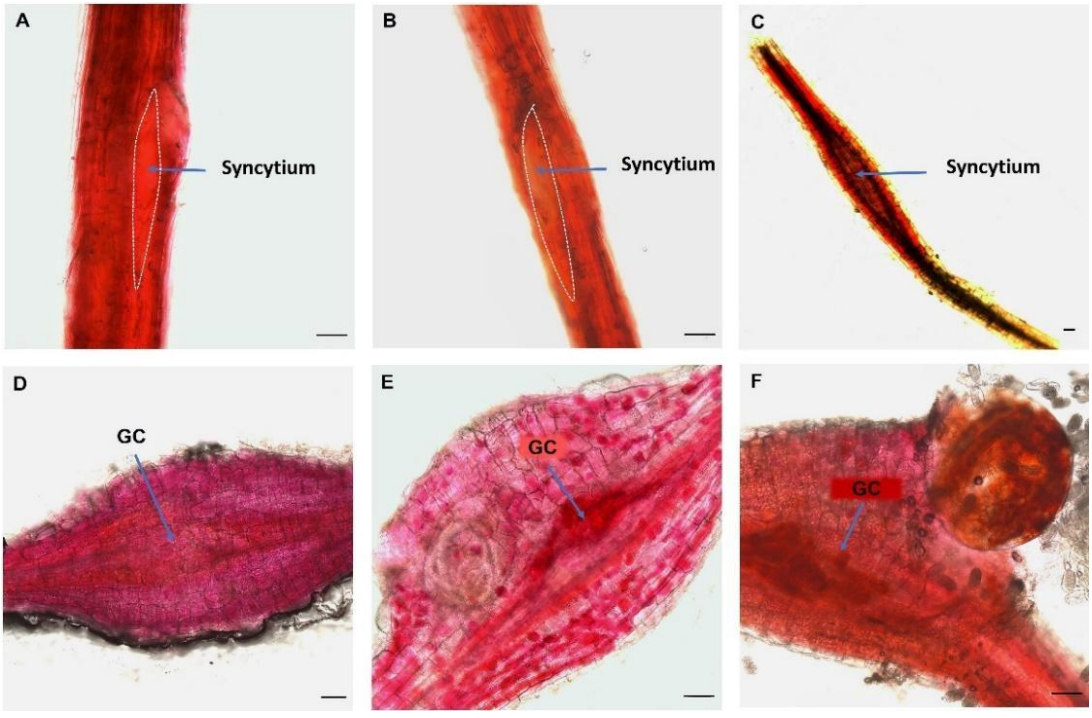

Figure 3.10. Cyst nematode and root-knot nematode infected potato roots express RUBY in nematode feeding sites over time post infection.

(A-C) RUBY expression in cyst nematode syncytia at **(A)** 4 weeks, **(B)** 6 weeks and **(C)** 8 weeks post-infection.

(D-F) RUBY expression in root-knot nematode-induced galls and giant cells at **(D)** 2 weeks, **(E)** 4 weeks and **(F)** 6 weeks post infection. GC = giant cells. Scale bar = 100 µm.

3.4.3 Monitoring of cyst and root-knot nematodes on RUBY Arabidopsis and potato

In addition to monitoring nematode feeding sites, the phenotype of nematodes parasitising RUBY plants was also explored. *Heterodera schachtii* on Arabidopsis roots consistently exhibited a transparent body colour with no visible betalain pigmentation in the nematodes throughout the entire life cycle (J2 to female) (Figure 3.11). No evidence of betalain ingestion or accumulation was observed in the body of *H. schachtii* for more than ten nematodes observed on each of more than two occasions.

Similar to *H. schachtii, G. pallida* individuals also displayed a transparent body phenotype throughout their developmental stages when parasitising potato roots expressing the 35S:RUBY construct (Figure 3.12 A, B and C). The developing females were removed from the roots and then placed on a microscope slide to be examined at higher magnification for additional confirmation that no red betalain pigment was present. The digestive and reproductive tracts were carefully dissected from some females, but both were found to be colourless (Figure 3.12 D).

An interesting and contrasting feature was found for the females of root-knot nematode developing on the 35:RUBY potato roots (Figure 3.13). It was noticed after 13 days of infection that red patches appeared in the young females (Figure 3.13 A). At regular intervals females were then carefully isolated from the galls and observed under a microscope. These red patches were present even at 45 dpi in mature egg-laying females. The digestive tract of developing root- knot nematode females appeared to be red whereas the reproductive tract was transparent and never pigmented. In addition, no betalain was ever observed in the developing eggs (Figure 3.13 D). The betalain pigment was clearly taken up from the giant cells and accumulated in the body of the feeding root-knot nematode female. The ingestion of betalains by cyst or root-knot nematodes has not previously been documented and the differences between the two genera are intriguing. Further investigations could explore the specific reason for the contrasting behaviour of both nematodes.

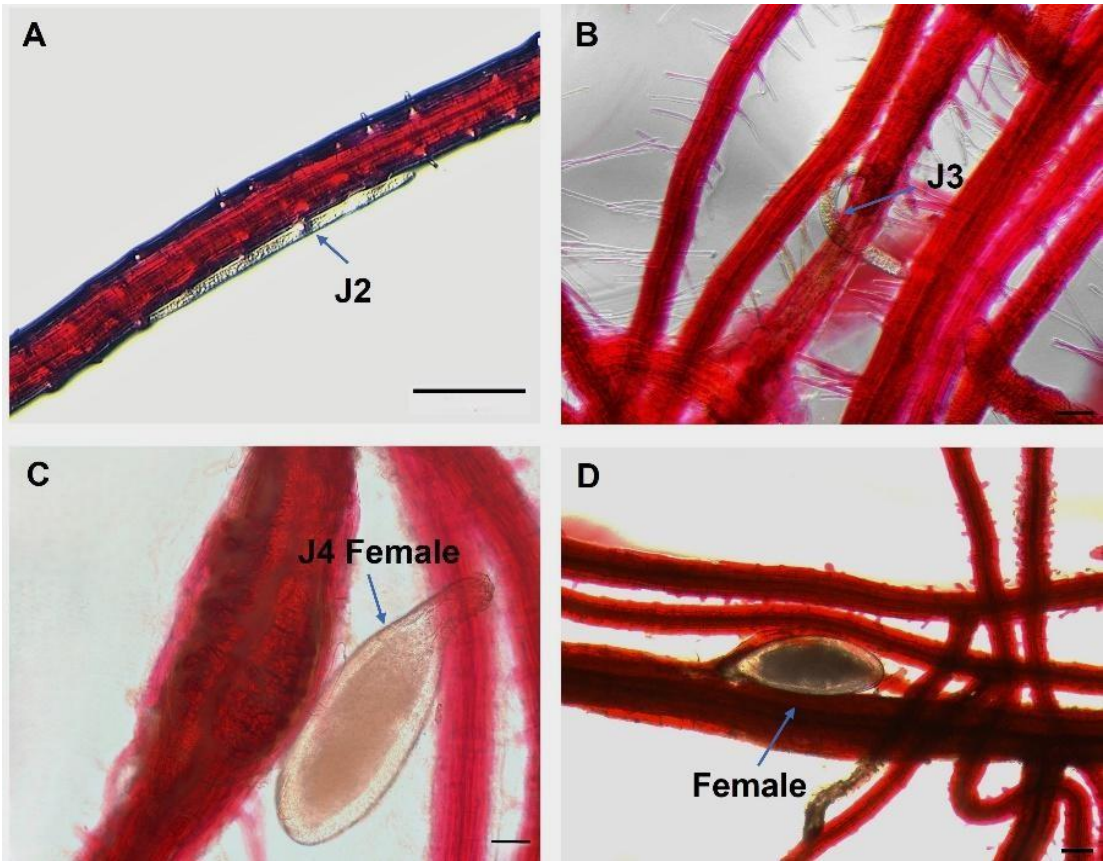

Figure 3.11. Developmental stages of *H. schachtii* visualised in RUBY expressing Arabidopsis.

A) Second-stage juvenile (J2); **B)** Third-stage juvenile (J3); **C)** Fourth-stage juvenile (J4) female;

D) Mature female. Scale bar = 100 µm.

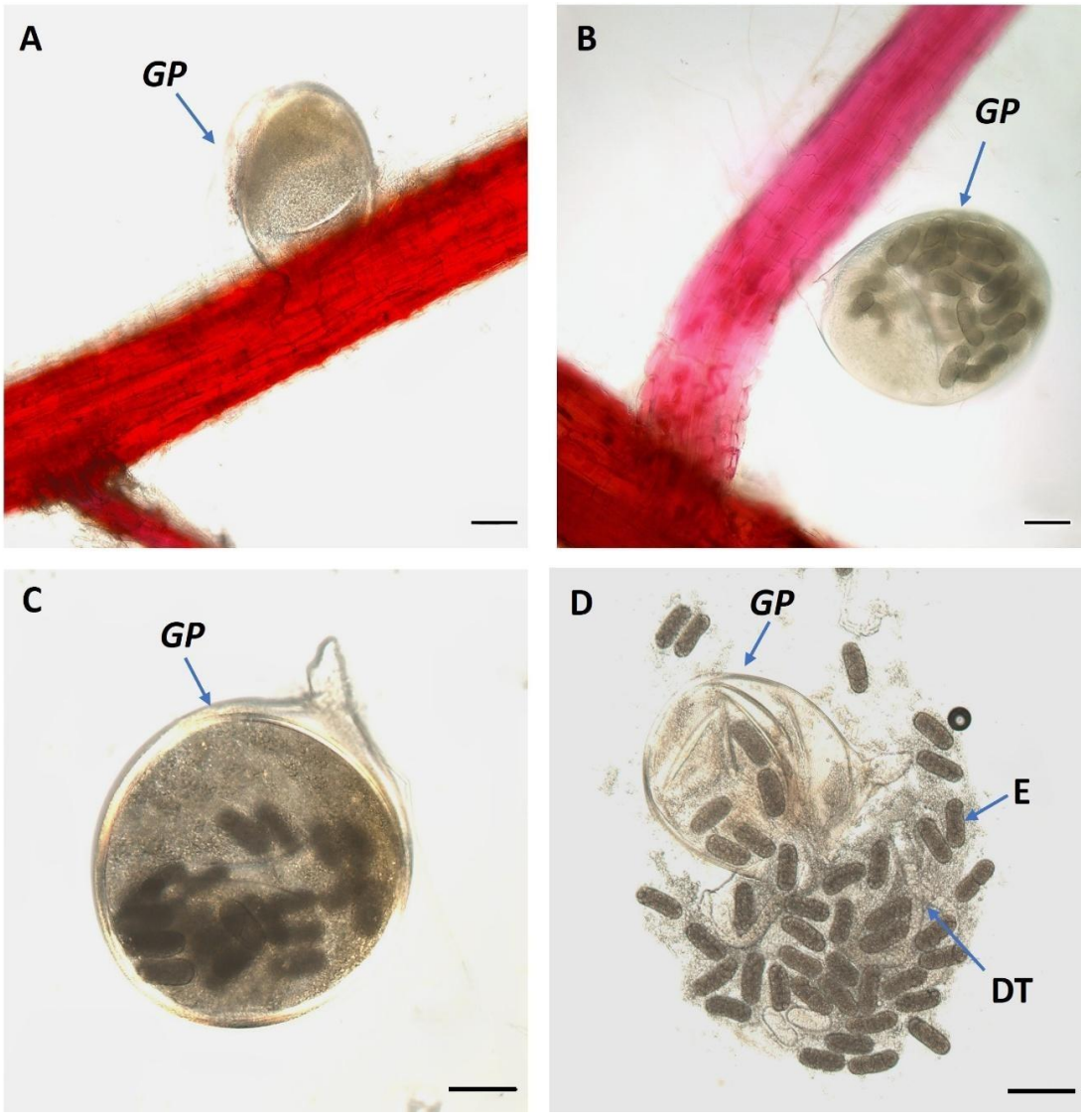

Figure 3.12. Betalain ingestion and accumulation in feeding females of the cyst nematode *Globodera pallida*.

Cyst nematode females exhibiting transparent colour during their development **(A)** 21 dpi, **(B)** 28 dpi and **(C)** 30 dpi. **D)** No evidence of betalain accumulation in the digestive tract and eggs at 30 dpi. GP = *Globodera pallida*; DT=Digestive tract and E= Eggs; scale bar represents 100 µm.

.

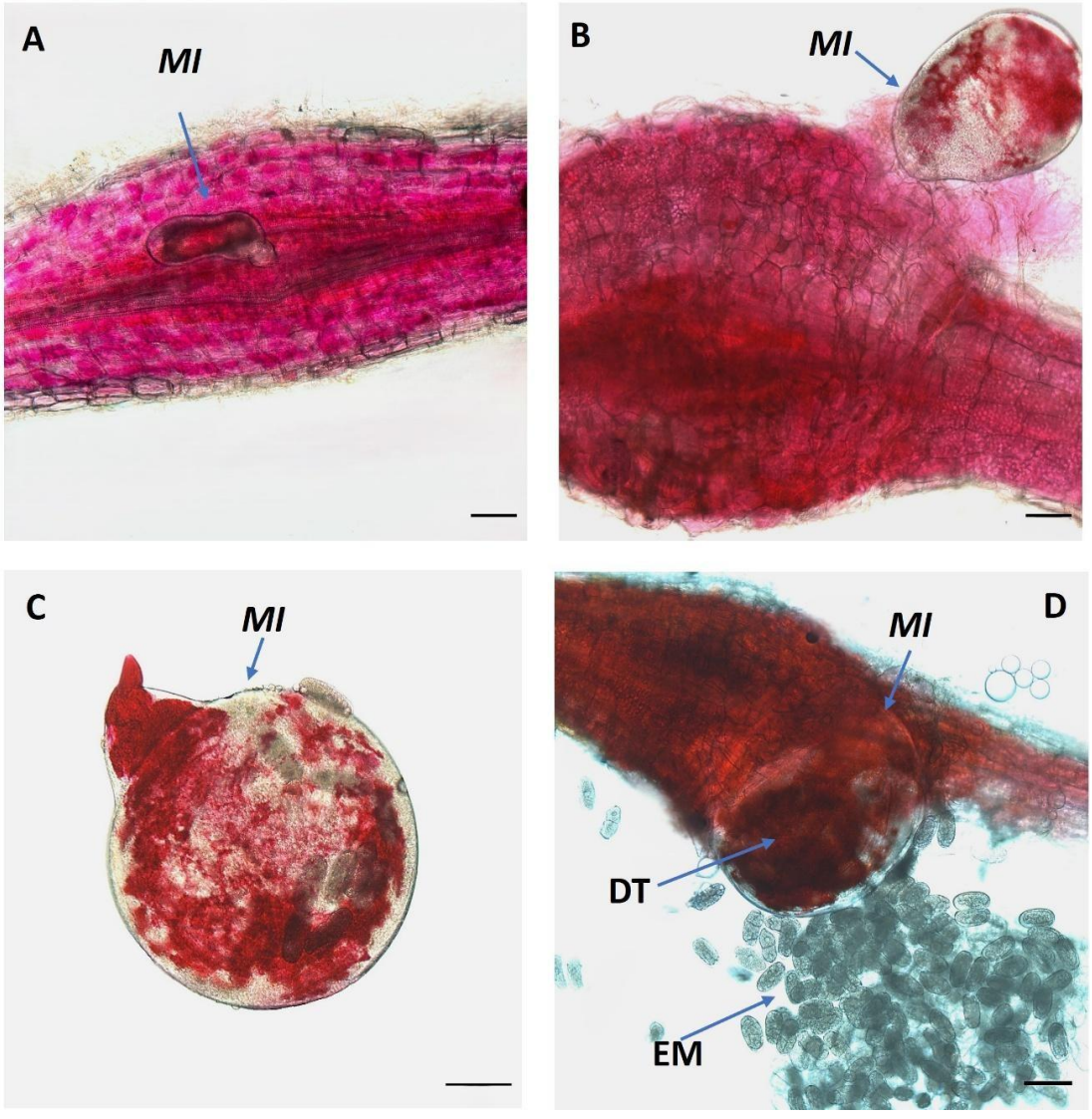

Figure 3.13. Betalain ingestion and accumulation in feeding females of the root-knot nematode *Meloidogyne incognita*

A-C) Accumulation of betalain pigments in the digestive track of root-knot nematodes at different time points, **(A)** 13 dpi, **(B)** 21 dpi and **(C)** 30 dpi. **D)** *Meloidogyne* females exhibited red pigmentation in their digestive part whilst their eggs remained transparent in colour at 35 dpi. MI = *Meloidogyne incognita*, DT=Digestive track and EM= Egg mass; Scale bar represents 100 µm.

3.4.4 Nematode access to vacuole and ingestion of RFP from vacuole

One hypothesis for the differential uptake and accumulation of betalain by cyst and root-knot nematodes was that the two types of nematodes could access different compartments of the giant cells or syncytia. Betalain is known to accumulate in the vacuoles of plant cells (Hu et al., 2025) and so we explored if the root-knot nematode *M. incognita* and the cyst nematode *H. schachtii* can access or ingest other vacuole-localized molecules such as proteins during parasitism. A previously characterised Arabidopsis marker line, VAC-RFP, with red fluorescent protein (RFP) targeted to the vacuole was used to investigate vacuolar uptake by feeding nematodes. RFP was readily detected in the roots of VAC-RFP Arabidopsis marker line plants (Figure 3.14 A & B). Strong RFP expression was particularly observed in root tips (Figure 3.14 A) and vascular tissue (Figure 3.14 B). The infected plant roots were monitored on a regular basis during the course of infection (1, 2, 3, 4 and 5 weeks post infection) using confocal microscopy. Throughout the developmental stages of nematode infection, RFP signal remained confined to the vacuoles of plant cells including uninfected root cells and feeding sites (giant cells of *M. incognita* and syncytia of *H. schachtii*). At multiple time points of infection, encompassing juveniles, feeding females and egg-laying mature female stages, RFP fluorescence was not detected in RKN intestines or surrounding tissues (Figure 3.14).

The cyst nematode *H. schachtii* was also evaluated for presence of RFP in feeding female stages. As with *M. incognita*, there was no evidence for ingestion of vacuolar RFP (Figure 3.15). Furthermore, disruption of vacuolar integrity was not observed in cells surrounding or within feeding sites of either the cyst or root-knot nematodes.

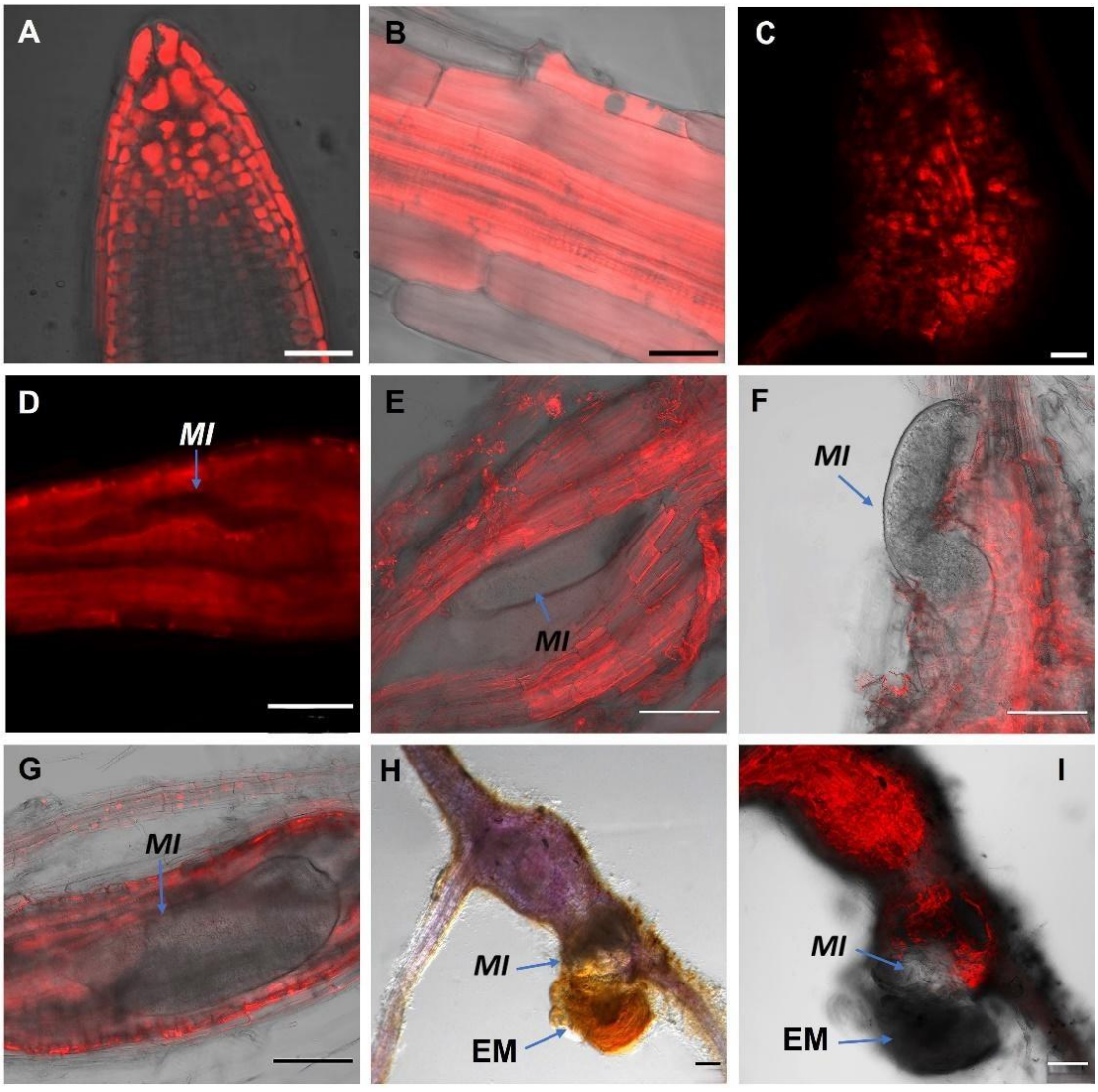

Figure 3.14. RFP uptake monitoring in root-knot nematode (*Meloidogyne incognita*) infected roots of Arabidopsis marker line (RFP targeted to the vacuole).

RFP fluorescence detected in vacuoles of **(A)** Arabidopsis root tip cells, **(B)** root vascular region and **(C)** a nematode-induced gall. There was no detectable RFP fluorescence in *Meloidogyne incognita* under confocal microscopy across all developmental stages; **(D)** juvenile J2, **(E)** juvenile J3, **(F)** J4 female, **(G)** developing female, **(H)** mature female under fluorescent microscope and (I) mature female under confocal.

MI = *Meloidogyne incognita*; EM=Egg mass and scale bar = 100 µm.

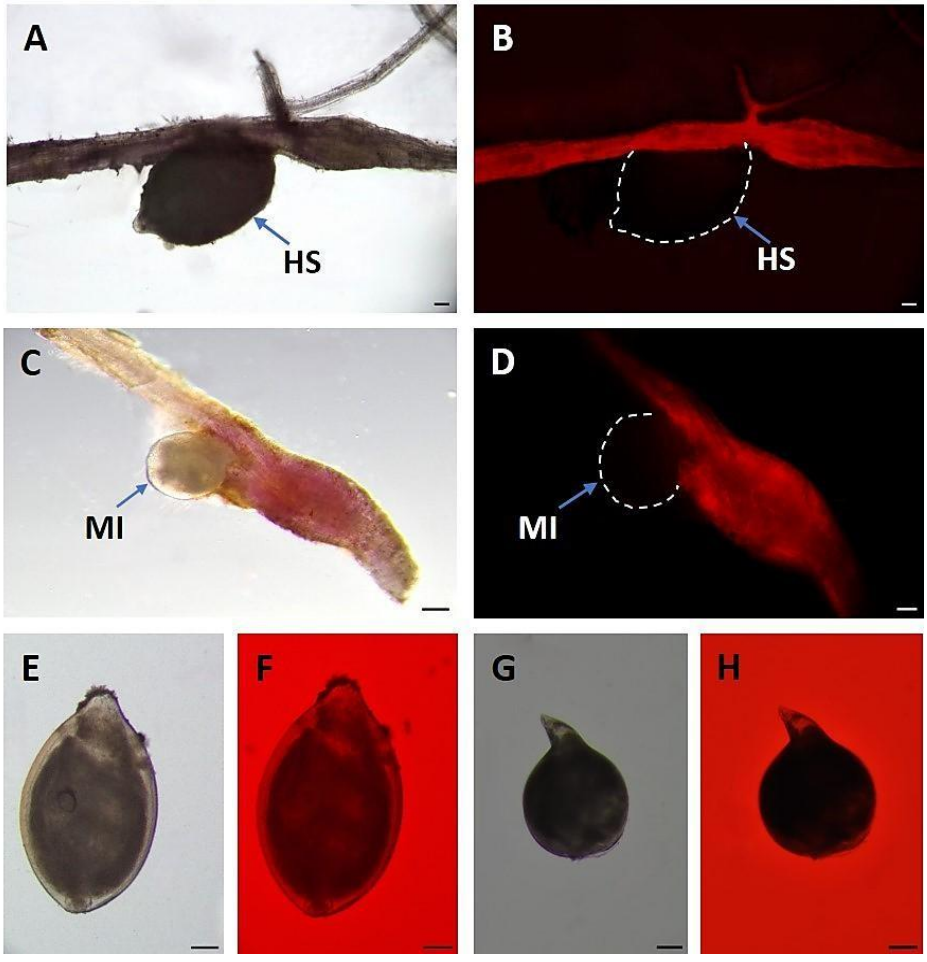

Figure 3.15. Root-knot nematode (*Meloidogyne incognita*) and cyst nematode (*Heterodera schachtii*) infection in Arabidopsis marker line VAC-RFP revealed no RFP in feeding females.

A) Mature female of *Heterodera schachtii* observed under bright field; **B)** Mature female of *Heterodera schachtii* observed under fluorescence microscope (RFP excitation filter with 540- 560 nm). **C)** *Meloidogyne incognita* female parasitizing Arabidopsis root seen under bright field; **D)** *Meloidogyne incognita* female parasitizing Arabidopsis root seen under fluorescence microscope (RFP channel). **E)** and **F)** *Heterodera schachtii* dissected from the Arabidopsis plant roots expressing RFP seen under bright field and under fluorescence microscope (RFP excitation filter with 540-560 nm) at 28 days post infection. **G)** and **H)** *Meloidogyne incognita* dissected from the Arabidopsis plant roots expressing RFP seen under bright field and fluorescence (RFP excitation filter with 540-560 nm) at 28 days post infection. *HS* = *Heterodera schachtii*, *MI* = *Meloidogyne incognita* and scale bar = 100 µm.

3.4.5 Betalain visualisation and AMF colonisation in AMF-inoculated *Nicotiana benthamiana* lines

Multigenic reporter constructs for AMF-responsive betalain expression were generated by Timoneda et al. (2021) for transformation of *N. benthamiana* (Figure 3.16 A). Transgenic lines expressing betalain under control of both the *NbPT5b* or *NbBCP1b* promoters were first validated for expression of betalain specifically in response to AMF colonisation.

AMF-inoculated plants of both lines produced betalain that was clearly visible by the naked eye as well as under the microscope after sectioning. AMF-inoculated *NbPT5b* plants (Figure 3.16 B) produced less betalain than the *NbBCP1b* plants (Figure 3.16 C). Further it was seen that control plants of both lines inoculated with mock AMF produced no betalain (Figure 3.16 D & E). Ink vinegar staining of pigmented roots of AMF-inoculated plants confirmed blue staining of the AMF and therefore AMF colonisation (Figure 3.17). However, the betalain pigmentation was lost during this staining process so it was not possible to directly correlate the overlap of betalain and ink staining. Additionally, AMF-inoculated roots of both *N. benthamiana* MycoRed lines harboured substantial AMF colonisation, hence both promoter constructs seemed to respond specifically as described by Timoneda et al. (2021).

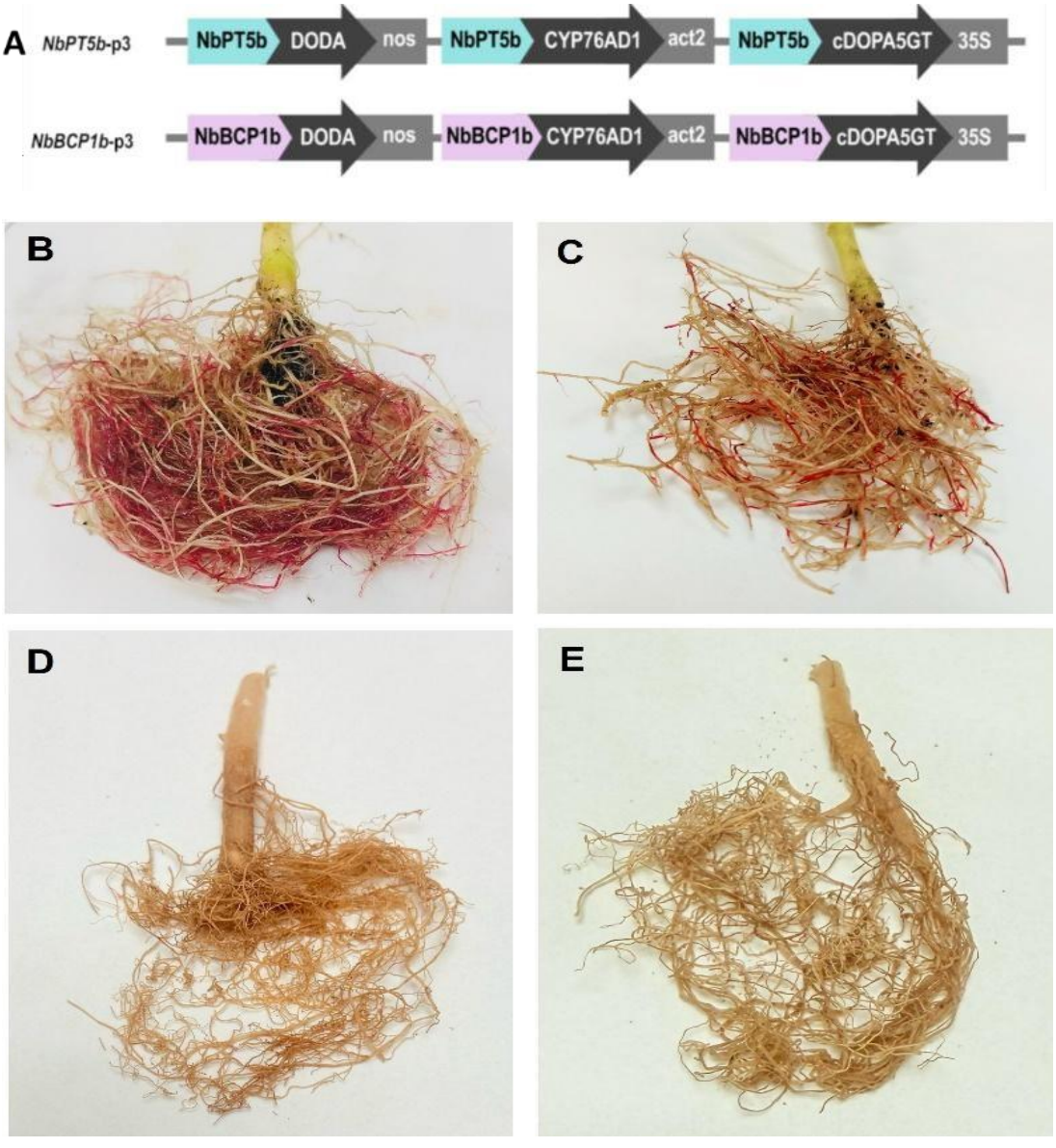

Figure 3.16. Betalain visualisation in response to AMF colonisation in *Nicotiana benthamiana* MycoRed roots.

A) Schematic diagram of inducible multigene vector constructs containing three betalain biosynthesis gene governed by the *NbPT5b* or the *NbBCP1b* promoters.

Expression of betalain under control of the **(B)** *NbBCP1b* and **(C)** *NbPT5b* promoter four weeks after inoculation with AMF. Mock inoculated roots did not express betalain in **(D)** *NbBCP1b* and **(E)** *NbPT5b* lines.

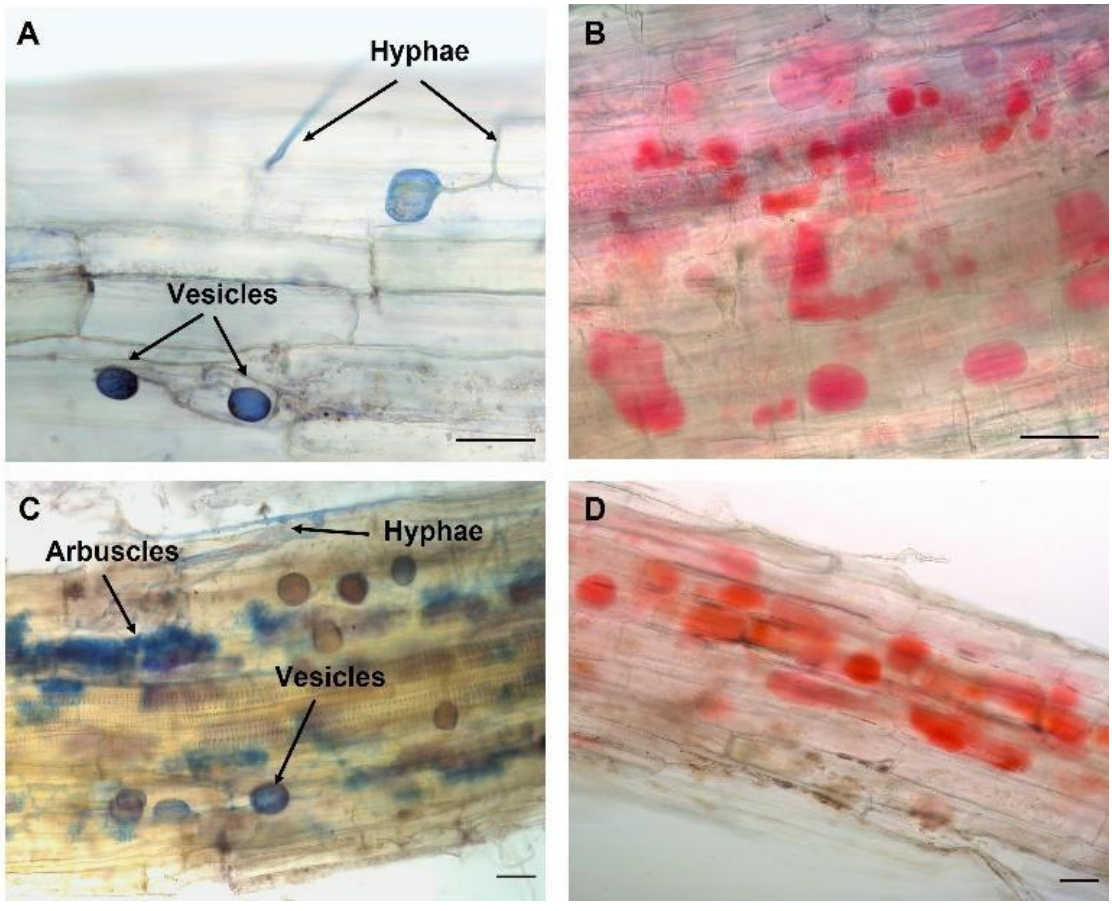

Figure 3.17. AMF colonisation in *Nicotiana benthamiana* roots.

Ink-vinegar staining confirmed the colonisation of AMF in **(A)** *NbBCP1b* and **(C)** *NbPT5b* reporter lines, whilst root transection and observation of betalain under the microscope also indicated colonisation in **(B)** *NbBCP1b* and **(D)** *NbPT5b* lines. Scale bar = 50 µm.

3.4.6 Absence of betalain accumulation in *Nicotiana benthamiana* roots following root-knot nematode infection

No visible accumulation of betalain pigments was detected in the MycoRed *Nicotiana benthamiana* roots infected only with root-knot nematode. Successful nematode infection was confirmed visually by the presence of galls and acid fuchsin staining of nematodes (Figure 3.18; Figure 3.20 C & D). Therefore, both the *NbBCP1b* and *NbPT5b* AMF-responsive promoters did not trigger betalain expression upon nematode infection.

3.4.7 Betalain visualisation in nematode and AMF co-infected *Nicotiana benthamiana* lines

In response to *M. incognita* infection and AMF colonisation, both *NbBCP1b* and *NbPT5b* promoter lines exhibited accumulation of betalain pigmentation or red root formation (Figure 3.19). The sectioning of red root regions further confirmed the presence of pigmentation, which was clearly visible under the microscope. Ink-vinegar staining of galls and nematode-infected red roots confirmed fungal colonization, while acid fuchsin staining further verified the presence of *Meloidogyne* in nematode and AMF-infected plants (Figure 3.20). Although both the *NbBCP1b* and *NbPT5b* lines produced betalain under nematode and AMF co-infection, the *NbPT5b* line exhibited weaker expression in response to AMF colonisation. Therefore, only the *NbBCP1b* line was selected to investigate spatial interactions between AMF and root-knot nematode.

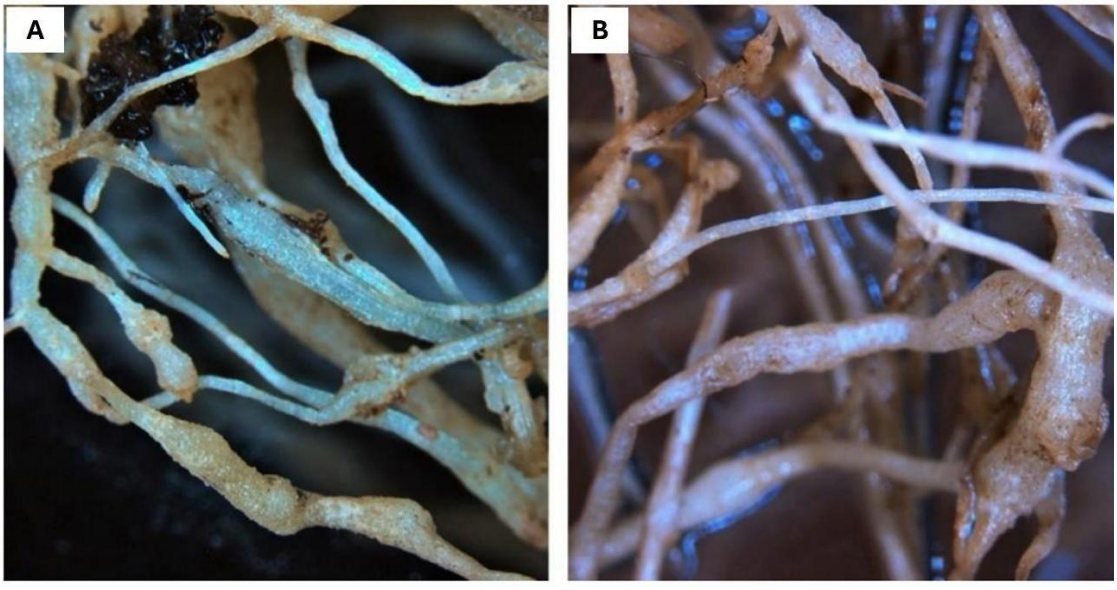

Figure 3.18. *Meloidogyne* infected *N. benthamiana* produced galls with no visible betalain expression.

A) *NbBCP1b* line produce galls in response to nematode infection.

B) *NbPT5b* line. produce galls in response to nematode infection.

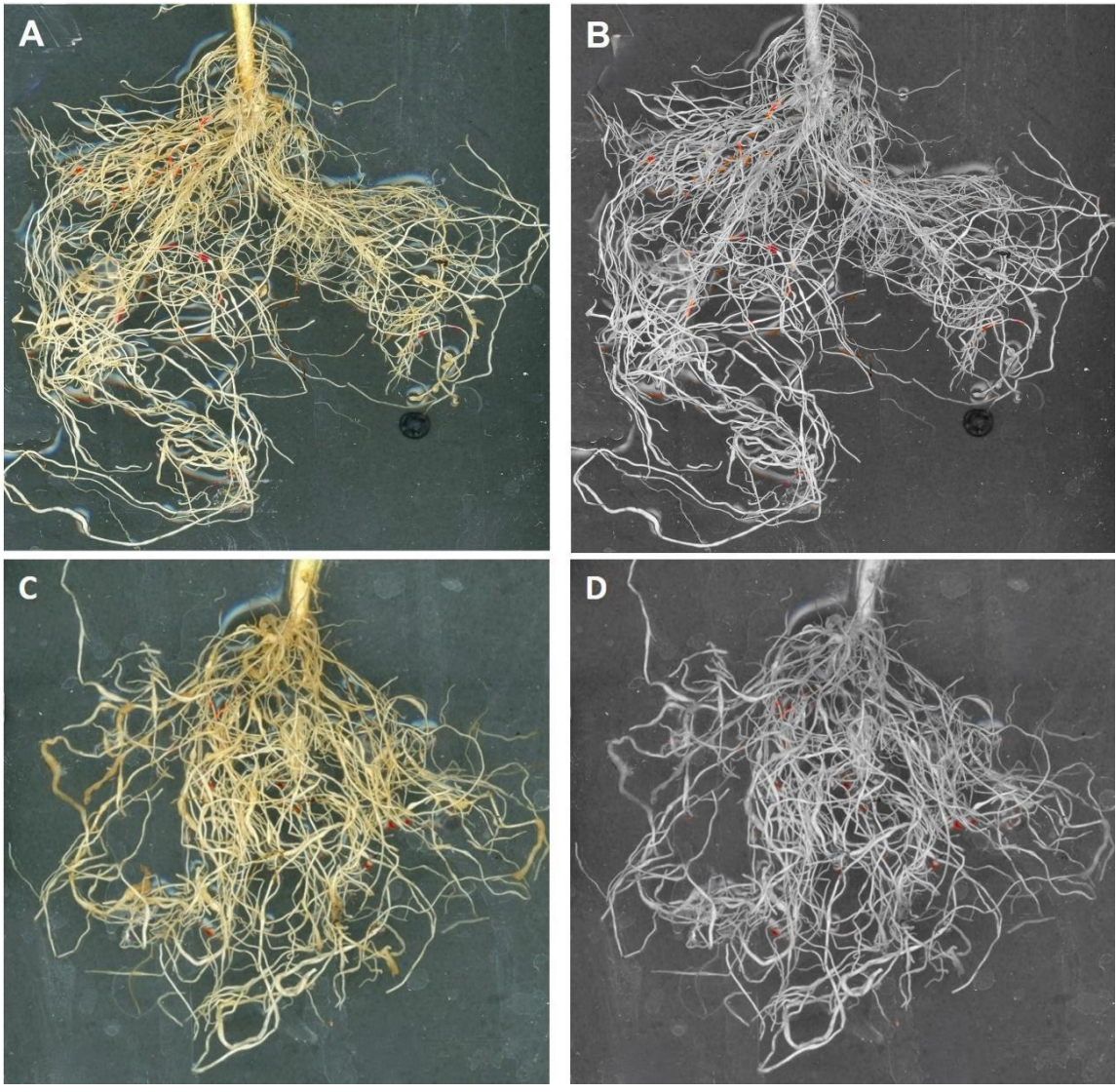

Figure 3.19. Expression of betalain in AMF and root-knot nematode infected *Nicotiana benthamiana* lines.

The *NbBCP1b* line **(A)** and *NbPT5b* line **(C)** produced betalain after six weeks of infection with *R. irregularis* and *M. incognita*. **B)** and **D)** Images are filtered for visualisation of betalain (red colour) only.

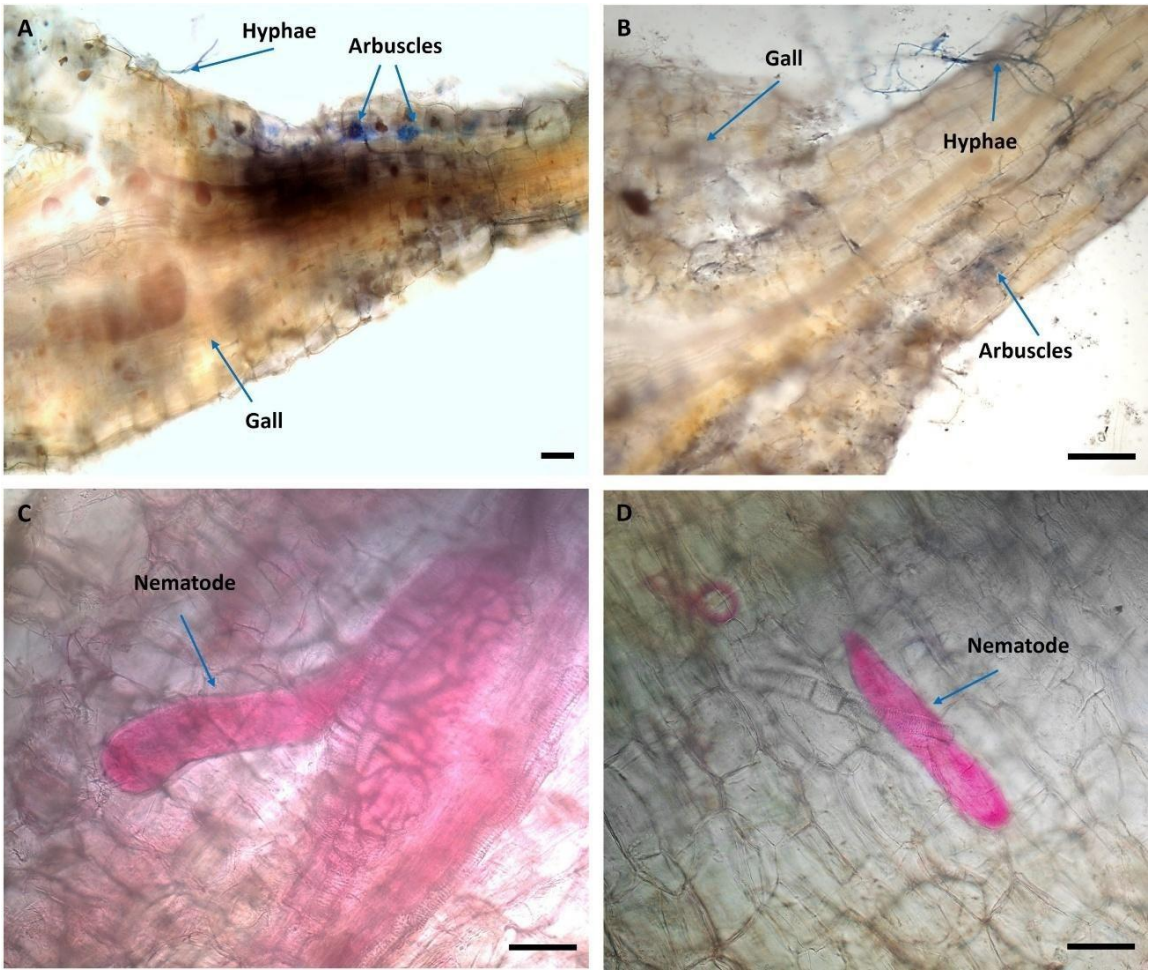

Figure 3.20. AMF (*R. irregularis*) colonisation and root-knot nematode (*M. incognita*) infection in infected *Nicotiana benthamiana* lines.

Ink-vinegar staining proved the occurrence of *R. irregularis* in **(A)** *NbBCP1b* line and **(B)** *NbPT5b* line after six weeks of infection with AMF and root-knot nematode at the same time point. The presence of root-knot nematode in **(C)** the *NbBCP1b* line roots **(D)** and *NbPT5b* line roots after acid fuchsin staining. Scale bar = 50 µm.

3.4.8 Spatial interaction between AMF and root-knot nematode

The MycoRed reporter lines provided an ideal resource to investigate the spatial interaction at a macro-scale between AMF colonisation and root-knot nematode infection sites without the need for staining. The *NbBCP1b* reporter line was selected for this work as it displayed the strongest and most consistent response to AMF colonisation. Among the randomly selected root segments with galls and without galls, the presence of red pigmentation was assessed. The majority of the roots were wholly unpigmented, while 13 root segments in each group displayed distinct red pigmentation. To further assess the potential relationship between nematode infection (as indicated by gall development) and AMF colonization, the percentage of red coverage was quantified in both galled and ungalled categories. A two-sample *t*-test was performed to test the significant difference between two groups. The proportion of each root length that was red did not differ significantly between galled and ungalled roots ($p=0.52$, $t\ stat=0.66<t\ Critical=2.2$) (Figure 3.21). The results therefore suggest that betalain accumulation, indicating AMF colonisation of the root, is not strongly influenced by gall formation.

When we analysed the infected roots visually or under the microscope, the position of galls and betalain pigmentation revealed that the red colour was generally between two galls or on both sides of the gall and was rarely associated with the galls themselves, whereas some areas of red pigmentation were present far away from galls (Figure 3.22). Furthermore, betalain synthesis was mainly observed in the comparatively thinner or younger roots rather than older roots.

The spatial interaction was then investigated more quantitatively. The distance between red roots areas and nematode induced galls was also measured to assess whether AMF colonisation was associated with gall location. Descriptive statistical analysis was done to determine the distribution pattern of these distances. The measurement of distance was also consistent with the visual or microscopic observation. The mean distance between galls and red roots was 0.93 mm (SD=1.36 mm) while maximum distance was 4.45 mm and minimum distance was 0 mm with a median of 0.25 mm. The standard deviation revealed moderated variability in the distance between the galls and red roots, suggesting some red roots were located at closer proximity to the galls while others were farther away. The boxplot represents that most of the red roots were clustered near the gall, whilst occasional outliers were present at greater distances (Figure 3.23).

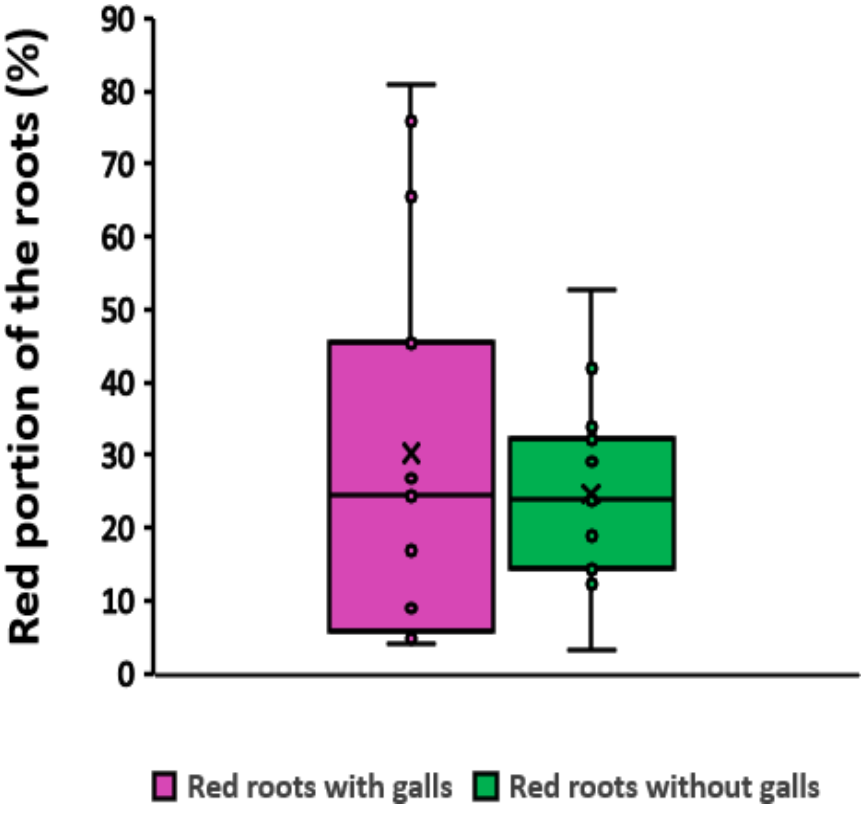

Figure 3.21. Relationship between red roots colonized by AMF with galls and red roots colonized by AMF without galls.

Boxes represent interquartile range, the line inside the boxes represents median value and the whiskers extend to the maximum and minimum values. Each dot indicates an individual sample (n=13).

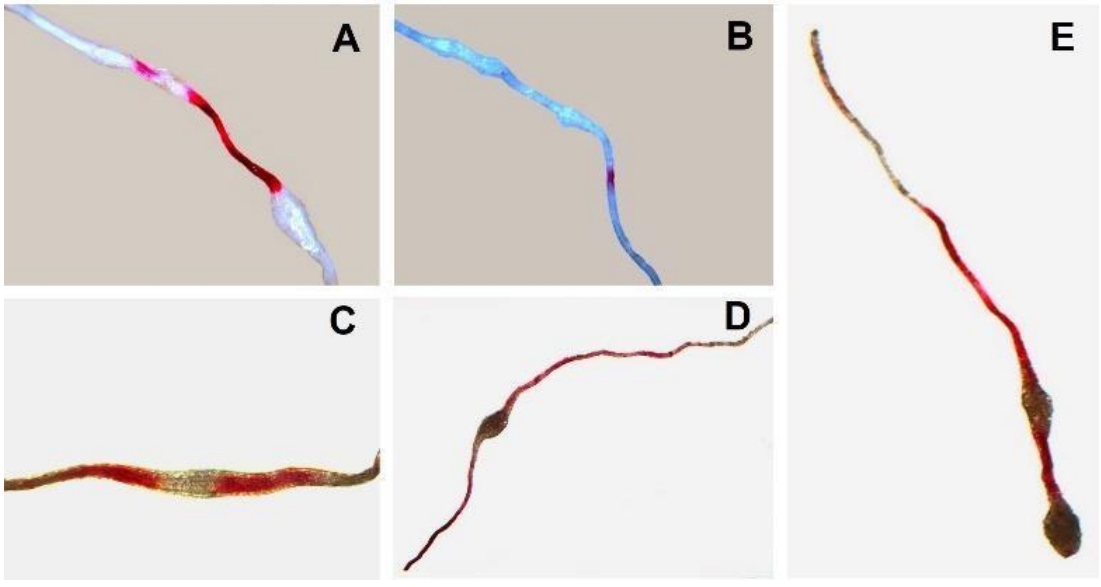

Figure 3.22. Examples of apparently random spatial expression of betalain in AMF and root- knot nematode infected *NbBCP1b* roots.

Betalain expression as a result of AMF colonisation appeared **(A)** between two galls induced by root knot nematode, **(B)** far away from a gall, **(C)** within gall, **(D)** on both sides of the gall and **(E)** in thinner roots adjacent to galls**.**

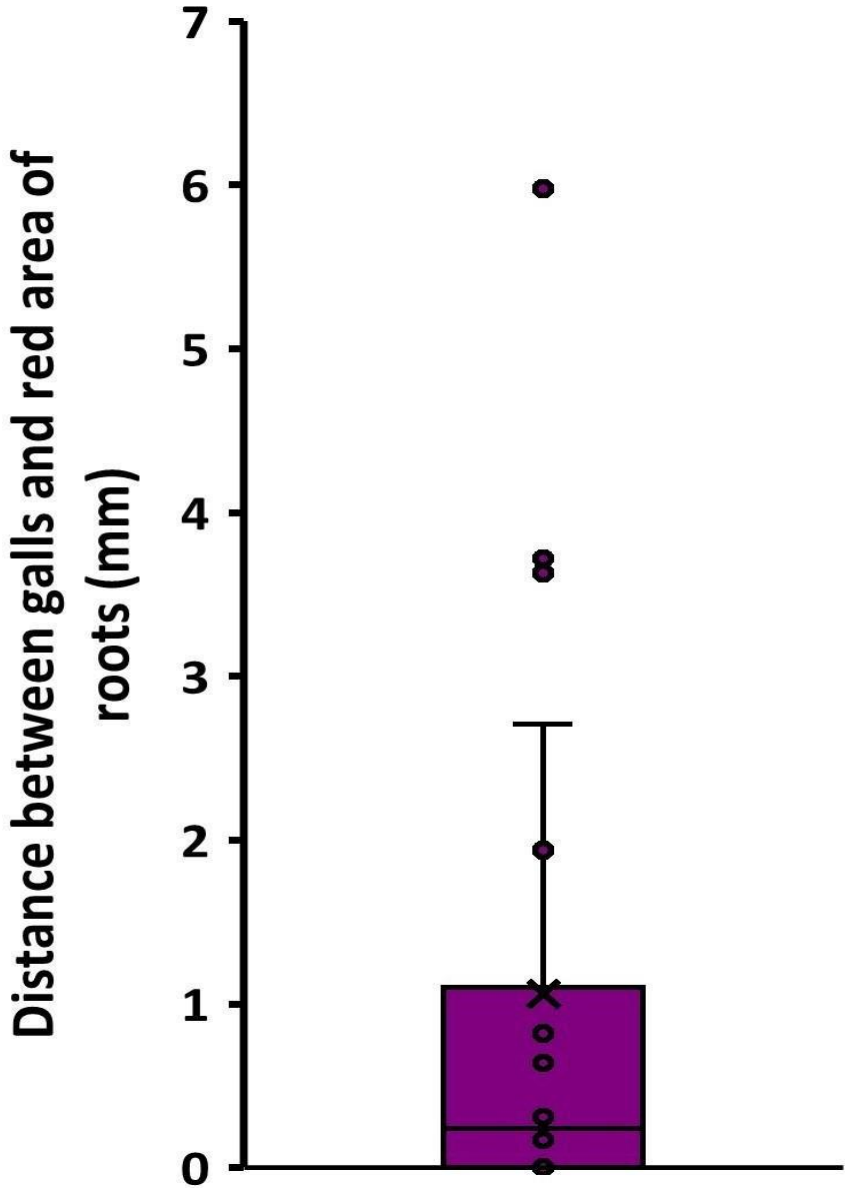

Figure 3.23. Distance between galls and red area of roots.

Boxes represent interquartile range, the line inside the boxes represents median value and the whiskers extend to the maximum and minimum values. Each dot indicates an individual sample (n=20).

3.5 Discussion

Two distinct betalain reporter systems that differ in how the betalain biosynthetic genes are controlled in the transgenic plant were utilised in this work. The aim was to assess the potential of using this new reporter system as an alternative to traditional GUS or GFP reporters to monitor plant gene expression during plant-nematode interactions.

3.5.1 Transgene expression and gene silencing in transgenic Arabidopsis and potato plants

In this chapter, the CaMV35S:RUBY reporter construct described by He et al. (2020) was used to investigate transgenic expression in Arabidopsis and potato plants for evaluating nematode infection. An efficient integration of the construct and functional expression of betalain was observed in both plant species, but varying degrees of gene silencing in Arabidopsis were observed. It was evidenced from our reverse transcriptase analysis that the construct becomes silenced in Arabidopsis if the very high level of constitutive over-expression becomes detrimental to the plant. A similar observation was reported by Baral et al. (2024), where gene silencing occurred in approximately 50% of transgenic *Arabidopsis* lines expressing RUBY under the CaMV35S promoter. Furthermore, Wang et al. (2023a) identified detrimental effects associated with RUBY over-expression driven by the same promoter, including excessive betalain accumulation in fruits, leaves, and flowers of tomato, which led to reduced growth, diminished pollen production, and a lower fruit set rate. In contrast, RUBY maintained high expression during the whole life span of the transgenic potato lines including all the mature tissues that exhibited stable and strong expression. This result is consistent with earlier findings that the CaMV35S promoter drives constitutive gene expression and red pigmentation was consistently observed across all tissues throughout the plant's developmental stages in tobacco (Jogam et al., 2024), Arabidopsis (He et al., 2020), *Plukenetia volubilis* (Yu et al., 2023), Maize (Lee et al., 2023) and tomato (Wang et al., 2023a).

Different factors are responsible for transgene silencing including strength of the promoter, number of transgene copies, DNA methylation, transgenic insert's repetitiveness and the expression level of the transgene (Stam et al., 1997). Among these factors, post-

transcriptional gene silencing (PTGS) and RNA-directed DNA methylation (RdDM) are mostly active in Arabidopsis, which identify and silence highly expressed or repetitive transgene sequences (Slotkin and Martienssen, 2007). One plausible explanation for the detected gene silencing of the highly expressed RUBY construct in Arabidopsis is the activation of the PTGS pathway. The utilization of the strong constitutive CaMV35S promoter in combination with transgene insertion might play an active role in triggering this gene silencing (Mlotshwa et al., 2010).

On the contrary, potatoes may possess a less responsive or weaker transgene silencing mechanism, or the chromatin context of transgene integration may have been more tolerant. Moreover, the Agrobacterium-mediated transformation for both cases might affect the epigenetic status of the integrated DNA, and different species might react differently to T-DNA integration at the molecular level (Jupe et al., 2019).

Additionally, the RNA expression levels of the three genes comprising the RUBY reporter system showed variability across transgenic *P. volubilis* and *N. benthamiana* hairy roots, as well as in transgenic *Arabidopsis* plants (Yu et al., 2023). Pigment production and RNA expression were found unstable over two generations in Arabidopsis, likely due to inefficient 2A peptide–mediated "self-cleavage" or ribosomal "skipping" mechanism (Kiryushkin et al., 2021). The RUBY "polycistronic" mRNA in *Arabidopsis*, which encodes three biosynthetic genes, may undergo unexpected post-transcriptional processing. While polycistronic mRNAs were once thought to be rare in eukaryotes, recent studies have identified 271 such loci in *Arabidopsis*, although the mechanisms governing their regulation remain largely unknown (Yu et al., 2023). Notably, there is currently no evidence for the existence of similar polycistronic mRNAs in potato or inefficient 2A peptide–mediated cleavage, highlighting a potential species-specific difference in transcript processing that warrants further investigation.

This finding suggests that Arabidopsis which is commonly used as a model for gene regulation studies, does not always accurately predict the behaviour of transgenes in crops such as potato, highlighting the importance of species-specific validation in the field of plant biotechnology. Construct design methods, such as the use of weaker (or tissue-specific) promoters, and of introns or insulating elements, may be necessary to

diminish silencing in Arabidopsis. Therefore, for the best possible application of the pigment- based reporter system (e.g. RUBY) in certain plant species, it is necessary to optimise and comprehend aspects that affect the system (Jogam et al., 2024; Wang et al., 2023). Promoter optimisation in tomato has been shown to reduce the detrimental phenotypes associated with excessive betalain accumulation (Polturak et al., 2017), demonstrating that the design of constructs is of critical importance. Studies suggest the effectiveness of reporters using radicle-specific promoters (e.g. pOsSli2) in several tiny-seeded and glume-bearing species, including tomato, tobacco, rapeseed and rice (Chen et al., 2015, Ma et al., 2007). Additionally, RUBY overexpression has been avoided in maize by integrating helper plasmid with genetically engineered T-DNA binary vectors (Lee et al., 2023). These optimisations could be considered in transgenic Arabidopsis plants for RUBY expression.

3.5.2 Betalain expression in nematode feeding sites and nematode interaction

One benefit of the RUBY reporter system was that it allowed us to investigate the expression of the CaMV35S promoter in nematode feeding cells, for which apparently conflicting results have been reported in the past. Previous experiments using the GUS reporter system with the 35S promoter had noted an apparent reduction in GUS expression in nematode feeding sites. Consistently, the downregulation of a GusA construct in the syncytial feeding cells of cyst nematodes (*H. schachtii*) and giant cells of root knot nematodes was reported under the control of the CaMV35S promoter (Goddijn et al., 1993) and a significant reduction of GFP levels was similarly observed in the syncytial structure while using the CaMV35S promoter (Urwin et al., 1997a). However, it remained uncertain whether this apparent reduction was due to the reduction of promoter activity (CaMV35S) or shortcomings of GUS substrate penetration into the nematode feeding sites and effective visualisation of GFP fluorescence through the more opaque walls of older syncytia. These observations are in contrast to the successful nematode resistance that has been achieved through CaMV35S-directed expression of anti-feedant proteins that must be produced in the syncytia and giant cells to be effective (eg. Urwin et al., 1997b; Urwin et al., 2001; Li et al., 2007). From our study, we found betalain expression directed by the CaMV35S promoter in the feeding sites of both root-knot nematode (*M. incognita*) and cyst

nematodes (*H. schachtii and G. pallida*). No down-regulation of RUBY was observed in giant cells or syncytia even at the later stages of the life cycles suggesting that the apparent down- regulation reported previously may have been largely due to the technical limitations. Furthermore, the use of traditional reporters such as GUS requires sacrifice of the whole plant and fluorescent proteins such as GFP or RFP require expensive fluorescent imaging to visualize the nematode infection or gene expression in nematode feeding sites (He et al., 2020). In contrast, our result clearly shows that the RUBY reporter system provides a visible, non- destructive alternative system for monitoring gene expression in real-time during nematode infection that may overcome such types of limitations.

During the infection of transgenic RUBY potato plants with root-knot nematodes and potato and Arabidopsis plants with cyst nematodes, an interesting observation was made that the betalain pigment was taken up from the giant cells and accumulated in the body of the feeding root-knot nematode female. On the contrary, betalain was never observed in cyst nematodes and they remained transparent in colour, indicating either limited ingestion of betalain pigment by cyst nematodes due to different mechanisms of uptake or variation in retention once the betalain is ingested. There might be several plausible explanations for this discrepancy such as differences in feeding strategies, internal structure of feeding cells or nematode access to different plant cellular compartments. Alternatively, the metabolic pathways for breakdown of compounds once ingested may differ between cyst and root knot nematodes.

Previously observed differences in the uptake of certain proteins by cyst and root-knot nematodes have been attributed to the distinct sieving characteristics of root-knot and cyst nematode feeding tubes. Within the feeding site, the nematodes of both types construct a replaceable feeding tube at the stylet orifice from gland secretions that acts as molecular sieve with a view to excluding large proteins or organelles (Razak and Evans, 1976). Root-knot nematodes produce feeding tubes within the giant cells to feed the developing females, whilst cyst nematode feeding tubes form during early infection (36h) and the tube walls are noticeably thinner than those of root-knot nematodes with a different structure as viewed using electron microscopy. Unlike the more selective cyst nematode feeding tubes, root-knot nematode feeding tubes permit uptake of larger macromolecules (Eves-van den Akker

et al., 2015). By analysing critically, it was established that the size exclusion limit of the cyst nematode feeding tube was likely in the region of 20-27 kDa (Bockenhoff and Grundler, 1994; Urwin et al., 1997a ; Urwin et al., 1998), whereas root knot nematodes can ingest up to at least 27 kDa (cytoplasmic GFP) (Urwin Lab, unpublished data) and most likely larger Cry toxins (Li et al., 2007). While the feeding tube is considered as a limiting factor for uptake of macro- molecules, it is unlikely to impact the uptake of betalain. Betalains are tiny, water soluble amino acid molecules (Gengatharan et al., 2015), hence these should be passed through the feeding tubes of both nematodes.

One previous experiment implied that cyst nematodes are unable to access the vacuole, hence, cannot uptake protein or vacuole-based nutrients from it (Hayes, 2022). Given that betalain pigments are localised in the plant vacuoles (Sadowska-Bartosz and Bartosz, 2021) in that case they would remain inaccessible to cyst nematodes. Feeding access to the vacuole had not previously been tested for root-knot nematode and how the feeding tube interacts with different compartments of the feeding site is unknown. For this reason, we initially hypothesized that maybe feeding root-knot nematodes can somehow access the vacuole and can ingest betalain while cyst nematodes cannot. To test this hypothesis, a previously characterised Arabidopsis marker line (VAC-RFP) was used for both infection with both cyst and root-knot nematodes. Neither *M. incognita* nor *H. schachtii* were observed to ingest vacuolar-targeted RFP as no red fluorescence was observed in the nematode digestive tract during their feeding process. This result indicates that root-knot nematode cannot access the vacuole and uptake vacuolar contents as the size of RFP should not exclude it from this nematode.

The opposing behaviour of up taking RFP and RUBY-derived betalain provide valuable insight of root-knot nematodes' access to cellular compartments and their feeding pattern. While vacuolar based RFP was not ingested by root-knot nematodes, betalain pigments were noticeably up taken. This suggests that betalains may be transported or leaked into the apoplast or cytoplasm under certain conditions hence being accessible to root-knot nematodes. There is a greater possibility of up-taking betalains from the cytoplasm rather than being directly ingesting from vacuoles. Accumulation of cytoplasmic GFP in the intestine of *M. incognita* was evidenced by a previous report (Urwin Lab, unpublished data)

and apoplastic type of protein assimilation was found in root-knot nematode-induced giant cells (Hoth et al., 2008).

In the case of cyst nematode induced syncytia, symplastic loading via plasmodesmata was observed, suggesting more selective feeding than that of root-knot nematodes (Hoth et al., 2008). During syncytial formation, the large central vacuole is replaced by numerous small vacuoles or vesicles, which are surrounded by the membranes comprising tonoplast intrinsic proteins (γ-TIP proteins) (Baranowski et al., 2019). These proteins have a role in cellular compartmentalization and regulate movement of tiny molecules and water between vacuole and cytoplasm (Maurel et al., 1993). These distinguishable attributes are supposed to play a key role in inaccessibility of vacuolar contents by cyst nematode. Overall, it is suggested that future studies to gain a deeper understanding of host–parasite interactions could include examining vacuolar integrity, comparing the localization of subcellular markers, visualizing nematode feeding behaviour, and analysing what the nematodes actually absorb.

3.5.3 Transgenic tobacco (*Nicotiana benthamiana*) lines infection with AMF and root-knot nematodes and their spatial interactions

In this experiment, we used two reporter lines of *N. benthamiana* that respond to AMF infection by producing betalain. We first tested the reported inducibility and specificity of the betalain expression in both lines to ensure that it was stably maintained in the generation of seeds that we had obtained. Overall, it was evident from our experiment that betalain production correlated with the presence of AMF in both reporter lines of *Meloidogyne* infected and AMF inoculated plants, whereas control plants (Mock AMF-inoculated) produced no visible betalain. This result supported the findings of Timoneda et al. (2021) and confirmed that the transgene expression was stably maintained even after a number of generations.

It was interesting to note that the *NbPT5b* lines produced less betalain than *NbBCP1* plants during AMF colonisation. Betalain colouration was produced in colonised roots and was associated with arbuscule presence and confirmed AMF induced expression of that promoter. The reduced betalain production in *NbPT5b* may be attributed to the expression

pattern of phosphate transporter 1 (PHT1), which is confined to arbuscule-containing cells and localised to the plant membrane surrounding arbuscules, where it facilitates phosphate uptake released by the fungus during symbiosis (Timoneda et al., 2021). Or the reason might be that reporter expression is deactivated by the existence of another microorganism. This is also supported by the absence of red pigmentation upon inoculation of reporter lines with spores of the oomycete root pathogen *Phytophthora palmivora* (Timoneda et al., 2021).

Regarding the spatial interaction between galls induced by *Meloidogyne* and red areas of root induced by AMF colonisation, the distribution pattern of betalain (red roots) and galls appeared as random, and betalain was expressed prominently in younger or thinner roots. The quantitative aspects revealed that the presence or absence of galls did not differ significantly with the percentage of red roots. This result contrasts with earlier findings, which reported the suppressive effect of AMF on the populations of plant-parasitic nematodes, primarily due to nutrient and space competition, induced systemic resistance or altered interactions in the rhizosphere (Schouteden et al., 2015). However, this suppression may not always affect spatial interaction unless the feeding cells extend towards the cortical regions (Schouteden et al., 2015). It was evident that AMF and nematodes were unlikely to compete for space while root-knot nematode infestations were reduced by the presence of AMF (Hol and Cook, 2005). This perspective is in line with our finding, suggesting that AMF and *Meloidogyne* association may not always provide direct spatial exclusion or competition.

A possible elucidation for the non-significant AMF and *Meloidogyne* association is due to their location within the roots. AMF produce arbuscules and colonize cortical cells, whereas *Meloidogyne* induce galls in central vascular tissues to establish their permanent feeding sites (Hol and Cook, 2005). This structural isolation abates direct physical competition between both organisms, allowing them to coexist without significantly disturbing their spatial distribution. Another aspect might include their temporal colonization, if AMF colonises prior to nematode inoculation, it might change root physiology to alter susceptibility to nematode infection. This hypothesis aligned with a study that noted no effect in case of AMF and *Meloidogyne* co-inoculation, while well-

established AM symbioses were found when AMF colonization preceded *Meloidogyne* infection (Anjos, et al., 2010). In order to elucidate the precise mechanisms, quantitative techniques based on in situ-hybridization or qPCR would provide specific insights into actual colonization and spatial interaction rather than applying only visual technique based quantitative estimation.

3.5.4 Conclusions

The results from this chapter demonstrated that the CaMV35S:RUBY reporter construct is a promising vector system upon which to build reporters to monitor early nematode infection non-destructively in real time. While both the constitutive CaMV35S:RUBY plants and the inducible betalain-based AM symbiosis reporter system offered valuable insights, the RUBY vector provided strong and consistent betalain production and has the advantage of a simpler cloning strategy for subsequent modification. Despite potential gene silencing in later growth of Arabidopsis plants, the consistent early expression of the betalain pigment throughout the plant and nematode life cycle, especially in potato makes RUBY a potential system for monitoring nematode infection. The use of inducible promoters or those with limited expression patterns would further reduce any problems with gene silencing. Based on these preliminary analyses, the CaMV35S: RUBY reporter construct was selected for our next phase of work.

The key findings from these experiments are:

- The CaMV35S:RUBY construct was expressed over the whole life cycle of transgenic potato plants while gene silencing was frequently observed in transgenic Arabidopsis plants. It was also expressed in the nematode feeding cells (syncytium and giant cells) throughout the development, no down-regulation was noted, suggesting that previous observations of apparent down-regulation of 35S were due to the technical limitations.

- Betalain was observed to accumulate within the body of feeding root-knot nematode females but was never detected in cyst nematodes. The way of solute transport or differences in vacuolar integrity may play key roles in this discrepancy.

- Lack of RFP fluorescence in both nematodes during infection of an Arabidopsis vacuolar RFP marker line clearly exhibited vacuolar inaccessibility of both nematodes.

- To understand better nematode biology and host-nematode interaction, future studies should include investigating selective feeding of nematodes and comparing the localization of subcellular markers for more precise insights.

- Betalain pigments confirmed the presence of AMF in both *NbPT5b* and *NbBCP1b* lines of *Meloidogyne* infected and AMF inoculated plants, whereas control plants (mock AMF-inoculated) produced no betalain.

- Weaker betalain expression was evident in *NbPT5b* promoter line in comparison to *NbBCP1b* line under AMF accumulation. The quantitative aspects of AMF-nematode spatial interaction in *NbBCP1b* line demonstrated a non-significant interaction.

Chapter 4

Development of Novel RUBY Reporter Constructs to Investigate Early Nematode Infection

4.1 Introduction

Reporter gene systems are widely used tools in plant biology to visualize gene expression and cellular responses in plants during biotic and abiotic stresses (He et al., 2020). The protein products of reporter genes exhibit detectable features that facilitate the identification and quantification of genes. Gene expression systems also enable the evaluation of gene and promoter function within whole plant tissue under both natural and controlled conditions (Jeong et al., 2024). These reporter genes, coupled with specific plant promoter regions have also been used to study gene expression relating to cellular and hormonal changes during the formation of nematode-induced feeding sites (Escobar et al., 1999). Research on plant host gene responses to nematode infection has traditionally focused on a limited number of known genes using promoter–reporter constructs (Fuller et al., 2007) or has used a promoter-tagging approach, where a promoterless GUS gene is randomly integrated into the plant genome. This latter method served as a powerful tool for identifying nematode-triggered gene activation within nematode feeding sites (Barthels et al., 1997) that could be followed by cloning of the associated plant gene to provide insight into the mechanisms of feeding site formation (Grunewald et al., 2008).

While traditional reporter systems like GUS, GFP, and LUC have been influential in studying gene expression, each has drawbacks related to sensitivity, stability, or reliance on external substrates. The recently developed RUBY reporter, which generates a vivid red pigment via betalain biosynthesis, presents a compelling alternative. Its substrate-free, non-invasive, and visually distinct signal makes it especially advantageous for monitoring dynamic biological processes in living plant tissues (He et al., 2020; Yu et al., 2023; Jogam et al., 2024; Kumar et al., 2025). The work described in Chapter 3 demonstrated the general potential of this RUBY reporter system in potatoes and the consistent and stable expression of RUBY driven by the CaMV35S promoter was also confirmed in nematode induced-feeding sites in that plant species.

However, that work only evaluated RUBY expression with the widely used strong, constitutive cauliflower mosaic virus (CaMV35S) promoter (Odell et al, 1985; Benfey et al., 1989; Amack et al., 2022). The CaMV35S promoter offers continuous gene expression which, depending on the transgene being controlled, can lead to metabolic burdens, off-target effects and deleterious effects on the plant (Agarwal et al., 2017). Even with relatively inert reporters such as GUS or GFP, the burden imposed can divert transcriptional/translational resources and potentially affect plant metabolism or growth. The RUBY reporter, on the other hand, is not 'metabolically neutral' and can affect redox status and perturb aromatic amino acid metabolism. High levels of betalain biosynthesis could reduce the pool of tyrosine available for protein synthesis metabolism and also divert precursors from other tyrosine-derived metabolites, such as alkaloids, tocopherols and plastoquinone (He et al., 2020). Such negative impacts were observed in this work (Chapter 3) when RUBY was expressed in Arabidopsis under the control of CaMV35S. Many seeds germinated poorly and the reporter gene construct became progressively silenced in plant tissues when the strong constitutive over-expression presumably became detrimental.

RUBY offers a valuable tool as a visual marker, and potential side-effects associated with its expression under constitutive promoter can be minimized by employing tissue-specific or root-inducible promoters. Such promoters ensure that RUBY is expressed only in target cells or under defined conditions, thereby preventing unnecessary accumulation in non-relevant tissues. In addition, restricting expression to specific sites can help mitigate gene silencing, as overexpression across the whole plant is avoided. A relevant precedent is the MycoRed system, a betalain-based, in vivo and non-invasive reporter driven by a root-inducible AM symbiosis promoter, which has been successfully applied for fungal visualization (Timoneda et al., 2021). By linking RUBY expression to nematode-inducible or root-inducible promoters similar to this approach, a reliable visual marker of infection particularly during the early stages or potentially at later stages could be generated. Such a RUBY system would provide a powerful tool for assessing nematode infection levels in soil-grown plants without the need for destructive staining or microscopy.

Therefore, we investigated promoters from potato genes known to be strongly upregulated in a susceptible potato cultivar during the early stage of potato cyst nematode infection for their potential to direct RUBY expression. Two potato genes, PGSC0003DMG400028755 (PG1) and PGSC0003DMG400010532 (PG2), were selected based on published transcriptomic data showing their significant upregulation in roots by *Globodera* infection (Walter et al., 2018). PGSC0003DMG400028755 was described as encoding a Pit-1

homologue homeobox transcription factor (Walter et al., 2018) although Pit-1 belongs to the POU-homeodomain group, which is absent in plants (Gold et al., 2014). Although its function in plants is not well-characterized, the upregulation of the PG1 homeobox gene in response to potato cyst nematode (PCN) infection suggested a potential role in regulating plant hormone signalling pathways or the host pathogen-interaction.

The second gene PGSC0003DMG400010532 encodes an auxin efflux carrier which has a crucial role in cell enlargement and cell differentiation by regulating polar auxin transport. It might contribute to plant susceptibility to nematode infection, by facilitating the formation of the cyst nematode feeding structure (Walter et al., 2018). Arabidopsis plants with mutations affecting the polar auxin transport system exhibited a significant reduction in cyst nematode infection, suggesting that proper auxin distribution is crucial for the establishment and success of nematode parasitism (Goverse et al., 2000).

The promoters of these genes, selected from a shortlist, are therefore promising candidates for driving nematode-inducible, root-specific transgene expression. Using the *RUBY* reporter gene, we evaluated their spatial and temporal activity to determine their promise for use in a system to report nematode infection akin to the MycoRed system for detecting AMF root colonisation (Timoneda et al., 2021). This approach provides a foundation for developing valuable tools for studying early plant-nematode interactions. Ultimately, these nematode-inducible promoters could also have utility in driving more precise, effective, and publicly acceptable nematode resistance strategies in potato and related crops.

4.2 Aims

- To generate a new RUBY plant transformation vector to facilitate promoter cloning in downstream applications
- To generate new RUBY constructs for testing nematode-responsive potato promoters.
- To investigate RUBY expression in transgenic potato plants derived from newly engineered constructs.
- To monitor RUBY expression dynamics in response to early nematode infection, with the goal of understanding promoter activity under biotic stress.

4.3 Materials and Methods

4.3.1 Generation of new RUBY vector

4.3.1.1 Cloning strategy for new RUBY vector construction

To construct a new vector that would allow introduction of alternative promoter regions to replace CaMV35S, the entire RUBY cassette (~4.0 kb) was amplified from the original CaMV35S construct (Figure 4.1) using PCR to facilitate subsequent directional cloning into the pBI121-GUS vector, replacing the GUS gene with the RUBY cassette.

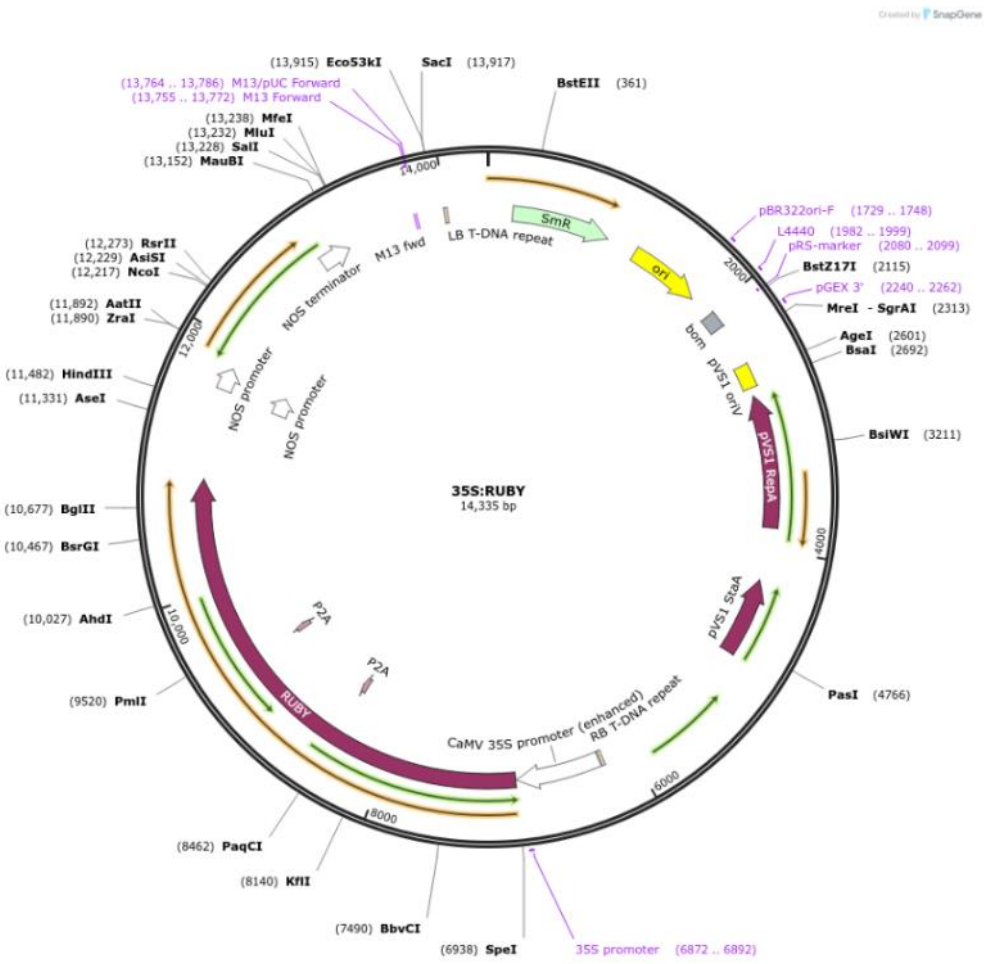

Figure 4.1. 35S:RUBY plasmid map derived from Addgene (Plasmid #160908).

4.3.1.2 Primer design and PCR amplification

The primers used for cloning, sequencing and checking the presence of RUBY are listed in Table 4.1. To optimize translational efficiency in plant systems, a plant-preferred Kozak sequence (AAACAAC, highlighted in red) was introduced immediately upstream of the start codon (ATG) of the RUBY gene in the RUBY Clone F primer. This primer also contained a XbaI restriction site (bold), whilst the RUBY Clone R primer contained a SacI restriction site (bold).

The entire RUBY cassette was amplified from the original 35S:RUBY plasmid DNA using RUBY Clone F and RUBY Clone R primers (Table 4.1) with 2X Phusion Mastermix (New England Biolabs) (**section 2.4.5**). The amplified DNA was analyzed by agarose gel electrophoresis (**section 2.4.6**), and the DNA product was purified using the E.Z.N.A Cycle Pure Kit (Omega Bio-Tek, USA) (**section 2.4.7**).

Table 4.1. Primer Sequences Used for RUBY Sequencing and Vector Construction

Use	Name of primer	Primer sequence
Confirming RUBY presence	RUBY check F	ATCCTCGCGATCTGGTTCAT
	RUBY check R	GCCGGCTGTAACACTATTCG
Amplification and cloning of RUBY cassette	RUBY Clone F	ACA**TCTAG**AAACAACATGGATCATGCGACCCTC
	RUBY Clone R	ACA**GAGCTC**TCACTATCACTGGAGGCTTG
Internal sequencing of RUBY clones	RUBY SEQ F	GATACCACATCCTCCACATTC
	RUBY SEQ R1	AACTTATGGTTCTCTGGGAAG
	RUBY SEQ R2	AGGACGGAGTCCGGCTCTTTG
Universal primers used for RUBY clone sequencing	M13 F	GTAAAACGACGGCCAGT
	M13 R	GGAAACAGCTATGACCATG
Internal sequencing of promoter clones	RUBY-PG2-SEQ2	GATGCACGGCGGTAATCTTG

4.3.1.3 A-tailing of PCR products

Phusion™ high-fidelity DNA polymerase generates blunt ends during amplification of DNA fragments. To resolve this and allow cloning into a T-vector, PCR amplified clean products were A-tailed to create A-overhangs (sticky ends) for use in cloning into the pGEM®-T Easy vector (Promega, USA). The A-tailing reaction was carried out by incubating the purified PCR

product (27 µl) with 4 µl of 10x Taq polymerase buffer, 4 µl of 2mM dATP, 1 µl of Taq polymerase, and 4 µl of ELGA water at 72 °C for 20 minutes.

4.3.1.4 Ligation

A-tailed fragment (3 µl) was directly ligated into 50 ng (1 µl) of pGEM®-T Easy vector with 1 µl of T4 DNA ligase, 5 µl of ligation buffer (2x). The total 10 µl ligation reaction was incubated at room temperature for one hour.

4.3.1.5 Transformation of *E. coli* competent cells

E. coli competent cells (DH5α strain, Invitrogen™ One Shot™ Top 10) were transformed by the heat shock method as described in **section 2.5.1** using 1 µl of ligation reaction mixture. Transformed cells were plated onto LB agar plates with ampicillin at a concentration of 100 µg/mL and X-gal (5-bromo-4-chloro-3-indolyl-β-D-galactopyranoside) at 40 µg/mL, then incubated overnight at 37°C.

4.3.1.6 Colony screening

Blue-white selection was employed initially to screen successful ligations. These screenings allowed for visual differentiation based on disruption of the gene within the multiple cloning sites of the pGEM-T easy vector. White colonies disrupted the coding sequence of lacZα and prevented β-galactosidase production that would otherwise incite hydrolysis of X-gal. Therefore, white colonies indicated successful DNA insertion, whereas blue colonies indicated an empty vector by retaining the intact lacZα gene. Several white colonies were cultured overnight in 5 mL of LB liquid medium in the presence of ampicillin for subsequent extraction of plasmid DNA (**section 2.5.4**).

4.3.1.7 Plasmid digestion

Twelve miniprep DNA samples were digested with EcoRI restriction enzyme, which cleaves on either side of the cloning site, in CutSmart buffer (New England Biolabs) to determine the successful cloning of the RUBY insert. The specific digestion reaction conditions are described in **section 2.5.5**. The digested products were analysed by 1% agarose gel electrophoresis as described in **section 2.4.6**, allowing visual confirmation of the expected fragment sizes.

4.3.1.8 Sequencing

DNA of the putative successful clones was prepared according to the guidelines (50 ng/µl) and sent to Genewiz from Azenta Life Science for sequencing. Initial sequencing was performed with universal M13F and M13R primers (Table 4.1), which flank the multiple

cloning site of the pGEM vector. Due to the large size of the RUBY cassette, the initial sequencing runs did not overlap. To bridge the sequencing gap, one forward and two reverse primers were designed (Table 4.1) based on known flanking sequences. These primers were used in subsequent sequencing reactions to ensure complete coverage of the RUBY cassette.

Overlapping sequence reads for each cloned RUBY insert were assembled into a single contiguous sequence and converted to protein sequence using the Expasy translate tool. Amino acid sequences were aligned using Clustal Omega software. For subsequent steps, clones with complete length coverage and 100% protein sequence fidelity were selected.

4.3.1.9 Clone selection and validation

Following sequence analysis, Clone 4 was selected as a representative for further validation and use in subsequent cloning. The plasmid DNA was subjected to digestion with XbaI and SacI restriction enzymes, both singly and together in CutSmart buffer (New England Biolabs). The digested products were electrophoresed (**section 2.4.6**) to confirm successful digestion.

4.3.1.10 Cloning of RUBY into pBI121-GUS vector

After restriction digestion and sequence validation, the pBI121-GUS vector and the chosen RUBY clone were digested using XbaI and SacI as above. The two digested vectors were purified using the E.Z.N.A® Cycle Pure Kit (**section 2.4.7**). Subsequently, ligation was performed using 10x ligation buffer (1µl), T4 DNA ligase (1µl), pBI121 vector (4µl), and pGEM:RUBY (4µl). The reaction mixture was incubated at room temperature for 2 hours, followed by 4°C overnight. DH5α *E. coli* competent cells were transformed as described in **section 2.5.1**, and the cells were grown on LB agar plates containing kanamycin. Minipreps were performed to extract transformed plasmid DNA following the guidelines of the E.Z.N.A® Plasmid DNA Mini Kit. The successful insertion of the RUBY cassette into the pBI121 vector was verified by digestion with XbaI and SacI enzymes and gel electrophoresis.

4.3.1.11 *Agrobacterium* infiltration for transient gene expression in tobacco

For this, three clones were introduced into *Agrobacterium tumefaciens* strain GV3101 for detecting functional expression of the pBI121:RUBY construct using the freeze–thaw method (**section 2.5.2.2**).

Tobacco (*N. benthamiana*) seeds were sown in compost and grown in glass house conditions at 22°C. After 2-3 weeks seedlings were transplanted into individual pots of compost and grown for a further 3-4 weeks. Overnight-grown *Agrobacterium* cultures (LB medium at 28°C)

were harvested by centrifugation and resuspended in infiltration buffer (10 mM MES, 10 mM $MgCl_2$, 150 µM acetosyringone) to an OD_{600} of 0.5–0.8. Leaf infiltration was performed by inoculating into the lower epidermis of tobacco leaves with a needleless 1 ml syringe. One plant was used for each pBI:RUBY clone. The plants were maintained under glasshouse conditions (22°C, 16 h light/8 h dark), and RUBY expression was confirmed visually after 24-72 hours of inoculation. Images were taken, and the clones showing clear red pigment development validated the functionality of the new pBI:RUBY vector.

4.3.2 Generation of nematode-responsive RUBY reporter constructs

4.3.2.1 Selection of potato promoters

Two nematode-responsive potato genes (PG1 and PG2) were selected based on prior transcriptomic data indicating their strong upregulation in root tissue during susceptible interactions with potato cyst nematodes (Walter et al., 2018) (Table 4.2). PG1 encodes a homeobox transcription factor, and PG2 encodes an auxin efflux carrier implicated in nematode feeding structure formation.

Table 4.2. Details of two selected potato genes

Gene	Gene code ID	Upregulation time	Potato variety	Gene function
PG1	PGSC0003DMG400028755	48 hours after inoculation	Desiree	Homeobox transcription factor
PG2	PGSC0003DMG400010532	48 hours after inoculation	Desiree	Auxin efflux carrier

4.3.2.2 Cloning of potato promoters into pBI121: RUBY construct

For this, the sequences of the predicted promoter regions of potato genes PG1 (2kb) and PG2 (1.7 kb) were synthesised by Azenta Life Sciences and cloned into pUC-GW-Amp vectors (Gateway® recombination sites and an ampicillin resistance gene) (Figure 4.2). A HindIII restriction site was included at the 5’ ends of the promoter sequences and a XbaI site at the 3’ ends to allow subsequent cloning into the newly constructed pBI121:RUBY vector.

As the PG1 promoter region has two internal XbaI sites, partial digestion was performed to selectively cleave at only the 3’ site, avoiding complete fragmentation of the insert. This allowed isolation of the desired fragment between a specific XbaI site and the single HindIII site for efficient downstream cloning (Figure 4.2). For this, approximately 4 µg (8 µL) of the PG1 promoter clone was digested in a total volume of 40 µL using NEB 2.1r buffer and 2 µL

of HindIII to ensure complete digestion. The reaction was incubated at 37 °C for 2 hours, after which 2 µL was removed to serve as a HindIII single-digest control for gel electrophoresis. Subsequently, 0.5 µL of XbaI was added directly to the same reaction to perform a partial double digestion. At 1, 3, 5, and 10 minutes post-addition, 10 µL aliquots were removed and immediately mixed with 3 µL of loading dye containing additional EDTA to halt enzyme activity. The dye mix was prepared in a 2:1 ratio of 6× loading dye to 0.5 M EDTA. All partial digests, along with the HindIII-only control, were run on two separate agarose gels. The target DNA band was identified based on expected size and isolated from the 5-minute and 10-minute digests on each gel. DNA fragments were purified using the MicroElute Gel Extraction Kit (**section 2.4.7**). The eluates from the first gel were combined into 20 µL, which was subsequently used to elute DNA from the gel slices of the second gel to increase final concentration. For ligation, 3 µL of the double-digested pBI vector (described below) was combined with 5 µL of the purified promoter fragment and 8 µL of NEB Instant Ligation Mix.

For PG2 cloning, the promoter clone and pBI121: RUBY DNA were subjected to double digestion with XbaI and HindIII. Each 20 µL reaction contained 3 µL promoter plasmid or 8 µL of pBI121:RUBY plasmid, 1 µL each of XbaI and HindIII, 2 µL of 10× CutSmart® Buffer, and nuclease-free water to volume. The digested plasmid DNAs were purified using the either the Cycle Pure (PG2 clone) or Microelute Cycle Pure (pBI121: RUBY) protocol (**section 2.4.7**). The purified pBI121: RUBY vector DNA (3 µL) was ligated with purified promoter plasmid DNA (PG2) using T4 DNA ligase, as described in **section 2.5.6**.

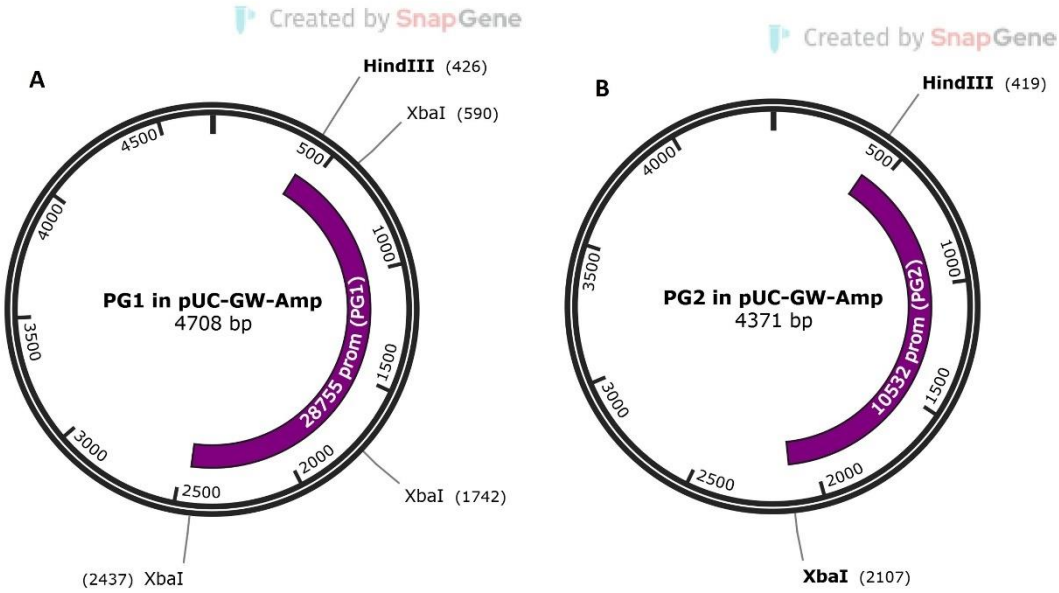

Figure 4.2. Illustration of vector maps of PG1-pUC-GW-Amp and PG2-pUC-GW-Amp constructs.

A) PG1-pUC-GW-Amp construct highlighting the 2 kb PG1 promoter regions with one HindIII and three XbaI restriction sites.

B) PG2-pUC-GW-Amp construct representing the 1.7 kb PG2 promoter regions with one HindIII and one XbaI restriction site.

4.3.2.3 *E. coli* competent cells transformation and sequencing analysis

E. coli competent cells (Stellar HST08 strain, Takara Bio Inc.) were transformed with the PG1 and PG2 ligation products (described in **section 2.5.1**). The transformed colonies were selected on LB agar plates supplemented with kanamycin (Table 2.1). Putative recombinant clones were cultured overnight in LB broth containing kanamycin, and minipreps were performed to isolate plasmid DNA (**section 2.5.4**).

To assess successful integration of the promoter regions into the pBI121:RUBY vector backbone, and replacement of the CaMV35S promoter, extracted plasmids were digested with XbaI and HindIII enzymes, and the resulting fragments were analyzed by agarose gel electrophoresis (**section 2.4.6**). Potentially correct clones were subjected to Sanger sequencing using the primers listed in Table 4.1 to further validate correct construct assembly. Sequence alignments confirmed proper orientation and integrity of the insert.

4.3.3 *Agrobacterium* Transformation

The validated pBI:PG1-RUBY and pBI:PG2-RUBY constructs were introduced into *Agrobacterium tumefaciens* (GV3101) using the freeze–thaw method (**section 2.5.2.2**). Both of the constructs were also introduced into *Agrobacterium rhizogenes* (R1000) for hairy root potato transformation using the electroporation method as described by Shen and Forde (1989).

To confirm successful Agrobacterium transformation with pBI:PG1-RUBY and pBI:PG2-RUBY, colony PCR (**section 2.5.3**) was conducted to amplify a short region of the RUBY DNA of interest using OneTaq® PCR Master Mix (New England Biolabs) (Table 2.2), with RUBY check primers (Table 4.1). Then PCR products were verified in 1% agarose gel electrophoresis (**section 2.4.6**).

4.3.4 Potato Transformation

4.3.4.1 Potato transformation using *Agrobacterium tumefaciens*

Transformed *Agrobacterium* colonies were cultured first in 5 mL of LB medium with kanamycin at 28°C overnight then 2 mL of this culture was used to inoculate 20 mL of the same medium which was again incubated at 28°C overnight the day before transformation. Four-week-old potato plants (‘Desiree’) grown in sterile culture on Multiplication Medium in magenta pots were used to prepare stem explants (0.5–1 cm). Multiplication Medium is LS basal medium with vitamins, 30 g/L sucrose, pH5.8 solidified with 5.5 g/L plant agar. The

explants were incubated for 15 minutes in an *Agrobacterium* suspension prepared by combining 5 mL of Agrobacterium culture with 45 mL of liquid MS30 basal salts with Gamborgs B5 vitamins. After removing the solution with a sterile syringe, explants were co-cultivated for 2 days on Co-Culture Medium with sterile filter paper placed on top of the agar. Co-Culture Medium is 0.1x MS basal salts, 1x Nitsch vitamins, 10 g/L sucrose, pH5.8, solidified with plant agar. Explants were then transferred to Callus Induction Media, which is MS30 containing NAA (0.1 mg/L), zeatin riboside (5mg/L), cefotaxime (500 mg/L), $AgNO_3$ (10 mg/L), and incubated at 19°C for three days. Explants were then transferred to fresh plates of Co-Culture Medium containing kanamycin (100 mg/L) for a further week. They were moved to Shoot Induction Media (SIM), MS30 with Gibberellic acid (0.3 mg/l), zeatin riboside, cefotaxime, and kanamycin for 4 weeks. Due to poor shoot regeneration, explants were subsequently cycled through SIM without zeatin riboside for two more weeks. The developing shoots were moved to 1/2 MS20 with kanamycin and cefotaxime for root development. If rooted, plants were then multiplied on MS30 media for further use.

4.3.4.2 Generation of potato hairy roots using *Agrobacterium rhizogenes*

Transformed *Agrobacterium* colonies were cultured in LB medium with kanamycin at 28°C for two days**.** Leaves from 4-week-old potato plants grown in sterile culture on solid MS20 medium were wounded with shallow cuts and incubated in *A. rhizogenes* suspension (½ MS30 medium) for 10 minutes. After rinsing (½ MS30 liquid medium) and blotting on sterile filter paper, leaves were placed on solid ½ MS30 medium with the abaxial side in contact with the medium. The plates were incubated at 20°C for 2–3 days in the dark. Infected leaves were then transferred to selection medium (½ MS30) containing kanamycin (50 mg/L) and cefotaxime (250 mg/L). Hairy roots emerging from wound sites were excised once they reached approximately 1 cm and sub-cultured individually on fresh selection medium. Root lines were maintained at 20°C in the dark and sub-cultured regularly by transferring fresh root tips onto new plates.

4.3.5 Monitoring transgenic potato plants for RUBY expression

Transgenic potato plants generated with pBI:PG1-RUBY and pBI:PG2-RUBY constructs were monitored for RUBY expression both visually and under a microscope. Red pigmentation, indicative of RUBY gene expression, was assessed in regenerated shoots and roots. Visual screening was conducted under natural and white LED light, while several roots were examined using a Leica M165 FC microscope to detect subtle expression patterns and imaged using GXCapture-T. Plants showing no visible pigmentation were randomly selected and their

transgenic status confirmed by PCR analysis. To confirm the presence of the RUBY gene, genomic DNA was extracted from leaves of all putative transgenic lines using the E.Z.N.A.® Plant DNA Kit protocol (**section 2.4.1**) and subjected to PCR analysis using RUBY check primers (Table 4.1).

4.3.6 Infection of transgenic potato roots with *G. pallida* in tissue culture and growth pouch

For the initial infection trial, one hairy root-transformed line carrying the pBI:PG1-RUBY construct and another *A. tumefaciens*-mediated transgenic plant lines carrying the pBI:PG2-RUBY construct was infected with *G. pallida*. The J2s were surface sterilized following the procedure described in **section 2.1.3.1**. A 30 µl aliquot of nematode suspension was applied to each root, applied across multiple sites on the root system. The plates were left to dry before being sealed with micropore tape and placed vertically and grown at 22 °C under a 16-hour light cycle. Plants grown under growth pouch conditions were infected using the same procedure described in **section 3.3.4.2.** In the time course of infection with nematodes, the plants were visualized for the infection under the microscope without staining. The infected roots were monitored after 48 hours, 4 dpi, 7 dpi and 2 weeks post infection and imaged using a Leica M165 FC microscope with GXCapture-T software. Red root signals were selectively enhanced by adjusting hue and saturation in GIMP 3.0.4, improving visual clarity and supporting more accurate RUBY detection.

4.4 Results

The RUBY reporter gene cassette, which was used in Chapter 3, encodes the coordinated expression of the betalain biosynthesis-related CYP76AD1, DODA, and Glucosyl Transferase genes to express a visible red pigment. Unfortunately, the existing vector with the CaMV35S promoter (He et al., 2020) had no suitable restriction sites for replacement of the 35S promoter that would allow the use of this reporter system with alternative, nematode-responsive promoters. Whilst a SpeI site was present at the 3' end of the 35S promoter, there was no unique site available at the 5' end (Figure 4.1). To initially address this, we explored introducing an XbaI site using site-directed mutagenesis. A suitable sequence location was identified where only two nucleotide substitutions were necessary to create the XbaI site, thereby minimizing the potential disruption to existing coding or regulatory elements. However, most likely due to the large size of the plasmid (>14 kB), this approach was unsuccessful, and no clones were recovered that included the desired change. An alternative strategy was therefore designed to amplify the entire RUBY three-gene cassette by PCR and at the same time add unique restriction sites to the primers so that the reporter could be transferred to an alternative plant transformation vector. This would also have the advantage of being able to use kanamycin selection for potato transformation, which is more robust and reliable than hygromycin in our hands.

4.4.1 Amplification and cloning of RUBY expression cassette

Gene-specific cloning primers were designed (Table 4.1) to target the RUBY coding region and PCR amplification was conducted using Phusion™ high-fidelity DNA polymerase, selected for its proof-reading ability and high accuracy in amplifying large target DNA (4.0 kb). Agarose gel electrophoresis of the PCR product confirmed amplification of the expected target DNA size corresponding to the RUBY cassette (Figure 4.3). This PCR reaction was cleaned and used as a template in the A-tailing reaction. The DNA overhangs allowed successful cloning into the pGEM-T Easy vector.

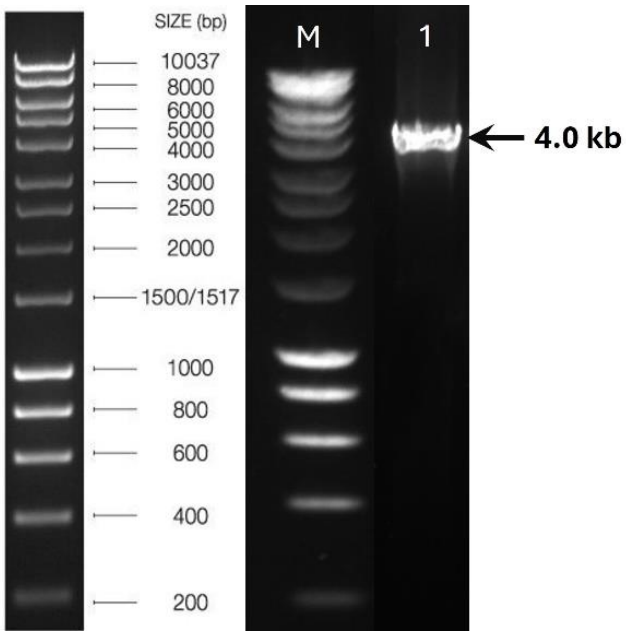

Figure 4.3. Successful amplification of RUBY DNA to clone into pGEM-T-Easy vector.

M= DNA marker (1 kb ladder).

Lane 1 is the amplification of RUBY DNA with an expected size of 4.0 kb.

4.4.2 Restriction analysis and sequence verification of pGEM:RUBY clones

Twelve selected clones that provided white colonies after *E. coli* transformation were subjected to EcoRI restriction digestion of the recombinant pGEM-T Easy vector. This showed that 11 of the 12 plasmids produced two distinct bands of the expected sizes on agarose gel electrophoresis and most likely contained the RUBY insert (Figure 4.4 A). Whereas Clone 10 contained a DNA insert of only ~250 bp (Figure 4.4 A), indicating that it did not harbour the desired insert. Although not all of the vector and insert bands resolved well in the first gel, subsequent analysis of nine clones confirmed that one band corresponded to the vector backbone (3.0 kb) and the second to the insert (4.0 kb), which was consistent with the expected size of the RUBY cassette (Figure 4.4 B). The absence of additional bands confirms that there were no internal EcoRI sites within the insert, and the insert was cloned in full. This result verified the successful insertion of the RUBY cassette into the pGEM-T Easy vector in nine clones.

All twelve clones were submitted for sequencing with M13F and M13R primers. Out of these, Clone 2 failed to produce any readable sequence, whilst Clones 1 and 7 produced poor quality sequence and, as expected, Clone 10 produced sequence that did not align with the expected RUBY sequence. Multiple amino acid sequence alignment of the eight remaining clones revealed that the terminal regions of the inserts all showed homology with the RUBY amino acid sequence confirming successful cloning (Figure 4.5). The central portion of the RUBY insert was not covered by the sequencing due to its large size (4.0 kb), which exceeds the typical read length limitations of standard Sanger sequencing. To resolve this, one forward sequencing and one reverse sequencing primer were designed for all eight clones, with an additional reverse primer designed for Clones 8 and 9 that yielded shorter sequences from the first run (Figure 4.5). Therefore, these clones were selected for additional sequencing to get the complete RUBY sequence and allow confirmation that the PCR amplification step had not introduced any errors.

Complete, high-quality sequence covering the entire RUBY cassette was finally obtained for five clones and no mutations, truncations, or frame shifts were detected, confirming the integrity and correctness of the cloned inserts. Since all clones were identical, Clone 4 was selected for downstream subcloning into the pBI121 vector backbone.

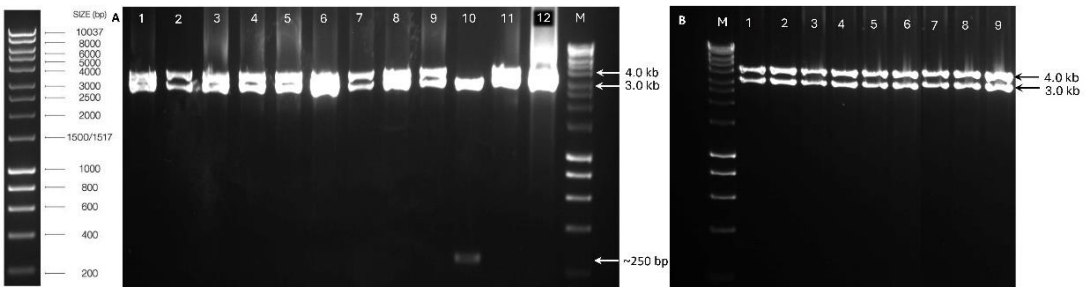

Figure 4.4. Digestion of pGEM-T-Easy vector containing the RUBY cassette with EcoRI restriction enzyme.

A) Digestion of 12 recombinant clones potentially harbouring the RUBY gene cassette, where Clone 10 exhibited a non-specific 250 bp DNA fragment. To obtain more clearly resolved bands nine clones were subjected to further gel electrophoresis as shown in **B)** Nine clones clearly displayed two distinct bands of approximately 4 kb corresponding to the RUBY insert and 3 kb band of the vector backbone. M= DNA marker (1 kb ladder).

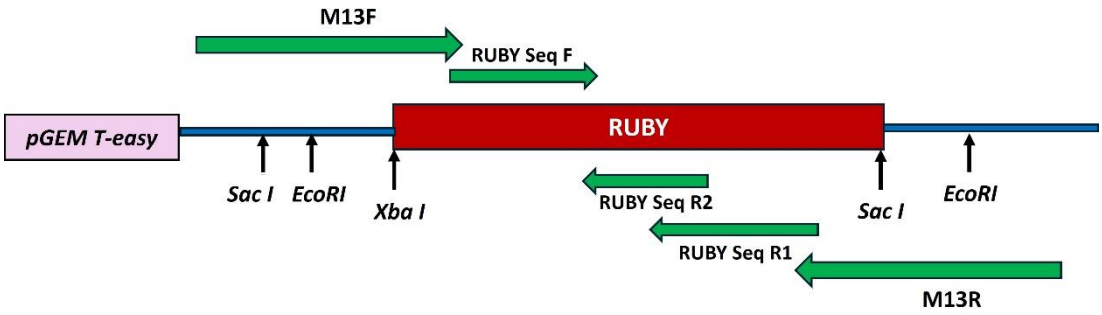

Figure 4.5. Sequencing strategy of RUBY cloned into pGEM T-easy vector.

Restriction enzyme sites utilised for checking successful ligation or for subcloning into pBI121 are highlighted together with the different primers used to generate the complete insert sequence.

M13F and M13R recovered the terminal regions of RUBY sequence, while RUBY Seq F, RUBY Seq R1 and RUBY Seq R2 primers recovered the internal sequence of original RUBY, thereby confirming successful cloning.

4.4.3 Transfer of the RUBY cassette into the pBI121 vector

The RUBY cassette was next transferred as a XbaI-SacI fragment from the pGEM vector to the binary vector pBI121, which contains the GUS gene under control of the CaMV35S promoter. This vector confers kanamycin resistance in the plant as the selectable marker. The functionality of the introduced XbaI and SacI sites in the selected pGEM:RUBY Clone 4 was first confirmed by digesting with the single enzymes separately. This was necessary as, due to the random orientation of the RUBY cassette in Clone 4, digestion with SacI alone would also release a DNA fragment of the correct size. The agarose gel electrophoresis showed two distinct bands upon digestion with SacI. The approximately 3 kb fragment size corresponds to the vector backbone and 4 kb for RUBY insert (Figure 4.6 A). More importantly, digestion of Clone 4 with XbaI produced a single band migrating slightly above 7 kb (Figure 4.6 A), which was consistent with the linearization of plasmid DNA at a single XbaI site. The pGEM:RUBY clone was then digested with both XbaI and SacI for subsequent cloning, and an aliquot of the digest was checked before proceeding. Upon double digestion, the plasmid was expected to cut into three fragments, however, approximately 3 kb, 4 kb fragments were clearly visible and another fragment of 50 bp was not recovered in the gel (Figure 4.6 B).

The vector pBI121-GUS was also digested with XbaI and SacI to remove the GUS reporter gene and replace it with the digested RUBY reporter gene. The purified, digested RUBY and pBI121 vectors were ligated and transformed into *E. coli* competent cells. Restriction digestion with XbaI and SacI confirmed successful ligation of the RUBY gene into the pBI121 vector. Three of four clones produced the expected digestion products, yielding distinct bands of approximately 12.86 kb for the vector backbone and 3.97 kb for the RUBY insert, thereby validating successful sub-cloning (Figure 4.7). A schematic presentation of the vector map of pBI:RUBY highlights cloning of the RUBY cassette into pBI121 binary vector in place of the GUS cassette (Figure 4.8).

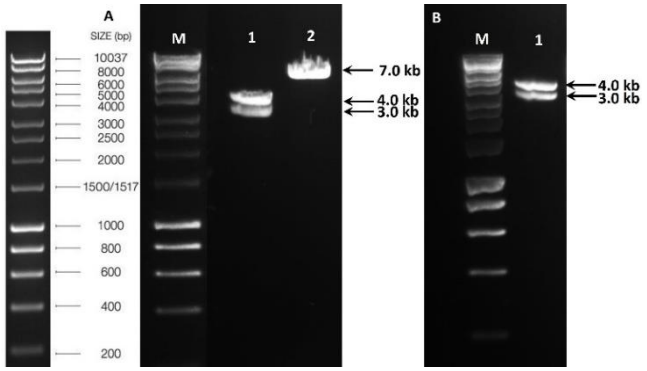

Figure 4.6. Digestion of pGEM-T easy recombinant with RUBY using XbaI and SacI.

A) Lane 1 represents single digestion with SacI which produced bands of approximately 3 kb and 4 kb corresponding to the size of vector and RUBY insert, respectively, confirming the presence of two SacI sites. Lane 2 shows pGEM:RUBY digested with XbaI where a single band of approximately 7 kb band, indicates successful digestion and plasmid linearisation. **B)** Double digestion with SacI and XbaI produced bands of approximately 3 kb and 4 kb of vector and RUBY insert size, respectively (Lane 1). M= DNA marker (1 kb ladder)

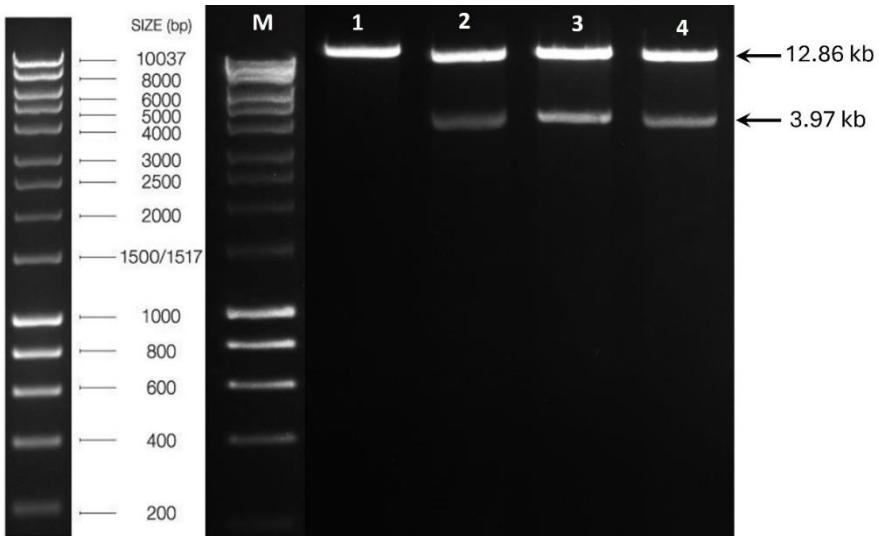

Figure 4.7. Restriction digestion of pBI121 recombinant vector containing RUBY using Xba1 and Sac1 enzymes.

M= DNA marker (1 kb ladder). Three clones (lanes 2-4) revealed successful digestion of pBI:RUBY plasmid producing two distinct bands of 12.86 kb and 3.97 kb corresponding to vector and insert size. Lane 1 produced only one band most likely indicating digestion at only one site. The three positive clones were subjected to Agrobacterium infiltration for RUBY expression.

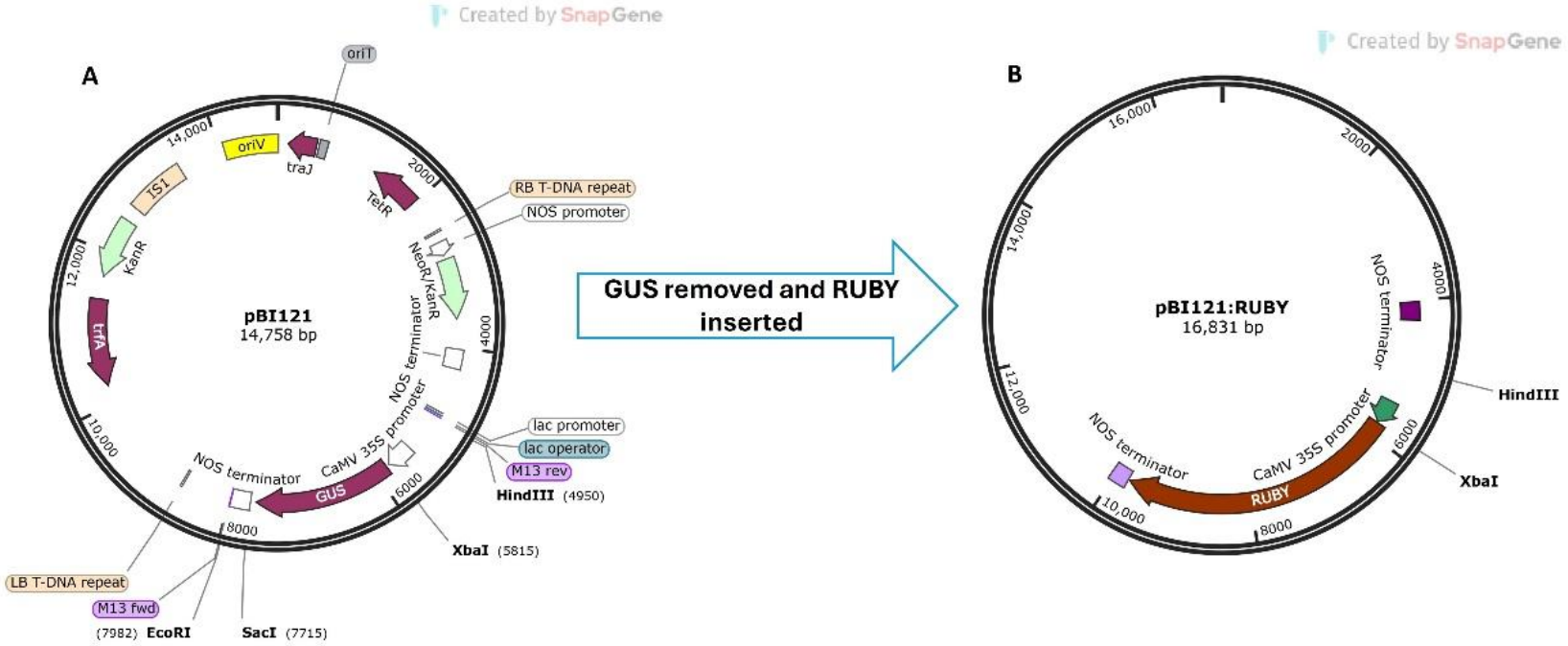

Figure 4.8. Schematic presentation of vector map of pBI121:RUBY as derived from cloning RUBY into pBI121 binary vector.

A) The original pBI121 vector demonstrating the GUS reporter gene under control of the CaMV35S promoter, which was digested at SacI and XbaI sites to excise the GUS cassette.

B) Recombinant pBI121 vector with RUBY reporter in place of GUS. CaMV 35S promoter, XbaI and HindIII restriction sites are highlighted in the map.

4.4.4 RUBY expression through Agrobacterium-mediated infiltration

To confirm that the RUBY cassette was still functional after transfer into the pBI121 vector, transient expression in *N. benthamiana* leaves via Agrobacterium transformation was performed. We introduced each of the three recombinant pBI:RUBY plasmids into the *Agrobacterium* strain GV3101 and subsequently infiltrated them into young leaves of tobacco. After infiltration, we observed clear phenotypic RUBY expression at 24 to 72 hours of inoculation. The infiltrated leaf areas of all the clones showed a noticeable red patch, consistent with the expected phenotype from RUBY gene expression. Temporal differences in expression patterns were observed among the three selected clones. Clone 2 expressed RUBY after 24 hours post-inoculation, Clone 3 after 48 hours, whilst Clone 4 expressed RUBY after 72 hours. Notably, clone 2 and clone 3 demonstrated strong RUBY expression, whereas clone 4 exhibited weaker expression (Figure 4.9). This expression acted as a visual marker, confirming that the RUBY gene cassette was successfully added to the vector and was also active in the plant. Clone 2 was therefore selected for further plasmid construction using potato promoters.

4.4.5 Development of a RUBY construct driven by potato promoters

Now that we had a RUBY vector with suitable restriction sites for introducing alternative promoters of interest, a shortlist of potential genes was collated from the literature. We wanted to test promoters that had not previously been characterised and so focused on transcriptomic studies of the early interaction of PCN with potato roots (Walter et al., 2018). The list of up-regulated genes reported in that work was first triaged by checking the genomic sequence for each gene and discounting any that had large regions of missing data in either the coding region or promoter region. The predicted amino acid sequences were subjected to BLAST analysis to determine if the gene model was likely to be correct, fused or truncated. For genes that were still retained, we focused on the N-terminal of the predicted protein to assess if the start codon was predicted correctly so that we could be confident in our designation of the promoter region. This process resulted in a final group of three genes of interest with confident gene models that had 1.7-2 kb of upstream region that did not overlap coding regions of other genes. After unsuccessful attempts to clone these promoters from potato genomic DNA, the promoter regions of two genes, designated PG1 and PG2 were synthesised and cloned into the plasmid vector pUC-GW-Amp.

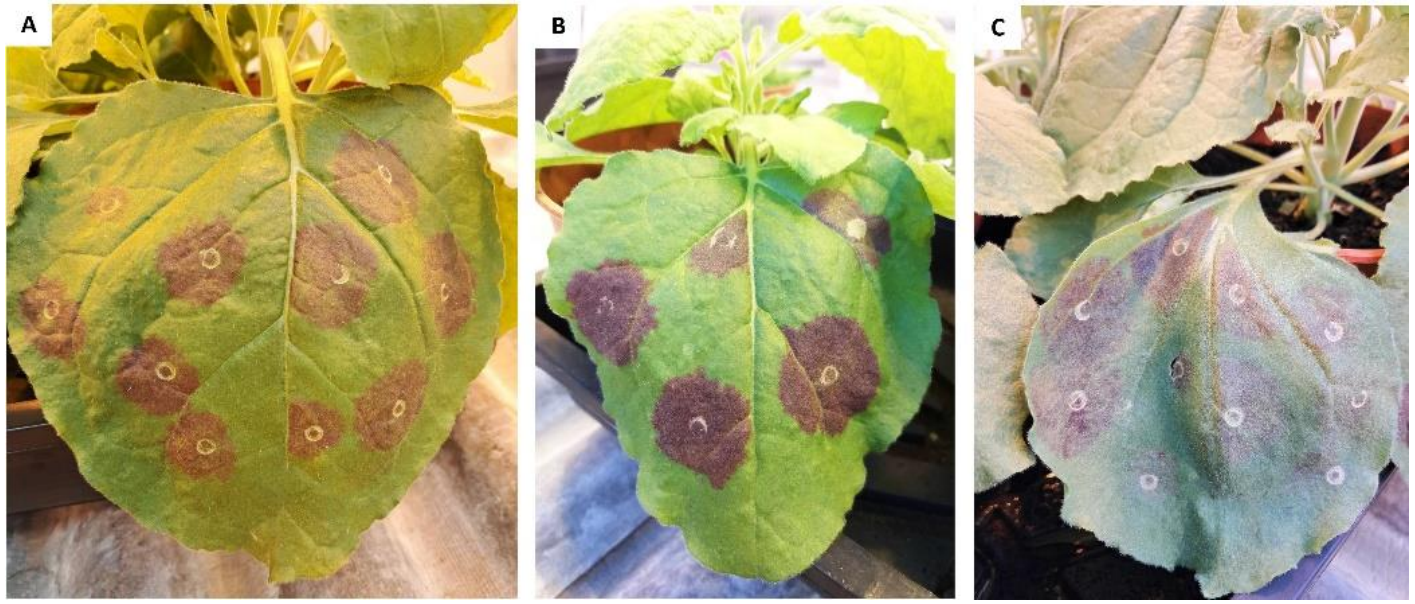

Figure 4.9. RUBY expression in tobacco leaves using pBI121:RUBY clones derived from Agrobacterium-mediated infiltration.

Noticeable red patches confirmed RUBY expression after 48 hours for Clone 3 **(A),** 24 hours for Clone 2 **(B)** and 72 hours for Clone 4 **(C)**.

The promoter fragments were excised through restriction digestion using XbaI and HindIII and agarose gel electrophoresis confirmed the presence of the expected DNA fragment sizes.

As the PG1 promoter sequence contained additional XbaI sites, partial digestion using XbaI in combination with a complete HindIII digest was performed to isolate the complete PG1 promoter fragment from the pUC-GW-Amp vector. The expected fragment size, corresponding to the region between the HindIII site at 426 bp and the XbaI site at 2437 bp, was approximately 2.0 kb, encompassing the full 2037 bp PG1 promoter (Figure 4.10). Agarose gel electrophoresis of time-course partial digests (1, 3, 5, and 10 minutes) revealed multiple digestion products, with a distinct ~2.0 kb band observed prominently in the 5-minute and 10-minute samples. The ~2.0 kb bands from both gels were excised and purified for downstream cloning.

Double digestion of the PG2 from pUC-GW-Amp vector with XbaI and HindIII restriction enzymes produced the expected fragments of interest: a 2.7 kb vector backbone and 1.7 kb promoter fragment (Figure 4.11). In addition, similar digestion of the pBI:RUBY vector to release the CaMV35S promoter ready for cloning produced a 16 kb vector backbone fragment and 865 bp of 35S promoter fragment, representing successful digestion (Figure 4.11).

Both of these promoter regions were successfully ligated into the pBI:RUBY binary vector, replacing the 35S promoter region. The recombinant constructs were transformed into *E. coli*, and eight colonies were screened by restriction digestion of miniprep DNA using XbaI and HindIII, followed by gel electrophoresis. In the case of the PG2 promoter, six clones (Clones 1, 2, 3, 6, 7, 8) successfully produced an approximately 16 kb vector backbone and a 1.7 kb promoter fragment. In contrast, DNA from minipreps 4 and 5 appears to contain both the pBI and pUC-GW-AMP vector backgrounds, a possible occurrence when mixing two plasmids in a ligation reaction (Figure 4.12 A). On the other hand, only one of the PG1 promoter clones contained the desired insert, with fragments of 1.15 kb, 695 bp and <200 bp excised from the vector, consistent with the presence of three XbaI sites within the promoter sequence (Figure 4.12 B). The remaining PG1 clones predominantly produced bands corresponding to the 35S promoter, indicating unsuccessful cloning. Based on these findings, Clones 2 and 6 of the PG2 promoter, as well as Clone 5 of the PG1 promoter, were selected for sequencing analysis.

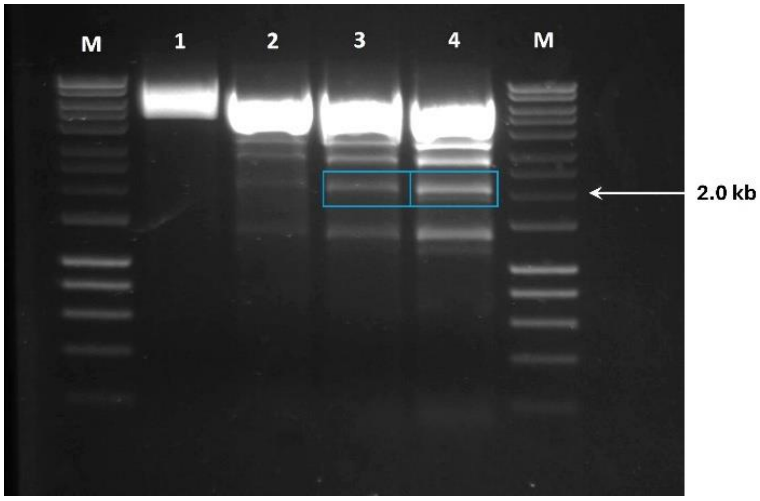

Figure 4.10. Partial digestion of PG1 promoter clone with XbaI restriction enzyme to isolate desired DNA fragment. Lane 1: HindIII control only, **Lane 2:** 3 mins digestion with XbaI, **Lane 3:** 5 mins digestion with XbaI. **Lane 4:** 10 mins digestion with XbaI. The ~2 kb band corresponding to the complete PG1 promoter region was excised for further cloning into the pBI:RUBY vector. M= DNA marker (1 kb ladder).

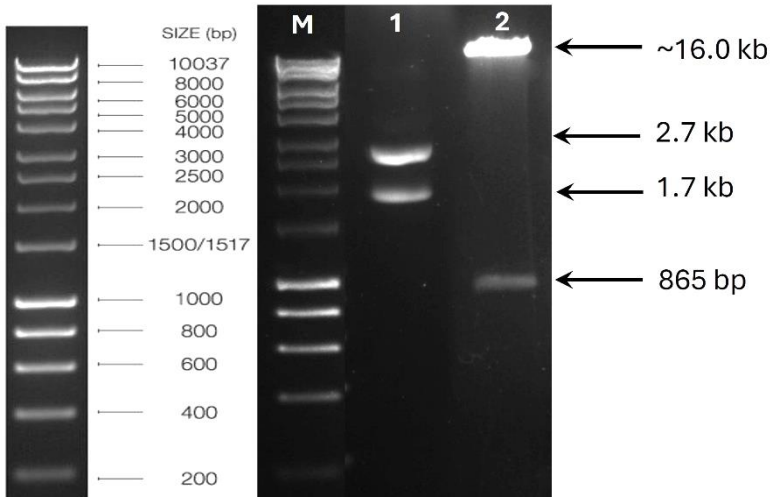

Figure 4.11. Double digestion of PG2 promoter clone and pBI:35S-RUBY with HindIII and XbaI restriction enzymes. Lane 1 (PG2 clone) produced 1.7 kb band corresponding to the size of the PG2 promoter and a 2.7 kb band representing the vector backbone. Lane 2 (pBI:35S-RUBY) exhibited an obvious 865 bp 35S promoter fragment and ~16 kb vector backbone upon double digestion. M= DNA marker (1 kb ladder).

Sequencing analysis of PG2:RUBY Clone 2 and Clone 6 and PG1:RUBY Clone 5 confirmed the correct insertion and orientation of the respective promoter fragments. All sequences matched the expected reference, specifically verifying the integrity of the junction between the promoter region and the RUBY gene, indicating successful cloning and integrity of the promoter regions. These results confirm the successful cloning of both PG1 and PG2 promoters for downstream applications. The vector map demonstrated the features of the new pBI:PG1-RUBY and pBI:PG2-RUBY constructs derived from pBI:35SRUBY construct (Figure 4.13).

4.4.6 *Agrobacterium* transformation using pBI:PG1-RUBY and pBI:PG2-RUBY constructs

Agrobacterium transformation was successfully carried out using the new binary constructs pBI:PG1-RUBY and pBI:PG2-RUBY. Both constructs showed efficient transformation into *A. tumefaciens* strain GV3101. This was confirmed by colony PCR, which amplified the RUBY DNA of interest. Among 16 tested colonies transformed with the pBI:PG1-RUBY construct, 8 colonies demonstrated strong amplification of the RUBY gene. An additional 5 colonies showed faint RUBY bands, while the remaining 3 colonies failed to amplify the RUBY fragment (Figure 4.14 A). For the pBI:PG2-RUBY construct, colony 15 exhibited a strong RUBY band comparable to the positive control, and 6 additional colonies also showed successful amplification. The remaining colonies did not produce detectable RUBY bands (Figure 4.14 B). These results demonstrate variable transformation efficiencies, with several colonies from both constructs suitable for further plant transformation experiments.

Hairy root transformation was also used because it allows for fast, efficient, and stable transgene expression in roots. This method does not require whole-plant regeneration, which makes it perfect for studying root-specific promoters such as PG1 and PG2. Both constructs were successfully transformed into *A. rhizogenes* as confirmed by colony PCR and it was revealed that RUBY DNA could be amplified from most of the colonies for both constructs (Figure 4.15).

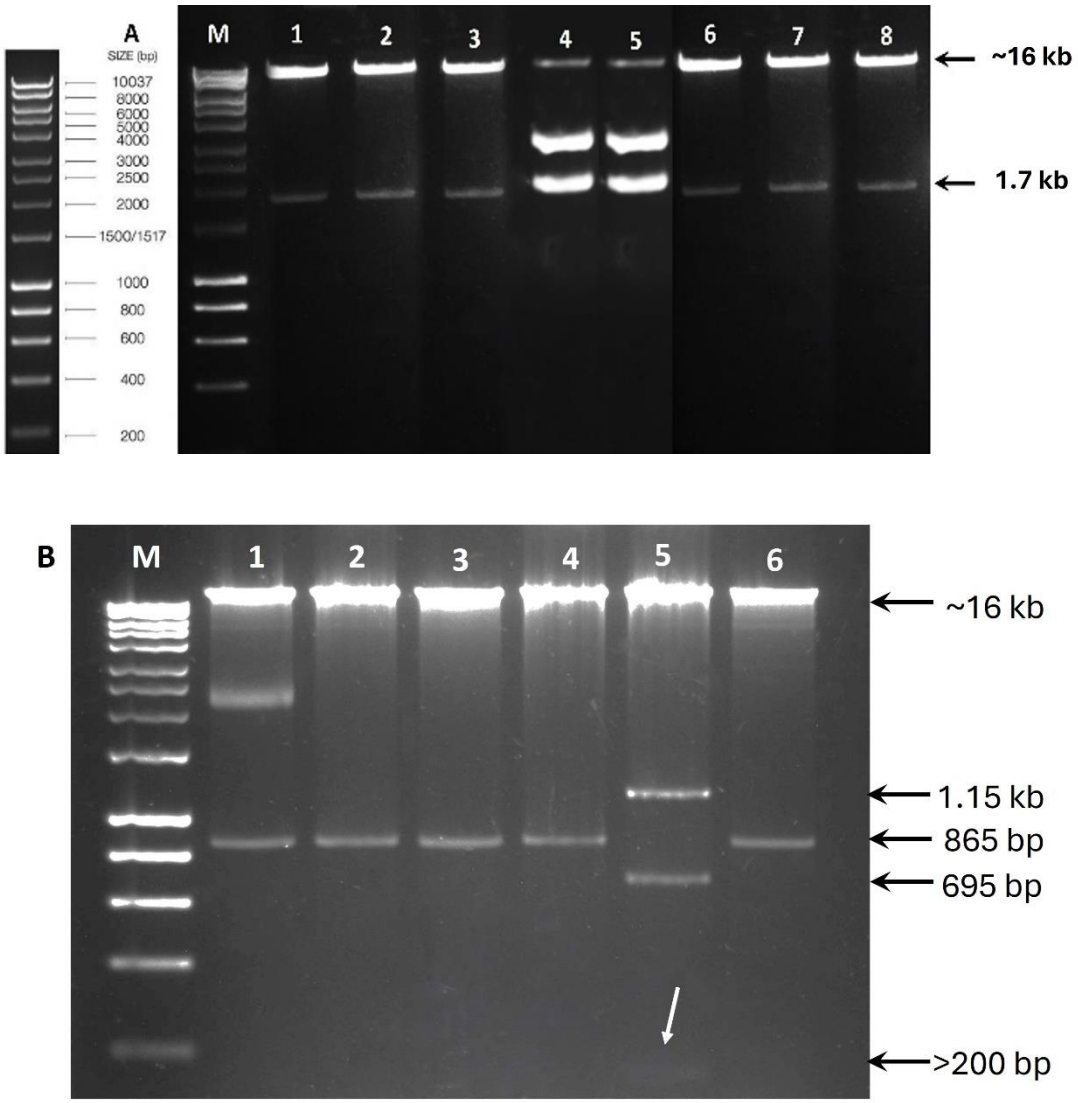

Figure 4.12. Restriction digestion of pBI: RUBY recombinant vector containing PG1 and PG2 promoters using XbaI and HindIII enzymes. A) Restriction digestion of eight clones (lanes 1-8) containing the PG2 promoter. Clones 1-3 and 6-8 provided two distinct bands of approximately 16 kb that aligns with the vector fragment and a 1.7 kb promoter fragment. Whereas Clones 5 and 6 appeared to contain both original plasmids. **B)** Restriction digestion of six clones (lanes 1-6) potentially containing the PG2 promoter. Only Clone 5 produced one expected ~16 kb vector fragment and three 1.15 kb, 695 bp, <200 bp promoter fragments, indicating the presence of three XbaI sites within the plasmid. In contrast, the other clones retained the original 35S promoter fragment. M= DNA marker (1 kb ladder).

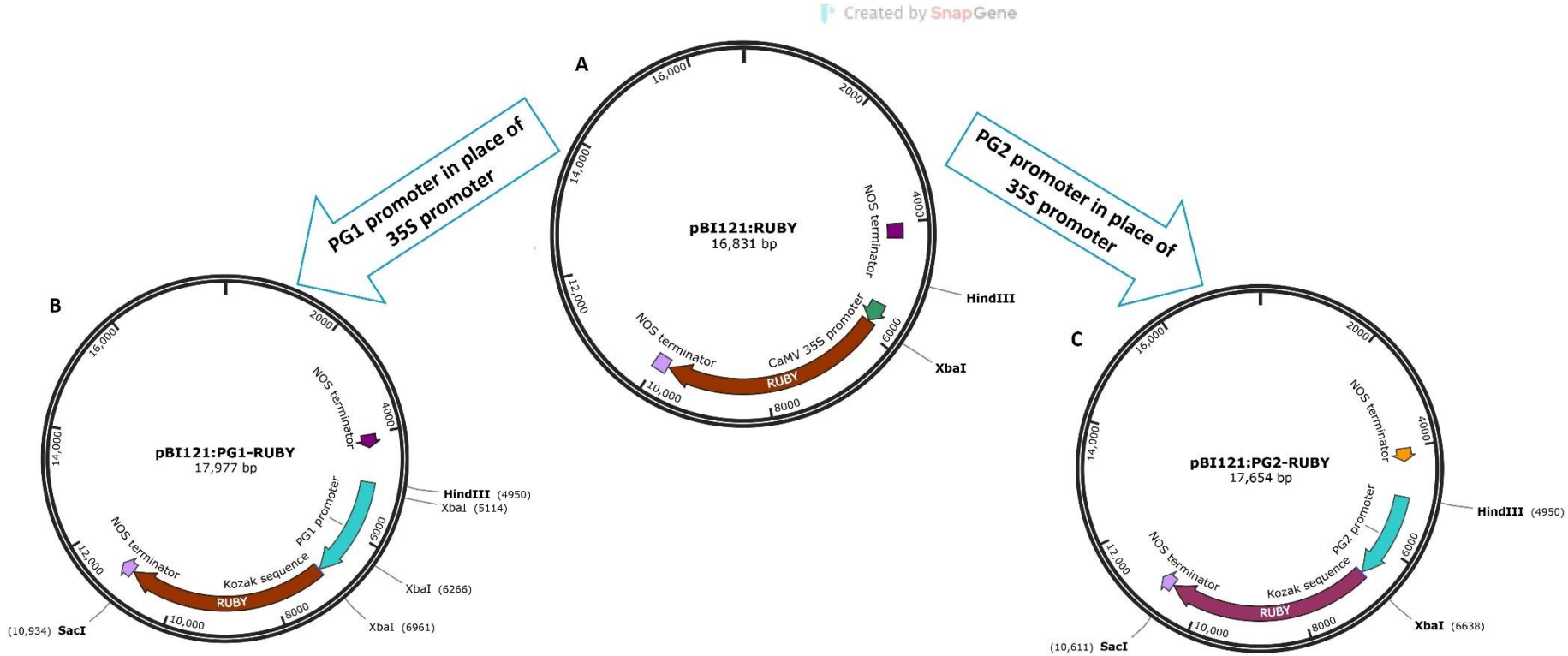

Figure 4.13. Schematic representation of generation of the new pBI:PG1-RUBY and pBI:PG2-RUBY constructs. A) pBI:RUBY vector highlighting RUBY cassette under 35S promoter with XbaI and HindIII sites**. B)** The PG1 promoter was placed upstream of RUBY replacing the 35S promoter to develop pBI121:PG1-RUBY construct. **C)** The PG2 promoter was placed upstream of RUBY replacing the 35S promoter to generate the pBI121:PG2-RUBY construct.

4.4.7 RUBY expression from the PG1 and PG2 promoters in transgenic potato lines

Transgenic plants generated using *A. tumefaciens* harbouring the pBI:PG1-RUBY and pBI:PG2-RUBY constructs were evaluated for RUBY expression. Phenotypic monitoring of transformed plants revealed that several transformed plants and their corresponding roots displayed distinct red pigmentation, indicating the functional activity of this promoter in the plants. Transformation with the pBI:PG1-RUBY construct produced nine regenerated lines to date, all of which successfully entered the vegetative growth stage (Figure 4.16 A). Although root development had not yet initiated in the transgenic PG1 lines, these lines were therefore not assessed for nematode infection.

Contrastingly, eight out of 14 regenerated lines of the pBI:PG2-RUBY construct produced roots on selective antibiotic media and one of those lines produced red roots demonstrating successful regeneration and transformation (Figure 4.16 B, C and D). Specifically, one transformed line with the PG2 promoter exhibited visual expression of RUBY in root tissues, while a few lines did not show any detectable red coloration (4.16 B and D).

A similar expression pattern was observed in the *A. rhizogenes*-transformed hairy roots of potato. While several hairy roots from both constructs developed intense red coloration consistent with RUBY expression, others remained unpigmented despite being PCR-positive for the transgene (Figure 4.17). A total of twelve transgenic lines were successfully generated using the pBI:PG1-RUBY construct, of which four exhibited red pigmentation in roots. Similarly, four lines were developed from the pBI:PG2-RUBY construct, with one line showing red coloration.

To confirm successful transformation, one representative line from each construct was randomly selected, PCR amplification of the RUBY sequence verified transgene integration (Figure 4.18). These findings demonstrate the functional activity of PG1 and PG2 promoters in potato roots in driving RUBY expression and highlight variability in expression levels among independent transformants. Nevertheless, satisfactory root growth was not observed either with the PG1 or PG2 constructs. The reduced root development suggested that the overexpression of betalain may have negatively impacted root architecture or hormonal balance involved in root elongation and differentiation.

In the case of the *A. tumefaciens* transformed lines, only a few of the potato lines could be confirmed as transgenic by visual production of betalain, PCR analysis of gDNA from four lines transformed with the pBI:PG1-RUBY construct and nine lines transformed with the

pBI:PG2-RUBY construct was used to confirm the presence of the transgene by amplification of RUBY sequence (300 bp). Whereas RUBY sequence was not amplified from wild type DNA (300 bp) (Figure 4.18). This result confirmed the presence of the RUBY gene under the control of the PG1 and PG2 promoters in most of the tested potato lines.

4.4.8 Initial trial for RUBY expression under the control of the PG1 and PG2 promoters in response to early nematode infection

In this study, PG1 roots were obtained from hairy root transformation, whereas PG2 roots were derived from fully regenerated potato plants produced via *Agrobacterium tumefaciens*–mediated transformation. Transgenic hairy roots carrying the pBI:PG1-RUBY construct and whole potato plants harbouring the pBI:PG2-RUBY construct were subsequently infected with *G. pallida* to evaluate promoter activity under nematode infection conditions.

In the case of hairy root cultures derived from the pBI:PG1-RUBY construct, neither sustained root growth nor nematode development was observed throughout the observation period. Juvenile nematodes were observed in and around the infected roots of PG1 promoter lines at 48 hours, 4 DAI and 7 DAI (Figure 4.19). However, no visible RUBY expression was detected at any time point of infection derived from hairy roots of PG1 construct. Since the infections were performed when the PG1 transgenic hairy roots had only recently rooted and were not yet fully established, this likely limited both nematode penetration and development in hairy roots.

In contrast, the transgenic potato line carrying the pBI:PG2-RUBY construct derived from *A. tumefaciens* transformation showed clear induction of RUBY expression following infection with *G. pallida*. RUBY signals were detectable as early as 48 hours post infection and remained visible at 4 days post infection, whereas uninfected roots showed no detectable RUBY expression at these time points. RUBY expression was continuously detected in infected roots throughout nematode development, including at 2 weeks post infection, when developing female nematodes were present (Figure 4.20).

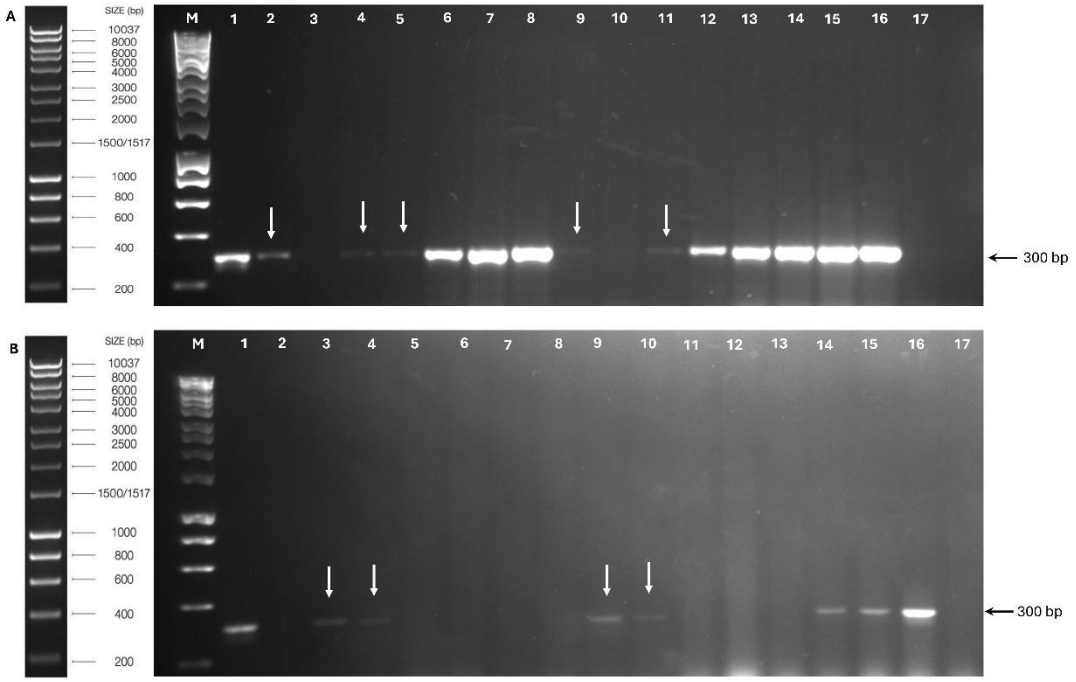

Figure 4.14. Colony PCR of *Agrobacterium tumefaciens* harbouring pBI121:PG1-RUBY and pBI121:PG2-RUBY constructs.

A) Thirteen colonies of pBI:PG1-RUBY amplified RUBY DNA where colonies 6-8 and colonies 13-16 demonstrated strong bands and colonies 2, 4, 5, 9, 11 exhibited faint bands (indicated by arrows). Colonies 3 and 10 did not amplified RUBY DNA.

B) Seven colonies of pBI:PG2-RUBY amplified RUBY DNA (lanes 3, 4, 9, 10, 14, 15, 16), arrows indicate faint bands. Other colonies did not produce any band. M= DNA marker (1 kb ladder).

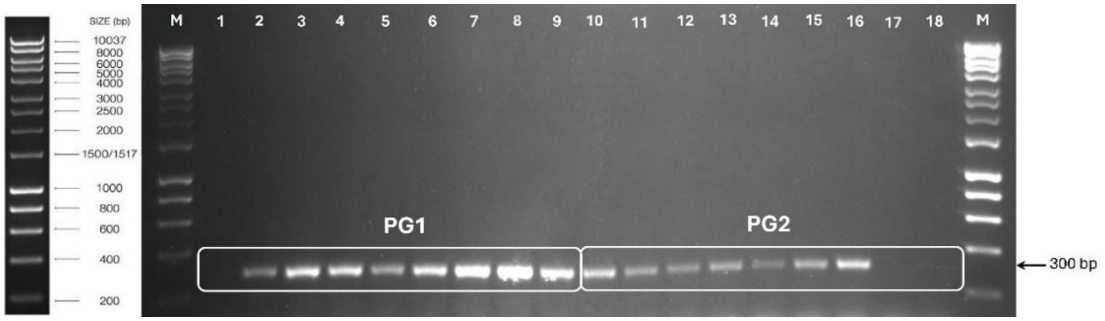

Figure 4.15. Colony PCR of *Agrobacterium rhizogenes* harbouring pBI:PG1-RUBY and pBI:PG2-RUBY constructs.

Eight colonies of pBI:PG1-RUBY (lanes 2-9) amplified RUBY DNA sequence and seven colonies of pBI:PG2-RUBY (lane 10-16) amplified RUBY DNA of 300 bp. Lane 1 and lane 18=Negative control (water only without colony), M= DNA marker (1 kb ladder).

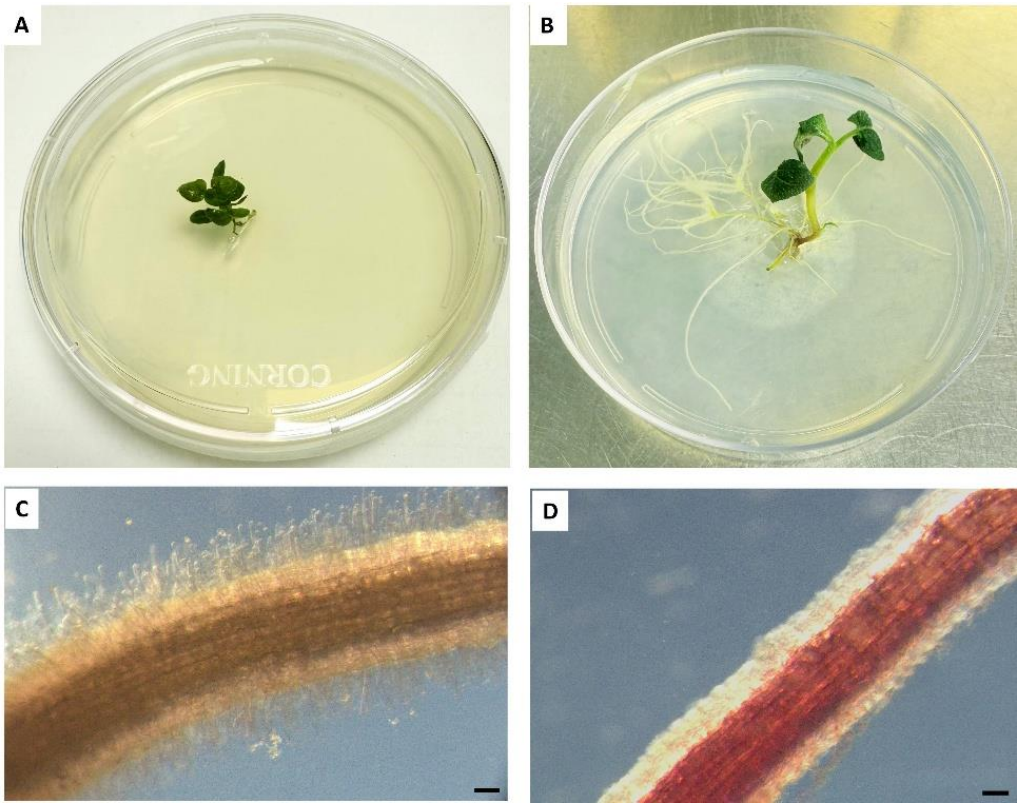

Figure 4.16. *Agrobacterium tumefaciens* mediated transgenic potato lines in tissue culture.

A) Transgenic potato line carrying the pBI:PG1-RUBY construct successfully developed healthy shoots, with root formation expected in the subsequent growth phase.

B) Transformed potato line carrying the pBI:PG2-RUBY construct developed extensive healthy roots.

C) Transformed root of one pBI:PG2-RUBY line exhibited no visible betalain pigmentation (microscopic view).

D) Transformed root of a second pBI121:PG2-RUBY line displaying visible betalain pigmentation (microscopic view).

Scale bar = 100 µm.

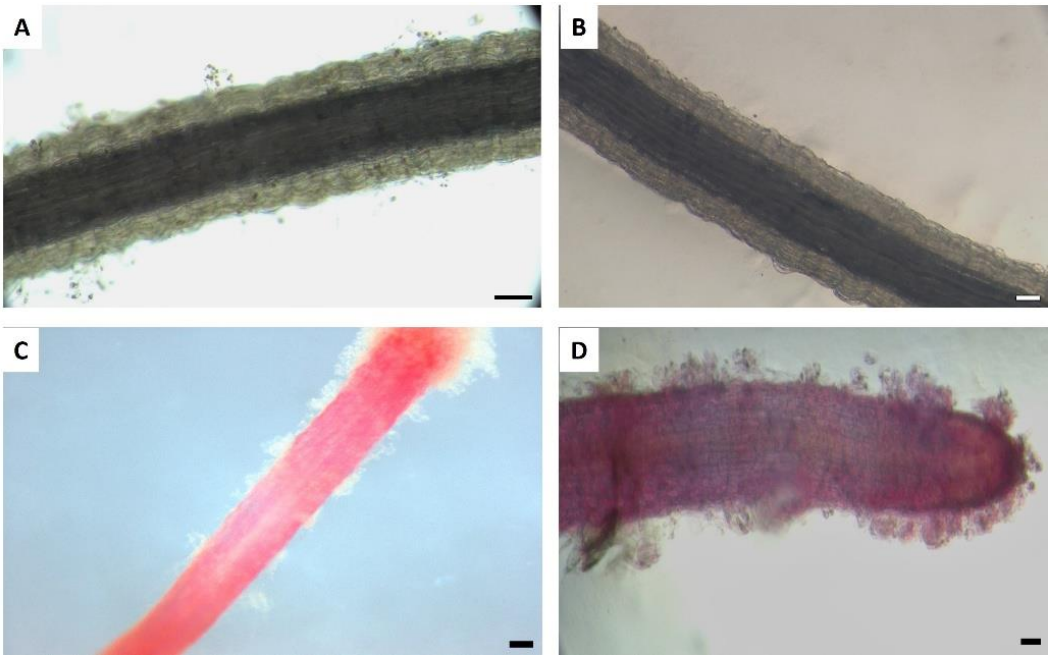

Figure 4.17. Phenotypic expression of RUBY in transgenic hairy root lines of potato under control of the PG1 and PG2 promoters.

Transformed potato hairy roots carrying the pBI:PG1-RUBY construct **(A)** and pBI:PG2-RUBY construct **(B)** showing no visible betalain pigmentation, while PCR analysis confirmed the presence of the RUBY sequence.

Transformed hairy roots of potato carrying the pBI:PG1-RUBY (**C)** and pBI:PG2-RUBY construct **D)**, respectively exhibiting visible betalain pigmentation.
Scale bar = 100 µm.

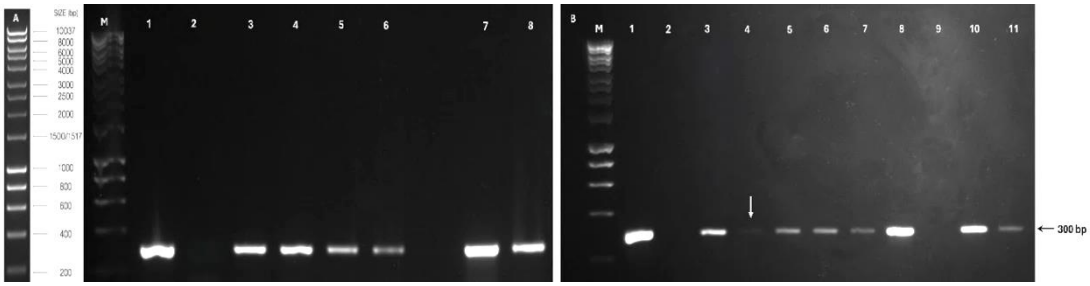

Figure 4.18. PCR amplification of RUBY sequence (300 bp) confirmed the presence of RUBY in transformed potato lines.

A) Lanes 3 to 6 represent RUBY sequence amplification from *A. tumefaciens* transformed potato lines containing the PG1-RUBY construct, whilst lanes 7 and 8 represent RUBY sequence amplification from *A. rhizogenes* transformed potato hairy root lines containing the PG1-RUBY and PG2-RUBY constructs, respectively. Lane 1= positive control RUBY DNA, lane 2 = negative control (DNA of wild type potato) and M= DNA marker (1 kb ladder).

B) Lanes 3-8 (faint band indicated by arrow) and lanes 10-11 represent amplified RUBY DNA from *A. tumefaciens* transformed potato lines containing the PG2-RUBY construct. Lane 1= positive control RUBY DNA, lane 2 = negative control (DNA of wild type potato) and M= DNA marker (1 kb ladder).

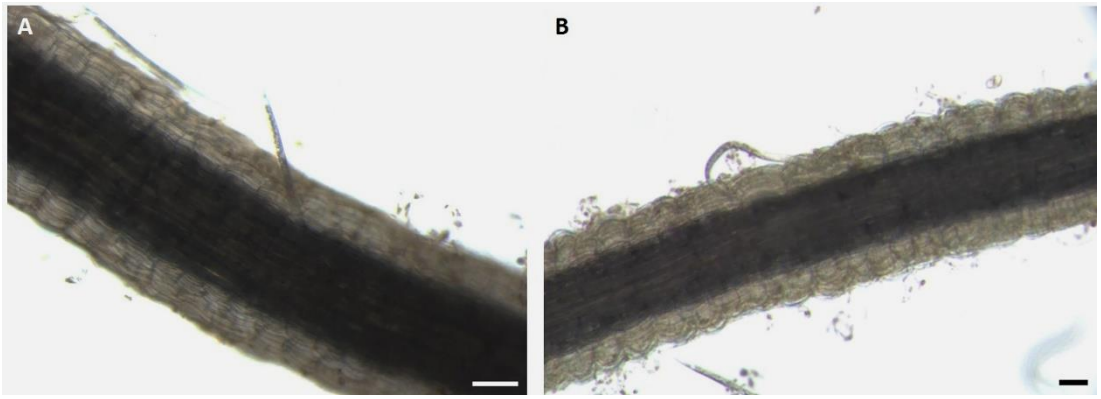

Figure 4.19. Assessment of RUBY expression under the control of the PG1 promoter in response to early nematode infection.

Transgenic potato line carrying pBI:PG1-RUBY construct showed no visible RUBY expression at 48 hours **(A)** and 4 days after infection **(B)** with *G. pallida*.

N = Nematode, scale bar = 100 µm.

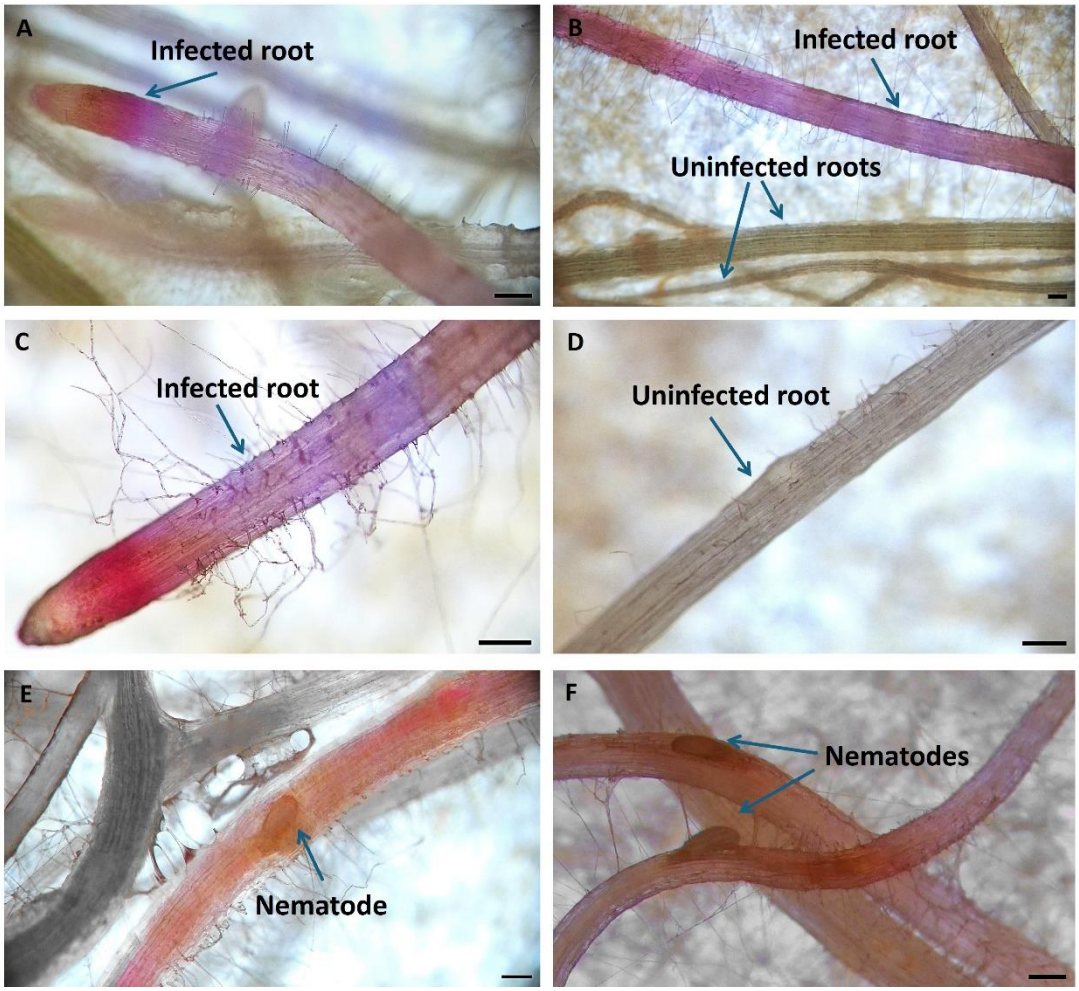

Figure 4.20. Assessment of RUBY expression under the control of the PG2 promoter in response to early nematode infection.

Transgenic potato line carrying pBI:PG2-RUBY construct showed visible RUBY expression at 48 hours **(A & B)** and 4 days post infection **(C)** with *G. pallida*. While uninfected roots expressed no visible RUBY at 48 hours **(B)** and 4 days post infection **(D).**

E & F) The infected roots continued to express RUBY at 2 weeks post infection and developing female nematodes were detectable on infected roots; red roots were selectively filtered by adjusting hue and saturation using GIMP 3.0.4 software, improving clarity and enabling more accurate RUBY detection.

Scale bar = 200 µm.

4.5 Discussion

4.5.1 Successful cloning of RUBY into the pBI121 vector

The successful cloning of the RUBY reporter gene cassette into the pBI121 binary vector represents a critical step in establishing a visible marker system for monitoring gene expression in plants under root inducible promoters. The pBI121 vector commonly referred to as pBI121-GUS, was selected as the vector backbone for RUBY cloning due to its compatibility in Agrobacterium-mediated transformation and its wide use in plant genetic transformation. This vector contains a T-DNA with CaMV35S promoter, nopaline synthase (NOS) terminator and multiple cloning sites, making it convenient for constitutive gene expression in a wide range of plants. pBI121 vector, originally designed for GUS expression, allows easy replacement of the GUS gene with other genes of interest. Additionally, the CaMV35S promoter positioned upstream of the multiple cloning sites can be replaced with alternative promoters, facilitating the development of plant expression vectors tailored to the regulatory characteristics of the introduced promoter (Gao et al., 2007). For example, the CaMV35S promoter of pBI121 was replaced by a cellulose synthase promoter to drive GUS reporter gene expression (Hai et al., 2016). Due to its reliable performance and ease of manipulation, we modified the vector by substituting GUS with RUBY to enable betalain-based visual identification under the control of root-inducible promoters.

The RUBY reporter gene was initially cloned into the pBI121 binary vector downstream of the constitutive CaMV35S promoter to serve as a positive control for visual RUBY gene expression. The CaMV35S promoter is widely used in plant biotechnology due to its strong, ubiquitous expression in most plant tissues (Amack et al., 2022; Singh et al., 2025).

Agrobacterium-mediated infiltration in tobacco leaves was performed to rapidly detect subcellular localisation and RUBY expression as a visual marker. Tobacco leaves inoculated by pBI121:35S-RUBY construct (three clones) transiently expressed robust red pigmentation in leaves, demonstrating that the RUBY gene was functional in the plant system and that the CaMV35S promoter can drive high-level expression. Furthermore, the spots were localised to Agrobacterium infiltrated areas with no visible red colour patches detected in non-inoculated leaves. Such localized expression reinforces the utility of RUBY as a precise marker for transient transformation efficiency.

However, there were temporal variations noticed among the clones. The onset of betalain pigmentation was observed within 1–3 days post-infiltration and intensified over time,

reflecting typical dynamics of transient gene expression via Agrobacterium. The somatic cells in the agroinfiltration zones have the potentiality to express a transgene within 3-5 days under the control of the 35S promoter (Kaur et al., 2021). Sometimes the target gene can be expressed in a short time (within 12 h of infiltration) and strong expression in the plant cells could be achieved after 2 to 4 days of infiltration (Zhou and Yu, 2013). Therefore, our finding confirmed that while temporal variations existed among the three clones, this variation among the three agroinfiltration events in our study likely arose from differences in *Agrobacterium* concentration, variation in transformation competency and metabolic activity of the infiltrated leaves, and physiological differences between plants, such as developmental stage or leaf expansion. Our findings confirmed that Agrobacterium-mediated expression enabled a rapid and robust expression pattern within just a few days post-infiltration.

4.5.2 Promoter selection and integration into pBI:RUBY vector

Promoter selection plays a pivotal role in determining the spatial and temporal expression patterns of a transgene. In this study, we aimed to integrate novel, relatively uncharacterised potato promoters upstream of the RUBY reporter gene in order to identify root-inducible promoters responsive to nematode infection. Although these promoter-RUBY constructs were successfully developed, their activity in response to nematode infection has not yet been assessed due to time constraints. RUBY has proven capability of visual betalain production under the control of diverse promoters such as Maize UBIQUITIN promoter, Arabidopsis seed-specific At2S3 promoter and YUC4 promoter (encodes auxin biosynthesis enzyme), DR5 promoter (auxin responsive) (He et al., 2020) and cassava vein mosaic virus promoter (CsVMV) in soybean roots (Mejias et al., 2025).

To identify potential nematode-responsive genes, we analysed the expression profiles of different genes active during nematode infection in susceptible potato cultivars. Different types of nematode responsive potato promoters were analysed in previous studies, for example, the GUS gene was upregulated in *G. pallida* infected feeding sites under control of a potato wound-inducible promoter (*wun1*) (Hansen et al., 1996) and five gene promoters (CYP97A29, DFR, FLS, NIK and PMEI) upregulated GUS upon *G. rostochiensis* infection in potato and tomato (Wisniewska et al., 2013). RNA-seq analysis revealed a diverse set of genes that were upregulated in potato roots in response to PCN infection at 48 hours post-inoculation, providing valuable insights into early molecular responses to nematode stress (Walter et al., 2018). Based on this analysis, we selected two upregulated genes (PG1 and

PG2) as candidates for promoter isolation (**section 4.3.2.3**). PG1 encodes a predicted homeobox transcription factor, which is hypothesized to participate in hormonal signalling pathways, potentially influencing stress related responses upon nematode infection. PG2 encodes an auxin efflux carrier, which may play a crucial role in the formation of the syncytium during nematode infection (Walter et al., 2018).

To isolate putative promoter regions, approximately 2 kb and 1.7 kb (PG1 and PG2, respectively) of genomic sequence upstream of the ATG start codon was extracted for each selected gene. These upstream regions were carefully evaluated to ensure they did not overlap with adjacent genes, and that the gene models appeared structurally plausible based on available annotation data. Sequences spanning one to two kilobases upstream of the transcription sites are commonly used in plant promoter studies, as they typically include core promoter elements (such as the TATA box and transcription start site) and proximal regulatory elements (enhancers and silencers) to trigger gene expression (Schmitz et al., 2022). Supporting this approach, several functional studies have successfully isolated promoters within the range of 1 to 2 kilobases which, when linked to a reporter gene, faithfully reproduce expression characteristics of the native gene. For example, the 1.5 kb promoter regions of two Arabidopsis genes (At1g74770 and At2g18140) up-regulated in roots infected with *M. incognita* directed strong GUS expression in infected roots, including galls, which was absent in non-infected roots (Kakrana et al., 2017). A ~3 kb promoter fragment of the sugar beet $Hs1^{pro-1}$ beet cyst nematode resistance gene fused to GUS was functional in both susceptible beet roots and Arabidopsis plants, driving feeding site-specific GUS expression. Further dissection of the specific regulatory regions defined elements present between –355 and +247 bp from the transcription start site as being required for syncytial expression, whilst the region between −1199 and −705 was necessary for higher levels of expression (Thurau et al., 2003). Similarly, deletion analysis of the CmLOX08 promoter from *Cucumis melo* evaluated fragments of 2,054 bp and shorter, effectively identifying regulatory regions relevant to stress responses, PsDREB2 promoter from *Paeonia suffruticosa* included a ~2.2 kb fragment upstream of the start codon, which contained multiple cis-acting elements—such as numerous TATA and CAAT boxes, along with stress-responsive motifs (Wang et al., 2019; Liu et al., 2019). Previous findings also identified upstream sequence of 1242 bp (-1548 to -306) as the key region for transcriptional regulation of *Ginkgo biloba* chalcone synthase gene promoter in Tobacco (Li et al., 2014). In another study, a 3.1 kb fragment of the promoter region of the *Populus trichocarpa* cellulose synthase

A4 gene (PtrCesA4 gene) was successfully cloned and used to replace CaMV35S promoter in the binary vector pBI121 (Hai et al., 2016).

4.5.3 PG1- and PG2-driven RUBY expression in transgenic potato plants.

Agrobacterium-mediated transformation using both *A. tumefaciens* and *A. rhizogenes* exhibited similar expression patterns for the PG1 and PG2 constructs. Differential expression patterns were detected in the transformed lines, which is a common issue of pigment-based reporters as varying levels of colour expression can arise due to transgene integration or positional effects (Yu et al., 2023). However, the restriction of RUBY expression to roots indicates that the promoter retains strong root-specific activity, as no pigmentation was detected in the leaves of plants transformed with either construct.

In several transgenic lines, betalain pigmentation was observed in roots even before nematode infection, suggesting possible basal activities in root tissues under non-infected conditions. Specifically, the PG2 promoter, associated with auxin efflux transport, may exhibit expression patterns influenced by local auxin gradients, potentially leading to background activation in roots even without nematode infection. Additionally, tissue culture conditions, root development, or wounding stress during transformation may have contributed to unintended promoter activation in the absence of infection response.

In other lines, visible betalain pigmentation was absent, yet PCR analysis confirmed the presence of the RUBY transgene, indicating successful transformation. This discrepancy could be explained by several factors such as the promoter might have remained inactive in the absence of nematode response as intended, a low expression level of RUBY might not be visually detectable or transformation may occur but transcription of betalain biosynthesis genes might be impaired (Kiryushkin et al., 2021) due to epigenetic gene silencing. Since betalain accumulation depends on the expression levels of its biosynthetic genes (Yu et al., 2023), environmental factors such as temperature, pH, light also contribute to reduced pigment production (Khidr et al., 2017; Jogam et al., 2024). Moreover, betalain synthesis also regulated by transcriptional regulation and other gene expression process (Polturak et al., 2018), suggesting that both environmental cues and molecular control jointly influence the observed expression patterns.

In the case of hairy root transformation, it was observed that although roots developed on selective antibiotic media, few lines with red roots were found from both constructs. Root growth was generally limited, and some contamination occurred. The effectiveness of *in vitro*

hairy root transformation is influenced by several imperative factors, including plant genotype, the developmental stage of the explant, the *Agrobacterium rhizogenes* strain, media composition, and the culture environment (Thwe et al., 2016). For successful *in vitro Agrobacterium*-mediated transformation using pBI:PG1-RUBY and pBI:PG2-RUBY constructs, it is essential to further optimize these parameters to enhance transformation efficiency and root development.

4.5.4 Initial trial for RUBY expression in response to early nematode infection

A contrasting response to nematode infection was observed between the two constructs, with pBI:PG2-RUBY showing a clear induction of expression, whereas pBI:PG1-RUBY did not exhibit a detectable response. The continuous detection of RUBY expression in infected roots throughout nematode development suggests sustained activation of the pBI:PG2-RUBY promoter in response to *G. pallida* infection.

Despite choosing the PG1 promoter gene based on RNA-seq analysis demonstrating significant upregulation within 48 hours post infection of PCN in susceptible potato roots, no visible betalain expression was detected in the transgenic roots up to 7 dpi. In contrast to PG2, the lack of detectable PG1-driven RUBY expression suggests promoter-specific differences in inducibility or strength when tested in a reporter system. This observation was unexpected, as the native genes driven by these promoters provided strong transcriptional activation during early stages of infection (Walter et al., 2018), suggesting the promoter regions may contain nematode-responsive regulatory elements.

The absence of visible red pigmentation in PG1 promoter line may be elucidated by several factors. Firstly, although the promoter sequences were transcriptionally functional in their native genomic background, their actions when isolated and employed upstream of the RUBY reporter even within the same species may not fully recapitulate their native regulation. In the genome, promoters often operate in coordination with additional regulatory elements such as enhancers, silencers, insulators, or boundary sequences that can reside tens or even hundreds of kilobases away, either upstream or downstream of the gene (van Arensbergen et al., 2014). Once excised and tested as isolated fragments, these contextual influences may be reduced or absent, potentially altering the strength, tissue-specificity, or inducibility of RUBY expression. Furthermore, differences in promoter length or omission of regulatory motifs beyond the chosen fragments may also limit their ability to reflect full native expression patterns.

Experimental limitations may also have contributed to the lack of detectable activity from the PG1 promoter. In hairy root transformation experiments, neither robust root growth nor nematode development was observed, which restricted reliable assessment of promoter responsiveness under infection conditions. In Agrobacterium-mediated stable transformation, root development was obtained only in transgenic plants carrying the pBI:PG2-RUBY construct. Consequently, transgenic plants harbouring the pBI:PG1-RUBY construct could not be evaluated for nematode infection, limiting direct comparison of promoter activity under these conditions.

Although expression profiling is a powerful tool, functional validation using reporter systems remains essential to confirm promoter inducibility under nematode infection. The clear activation of PG2 in the current study underscores the importance of optimized infection timing and the use of well-established transgenic material to reveal promoter responsiveness. In contrast, the lack of detectable RUBY expression from PG1 highlights that promoter activity predicted from transcriptomic data may not always translate into visible reporter expression, potentially due to insufficient strength, delayed activation, or the absence of contextual regulatory elements. Future studies should employ fully developed transgenic lines across multiple stages of nematode development and incorporate complementary approaches such as qRT-PCR of RUBY transcripts or quantitative measurement of betalain accumulation to capture subtle, transient, or spatially restricted promoter activity that may not be visually apparent.

4.5.5 Conclusions

The experiment was conducted with the aim of generating novel RUBY constructs driven by root-expressed, nematode-inducible promoters and investigating RUBY expression during the transgenic process as well as in response to nematode infection. The key findings of this experiment are summarised below:

- The entire RUBY cassette containing three betalain biosynthesis key genes (CYP76AD1, DODA, and glucosyl transferase) linked by “2A” peptides, was successfully cloned into pBI121 binary vector.
- *Agrobacterium*-mediated transient infiltration of pBI:35S-RUBY construct resulted in strong betalain pigmentation in tobacco leaves, confirming functional betalain production driven by the CaMV35S promoter in the new construct.
- By integrating two candidate promoter sequences upstream of the RUBY gene, two constructs (pBI:PG1-RUBY and pBI:PG2-RUBY) were generated, enabling visualization of transcriptional activation in roots of transgenic potato plants.
- The newly developed RUBY constructs demonstrated root-specificity in transgenic potato lines. Using the pBI:PG2-RUBY construct, RUBY expression was specifically activated in roots in response to nematode infection, demonstrating the promoter’s inducibility under these conditions. However, further experiments using pBI:PG1-RUBY construct are essential to functionally validate the promoter responsiveness to nematode infection.

Chapter 5

Screening and Characterising the Resistance Response of *Solanum spp*. to Potato Cyst Nematodes

5.1 Introduction

Potato is regarded as the world's third most and the UK's second most important staple crop (Campbell, 2024), which is threatened by an array of diseases and pests. Notably, potato cyst nematode (PCN) is one of the major threats to potato production (Orlando and Boa, 2023; Spychalla and Jong, 2024). Infection with PCN causes serious crop losses as a result of the damage caused by the prolonged feeding of the parasitic nematodes as well as the earlier intracellular migration of the J2s. Therefore, there is a pressing need to develop sustainable control methods against PCN. The existing management strategies basically based on integrated pest management including treatment of soils, use of certified seeds and resistant varieties, trap cropping, and applying nematicides (Back et al., 2018; Sasanelli et al., 2021; Price et al., 2024). There are no chemical treatments specifically targeting PCN management; instead, broad-spectrum nematicides are used, but their application is increasingly restricted due to environmental concerns and lack of specificity (Price et al., 2024). Apart from chemicals, crop rotation and biological control are applied in agricultural practices. However, the natural enemy sources for nematodes are limited and crop rotation can cause yield reduction due to the forced utilization of suboptimal farmland. Therefore, several research programmes have focused on the development of natural resistance against potato cyst nematode worldwide (Koropacka, 2010).

Using resistant crop varieties has become a key eco-friendly and efficient component of the integrated management strategies. Various wild relatives as well as landraces of the cultivated potato crop have been considered for providing a source of resistance genes against potato cyst nematode which have been used successfully in breeding programmes (Gartner et al., 2021).

So far, more than fifty tuber forming *Solanum* species have been found that confer resistance to *G. pallida* and/or *G. rostochiensis* in the case of at least one PCN pathotype and one plant

accession (Castelli et al., 2003). Initial approaches to identify potato cyst nematode resistance sources in potato screened almost 1,200 wild accessions from the Commonwealth Potato Collection and this led to the first identification of the resistance locus H1 against potato cyst nematode from *S. tuberosum ssp. andigena*. This locus provided almost complete resistance against *G. rostochiensis* (pathotypes Ro1 and Ro4) (Ellenby, 1952) but no resistance to *G. pallida*. H1 has been widely used by potato breeders (Blok et al., 2018).

Although the H1 resistance gene has been widely deployed, its use has coincided with a rise in *G. pallida* prevalence in the UK (Minnis et al., 2002). For a long time, no highly effective resistance gene was available for *G. pallida*, and achieving durable resistance remains challenging due to its greater genetic diversity and variability in virulence. Consequently, resistance to *G. pallida* may be less stable than H1 (Hockland et al., 2012; Phillips and Trudgill, 1998). The dominant gene Gpa2 related to *G. pallida* resistance (pathotype Pa2) was identified in *S. tuberosum ssp. andigena* (van der Voort et al., 1999). The dominant gene H2 was detected in *S. multidissectum*, which provided resistance to *G. pallida* (pathotype Pa1) (Strachan et al., 2019). However, there is a continuous need for exploring other sources. Numerous wild species of Solanum could be effective sources of resistance to nematodes (Milczarek et al., 2020). A range of Solanum species with resistance has been explored from *S. gourlayi, S. sparsipilum, S. kurtzianum* and *S. acaule* (Castelli et al., 2003). *Solanum gourlayi* was one source of resistance against *G. pallida* that was detected among accessions of wild species of Solanum (Ruiz de Galarreta et al., 1998; Castelli et al., 2005). *G. pallida* resistance gene Gpa VI^{1}_{spg} was also derived from wild potato species *S. spegazzinii* recently (Gartner et al., 2024).

Recent work by Witek et al. (2021) demonstrated that *S. americanum* could act as a source of R genes for another devastating potato pathogen, *Phytophthora infestans*. Indeed, the researchers were able to identify not just a single R gene, but also an additional eight alleles of this gene, all of which conferred resistance to *P. infestans*. Hence, the finding is a significant advancement towards the development of effective, durable resistance to *P. infestans* in potato. Given the relative lack of commercially acceptable *G. pallida* resistant cultivars, it is hoped that similarly effective R genes to potato cyst nematodes may also be identified from the *S. americanum* genome.

Solanum is the largest genus in the Solanaceae family, containing over 1,500 species, including key crops like potato, tomato, and eggplant, which have well-characterized genomes (Witek et al., 2021). *Solanum americanum*, a diploid species within the *Solanum*

nigrum complex, is often misidentified as *S. nigrum* but has been confirmed as a distinct species through molecular and morphological evidence (Ud-Din et al., 2009; Bello et al., 2013) (Figure 5.1). *S. americanum* is commonly known as 'black nightshade' due to its blackish-purple berries (Haque et al., 2018). Like potato, *S. americanum* evolved in the Americas but has since become globally distributed, being present in almost all tropical and sub-tropical regions where it often acts as a weed in crop fields (Ogg et al., 1981). Most previous research into *S. americanum* has thus either focused on its control as a weed or on its traditional culinary and medicinal uses. Apart from resistance to potato late blight and bacterial wilt, *S. americanum* also harbours diverse genetic resources that may contribute to resistance against other plant diseases, making it a valuable species for crop improvement (Witek et al., 2021).

It is hypothesized that different resistant Solanum accessions have different and maybe multiple resistance genes, as the infection phenotypes vary. For example, some roots show no infection at all, some contain only J2 nematodes that never develop further, and others have very few nematodes, but those present show some development. This is probably related to the timing of the resistance response – there could be a hypersensitive response whilst the nematode is migrating through the root, or there may be a later response that prevents feeding site development.

Recent studies highlighted the interaction between potato cyst nematode and *S. sisymbriifolium* (Wixom et al., 2020; Varandas et al., 2024). *S. sisymbriifolium* is used as an efficient trap crop for potato cyst nematode as it stimulates hatching of J2s but is highly resistant to *G. pallida* therefore the nematodes cannot complete their lifecycle (Scholte and Vos, 2000). A hypersensitive response involving reactive oxygen species is assumed to play an active role in the defence response and resistance of *S. sisymbriifolium* (Wixom et al., 2020). During nematode infection, reactive oxygen species (ROS) are generated as a plant defensive component (Hasan et al., 2024). ROS act as highly toxic molecules that can interfere with the invading pathogen and incite a defence response (Chamnongpol et al., 1998; Ali et al., 2018; Leonetti and Molinari, 2020). ROS increases strongly and rapidly in the apoplast creating severe damage to carbohydrates, lipids, proteins and nucleic acids (García-Caparrós et al., 2021). Although ROS are recognised to play a role in plant defence, the precise function and timing of their generation in resistant versus susceptible Solanum lines are still unknown. This study assesses the ROS accumulation in order to better understand the nature of the resistance mechanisms.

Building upon previous screening of 41 Solanum accessions for resistance to *G. pallida*, a subset comprising nine *S. americanum* accessions, one *S. nigrum* accession and two unidentified *Solanum* spp. accessions were selected for initial resistance and phenotypic screening against *G. pallida*. Based on this screening, the present study examined the phenotypic assessment of offspring produced by crossing susceptible and resistant lines and eventually characterized the resistance responses of selected Solanum genotypes against *G. pallida*. This work will contribute to the long-term management strategies of potato cyst nematode by developing our knowledge of resistance traits to support forthcoming breeding programmes.

Figure 5.1. Morphological features of *Solanum* spp.

A) *Solanum americanum* and **B)** *Solanum nigrum*.

5.2 Aims

- To develop a faster method of phenotyping that included determining the best level of *G. pallida* infection to reliably distinguish between levels of resistance/susceptibility in *Solanum* plants.

- To examine F2 plants derived from crosses between susceptible and resistant parents to determine susceptible or resistant phenotypes for subsequent genomic analysis.

- To conduct a tissue culture-based assay for characterising the resistance response following *G. pallida* infection in more detail at the cellular level in aseptic conditions.

5.3 Materials and Methods

5.3.1 Initial Screening of *Solanum spp* accessions

An initial screen was performed on 41 Solanum accessions, followed by repeat testing of selected 12 accessions using a pot assay with cyst-infested soil. Seeds were sown in compost and seedlings were allowed to establish before being transplanted into a 1:1 mixture of compost and sand-loam soil. Plants were grown until they reached a suitable size for nematode inoculation. Six plants from each *Solanum* line were then transferred to individual 3-inch square pots containing sand-loam soil pre-infested with *Globodera pallida* cysts at a concentration of 10 eggs g^{-1} soil. Two to three days after transplanting, 25 ml of neat potato root exudate was applied to each pot to stimulate nematode hatching.

After 30 days in infested soil, plants were removed from pots and roots were washed thoroughly under running tap water. Roots were stained with acid fuchsin following a standard procedure (**section 2.2.1**). Stained roots were examined under a light microscope, and nematodes present were counted and categorised as J2, J3/J4, adult females, or males.

5.3.2 Root trainer trials for development of a faster method of phenotyping *S. americanum*

The preliminary method used for phenotyping of Solanum accessions provided valuable information regarding the progression of the plant-nematode interaction. However, it was very laborious as well as time consuming, and would not be feasible for the large number of individual F2 plants that would need to be evaluated. Therefore, it was necessary to develop a faster method of phenotyping infected *S. americanum* plants in order to be able to phenotype F2 populations. In contrast to the preliminary method, the root trainer system offers a rapid, cost-effective, and higher-throughput alternative. The vertical design promotes downward root growth along the container walls, enabling mature *G. pallida* females to develop on the root surface where they are clearly visible. Importantly, the book-style opening of the root trainers allows direct visualisation and counting of females without the need for staining, greatly reducing labour and processing time.

To develop a faster, higher-throughput method of reliably phenotyping the resistance of *S. americanum* plants, the susceptible parent accession SP2273 that had been used in crosses

with resistant accessions SP1101 and SP2299 was evaluated in different combinations of soil type and inoculation levels of *G. pallida*.

For this, seeds of *S. americanum* SP2273 were sown in a peat-based compost growth medium (No.2 Potting Supreme; Petersfield Growing Mediums) and once they were large enough to transplant, seedlings were transferred into root trainers containing a range of soil conditions and cysts to provide two different inoculum levels of *G. pallida* as illustrated in Figure 5.2.

All the root trainers contained a different combination of these conditions to assess which provided a good level of nematode infection on the susceptible accession and made it easiest to count the number of nematodes present on the surface of roots. Five replicate Solanum plants were established in each soil combination. Five days after transplanting, 12.5 ml neat tomato root exudate were applied to each root trainer to stimulate hatching of *G. pallida*. Plants without root exudate received an equal volume (12.5 mL) of sterile water in place of root exudates to ensure consistent treatment conditions. Subsequently the number of mature female nematodes present on the surface of the roots on the two opposite ridged sides when the root trainers were opened up (Figure 5.3) was then counted under a stereobinocular microscope at both 5 and 6 weeks after transplanting to determine when the nematodes were most easily observable.

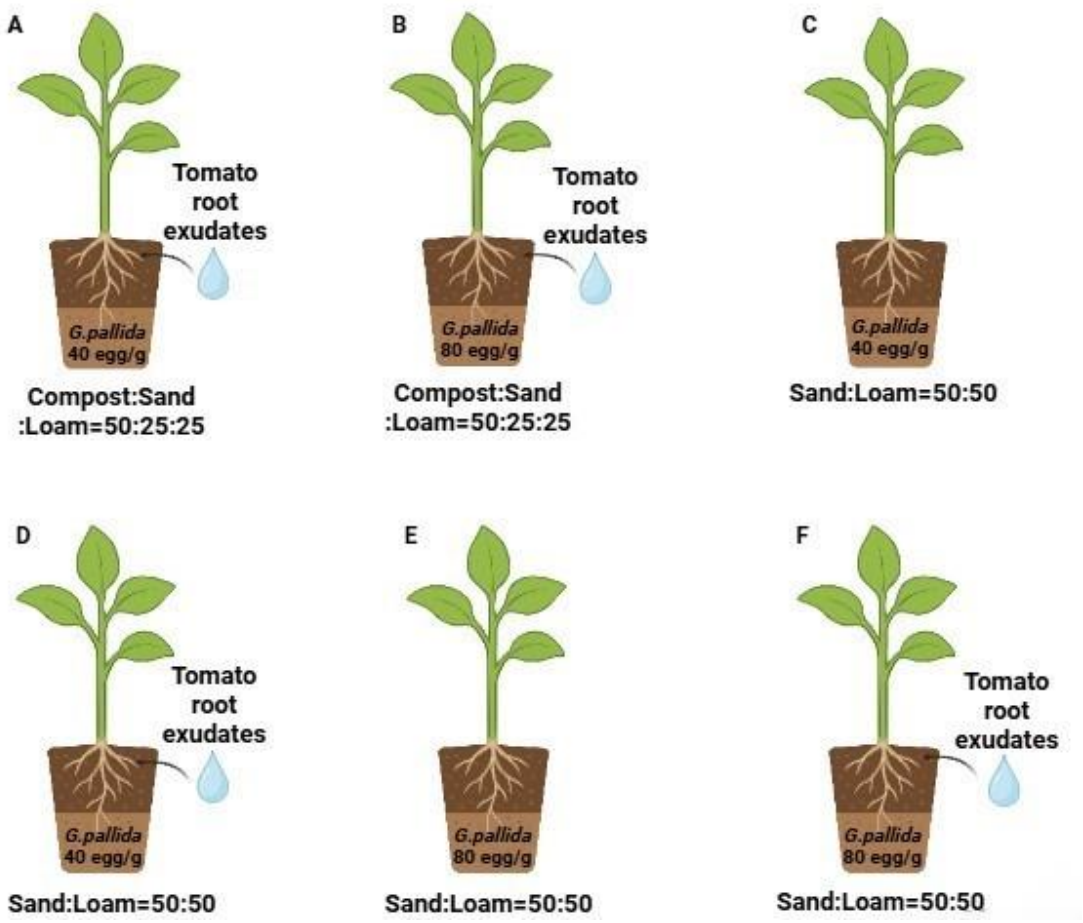

Figure 5.2. Schematic diagram of different soil and inoculum combinations used in root trainers.

A) Compost and sand-loam were mixed (50:25:25) with *G. pallida* (40 egg/g soil) infected soil and tomato root exudates were applied; **B)** Compost and sand-loam were mixed (50:25:25) with *G. pallida* (80 egg/g soil) infected soil and tomato root exudates were applied; **C)** Only sand-loam were mixed (50:50) with *G. pallida* (40 egg/g soil) infected soil and no tomato root exudates were applied; **D)** Only sand-loam were mixed (50:50) with *G. pallida* (40 egg/g soil) infected soil and tomato root exudates were applied; **E)** Only sand-loam were mixed (50:50) with *G. pallida* (80 egg/g soil) infected soil and no tomato root exudates were applied; **F)** Only sand-loam were mixed (50:50) with *G. pallida* (80 egg/g soil) infected soil and tomato root exudates were applied.

Figure 5.3. Establishment of Solanum plants in root trainers for phenotypic screening.

5.3.3 Phenotyping of F2 crosses of susceptible and resistant *S. americanum* accessions

Seeds for F2 offspring of a cross between each of the resistant accessions SP2299 and SP1101 and the susceptible SP2273 accession were obtained from Dr Kamil Witek at the Sainsbury Laboratory, Norwich, UK. Seeds were sown in a compost growth medium as in **section 5.3.2** and once they were large enough to infect, 60 plants for each cross were transplanted into root trainers containing a 50:25:25 mix of sterile compost and sand-loam which was infested with *G. pallida* cysts to a degree of 80 egg/g. Five days after the plants were transferred to the root trainers, 12.5 ml of neat tomato root exudate (**section 2.1.2**) was applied to each plant to ensure stimulation of nematode hatch.

Plants were then allowed to grow for between 5 and 6 weeks. Subsequently, the number of female nematodes or cysts present on the surface of the roots of each plant was observed and counted by light microscopy using a stereobinocular Leica M165 C microscope. To categorize the degree of resistance, a standard PCN resistance scoring notation (a scale of 1-9, 9 being the maximum resistance) was employed (EPPO, 2006). To obtain clear interpretation and facilitate plotting of a histogram a slight modified version of this standard notation based on our initial infection trend was used (Table 1). The histogram of frequency distribution was prepared using R programming and RStudio software (version 4.2.3). A goodness-of-fit test (chi-square) was conducted to assess whether the observed distribution of resistant and susceptible plants deviated from the expected distribution ratio (3:1 or 15:1).

Table 5.1. Scoring of PCN resistance levels

Number of females	Score	Resistance level
0-1	9	Highly resistant
2-3	8	Resistant
4-5	7	Moderately resistant
6-10	6	Slightly resistant
11-15	5	Intermediate
16-25	4	Moderate susceptible
26-50	3	Susceptible
51-100	2	Highly susceptible
>100	1	Extremely susceptible

5.3.4 Growing of *S. americanum* in tissue culture

Seeds of resistant accession SP2299 and the susceptible accession SP2273 were grown in tissue culture after sterilizing in 20% bleach solution for 25 minutes followed by 5 times washing in sterile ELGA water whilst working in a flow-hood. Sterilised seeds were germinated on MS30 solid medium (**section 2.3.2**) in deep 9 cm tissue culture dishes. When the seedlings were of a sufficient size for transplanting, they were transferred to square plates of the same media but containing 1% plant agar for growing vertically. After 2-3 days, the plants were infected with a J2 suspension of *G. pallida* (1 nematode per ul within sterile water and infecting three root tips of each plant with around 30 ul/root). Before infection, *G. pallida* J2s were sterilized following the standard procedure (**section 2.1.3.1**). Over the time course of infection up to 30 dpi, the plates were observed regularly under a stereo binocular microscope to monitor infection and nematode development. After 30 days of infection, the roots were stained with acid fuchsin (**section 2.2.1**) and observed under the microscope, when nematodes were detected then images were captured using a Leica M165 C microscope with Q IMAGING camera and Q Capture Pro 6.0 software.

5.3.5 MS media trial for growing of *Solanum* accessions in tissue culture

MS medium plates with three different levels of sucrose were prepared by supplementing with 10 g/l, 20 g/l and 30 g/l sucrose to evaluate the optimal media conditions for *in vitro* growth of the Solanum accessions in tissue culture, with the aim of determining the best performing media for further analysis. Tomato plants, which are known to be susceptible hosts for nematode infection, were also grown on media with the same sucrose concentrations to enable a comparative assessment between these two Solanum species. Three to five plants were grown on these media and subsequently infected with *G. pallida* as mentioned above (**section 5.3.4**). Plants were then stained using acid fuchsin as described in **section 2.2.1** after 5 weeks of infection and the number of females was counted using light microscopy as described above.

5.3.6 Testing the use of Plant Preservative Mixture (PPM) in MS media trial for growing of *Solanum* accessions

After selecting the optimal MS medium for growing *Solanum* lines, we also performed a trial using PPM (Plant Cell Technology) in the medium to suppress microbial contamination and improve plant growth. However, we first needed to find out whether PPM can cause any

effect on nematode growth and development. Five plants were cultured on media supplemented with PPM at 2 ml/L, while eight plants were grown on equivalent media without PPM. The experimental protocols for growing plants and infecting with *G. pallida* were then followed as above (**section 5.3.5**.). The number of female nematodes per plant was counted both before and after staining with acid fuchsin and the numbers compared between plants grown on media with and without PPM.

5.3.7 Characterization of the resistance response in sterile conditions

Five Solanum accessions resistant to *G. pallida* were selected for analysing the resistance response in detail. One known susceptible accession was included as a control. For each accession, ten replications were included for both infected and uninfected plants. Seeds were sown on MS30 medium containing 2 ml/l PPM, then transplanted and infected with *G. pallida* as described in Section 5.3.4. Uninfected control plants were mock-inoculated using sterile water, to control for any mechanical damage occurring to the roots during the inoculation procedure. Data were collected at two time points (4 dpi and 7 dpi). At each time point, plants were harvested, adhering agar gently removed and the roots stained with DAB solution (details in **section 2.2.3**) to visualise ROS for detecting resistance responses. Subsequently, the number of brown spots indicative of ROS activity were counted in each root system after capturing images under a Leica M165 C microscope with a Q IMAGING camera and Q Capture Pro 6.0 software. The total length of roots of the stained plants were measured and the number of brown spots expressed per centimetre (cm) length of root for further analysis. Data were analysed to compare resistance responses among the resistant lines and the susceptible control, and to assess the effects of infection over time.

5.3.8 Statistical analysis

Statistical analysis was performed using R programming and RStudio software (version 4.2.3). A Shapiro-Wilk test was applied to test the normality of data. Data that included a comparison between only two variables were analysed using an independent two sample t-test. Where more conditions were being tested, data were analysed using a one-way or three-way analysis of variance (ANOVA). Tukey's Honest Significant Difference (HSD) post hoc test was then performed for comparing the means of data ($P<0.05$).

5.4 Results

In preliminary work, a small number of Solanum accessions were identified that were able to support good development of *G. pallida* to adult females and were therefore classed as 'susceptible'. The expectation, based on the available literature, was that *S. americanum* would be resistant to, or a non-host for PCN, however it was important to identify any susceptible accessions that could be used in a subsequent mapping approach by crossing with resistant accessions. Accessions SP2273, SP2360, SP3376 were fully susceptible, showing high levels of nematode infection with both females and males developing well. When the screening originally took place, all three of these were presumed to be *S. americanum*, but during the project, genome sequencing by our collaborators identified that SP3376 was in fact another, as yet unidentified, Solanum species. SP3376 was therefore not taken forward for use in crosses.

A shortlist of other accessions, chosen to span a range of resistance phenotypes, was taken forward for additional screening and more detailed characterisation. Partially resistant accessions were SP3371, SP2308 and SP1101, which supported development of both females and males, but in very much smaller numbers than the susceptible accessions. Other accessions were classified as resistant, but they differed in their resistance phenotype. For example, infected roots of the SP3393 accession contained only J2 stage nematodes and those were in relatively low numbers (<20 per plant). In contrast, while roots of accession SP2299 also contained almost exclusively J2 nematodes, these were present in larger numbers (100 per plant). Quite often in these lines many of the J2s were observed in necrotic regions of the roots, showing that whilst the plants were susceptible to invasion, they were able to suppress nematode development, most likely via a hypersensitive response. The roots of one accession, SP1032, contained small numbers of J2 and/or adult male nematodes Finally, no nematodes of any developmental stage were observed in the roots of accession SP3052 (Greenwood, 2022; unpublished data). Based on these preliminary findings, susceptible accession SP2273, resistant accessions SP2299, SP3393, SP1032 and partially resistant accessions SP1101 and SP2308 were selected for subsequent studies.

5.4.1 Root trainers enabled an effective high throughput assay

In preliminary tests of resistance status, both the initial screen of 41 different *Solanum* accessions and the follow-up repeat testing of 12 selected accessions was based on growing plants in pots of cyst-infested soil, staining the root systems with acid fuchsin, then counting

the nematodes and noting their developmental stages under the microscope. Whilst this did provide valuable information regarding the progression of the plant-nematode interaction it was very laborious as well as time consuming and would not be feasible for the large number of individual F2 plants that would need to be evaluated. In that case, the important phenotypic distinction would be between those plants that allowed development of mature females and those that did not, hence the root trainer method was developed.

As there were no previous reports of growing and infecting *S. americanum* plants in root trainers an initial optimisation experiment was carried out to determine the best set-up to use. Female nematodes were visible on susceptible *S. americanum* SP2273 plants grown in root trainers at five to six weeks post transfer of seedlings into the *G. pallida*-infested soil (Figure 5.4), demonstrating that this technique can be used to identify a plant's infection status. Female nematodes were visible on the roots after 5 weeks but were more easily detected after 6 weeks as they were slightly larger. Additionally, the high sand content of the sand-loam soil made it difficult to reliably identify all nematodes present due to the similar appearance of untanned female nematodes and some sand grains. This problem was largely alleviated by mixing the sandy loam soil with equal parts compost which made the nematodes significantly easier to locate against the darker soil background.

The numbers of female nematodes visible on the roots of each plant were counted and the data analysed to determine the effects of soil type, inoculum level and root exudate addition on infection rate. A one-way ANOVA test showed a highly significant variation among all the treatments ($p<0.001$, $F=16.2$), with a Tukey HSD posthoc test determining that the plants grown in compost and sand loam, at the higher inoculation rate of 80 eggs/g *G. pallida* cysts harboured significantly more female nematodes (31±3.83 per plant; Figure 5.5). There was no significant difference in infection level between all other treatments. In particular, the addition of tomato root exudate to the soil significantly increase infection (Figure 5.5), suggesting that the root exudate of the susceptible *S. americanum* accession SP2273 was able to stimulate hatching of *G. pallida*.

Based on these results, the conditions chosen for use in future experiments, were compost:sand:loam (50:25:25) with an inoculum level of 80 eggs/g *G. pallida* and the addition of tomato root exudate to ensure a good rate of hatch, irrespective of which accession was used.

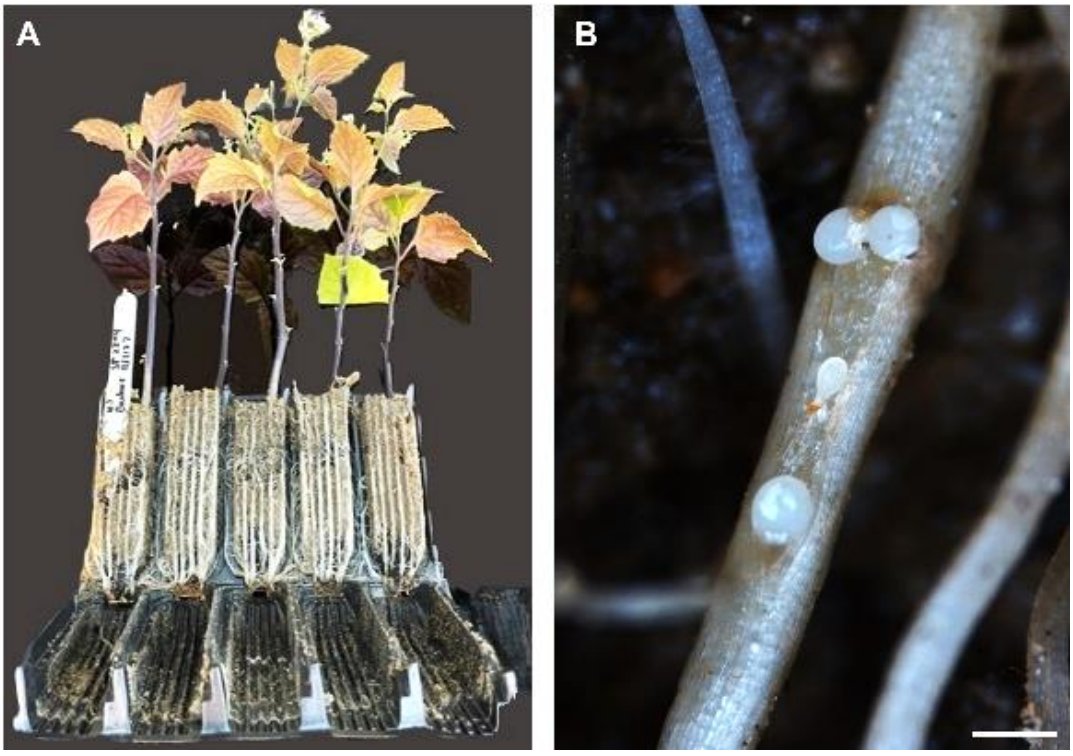

Figure 5.4. Root trainer high throughput assay.

A) Photograph of *S. americanum* plants in root trainers. The sides of the root trainer pots can be folded down to reveal the roots for inspection.

B) Four female *G. pallida* cyst nematodes visible on roots of a susceptible *S. americanum* plant grown in a root trainer. Scale bar=500 µm.

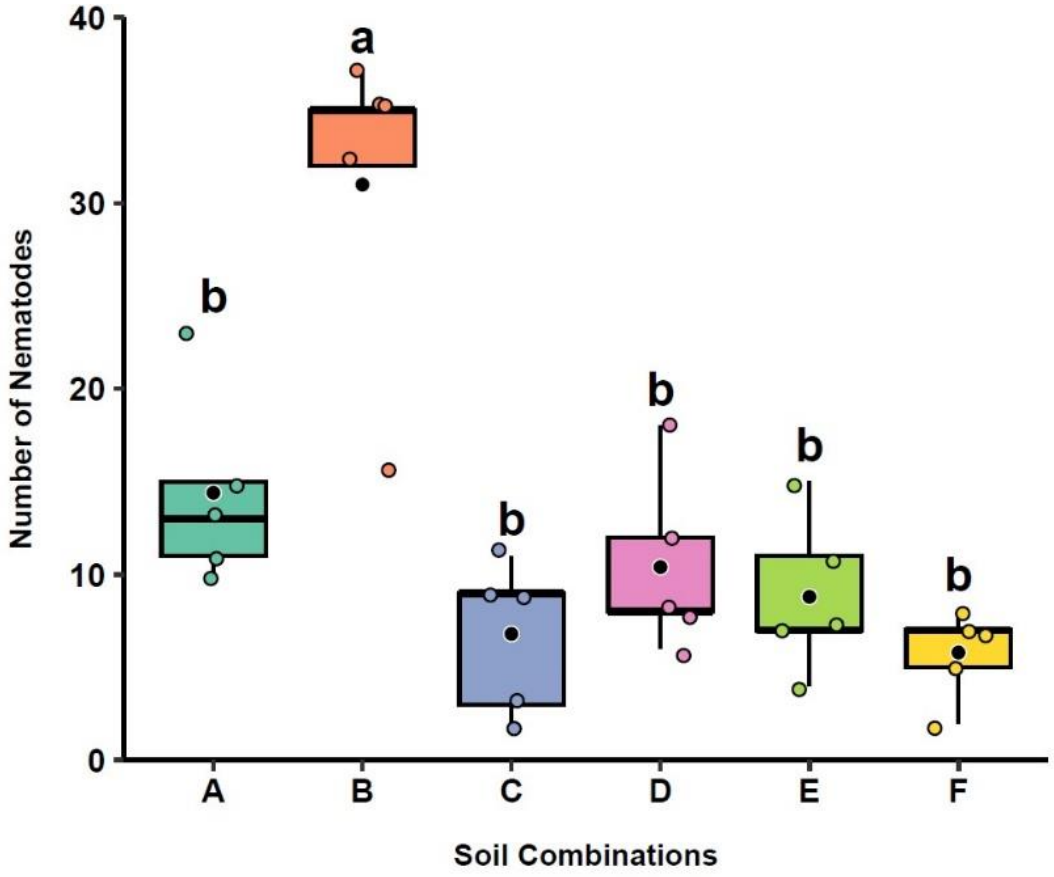

Figure 5.5. Infectivity of the cyst nematode *G. pallida* in *S. americanum* accession SP2273 under different soil combinations in root trainers.

The number of female nematodes visible on the roots were counted per plant after opening the root trainers. **A)** Compost and sand-loam (50:25:25) with *G. pallida* (40 eggs/g soil) and tomato root exudates; **B)** Compost and sand-loam (50:25:25) with *G. pallida* (80 eggs/g soil) and tomato root exudates; **C)** Only sand-loam (50:50) with *G. pallida* (40 eggs/g soil) and no root exudates**; D)** Only sand-loam (50:50) with *G. pallida* (40 eggs/g soil) and tomato root exudates; **E)** Only sand-loam (50:50) with *G. pallida* (80 eggs/g soil) and no tomato root exudates; **F)** Only sand-loam (50:50) with *G. pallida* (80 eggs/g soil) and tomato root exudates. Boxes represent interquartile range, the bold line inside the boxes represents median value, black dot inside the boxes exhibit mean value and the whiskers extend to the maximum and minimum values within 1.5x interquartile range. Each dot indicates an individual sample (n=5). Treatments sharing the same letter are not significantly different ($p < 0.05$) in a Tukey HSD test following one-way ANOVA.

5.4.2 Phenotyping of F2 plants arising from a cross between SP2273 and SP1101

F2 seeds were available after selfing of F1 plants from an initial cross between the susceptible *S. americanum* accession SP2273 and the partially resistant accession SP1101. We examined 60 individual plants arising from these seeds to assess the segregation of the resistance/susceptibility trait for subsequent genomic analysis. There was a significant variation in the number of female nematodes found in these plants.

Considering the scale of 0-10 females/plant as resistant and >10 females/plant as susceptible according to the trend of the experiment conducted initially as mentioned above, it was revealed among 60 plants that 44 plants were identified as resistant with 13 plants being highly resistant (0-1 females/plant). Whereas 16 plants were susceptible producing >10 females/plant (Figure 5.6). These distributions clearly revealed a ratio between resistant: susceptible at approximately 3:1 that supports Mendel's observed 3:1 phenotypic ratio in case of a heterozygous population, where there is a single dominant resistance gene.

A chi-square (χ^2) goodness-of-fit test was also performed to compare the observed segregation (44 resistant and 16 susceptible) with the expected 3:1 Mendelian ratio for a single dominant gene. The calculated χ^2 value was 0.089 (df = 1, p = 0.76), indicating no significant deviation from the expected ratio. This suggests that resistance segregates according to the expected 3:1 pattern, consistent with single-gene dominant inheritance.

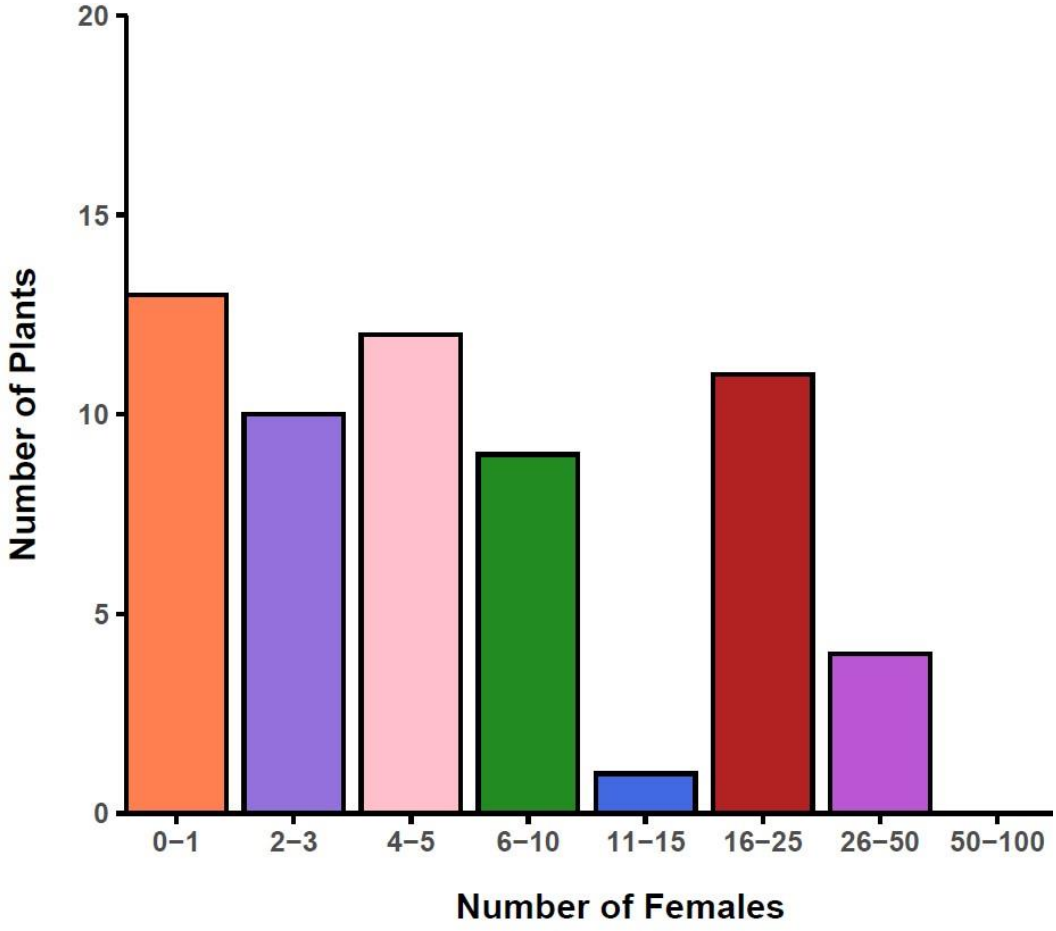

Figure 5.6. Frequency distribution of number of *G. pallida* potato cyst nematode females among 60 Solanum F2 cross (SP2273xSP1101) plants.

5.4.3 Phenotyping of plants arising from a cross between SP2273 and SP2299 accessions

We also examined another 60 F2 cross (SP2273xSP2299) plants individually to assess the segregation of inheritance for subsequent genomic analysis.

Following the designated resistance scale, it was revealed from 60 plants that 58 plants were identified as resistant with 49 of those plants being highly resistant (0-1 females/plant). On the other hand, only 2 plants were susceptible producing >10 females/plant (Figure 5.7). This type of segregation (29:1) indicates the strong biased distribution towards a resistant population.

As expected, the chi square (χ^2) goodness-of-fit test between observed resistant (58) and susceptible phenotypic (2) ratio revealed a highly significant *($p<0.0001$)* deviation from a 3:1 ratio, indicating more than one resistance locus. Conversely, the segregation did not significantly deviate from an expected 15:1 ratio ($\chi^2 = 0.87$, df = 1, $p \approx 0.35$, not significant) that would be typical for two unlinked, dominant genes.

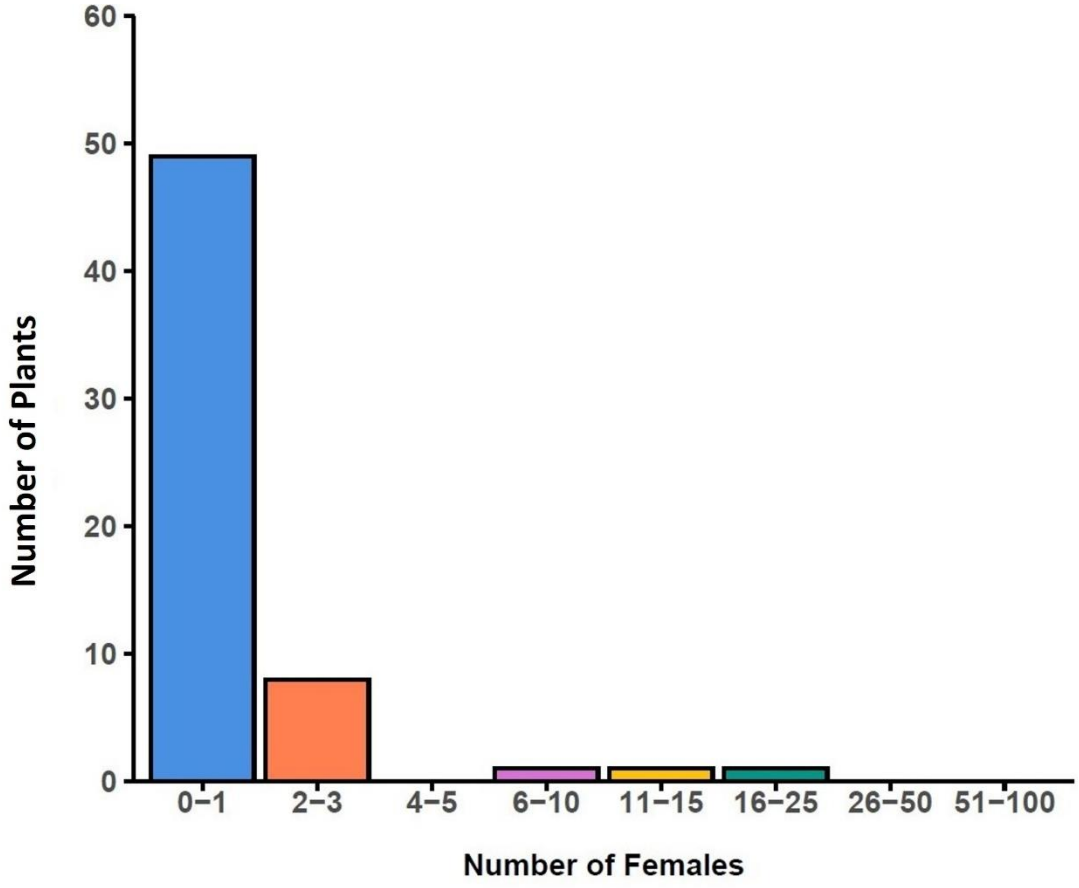

Figure 5.7. Frequency distribution of number of *G. pallida* potato cyst nematode females among 60 Solanum F2 cross (SP2273xSP2299) plants.

5.4.4 Growth of susceptible and resistant *S. americanum* accessions in tissue culture

All previous work with the *S. americanum* accessions had been carried out in glass house conditions with infection from soil-borne cysts of *G. pallida*. This was to replicate the natural infection scenario as closely as possible, however it was difficult to characterise the resistance responses in detail in those conditions. Therefore, we explored how best to set up a robust infection system in tissue culture.

In preliminary tests of Solanum plants grown in tissue culture conditions in MS30 media and inoculated with *G. pallida* J2s, accession SP2299 (Resistant) showed no development of female nematodes whilst only a few females developed on roots of SP2273 (Susceptible) as expected (Figure 5.8). In the case of the resistant SP2299 accession a few J2s, but no other stages, were found after 35 days of infection. We also kept some plates for longer for further observation. However, the further development of J2s was not seen even after 50 to 60 days of infection. Although few nematode infections were observed, the numbers of J2s in SP2299 and females in SP2273 was much lower than expected. The growth of the plants that did germinate in this media was good, although the seeds revealed poor and/or delayed germination. It was suggested (Forte et al., 2019) that the fluctuation of day and night temperature, rather than the constant controlled temperature facilitates the germination of *S. americanum* seeds. So, to encourage germination, we kept the petri dishes with sown seed in the same glass house conditions as used for all the other Solanum work. Once the seed germinated, we transferred the petri dishes back to the tissue culture facility. Once the germinated plants were placed in tissue culture they continued to grow well. After 30 days of infection, the plants were still green with vigorous root systems but after 50 to 60 days of infection, the plants started to dry as the media became desiccated. Therefore, we concluded from these preliminary results that we needed to determine the most appropriate media and conditions not only for the plants but also for nematode infection and development.

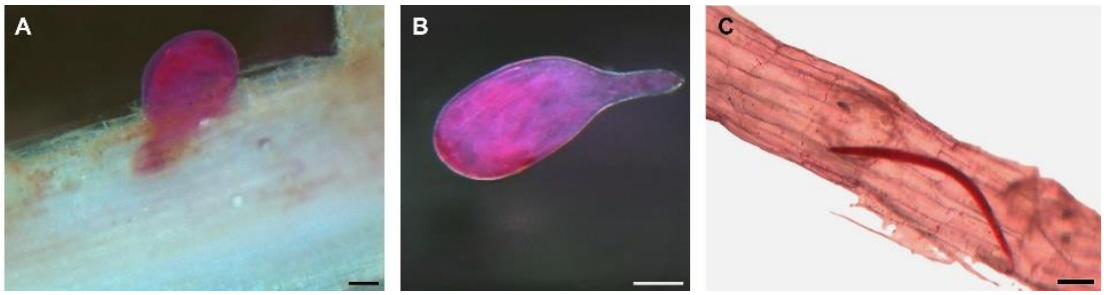

Figure 5.8. Potato cyst nematode development in susceptible and resistant lines at 35 days post infection.

A) Mature developed female in infected susceptible accession SP2273.

B) Mature female *G. pallida* dissected from a root of SP2273.

C) Only 2nd-stage juveniles (J2) were detected in roots of the resistant accession SP2299 with no development of females observed.

Scale bar=100µm.

5.4.5 Optimisation of media for growth of *Solanum* accessions in tissue culture

There is not much precedent for working with *S. americanum* in tissue culture and so we carried out an initial test, based on information found in the literature and for similar plants, to determine what media or media composition would be suitable and if we could achieve a good level of nematode infection and development under those conditions.

To select the optimal media composition, MS media supplemented with varying sucrose levels were evaluated against the number of female nematodes of *G. pallida* that developed on the susceptible accession SP2273. Tomato plants were also infected as a reference species of a susceptible host for potato cyst nematode. This allowed for comparative assessment of growth responses and infection potential under identical media conditions. Acid fuchsin staining of infected plants confirmed the infection level, allowing microscopic identification of nematodes and accurate quantification (Figure 5.9).

For comparing the effect of different sucrose concentrations on the number of females, two-way ANOVA was performed. Under the varied tested media conditions, non-statistically significant effects of plant species ($p = 0.685$), MS media sucrose concentration ($p = 0.223$), or their interaction ($p = 0.549$) on the number of nematode females were found. Among all the media conditions, the maximum number of mean (±SE) females was observed in MS20 medium for both *Solanum* (7.33 ± 3.38) and tomato plants (10.33 ± 4.37). These values were statistically similar to MS30 for Solanum (5.67±3.48) and tomato (3±1). Similarly, MS10 medium resulted in mean female counts of 4.40 ± 0.68 in *Solanum* and 6.00 ± 1.92 in tomato (Figure 5.10). Although MS20 medium supported the highest mean number of nematode females in both Solanum and tomato plants, nematode development in MS30 medium was not statistically different. Moreover, Solanum plants exhibited better overall growth performance in tissue culture when maintained on MS30. Therefore, MS30 was selected for subsequent experiments, as it provides conditions conducive to both healthy plant growth and nematode development, which are critical for long-term *in vitro* studies. This selection also aligns with the use of standard MS30 medium reported in earlier studies (Haque et al., 2018).

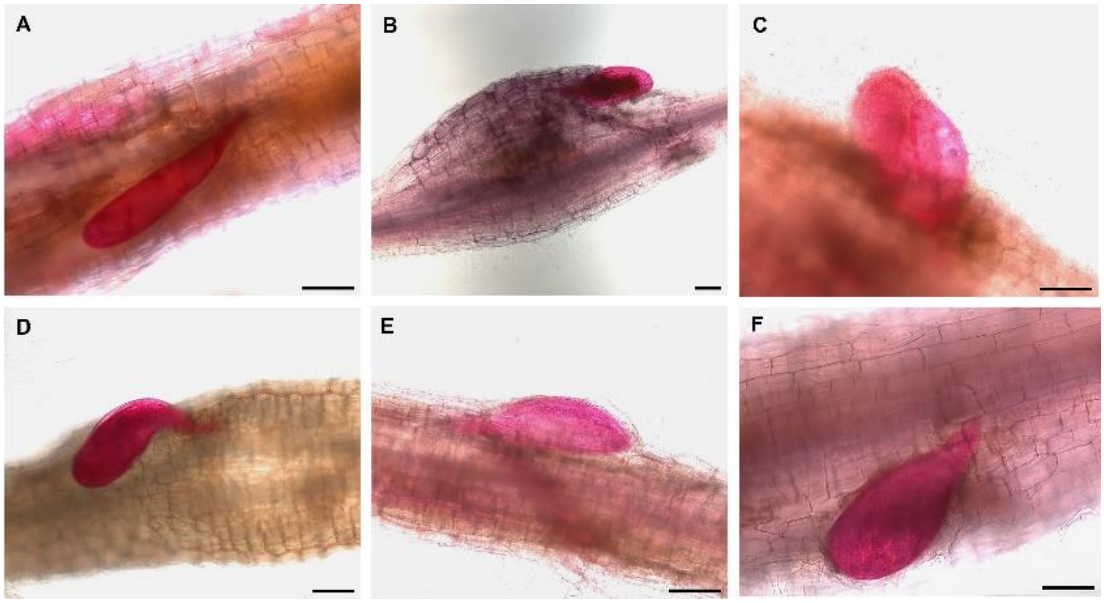

Figure 5.9. Development of *G. pallida* females in infected tomato and Solanum plants grown on MS medium containing different concentrations of sucrose at 5 weeks post infection.

A-C) Infected tomato roots on MS media containing **A)** 10 g/l sucrose; **B)** 20 g/l sucrose; **C)** 30 g/l sucrose.

D-F) Infected roots of *S. americanum* accession SP2273 on MS media containing **D)** 10 g/l sucrose; **E)** 20 g/l sucrose; **F)** 30 g/l sucrose.

Female nematodes are stained pink with acid fuchsin.

Scale bar=100µm.

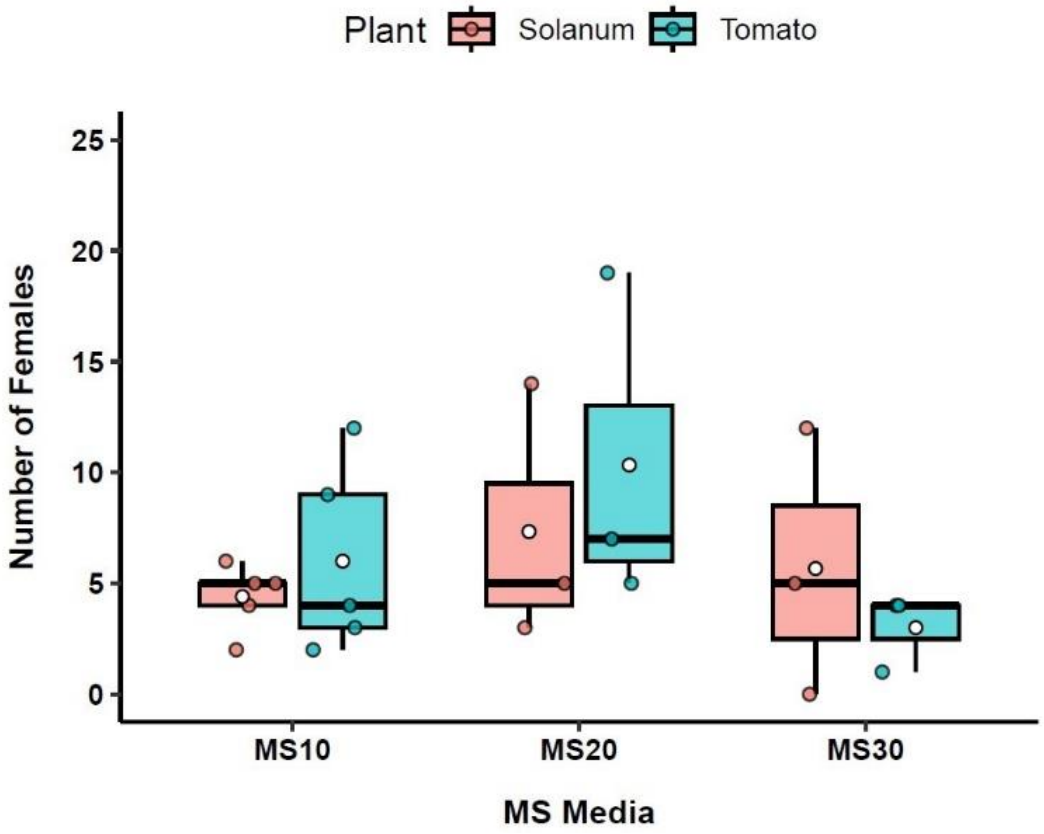

Figure 5.10. Interaction between number of *G. pallida* females and different MS media at 5 weeks post infection.

Boxplot represents interquartile range, the bold line inside the boxes represents median value, white dots inside the boxes exhibit mean value and the whiskers extend to the maximum and minimum values within 1.5x interquartile range. Each dot indicates an individual sample (n= 5 for MS10, n=3 for MS20 and MS30). A non-significant interaction was found using two-way ANOVA.

It had been apparent in the previous tests that variable numbers of plants were lost to contamination leading to difficulty in obtaining sufficient plants at the same stage for infection tests and variable numbers of replicates. The feasibility of using Plant Preservative Mixture (PPM) in the MS media was investigated with the aim of reducing the microbial contamination during infection assays. Before using PPM routinely in experiments, we needed to determine if it had any effect on growth and development of *G. pallida*. Female nematodes in the infected Solanum plants grown with and without PPM in the media were counted both before and after staining to ensure accurate quantification and mitigate for potential loss of mature females during the acid fuchsin staining process. All the tested media conditions provided substantial development of female nematodes (Figure 5.11), suggesting that the presence or absence of PPM did not substantially affect the invasion or development of nematodes (Figure 5.12).

A one-way ANOVA test comparing the number of females counted in the stained/unstained roots growing on media with or without PPM confirmed statistically non-significant variation among the groups ($F_{22} = 1.402, p = 0.269$) (Figure 5.12). The mean (±SE) number of females was higher (7.0±2.6) before staining than after staining (5.13±1.22) in media containing no PPM, indicating the loss of a few females during the staining process. Conversely, a higher number of females (11.4±2.46) was observed after staining compared to before staining (8.2±1.93) for the PPM supplemented media, suggesting improved visualisation and accurate identification of nematodes post-staining. Thus, within the scope of this data, variations in female counts across PPM effect levels can be attributed to random variation rather than to any treatment effect. This supported the inclusion of PPM in the medium for future experiments and resulted in improved control of microbial contamination.

Figure 5.11. Impact of Plant Preservative Mixture (PPM) on development of *G. pallida* at 5 weeks post infection

The development of *G. pallida* females on roots of *S. americanum* accession SP2273 growing on media **(A)** lacking PPM and **(B)** supplemented with PPM.

Scale bar=100µm.

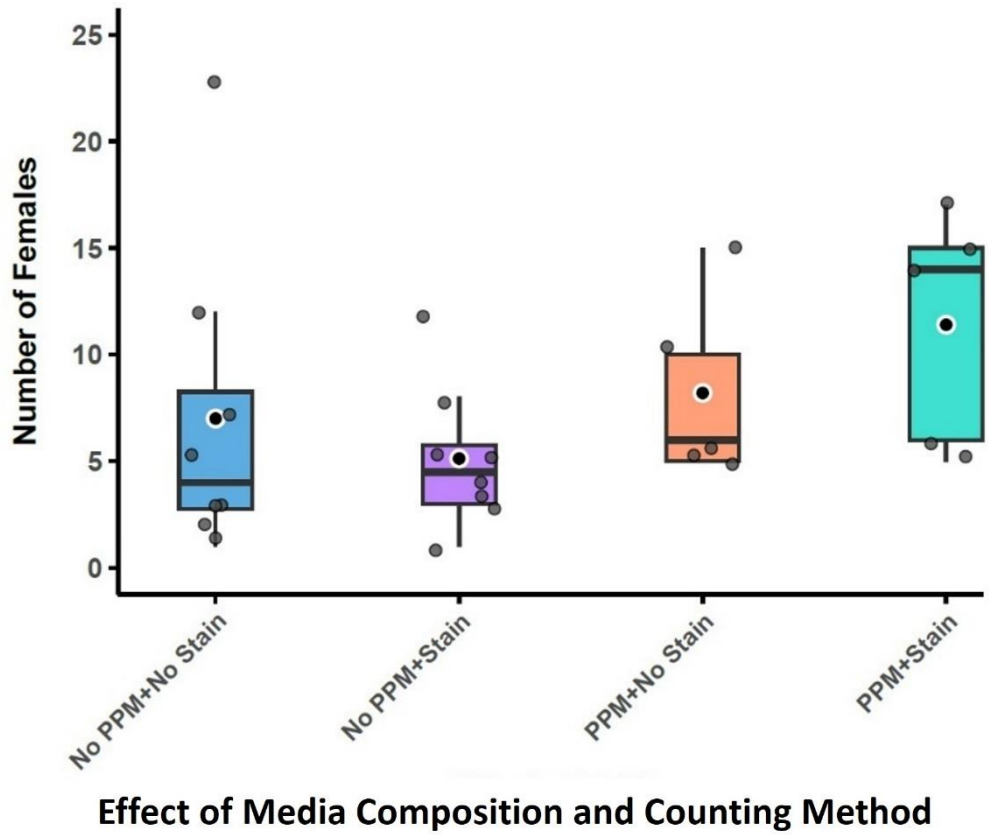

Figure 5.12. Effect on development of *G. pallida* females at 5 weeks post infection of using Plant Preservative Mixture (PPM) (2 ml/L) in the MS medium for growing of *Solanum* accessions.

Boxes indicate interquartile range, the bold line inside the boxes represents median value, black dots inside the boxes exhibit mean value and the whiskers extend to the maximum and minimum values within 1.5x interquartile range. Each dot indicates an individual sample (n=8 for without PPM and n=5 for with PPM). One-way ANOVA test proved statistically non-significant variation among the groups (*p = 0.269*).

5.4.6 Quantification of ROS accumulation in Solanum accessions in response to *G. pallida* infection

To assess the role of R genes in *Solanum* accessions, the timing and intensity of reactive oxygen species (ROS) production was monitored following nematode infection, as early and robust ROS accumulation is often indicative of effective R gene-mediated recognition and defence activation. To this end, ROS accumulation was determined by quantifying the DAB-stained spots, which act as a visible marker of ROS production and thus of oxidative stress. As ROS accumulation represents the early, initial stage of a defence response, the number of ROS spots per cm root were measured at two different time points (at 4 days post inoculation and 7 days post inoculation) to assess the dynamics of the response over time in the different Solanum accessions. Uninfected plants were included as a control for background ROS production that may be due to damage during the removal of roots from the media and during the staining process. The number of ROS spots varied considerably under infected and non-infected conditions in different Solanum accessions and there was visibly less DAB staining in the non-infected roots (Figure 5.13).

Three-way ANOVA was used to detect significant differences in level of ROS in roots of a range of infected and non-infected Solanum accessions at both four and seven dpi with *G. pallida* J2s. The three-way interaction (among the infected/uninfected accessions at 4 and 7 dpi) results represented a significant variation ($F_{5,96}=2.85, P=0.019$) among all the treatment combinations (Figure 5.14).The interaction between infection and the number of days after infection was highly significant ($F_{1,96} = 16.90$, $p < 0.0001$), showing that the effect of infection on ROS levels changed over time. In addition, the interaction between the different lines and the number of days after infection was also significant ($F_{5,96} = 6.97$, $p < 0.0001$), indicating that the lines responded differently depending on how many days had passed after infection. Among all the resistant lines, infected SP3393 line produced the maximum number (Mean±SE=5.94±0.49) of ROS spots at 4 dpi, followed by infected SP2299 at 4 dpi (Mean±SE=5.48±0.82) which was statistically similar to infected SP2273 at 4 dpi (Mean±SE=5.1±1.2), infected SP2308 at 4 dpi (Mean±SE=4.68±0.88), infected SP1032 at 7 dpi (Mean±SE=3.19±1.76) and infected SP1101 at 4 dpi (Mean±SE=3.46±0.39) and 7 dpi (Mean±SE=4.16±1.36). In contrast, minimum ROS levels were consistently observed in all uninfected roots at both 4 and 7 dpi. These values were not significantly different from one another and uniformly lower, indicating a lack of oxidative burst in the absence of nematode infection.

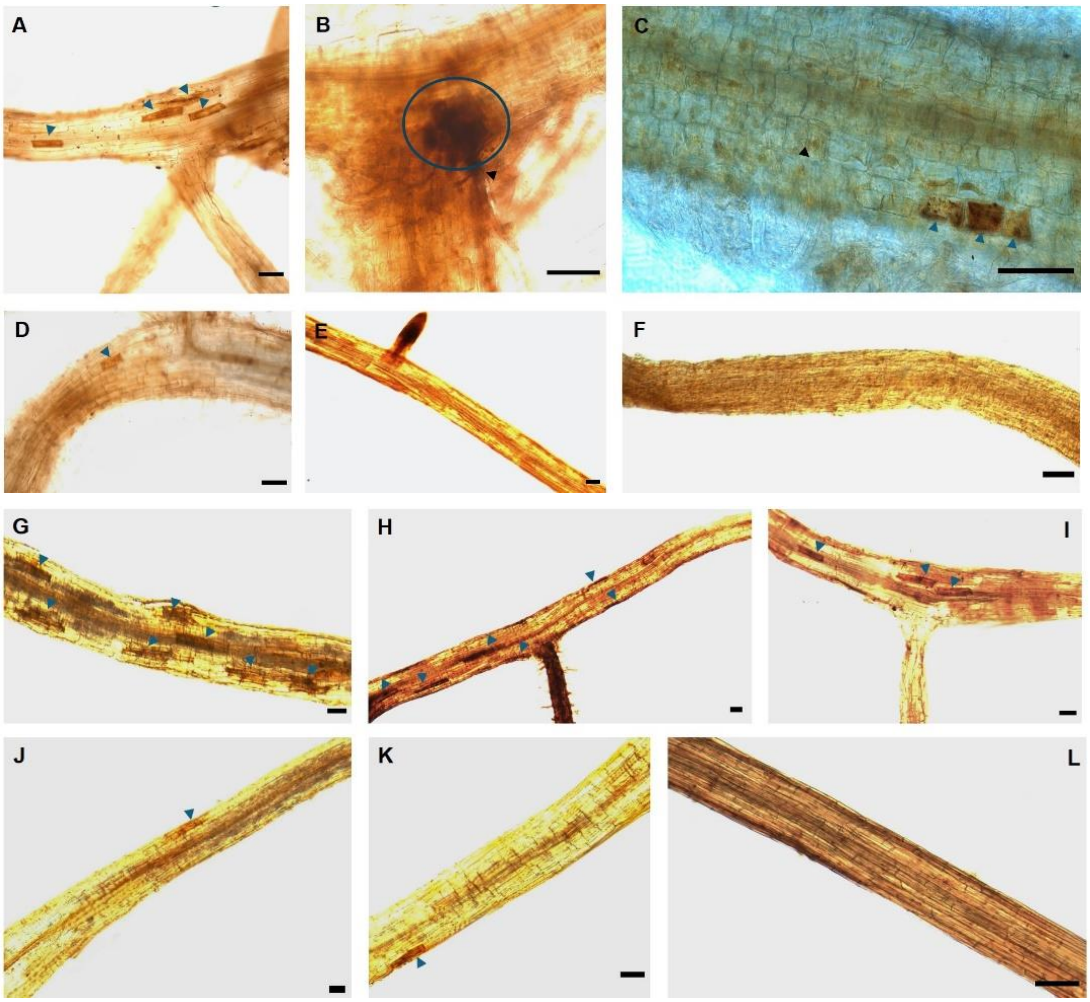

Figure 5.13. Detection of significantly higher reactive oxygen species (ROS) in *G. pallida*-infected Solanum roots than the non-infected controls.

Maximum number of ROS are accumulated in infected SP2299 at 4 dpi **(A)**, SP1101 at 7 dpi **(B)**, SP1032 at 7 dpi **(C)**, SP3393 at 4 dpi **(G),** SP2308 at 4D dpi **(H)** and SP2273 at 4 dpi **(I)**. Minimal to no spot formation was found in control (inoculated with water) plants; SP2299 **(D)**, SP1101 **(E)**, SP1032 **(F)**, SP3393 **(J)**, SP2308 **(K)** and SP2273 **(L)**. Blue arrows represent ROS spots and black arrows indicate nematode. Scale bar=100 µm.

The mean ROS value in uninfected Solanum accessions ranged from 0.21 to 1.96, reflecting ROS production due to basal immune response, mechanical or environmental stress rather than an induced defence response. These patterns of findings justify the role of nematode infection in triggering ROS production and also suggest that ROS levels remain strongly regulated under non infected conditions across different Solanum accessions and time points.

In the case of the nematode-induced ROS level amongst the different Solanum accessions, a non-significant interaction ($F_{5,96}=0.75$, $P=0.589$) was revealed, suggesting no overall differences in ROS accumulation among the resistant accessions and susceptible accession SP2273. Stated differently, there was not enough variance in ROS levels between the genotypes to be considered statistically significant. This implies that other factors, such as infection state and time after inoculation, may have a greater influence on ROS responses and that ROS accumulation is not necessarily correlated with the genetic resistance status of the Solanum accessions under the investigated conditions.

To assess the trend of increasing or decreasing reactive oxygen species (ROS) in infected Solanum accessions over time, a T-test was performed separately for each accession to evaluate the significant changes in ROS between 4 and 7 dpi. This analysis better highlighted changes in oxidative burst over the course of infection and different trends between accessions (Figure 5.15). There was no significant difference ($p = 0.60$ and 0.64, respectively) between the ROS level at 4 dpi and 7 dpi for resistant Solanum accessions SP1032 and SP1101. For the other resistant accessions (SP2299, SP2308 and SP3393), the ROS level declined significantly from 4 dpi to 7 dpi. Among these, SP3393 and SP2299 accessions exhibited statistically highly significant difference ($p<0.01$) and SP2308 showed statistically ($p<0.05$) significance difference between ROS levels at two time points. Interestingly, the susceptible accession SP2273 also exhibited a reduction of oxidative burst over the early infection period between 4 and 7 days post inoculation which was statistically significant ($p=0.02$). Overall, the result demonstrates an early resistance response in resistant Solanum accessions SP2299, SP2308 and SP3393 whereas the other two resistant accessions SP1032 and SP1101 exhibited a delayed resistance response that may have become more apparent at a later time point.

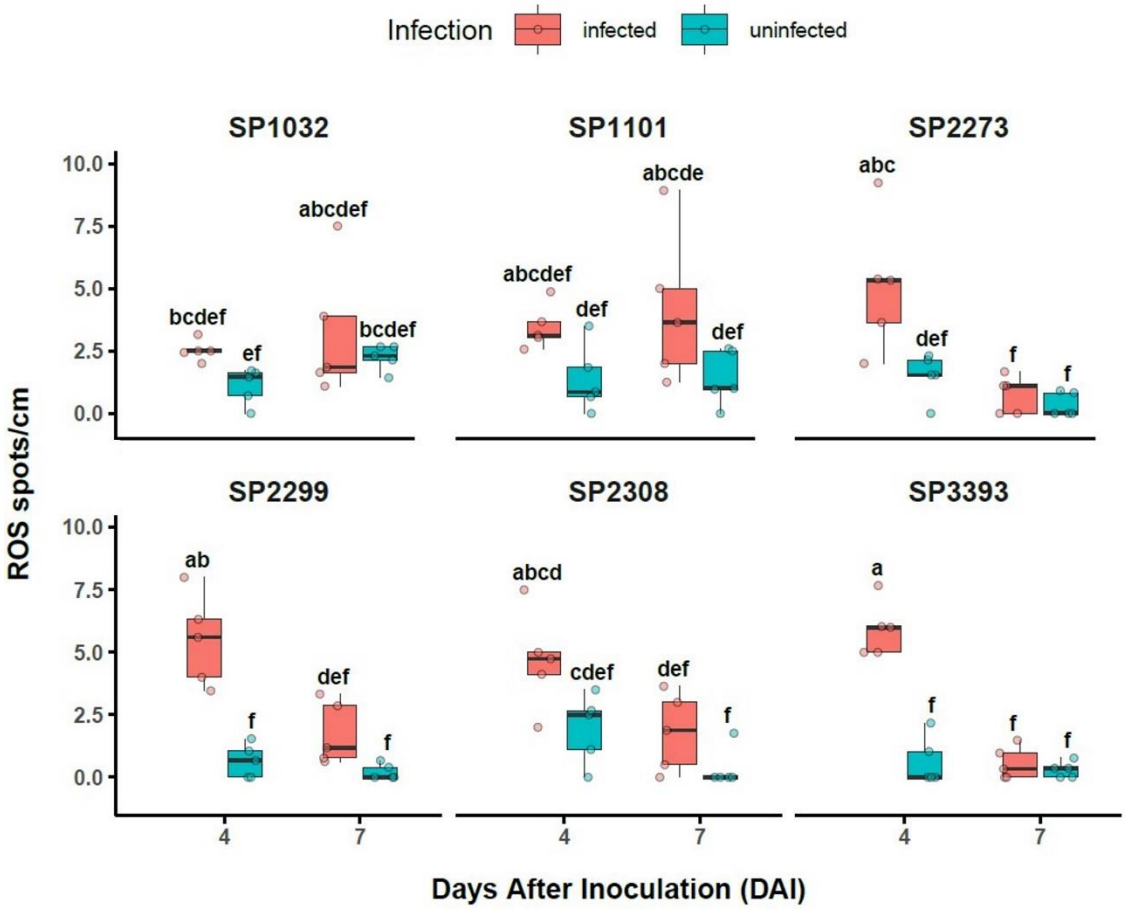

Figure 5.14. The level of reactive oxygen species (ROS) across different infected and non-infected resistant and susceptible Solanum accessions at different time points.

ROS accumulation was assessed in five resistant accessions and one susceptible accession (SP2273) in response to *G. pallida* infection or in non-infected control conditions at 4 and 7 days after inoculation. Boxes represent interquartile range, the bold line inside the boxes represents median value, and the whiskers extend to the maximum and minimum values within 1.5 x interquartile range. Each dot indicates an individual sample (n=5). Treatments sharing the same letter are not significantly different ($p < 0.05$) in a Tukey HSD test under three-way ANOVA (*P=0.019*).

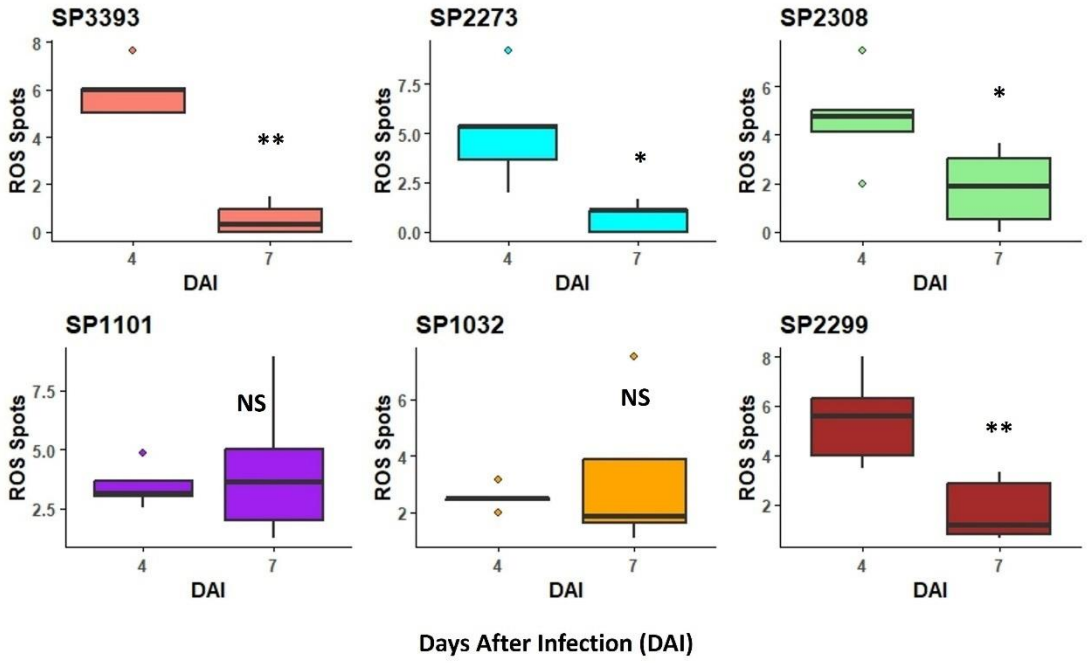

Figure 5.15. Level of reactive oxygen species (ROS) in different infected Solanum accessions at 4 and 7 days after inoculation.

Each graph shows a distinct Solanum accession evaluated at two time points after infection. Boxes represent interquartile range, the bold line inside the boxes represents median value, and the whiskers extend to the maximum and minimum values within 1.5 x interquartile range. A T-test was performed for each Solanum accession. There was no significant change in ROS levels between the two time points for accessions SP1032 and SP1101. Accessions SP2273, SP2299, SP2308 and SP3393 all exhibited a significant decrease of ROS accumulation between the two time points, suggesting an early resistance response. Each data point denotes the individual value (n=5). NS=Statistically Non-significant, * = $p < 0.05$ (statistically significant) and ** = $p < 0.01$ (highly significant).

5.5 Discussion

Given the relative lack of commercially available *G. pallida* resistant cultivars, especially for the fresh market, this study aimed to identify sources of effective R genes to potato cyst nematodes from the *S. americanum* genome. To that end, we first optimized soil mixtures in root trainers for cultivating F2 populations derived from a cross between resistant and susceptible *S. americanum* parents, in order to assess their infection phenotypes. In parallel, several *S. americanum* resistant and susceptible accessions were investigated for their physiological responses and optimal tissue culture conditions were established. The results suggested that root-trainers containing a mix of compost and sand-loam with high nematode inoculum and supplementation with potato root exudate significantly increased *G. pallida* populations, providing a more robust resistance screening system for F2 offsprings. Segregation patterns of resistance in F2 populations indicated the presence of two or more highly effective unlinked dominant genes conferring resistance to *G. pallida*. Our findings confirm the heritability of resistance traits and reveal the genetic diversity within the *Solanum* populations.

5.5.1 Root trainers enabled an effective high throughput assay

Root trainers have emerged as an effective, practical and cost-effective method for phenotypic screening of plant roots (Wharton et al., 2025) or plant responses to plant parasitic nematodes (Strachan et al., 2019, Gartner et al., 2024). However, they had not previously been used for screening *S. americanum* plants for nematode resistance and so the timescales and infection levels needed to be optimised for this species. In the present study, the use of root trainers facilitated clear visualisation of mature *G. pallida* females in the susceptible *S. americanum* accession SP2273 within five to six weeks after planting into cyst-infested soil. This time scale is consistent with the lifecycle of the same nematodes when infecting potato plants (Gartner, 2021); hence root trainers provide a reliable window for phenotypic screening during potato cyst nematode infection of *S. americanum* and related Solanum species.

Root trainers facilitate uniform root development due to their modular design and unlike a traditional pot system, this assay allows downward root growth along the surface of the container. This result is supported by a finding of Wharton et al. (2025) who observed the growth of roots predominantly in the bottom plane of root trainers. The design of the root trainers, which can be opened in a book style fashion, and pattern of root growth permit the

easy observation of root development. This design is appropriate for the detection of species such as cyst nematodes that become visible on the root surface as they mature. Therefore, this assay is useful particularly in the case of screening large populations such as F2 generations, where consistency and throughput are crucial.

5.5.2 Phenotyping of F2 (SP2273 X SP1101 and SP2273xSP2299) cross plants

To test the inheritance of resistance to *G. pallida*, two sets of F2 progenies derived from susceptible (SP2273) and resistant (SP1101 or SP2299) accessions of *S. americanum* were phenotyped individually. This analysis was conducted to investigate segregation patterns that can be used as identifying potential sources of novel potato cyst nematode resistance genes. DNA was also extracted from a leaf of each infected plant that we had planned to use subsequently for correlating the presence of specific R-gene loci with the resistance/susceptibility phenotype.

These distributions of resistance phenotypes in the first F2 cross (SP2273 X SP1101) clearly revealed a ratio of 3:1 (resistant: susceptible) highlighting the likely presence of single dominant R gene (Janssen et al., 1991) in SP1101. Conversely, the second F2 population (SP2273xSP2299) reveals the likely presence of multiple genes conferring a complex inheritance pattern of the high observed resistance. These patterns of inheritance are further reinforced by initial phenotypic screening against *G. pallida* (Greenwood et al., 2022). In the susceptible SP2273 line, good infestations with well-developed female nematodes were observed. Whereas only very few males and females with some second and third stage juveniles were detected in resistant line SP1101, suggesting the invasion of nematodes, but little further development or poor establishment of feeding sites. This indicates a post-invasion or delayed resistance strategy that probably involves localised defence responses such as hypersensitive cell death or disruption of syncytium formation. This might be due to the presence of a resistance gene with a similar mode of action to H1 (Rice et al., 1985) and *Hero A* (Sobczak et al., 2005). This type of resistance is also associated with 'male-biased' resistance which is sometimes found in cyst nematodes. In this case development of males occurs, but further development of females is not supported due to poor syncytium formation (Sobczak et al., 2005; Zheng et al., 2021).

In contrast, resistant parent line SP2299 displayed no evidence of any nematode development beyond the J2 stage. This indicates a possibility of a resistance mechanism involving structural barriers that prevented migration of the nematodes in the root beyond

the initial penetration (Lee et al., 2017). However, it had been noted that many of the J2s found in stained roots of SP2299 were in necrotic regions of root, suggesting a possible hypersensitive response to nematode migration. The complete absence of any nematode developmental stages beyond J2 in this accession also aligns with the high level of resistance phenotype and extremely skewed segregation ratio (29:1 = resistance : susceptible) in the F2 generation which was statistically similar to 15:1 ratio, this finding supported the existence of multiple resistance genes. This pattern of resistance is consistent with the presence of two unlinked resistance genes (15:1) in *S. americanum* F_2 progeny against *Phytophthora infestans* (Witek et al., 2021).

This divergence of the resistance response phenotype highlights the involvement of diverse types of gene interactions or resistance mechanisms. The near-complete resistance response in SP2273 x SP2299 populations represents high durability of resistance, justifying SP2299 as a potentially valuable source of resistance in breeding programmes. Moreover, the presence of different effective resistance phenotypes in both *S. americanum* accessions could imply the existence of both qualitative and quantitative resistance components. This aligns with previous findings where resistance to *G. pallida* was influenced by both major genes and minor QTLs (Bryan et al., 2002). To study the genetic basis of these discoveries and create molecular markers for marker-assisted selection, future genomic investigations like genome-wide association studies (GWAS) or QTL mapping will be crucial.

5.5.3 Optimal media trial for growing *Solanum americanum* plants in tissue culture

The MS media trial conducted in this study provided valuable insights into the optimal *in vitro* growth conditions for *S. americanum* under cyst nematode-infected conditions. Although there are few studies available for growing *S. americanum* plants in tissue culture, previous work suggests the potential of full or 1.5x strength MS medium supplemented with cytokinin and auxin for increasing flowering and fruit setting (Haque et al., 2018, Ramar et al., 2014). However, there are no studies addressing both the growth of *Solanum* species, and the development of potato cyst nematodes in tissue culture. The present study indicates that MS30, a standard medium optimized for tomato (Kaul et al., 2025) and potato (Hajra et al., 2021), effectively supports the growth of *S. americanum* and the development of potato cyst nematodes, making it a reliable choice for dual-host–pathogen assays.

Furthermore, a successful strategy was employed for reducing microbial contamination during the *in vitro* trial by adding the Plant Preservative Mixture (PPM) to the growth media.

In nematode bioassays and plant tissue culture, contamination is a frequent problem, especially when dealing with full life-cycle nematode infection assays that require prolonged growth times. In this study, PPM effectively maintained aseptic conditions without the need for recurrent subculturing or other antibiotics. Interestingly, PPM had no negative effects on *G. pallida* infectivity or development; nematode penetration, establishment, and progression to later developmental stages were similar to those of treatments without PPM. The active ingredients in PPM are 5-chloro-2-methyl-3(2H)-isothiazolone (CMIT) and 2-methyl-3(2H)-isothiazolone (MIT). These are often used in combination as a powerful biocide and preservative in consumer products such as paint, and household cleaners although their use in cosmetic products has been restricted or banned in the EU (Regulation (EC) No 1223/2009, Annex V). There is scarce information about the effect of the CMIT/MIT combination on nematodes, but one study found that exposure to CMIT/MIT induces metabolic toxicity in *C. elegans* via the O-linked N-acetylglucosamine transferase pathway, altering oxidative stress responses, fatty acid metabolism, and locomotory behaviour (Kim and Choi, 2019). Early stages of *C. elegans* seemed to be particularly sensitive to the effects. We found no evidence that the early developmental stages (J2s) of *G. pallida* were similarly affected. Due to its biological compatibility with both *G. pallida* and the host plant (*S. americanum*), PPM can be used as a supplement in *in vitro* nematode infection systems.

5.5.4 Quantitative ROS accumulation in Solanum accessions

An oxidative burst is considered as one of the most important defence reactions during host-pathogen interactions constituting localised and transient release of reactive oxygen species (ROS) (Hasan, 2019). During pathogen infection in resistant plant species, ROS detoxifying enzymes such as APX (Ascorbate Peroxidase) or CAT (Catalase) are suppressed, resulting in more ROS accumulation leading to a hypersensitive response (HR) (Das et al., 2008). This HR expression is a distinct phenotypic evidence of plant resistance. The nematode resistance genes in resistant plants trigger HR which targets nematodes invading cells. A key factor in this defence mechanism is the precise timing of hydrogen peroxide (H_2O_2) production, which plays a crucial role in preventing the nematodes establishing successfully (Chen et al., 2020; De Kock et al., 2024). Several techniques are employed to quantify ROS accumulation. In our present study, we used the polymerization of 3, 3-diaminobenzidine (DAB) stain-based method to measure ROS level in different resistant accessions under infected and uninfected conditions at two time points of early infection. The resulting polymer is a highly stable, dark

brown, and insoluble product that remains fixed, making it easy to observe visually (De Kock et al., 2024).

The results from DAB staining revealed a significant amount of ROS accumulation in infected Solanum genotypes at both time points of infection (4 and 7 dpi) compared to uninfected control plants. This indicates that potato cyst nematode infection triggers an oxidative response in both susceptible and resistant lines. The absence or low levels of ROS accumulation in uninfected lines represents lack of basal oxidative activity under non-stressed conditions. This result supports the hypothesis that ROS accumulation is incited by the pathogen and plays a key role in the initial recognition or stress response to nematode invasion in plants. This finding aligns with previous reports highlighting increased ROS production is correlated with nematode invasion in plant roots (Siddique et al., 2014, Chen et al., 2020).

In respect of changes in ROS level at different timepoints of infection in the resistant lines, differential temporal resistance responses were found. The resistant Solanum accessions SP2299, SP2308 and SP3393 exhibited early resistance responses, whereas a more delayed resistance response was employed by resistant accessions SP1032 and SP1101. The early responses demonstrated a defence reaction soon after nematode infection or restricted nematode invasion into infected roots, which is common in *Meloidogyne spp*. (Bleve-Zacheo et al., 1998; Paulson and Webster, 1972) but not typically identified in the case of cyst nematodes (Sobczak et al., 2005). The early resistance response detected in SP2299, SP2308 and SP3393 lines aligns with the initial phenotyping, particularly in SP2299, which effectively restricted invasion and migration of J2 nematodes. Furthermore, the SP2299 accession when crossed with the susceptible SP2273 also produced highly resistant F2 phenotypes. SP3393 showed the highest level of nematode-induced ROS among all the Solanum accessions, consistent with its initial phenotyping, in which there was evidence for invasion of only a few J2s with no subsequent development of J3, male or female *G. pallida*. In contrast, the ROS level increased gradually over time in the SP1032 and SP1101 accessions, exhibiting a more delayed resistance response. *Globodera*-infected resistant plants generally demonstrates a "hypersensitive-like" or "delayed hypersensitive" reaction. It was evident from such response that the cyst nematode feeding sites deteriorate slowly or develop abnormally after syncytium induction (Grymaszewska and Golinowski, 1998; Holtmann et al., 2000; Rice et al., 1985; Wyss et al., 1984). Previous studies also suggested variation in hypersensitive response (HR) in different plant species at different time points. For example, HR was found

in tomatoes as early as 24 hours after inoculation, while it was detected in pepper, soybean, or coffee at 1-3, 2-3, and 4-6 days after inoculation, respectively (Das et al., 2008). These discrepancies could be explained by changes in the speed of downstream defence responses, the efficacy of signal transduction, or pathogen recognition receptors, particular resistance gene and plant nematode interaction (Williamson and Kumar, 2006). This temporal variance in resistance responses in different Solanum accessions focuses the dynamic nature of the resistance mechanisms, including both delayed and early regulatory processes.

Nevertheless, statistically similar levels of ROS accumulation were observed in susceptible and resistant Solanum accessions, this implies that the resistance phenotype may not be determined solely by the ROS response. The oxidative burst and XR (rapid ion fluxes across the plasma membrane) are likely required but might not be generally enough to start cell death (Morel and Dangl, 1997). The outcome of the interaction may be determined by downstream reactions, such as gene expression, cell wall reinforcement, basal defence reactions, or hormone signalling, whereas ROS may serve as a general early indication of stress or damage (Torres et al., 2006). Non-significant difference between ROS activity in resistant and susceptible lines was also supported by previous findings in cowpea. This can be explained by the absence of biphasic manner of ROS production in cowpea, which instead exhibits an oxidative burst as part of the basal defence response rather that Rk-gene-mediated resistance upon root-knot nematode infection (Das et al., 2008). Future work could focus on more sensitive and quantitative approaches, such as fluorometric detection of H_2O_2, *in situ* imaging using ROS-specific dyes (e.g., 2',7'-Dichlorodihydrofluorescein diacetate (H_2DCF-DA), or expression profiling of ROS-related genes (e.g., *RBOH*, *CAT*, *APX*) to better resolve the dynamics of ROS during different developmental stages of nematodes in susceptible and resistant accessions.

5.6 Conclusions

The work conducted in this project has successfully established that there is variable resistance to *G. pallida* amongst different *S. americanum* accessions. Additionally, the variation in infection phenotype observed between the F2 offspring examined indicates that resistance and susceptibility are, at least in part, heritable traits with most offspring having a phenotype similar to one of the parents. Thus, this project has laid the groundwork for further research.

The key findings from the experiments are:

- Root trainers were determined to be an effective assay for screening large Solanum populations under *G. pallida* infection, exhibiting their potential as a high throughput and reproducible method for resistance screening with this plant:nematode combination.

- The combination of compost with sand-loam (1:1), root exudate stimulation, and a standardized cyst nematode inoculum of 80 eggs/g soil was an effective setup for promoting infection by *G. pallida* and reliable resistance phenotyping of *Solanum* accessions.

- The phenotypic segregation patterns observed in the F_2 populations not only confirmed the inheritance of resistance traits but also highlighted the complexity and diversity of resistance mechanisms within the *Solanum* gene pool. This insight is essential for developing effective and sustainable breeding strategies against potato cyst nematodes.

- The successful development of *Solanum* plants under tissue culture conditions using standard MS30 medium supplemented with Plant Preservative Mixture (PPM) demonstrates the effectiveness of this approach for maintaining sterile cultures and promoting healthy plants as well as nematode development.

- ROS-based characterisation of resistance responses revealed the intricate and dynamic nature of defence signalling in resistant Solanum accessions, as demonstrated by the early and late oxidative bursts.

Chapter 6

General Discussion

The project was based on two broad objectives. Firstly, the non-destructive betalain-based RUBY reporter construct was successfully validated in transgenic Arabidopsis and potato as well as during the interactions with root-knot and cyst nematodes. Subsequently, this reporter system was used to generate successfully novel RUBY reporter constructs with root-specific, nematode-inducible promoters, providing molecular tools for studying spatial and temporal regulation of gene expression in potato roots in response to nematode infection. Another aspect was screening of diverse *Solanum americanum* accessions against the potato cyst nematode *G. pallida* to characterise the resistance phenotypes for using in the mapping of potential resistance loci. Together, these approaches expand molecular tools for gene expression studies while also identifying valuable genetic resources for breeding nematode-resistant potato cultivars.

6.1 The utility of the RUBY reporter system to investigate early nematode infection under field conditions

In this study, two different betalain-based reporter systems were employed, each using distinct regulatory strategies to control the expression of betalain biosynthetic genes in transgenic plants. The aim was to evaluate whether this novel reporter system could serve as a robust alternative to conventional GUS or GFP reporters for monitoring plant gene expression during plant–nematode interactions. As an initial assessment, a CaMV35S-driven RUBY construct was introduced into Arabidopsis and potato plants, allowing examination of RUBY expression in nematode-induced feeding sites. In parallel, previously characterised *Nicotiana benthamiana* lines carrying RUBY under AM symbiosis–specific promoters were evaluated to explore whether an inducible betalain system could also respond visibly to AMF-nematode interaction.

Both the constitutive and inducible RUBY reporter systems produced clear betalain accumulation during the course of infection. Although each approach offered useful insights, the CaMV35S:RUBY construct that utilised a translational fusion system to deliver the three enzymes required for betalain synthesis provided consistently strong pigmentation and, importantly, a more straightforward cloning strategy for downstream modifications. Owing

to this simplicity, the RUBY framework was subsequently used to engineer nematode-responsive, root-specific constructs to monitor transcriptional activation during infection. Two promoter-driven constructs (pBI:PG1-RUBY and pBI:PG2-RUBY) were successfully developed, and transgenic potato lines expressing these constructs displayed visible reporter activation in roots. Notably, the pBI:PG2-RUBY construct also drove clear RUBY accumulation specifically in roots during nematode infection, confirming its responsiveness.

Together, these findings demonstrate the potential of the RUBY reporter system as a practical visual tool for assessing early nematode infection. By enabling rapid, non-destructive, and equipment-free visual assessment, the system provides a strong foundation for evaluating its advantages and limitations relative to existing reporter technologies. Importantly, these results justify further investigation into the applicability of RUBY beyond laboratory conditions and support its development as a candidate reporter for use in the field condition.

6.1.1 RUBY as a versatile tool in molecular biology

The betalain-based RUBY reporter demonstrates a major advance in visual marker systems for biology offering cost-effective, non-invasive, continuous gene expression in all types of plants and animals (He et al., 2020; Yang et al., 2023; Sun et al., 2023). It has already proven highly effective not only as a transformation marker but also as a versatile tool for analysing gene expression, protein–protein interactions between pathogen effectors and plant resistance proteins, protein–DNA interactions and tracking various cellular processes (Chen et al., 2023; Sun et al., 2023). With its expanding capabilities, RUBY offers a robust strategy for high-throughput screening of molecular regulators, including transcriptional activators and repressors, pre-mRNA splicing factors, RNA silencing components, and DNA-binding proteins, thereby advancing functional genomics and molecular biology research (Sharifova et al., 2025). Furthermore, a redesigned RUBY system driven by stress-responsive promoters offers the potential for real-time, field-based detection of environmental stresses or pathogen attack. This innovation could significantly enhance precision agriculture by enabling timely monitoring and more efficient resource management.

To enable early detection of biotic and abiotic stresses using visual reporters like RUBY, it is essential to develop natural or synthetic promoters with high specificity to individual stress signals. While several stress-responsive elements have been identified, many exhibit cross-reactivity, responding to multiple stress types. In addition to developing stress-specific

reporter systems, successful field deployment will require complementary technologies such as aerial imaging for signal detection and computational models for data interpretation (Sharifova et al., 2025). By integrating RUBY into precision agriculture frameworks, researchers and growers can achieve dynamic, field-based insights into biotic stresses like pathogen invasion, ultimately improving decision-making and resource management. Our finding has opened promising avenues for field application, enabling non-invasive, real-time visualization of nematode infection in crops and facilitating early intervention strategies for sustainable pest management.

6.1.2 Limitations of the RUBY reporter system

The RUBY reporter system has shown considerable utility in recent studies; however, several limitations must be acknowledged when evaluating its broader applicability (Table 6.1). First, betalain pigments synthesized by RUBY are predominantly confined within vacuoles and do not diffuse beyond their site of production. This spatial confinement limits the utility of RUBY for subcellular localization studies, especially in comparison to fluorescent protein-based reporters (He et al., 2020). Second, the intense pigmentation associated with RUBY expression may result in substantial consumption of tyrosine, a key precursor in multiple metabolic pathways. This metabolic competition could potentially interfere with the biosynthesis of other essential compounds, thereby contributing to growth inhibition in transgenic plants (Lee et al., 2023; Tse et al., 2024).

Another shortcoming includes the expression instability that has been observed in certain transgenic events, with some lines exhibiting gene silencing (Baral et al., 2024). This phenomenon may be attributed to the use of a single constitutive promoter to drive the expression of all three betalain biosynthetic genes, potentially triggering co-suppression (Hu et al., 2025). Additionally, gene silencing may represent a plant defence mechanism against the expression of foreign genes. Finally, the current methodologies for quantifying RUBY expression (spectrophotometric analysis and image-based intensity measurements) lack the sensitivity and precision of more advanced reporter systems. These limitations hinder the accurate detection of subtle molecular events and weak physiological responses (Chen et al., 2023; Liu et al., 2024). Taken together, while RUBY offers a visually detectable and non-destructive means of monitoring gene expression, these constraints must be carefully considered when selecting it for specific experimental applications.

Table 6.1. The pros and cons of the RUBY system

Pros	Cons
Non-destructive and visually detectable: Betalain pigments allow real-time, non-invasive monitoring of gene expression without the need for expensive substrates or specialised equipment.	**Restricted subcellular resolution:** Betalains accumulate within vacuoles and cannot provide fine subcellular localisation compared with fluorescent reporters (e.g., GFP).
Cost-effective and equipment-free: Detection relies on visible red pigmentation, reducing reliance on microscopes, fluorimeters, or imaging systems.	**Metabolic burden:** High RUBY expression may consume substantial tyrosine, potentially altering metabolic pathways and contributing to growth inhibition.
Versatile applications: Effective for transformation screening, tracking gene expression, monitoring protein–protein and protein–DNA interactions, and studying cellular processes.	**Potential for gene silencing:** RUBY expression under the control of constitutive promoter (CaMV35S) triggers gene silencing mechanisms in transgenic events of Arabidopsis plants.
Amenable to high-throughput functional screening: Suitable for assessing transcription factors, RNA silencing components, DNA-binding proteins, and other molecular regulators.	**Expression instability between lines:** Variation among independent transformants can reduce reproducibility and complicate quantitative comparisons.
Compatible with inducible and stress-responsive promoters: Facilitates development of biosensors for environmental stimuli, pathogens, or stress exposure.	**Limited quantitative sensitivity:** Current detection methods (spectrophotometry, image-based analysis) lack the precision of luminescent or fluorescent reporters for subtle responses.
Potential for field-level applications: Visual detection of infection or stress without laboratory equipment enables opportunities in precision agriculture.	**Field detection challenges:** Reliable field implementation may require aerial imaging systems, sensors, or computational tools for accurate signal interpretation.

6.1.3 Field application potential of the RUBY reporter system for visual detection of nematode infection in crops

Betalain pigments produced by the RUBY reporter system enable clear visual identification of nematode infection without the need for specialized equipment, making it a highly practical tool for field-based diagnostics.

6.1.3.1 Use of natural systemic defence signals

Root infection by nematodes is known to trigger systemic signalling cascades involving phytohormones such as jasmonic acid, salicylic acid, and ethylene, as well as reactive oxygen species and electrical signals (calcium fluxes), which move from the infection site in the roots to distal tissues in the shoot (Wang et al., 2019). By placing the betalain biosynthetic reporter cassette (RUBY) under the control of promoters responsive to these systemic signals (or a synthetic promoter gated by a mobile trans-activator produced in infected roots), it should be possible to convert otherwise invisible molecular responses into a visible colour change in the leaves (Figure 6.1). This approach is consistent with the finding that root infection by *Meloidogyne* spp. triggers electrical signals or ROS into jasmonic acid signalling loops affecting shoots, and that *Heterodera schachtii* modifies shoot hormone profiles (JA, SA, ET) and defence markers following root parasitism (Kammerhofer et al., 2015; Wang et al., 2019).

The promoters of pathogenesis-related genes (eg. PR1 or PR5), which play a role in salicylic acid (SA)-mediated systemic acquired resistance (SAR) (Pape et al., 2010), could be harnessed so that elevated SA levels in leaves after root nematode infection drive betalain accumulation. When SA levels rise systemically in leaves, SA-responsive transcriptional regulators like NPR1/TGA complexes bind to certain PR promoters, inducing strong expression. In the absence of SA, NPR1 (Non-Expressor of Pathogenesis-Related genes 1) forms inactive oligomers in the cytoplasm. Accumulation of SA triggers a change in cellular redox state causing NPR1 to reduce into monomers, which then move into the nucleus and interact with TGA transcription factors to form activator complexes, promoting PR-gene transcription (Seyfferth and Tsuda, 2014).

Alternatively, nematode feeding also stimulates jasmonic acid (JA) and ethylene signalling cascades, which are typically dominant in plant responses to root-feeding pests. In this case, JA-responsive promoters such as *VSP2* (vegetative stage protein 2) or *LOX3/LOX4*

(Lipoxygenase 3 or 4) that are induced in leaves upon nematode infection (Wondafrash et al., 2013) could be used to activate RUBY in the foliage.

VSP2, LOX3, and LOX4 promoters are activated not only by biotic stresses like herbivory and pathogen attack but also by certain abiotic stresses, which can lead to systemic jasmonate signaling. For instance, LOX3 and LOX4 are the key enzymes in the jasmonate biosynthesis pathway and are strongly induced by repetitive wounding, contributing to growth restriction and defense activation even in the absence of direct pathogen challenge (Yang et al., 2020). Moreover, jasmonates are known to mediate plant responses to both biotic and abiotic stimuli, including drought, salinity, and mechanical damage, through complex hormonal crosstalk involving salicylic acid (SA) and other phytohormones (Santino et al., 2013). Therefore, while the use of such promoters in RUBY reporter construct can provide a broad and sensitive readout of plant stress responses, it may also result in unintended activation under non-pathogenic or environmental conditions.

Therefore, beyond natural promoters, synthetic two-component systems offer additional flexibility, such as nematode-inducible, root-specific promoters can be used to drive the expression of mobile transcription factors or peptides, which then migrate to the shoot and specifically activate RUBY expression in leaves. This modularity provides an opportunity to distinguish nematode attack from abiotic stress or other pathogens or adjust latency (matching the time window when systemic signals are strongest) and optimize deployment across host backgrounds. Such tuning is essential for field applications, where false positives from wounding or drought could compromise reliability, and where early detection of nematode infestation could have a tangible impact on management practices.

6.1.3.2 RUBY expression in leaves using a dual promoter construct

For greater specificity, a more synthetic nematode-inducible root-specific promoter (such as those expressed in feeding sites) could drive a mobile transcriptional activator in the root, while RUBY in the shoot is placed under a JA/SA-responsive promoter. During cyst-nematode (*H. schachtii*) infection, plant defensin promoter genes (e.g., Pdf2.1) strongly express in syncytia (Siddique et al., 2011). Similarly, a giant-cell specific tobacco promoter (TobRB7) expresses during development of feeding sites (Opperman et al., 1994). Using a tissue-specific promoter to control a transcription factor is an effective way to activate and increase the expression of any target gene, by binding to short upstream activation sequences (UAS). GAL4–VP16 (or GAL4–VP64 used in CRISPR system) is a synthetic transcription factor

combining the yeast GAL4 DNA-binding domain, which targets upstream activation sequences (UAS), with the potent VP16 activation domain from Herpes Simplex Virus, enabling strong and specific activation of gene expression (such as GUS) in engineered systems (Sevin-Pujol et al., 2017).

The nematode feeding site-induced promoters could be used to express such a mobile trans-activator (e.g. GAL4–VP64) tagged for phloem movement (with a FT mobility domain) or carrying a tRNA-like sequence (TLS) on its mRNA. The *FLOWERING LOCUS T (FT)* protein is a well-characterized phloem-mobile signal in Arabidopsis and other plants; fusing its mobility domain to the activator enables cell-to-cell and long-distance transport through the phloem (Corbesier et al., 2007). Alternatively, adding a TLS motif on its mRNA mimics endogenous mobile RNAs, allowing the transcript itself to move through the phloem. Reporter transcripts harbouring TLS-containing mRNAs moved from transgenic roots into wild-type leaves and were even translated after transport in Arabidopsis (Zhang et al., 2016).

Then the RUBY reporter cassette could be placed under a hormone-responsive promoter (e.g. PR1 for SA/SAR or VSP2/LOX for JA) fused to a minimal promoter with GAL4 UAS repeats to express in leaves (Figure 6.2). The leaf turns red only when the nematode feeding site in the root produces the mobile activator, and the systemic SA/JA signal triggers expression of the hormone-responsive promoter in the leaf. Chen et al. (2023) demonstrated that RUBY, through its interaction with the upstream activating sequence of the yeast GAL4 transcription factor, functions as an inducible reporter system for assessing protein–protein interactions between plant resistance proteins and pathogen effectors. This modular layout combines feeding-site promoters with mobility elements so that the reporter activates only when nematode attack in roots coincides with systemic leaf signals, providing a field-visible readout while minimizing false positives from unrelated stresses.

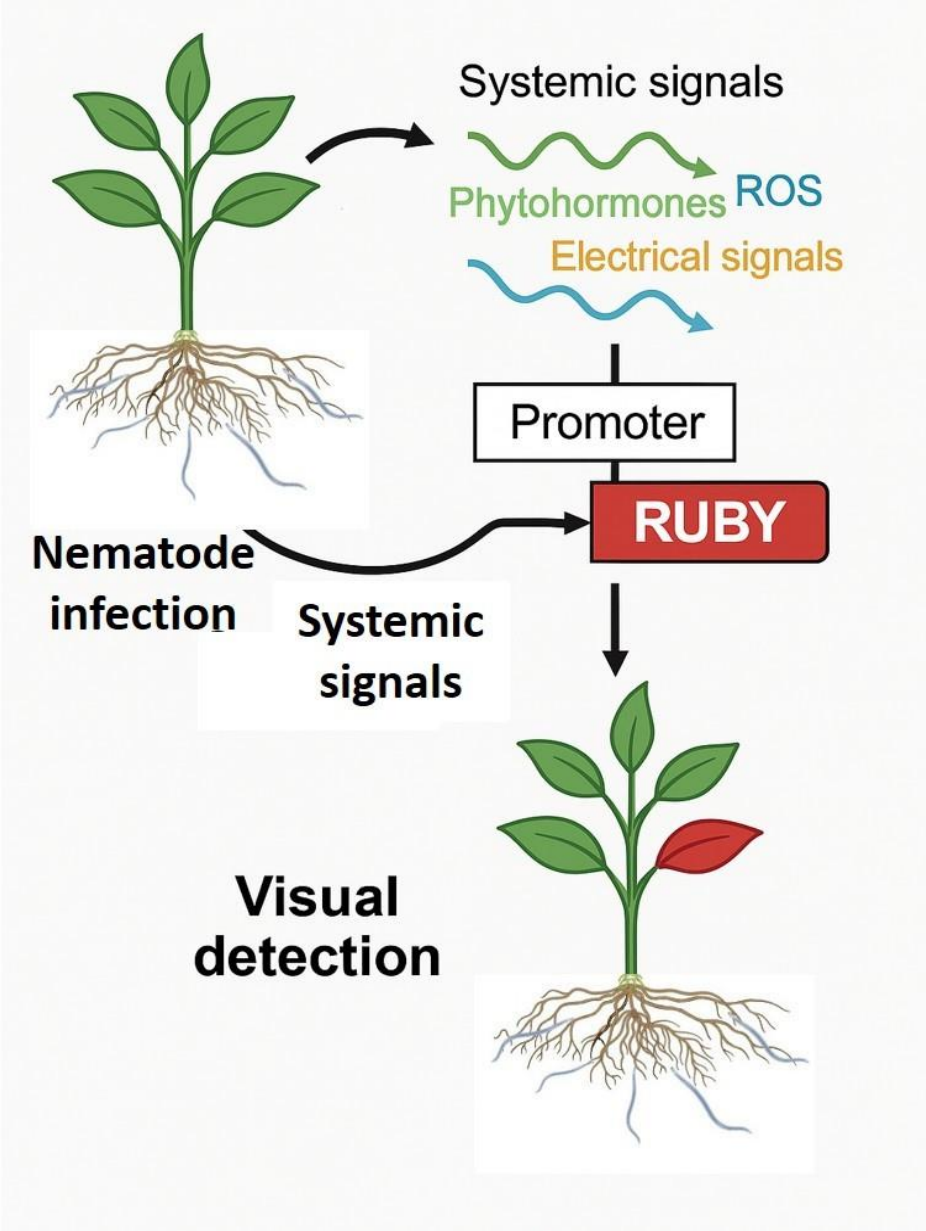

Figure 6.1. Schematic diagram of strategy of nematode infection in roots triggers systemic signals that activate the RUBY reporter in leaves for visible detection.

Plants transmitting systemic signals (e.g., phytohormones, ROS, electrical signals). Upon nematode infection in the roots, these signals activate a responsive promoter (jasmonic acid/ethylene responsive) that drives RUBY gene expression, resulting in red pigmentation in the leaves for easy visual identification of infected plants.

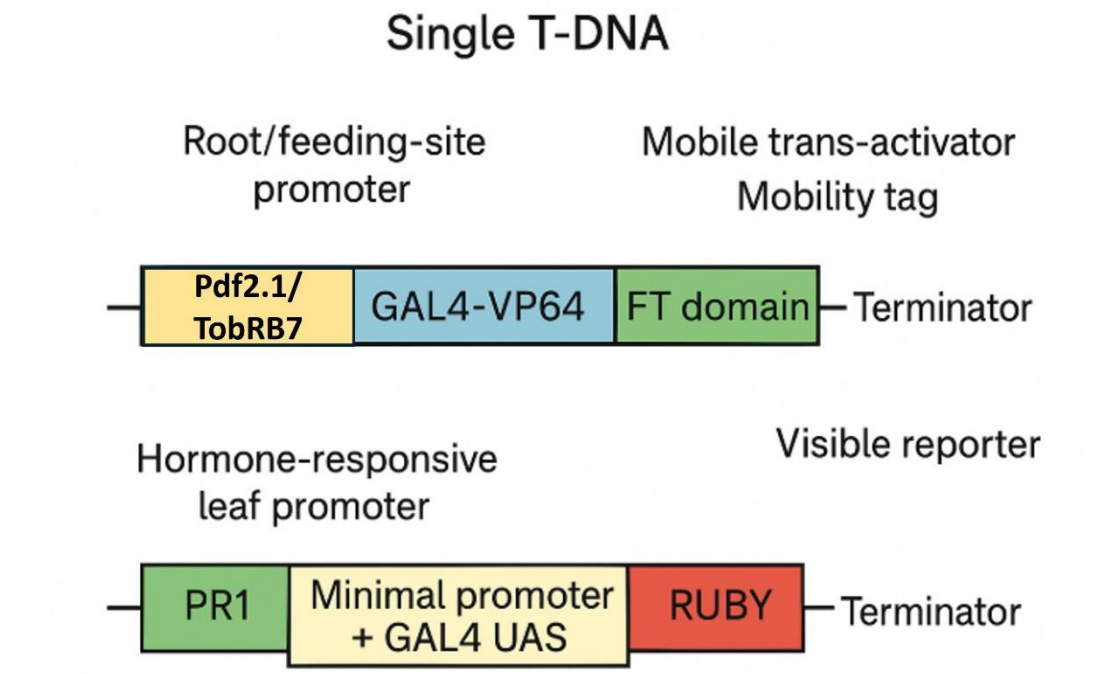

Figure 6.2. Strategy of expressing RUBY in leaves using a dual promoter T-DNA construct

The root/feeding-site promoter (Pdf2.1/TobRB7) drives expression of a mobile GAL4–VP64 trans-activator fused to an FT mobility domain. A separate hormone-responsive leaf promoter (PR1) controls a minimal promoter with GAL4 UAS, activating the RUBY reporter gene for visible output.

6.2 Introgression of resistance traits from non-tuberous *Solanum* species into *Solanum tuberosum*

Our project has laid the foundational groundwork necessary to identify one or more resistance (R) genes that confer resistance to potato cyst nematodes. Wild, non-tuberous *Solanum* species such as *S. americanum* are generally recognized for their resistance to PCN. Our findings confirm the heritability of these resistance traits and highlight the genetic diversity present within *Solanum* populations. This diversity will be instrumental in mapping resistance loci, enabling the identification of specific *G. pallida* resistance genes. Ultimately, these resistance sources can be introgressed or otherwise introduced from wild *Solanum* species into modern cultivars through targeted breeding strategies.

The transfer of resistance genes from non-tuber forming *Solanum* species to cultivated potato (*Solanum tuberosum*) has emerged as a pivotal strategy in breeding for durable resistance against major biotic stresses, particularly late blight and nematode infestations. Wild *Solanum* species such as *S. bulbocastanum*, *S. demissum*, and *S. americanum* harbour a rich repertoire of resistance (R) genes, many of which are absent in commercial cultivars due to their narrow genetic base. However, the sexual incompatibility between wild and cultivated species often due to differences in ploidy and endosperm balance number poses a significant barrier to conventional breeding (Spychalla and Jong, 2023). The success of this approach lies in combining the genetic diversity found in wild relatives with modern molecular and genomic tools that accelerate the identification and deployment of resistance. To overcome these limitations, advanced techniques such as somatic hybridization, protoplast electrofusion, and marker-assisted selection have been employed.

A key example is provided by the broad-spectrum resistance genes *Rpi-blb1* and *Rpi-blb3* from *S. bulbocastanum*, which were transferred into potato pre-breeding lines through somatic hybridization, followed by backcrossing and molecular validation with gene-specific markers and effector-based assays. These genes confer robust resistance to *Phytophthora infestans* even under severe disease pressure, while the resulting potatoes maintain agronomic performance comparable to elite cultivars (Rakosy-Tican et al., 2020). Similarly, the cloning of *Rpi-amr1* from *S. americanum* represents a major breakthrough. This gene encodes an NRC helper-dependent CC-NLR protein and provides resistance against all nineteen tested *Phytophthora infestans* isolates. Importantly, association genomics and long-read Resistance gene enrichment sequencing (RenSeq) revealed multiple alleles of *Rpi-*

amr1 across diverse *S. americanum* accessions, underscoring the potential for durable resistance through allele mining and exploitation of natural diversity (Witek et al., 2021). In this case, the cloned *R* gene was introduced directly into the commercial potato cultivar Maris Piper, by Agrobacterium-mediated transformation and functioned appropriately in its new genetic background. This example does highlight a key consideration that needs to be taken into account when transferring *R* genes between less closely related species. Whilst direct transformation allows the precise transfer of a single gene, helper proteins and other signalling components may be required for full functionality Helper Nucleotide-binding Leucine-rich Repeat protein (NLRs), particularly those in the NRC (NLR Required for Cell death) family, are essential for the function of many sensors NLRs (Wu et al., 2017), including Rpi-amr1 from *Solanum americanum*. These helper NLRs do not detect pathogen effectors directly but facilitate immune signalling by forming resistosomes upon activation (Jones and Dangl, 2006). However, if compatibility is limited, it may be necessary to identify and co-express a specific helper NLR from *S. americanum* to ensure full functionality of the introduced resistance gene.

Progress towards potato cyst nematode resistance further illustrates how these strategies can be applied beyond late blight. Advances in high-resolution sequencing, including Resistance gene enrichment sequencing and SMRT-AgRenSeq-d, have allowed precise identification of nucleotide-binding leucine-rich repeat resistance candidates by comparing resistant and susceptible phenotypes. This has recently led to the identification of nine strong candidates for the *G. pallida* resistance gene GpaV (Wang et al., 2023b). Other studies have demonstrated the successful use of wild *Solanum spegazzinii* as a source of resistance to *G. pallida* Pa1 and Pa2/3. When introgressed into *S. tuberosum* cultivar Mayan Gold, bulk-segregant analysis with genetic mapping enrichment sequencing and genotyping-by-sequencing pinpointed linked single nucleotide polymorphisms on chromosome VI, which were subsequently converted into allele-specific polymerase chain reaction markers for use in breeding nematode-resistant cultivars (Gartner et al., 2024). In a parallel case, the H2 resistance gene from wild diploid *Solanum multidissectum* was mapped to chromosome V of *S. tuberosum*, with resistance to *G. pallida* Pa1 confirmed as a single dominant gene. The use of Resistance gene enrichment sequencing, generic mapping enrichment sequencing, and Kompetitive Allele Specific PCR markers enabled precise tracking of this gene, highlighting once again the importance of integrating genomic tools with classical inheritance studies (Strachan et al., 2019).

For further advancement, the integration of transgenic and genome editing technologies offers a way to complement conventional introgression. Transgenic approaches have already demonstrated how cloned resistance genes can be directly introduced into potato genomes, evading crossability barriers and enabling the stacking of multiple resistance loci for enhanced durability. Meanwhile, tools such as RNA interference and CRISPR-Cas9 genome editing are expanding the capacity to engineer resistance precisely, including against pests and pathogens that are difficult to control through introgression alone (Bakhsh et al., 2020).

From our study, we identified novel resistance sources within *Solanum americanum* species against *Globodera pallida*. Analysis of segregating F_2 populations indicated the involvement of either a single dominant resistance gene or multiple unlinked loci. Furthermore, we demonstrated that resistance is accompanied by dynamic defence signalling, characterized by early and late oxidative bursts, by evaluating robust physiological response to nematode infection. These insights are instrumental for guiding the transfer of resistance (R) genes from *Solanum americanum* into cultivated potato varieties through transgenic approaches.The first step would involve fine mapping the resistance loci we have identified in our resistant accessions using segregating populations. These loci can then be resolved at the sequence level using targeted enrichment strategies such as Resistance gene enrichment sequencing (RenSeq) combined with long-read sequencing, as was applied by Witek et al. (2021) to capture the complex NLR repertoire of *S. americanum*. Once candidate resistance genes are identified, functional testing through transient assays in solanaceous model systems (e.g. *Nicotiana benthamiana*) or stable complementation in susceptible potato backgrounds would enable the causal genes to be confirmed.

Following validation, the cloned R genes could be deployed into cultivated potato using transgenic or cisgenic transformation. This route has the advantage of avoiding the lengthy backcrossing required by conventional breeding, while ensuring that resistance can be introduced directly into elite germplasm without linkage drag. Previous finding identified multiple independent loci from different resistant *S. americanum* accessions could be cloned and combined in single constructs for transfer into potato (Witek et al., 2021). Such gene stacking is particularly important for PCN, where high evolutionary potential may allow single resistance genes to be overcome; combining several non-redundant R genes is therefore expected to increase durability and broaden the spectrum of resistance.

When combined, these findings show that wild species of Solanum continue to be essential sources of resistance. Harnessing this diversity in an efficient and effective way is becoming

interestingly feasible by combining traditional breeding with cutting-edge genomic and biotechnological techniques.

6.3 Limitations of the study

While this research provides valuable insights into plant–nematode interactions and advances the development of molecular tools for visualising early infection processes, several limitations should be acknowledged to contextualise the findings and guide future work.

First, although the RUBY reporter system proved effective under controlled laboratory conditions, its performance under variable environmental and field conditions remains untested. Factors such as light, soil composition, microbial communities, and abiotic stress may influence betalain synthesis and accumulation. Therefore, the reliability, sensitivity, and stability of RUBY-based visualisation outside controlled environments require further validation. Additionally, while the betalain pigment was ingested by female root-knot nematodes, it was not taken up by cyst nematodes during the course of infection. The underlying reasons for this discrepancy remain unclear, as it was beyond the scope of the present study. Therefore, further experiments will be required to elucidate the mechanisms governing these differential uptake patterns.

Although the *CaMV35S:RUBY* system and root-inducible constructs showed strong potential for visual detection of early nematode infection, several limitations remain. The quantitative accuracy of RUBY as a reporter was not validated, and its sensitivity to weak or transient promoter activity is still unknown. Additionally, only a limited set of promoters and nematode interactions were tested, meaning broader applicability requires further evaluation.

Finally, the screening of *Solanum americanum* accessions successfully identified genetic diversity and heritable resistance to potato cyst nematode; it captures only the initial components of the defence process. Early indicators such as ROS provided valuable insight into the onset of resistance but do not reveal the full sequence of downstream molecular and genetic events that determine the final resistance outcome. A more comprehensive characterisation incorporating transcriptomics, metabolomics, or fine-mapping approaches will be required to fully elucidate the genetic basis of resistance. The study provides an essential foundation but does not yet identify specific resistance loci or R-genes.

6.4 Avenues for future work and prospects

Building on the findings of this study, several promising avenues for future research can further advance the application of betalain-based RUBY reporter systems and the genetic investigation of potato cyst nematode resistance in *Solanum americanum* accessions.

6.4.1 Advancing the RUBY reporter system

The RUBY reporter demonstrated clear potential for visualising gene expression during transgenic events and early nematode infection under controlled conditions. However, additional development is required to optimise its use in research and field diagnostics. Future work should focus on evaluating the performance and stability of RUBY constructs under field or variable environmental conditions. Factors such as fluctuating light, soil composition, nutrient availability, and microbial diversity may affect betalain biosynthesis and pigment accumulation. Testing the system under these conditions will help determine its robustness and guide improvements in construct design.

Another important direction is the development and screening of synthetic root-inducible promoters that perform reliably under field conditions representing an important opportunity to extend the applicability of this work beyond controlled environments. Such promoters have strong potential for use in the diagnosis and monitoring of nematode infection by enabling visible identification in intact plants. When coupled to visible RUBY reporter systems, such promoters could allow rapid, non-destructive identification of infected or resistant individuals, including under field or semi-field conditions (details in **section 6.1.3**).

Additionally, investigating the molecular basis of the observed differences in betalain uptake between root-knot and cyst nematodes represents an important avenue for future research. Comparative analyses using approaches such as transcriptomics, targeted gene expression studies, or advanced microscopy could help identify differences in feeding site organisation, nutrient uptake pathways, or cellular transport mechanisms between these nematode species. Such studies may clarify whether betalain accumulation reflects active uptake, passive diffusion, or differences in feeding behaviour and tissue permeability. Gaining insight into these mechanisms would advance understanding of nematode biology and plant-nematode-interactions. This would also support further refinement of the RUBY reporter system, enabling more informed interpretation of reporter signals and broader application across nematode species.

6.4.2 Dissecting resistance mechanisms in *Solanum americanum*

This study identified clear phenotypic variation and heritable resistance to *G. pallida* within *S. americanum* populations. The next step is to pinpoint the genetic determinants underlying this resistance. Fine-mapping of the resistance loci using segregating populations will be essential for narrowing candidate regions. Subsequently, targeted sequencing approaches such as Resistance gene enrichment sequencing (RenSeq), long-read sequencing, or AgRenSeq can be employed to resolve complex NLR gene families and identify candidate R genes.

Functional validation of these candidate genes through transient assays in *Nicotiana benthamiana* or stable transformation into susceptible potato backgrounds will be required to confirm causal resistance factors. Once validated, these genes can be introduced into cultivated potato using transgenic or cisgenic approaches, offering a route to deploy resistance without the genetic drag associated with traditional introgression. Stacking multiple non-redundant R genes from diverse resistant *S. americanum* accessions will be particularly valuable for achieving durable, long-term resistance against *G. pallida*.

6.4.3 Prospects for breeding and crop protection

The combined advances in visual RUBY reporter technology and resistance gene discovery have significant implications for sustainable crop protection. A refined RUBY system could serve as an early-warning tool for detecting nematode activity in the field, enabling timely interventions and reducing reliance on chemical nematicides. Similarly, the identification of novel resistance genes from *S. americanum* provides valuable genetic resources for breeding potato cyst nematode-resistant potato cultivars.

As genomic resources and biotechnological tools continue to develop, integrating R-gene cloning, gene stacking, and precision diagnostics will accelerate the deployment of durable nematode resistance in commercial potato varieties. Ultimately, this research lays the groundwork for combining molecular tools and natural genetic diversity to support resilient and sustainable potato production systems.

6.5 Conclusions

This project was designed around four specific objectives, aimed at developing resources and insights for understanding and managing potato–nematode interactions.

- The first objective focused on the application of the non-destructive, betalain-based RUBY reporter system. The construct was successfully integrated and expressed in transgenic events of potato and Arabidopsis, where its activity could be readily visualized without the need for destructive assays. Importantly, the RUBY reporter was evaluated during plant–nematode interactions, specifically with both root-knot (*Meloidogyne incognita*) and cyst nematodes (*Globodera pallida* and *Heterodera schachtii*) in transgenic potato and Arabidopsis plants. The expression analysis demonstrated the feasibility of using RUBY as a sensitive and visually tractable marker system in nematode feeding sites under the control of strong constitutive promoter (CaMV35S).

- The betalain-based MycoRed reporter system was employed to resolve the spatial interaction between root knot nematode and arbuscular mycorrhizal fungi. Betalain pigmentation was detected in both NbPT5b and NbBCP1b reporter lines following *Meloidogyne* infection and AMF inoculation, whereas no pigmentation was observed in the mock-inoculated controls. This confirms that the MycoRed system successfully reported AMF colonisation even in the presence of nematode infection, enabling visual localisation of AMF structures within infected root tissues. These observations demonstrate that the reporter system can be used to resolve the spatial overlap between root-knot nematodes and AMF during co-colonisation.

- CaMV35S:RUBY was employed to generate novel reporter constructs with root-specific, nematode-responsive promoters, thereby expanding the selection of molecular tools available for studying spatial and temporal regulation of gene expression in potato roots in response to early nematode infection. By enabling visible, non-destructive tracking of gene activity in real time, RUBY offers a powerful platform for investigating early nematode infection. Since RUBY enables the visual identification of nematode infection without requiring specialized equipment, it holds strong potential for application under field conditions. With careful construct design and optimization, RUBY could be developed into a practical diagnostic tool for rapid detection of nematode infections in potato and other crops.

- The final objective of the project addressed the identification and characterisation of nematode resistance within wild *Solanum americanum* populations. A diverse group of accessions was screened against potato cyst nematode (*G. pallida*), enabling the detection of variation in resistance responses. By characterising resistance phenotypes through early physiological responses, this study provides critical insights into the initial stages of plant defence, offering a foundation for understanding the mechanisms underlying cyst nematode resistance. The identification of heritability of resistance traits and the genetic diversity among *S. americanum* accessions represents a critical step toward the mapping of resistance loci and the eventual discovery of novel R-genes. These findings contribute to the long-term goal of developing potato cultivars with durable and broad-spectrum nematode resistance by applying transgenic approaches and transferring resistant genes from *S. americanum* into cultivated potato varieties, thereby enhancing field performance and contributing to sustainable crop production.

Chapter 7

References

ADAS. 2020. *Potato cyst nematode: Controlling the potato pest threat.* ADAS News. Available at:https://adas.co.uk/news/potato-cyst-nematode-controlling-the-potato-pest-threat/ [Accessed 9 August 2025].

Agarwal, P.K., Gupta, K., Lopato, S. and Agarwal, P. 2017. Dehydration responsive element binding transcription factors and their applications for the engineering of stress tolerance. *Journal of Experimental Botany*, 68, pp.2135–2148.

Alam, J. and Cook, J.L. 1990. Reporter genes: application to the study of mammalian gene transcription. *Analytical biochemistry*, *188*(2), pp.245-254.

Ali, M., Cheng, Z., Ahmad, H. and Hayat, S. 2018. Reactive oxygen species (ROS) as defenses against a broad range of plant fungal infections and case study on ROS employed by crops against Verticillium dahliae wilts. *Journal of plant interactions*, *13*(1), pp.353-363.

Ali, M.A. and Abbas, A. 2016. Analysis of reporter proteins GUS and DsRed driven under the control of CaMV35S promoter in syncytia induced by beet cyst nematode *Heterodera schachtii* in Arabidopsis roots. *Advancements in Life Sciences*, *3*(3), pp.89-96.

Ali, M.A., Abbas, A., Kreil, D.P. and Bohlmann, H. 2016. Overexpression of the transcription factor RAP2.6 leads to enhanced callose deposition in syncytia and enhanced resistance against the beet cyst nematode *Heterodera schachtii* in *Arabidopsis*. *Advances in Life Sciences*, 3(3), pp.73–84.

Ali, S. and Kim, W.C. 2019. A fruitful decade using synthetic promoters in the improvement of transgenic plants. *Frontiers in plant science*, *10*, p.1433. doi: 10.3389/fpls.2019.01433.

Amack, S.C. and Antunes, M.S. 2020. CaMV35S promoter–A plant biology and biotechnology workhorse in the era of synthetic biology. *Current Plant Biology*, *24*, p.100179. https://doi.org/10.1016/j.cpb.2020.100179.

Amack, S.C., Ferreira, S.S. and Antunes, M.S. 2022. Tuning the transcriptional activity of the CaMV 35S promoter in plants by single-nucleotide changes in the TATA box. *ACS Synthetic Biology*, *12*(1), pp.178-185. https://doi.org/10.1021/acssynbio.2c00457.

Anjos, É.C.T.D., Cavalcante, U.M.T., Gonçalves, D.M.C., Pedrosa, E.M.R., Santos, V.F.D. and Maia, L.C. 2010. Interactions between an arbuscular mycorrhizal fungus (*Scutellospora heterogama)* and the root-knot nematode (*Meloidogyne incognita*) on sweet passion fruit (Passiflora alata). *Brazilian Archives of Biology and Technology*, *53*, pp.801-809. doi: 10.1590/S1516-89132010000400008.

Back, M. A., Cortada, L., Grove, I. G. and Taylor, V. 2018. Field management and control strategies. In: Cyst Nematodes, eds R. N. Perry, M. Moens, and J. T. Jones (Wallingford: CAB International), 305-336.

Bakhsh, A., Dangol, S.D., Naeem, M., Azimi, M.H. and Yasmeen, A. 2020. Genetic approaches for engineering biotic stress resistance in potato (Solanum tuberosum L.). *JAPS: Journal of Animal & Plant Sciences*, *30*(1).

Baral, B., Riihelä, S., Kemppinen, J., Sierla, M. and Brosché, M. 2024. Seeing the invisible: Tools to teach and study plant transcriptional responses. *Plant Physiology*, *196*(3), pp.1729-1732.

Baranowski, Ł., Różańska, E., Sańko-Sawczenko, I., Matuszkiewicz, M., Znojek, E., Filipecki, M., Grundler, F.M. and Sobczak, M. 2019. Arabidopsis tonoplast intrinsic protein and vacuolar H+-adenosinetriphosphatase reflect vacuole dynamics during development of syncytia induced by the beet cyst nematode Heterodera schachtii. *Protoplasma*, *256*(2), pp.419-429.

Barcala, M., García, A., Cabrera, J., Casson, S., Lindsey, K., Favery, B., García-Casado, G., Solano, R., Fenoll, C. and Escobar, C. 2010. Early transcriptomic events in microdissected Arabidopsis nematode-induced giant cells. *The Plant Journal*, *61*(4), pp.698-712. doi: 10.1111/j.1365-313X.2009.04098.x.

Barcala, M., García, A., Cubas, P., Almoguera, C., Jordano, J., Fenoll, C. and Escobar, C. 2008. Distinct heat-shock element arrangements that mediate the heat shock, but not the late-embryogenesis induction of small heat-shock proteins, correlate with promoter activation in root-knot nematode feeding cells. *Plant molecular biology*, *66*(1), pp.151-164.

Barker, K.R., Hussey, R.S., Krusberg, L.R., Bird, G.W., Dunn, R.A., Ferris, H., Ferris, V.R., Freckman, D.W., Gabriel, C.J., Grewal, P.S. and MacGuidwin, A.E. 1994. Plant and soil nematodes: societal impact and focus for the future. *Journal of Nematology*, *26*(2), p.127.

Barthels, N., van der Lee, F.M., Klap, J., Goddijn, O.J., Karimi, M., Puzio, P., Grundler, F.M., Ohl, S.A., Lindsey, K., Robertson, L. and Robertson, W.M. 1997. Regulatory sequences of Arabidopsis drive reporter gene expression in nematode feeding structures. *The Plant Cell*, *9*(12), pp.2119-2134.

Bebber, D.P., Holmes, T. and Gurr, S.J. 2014. The global spread of crop pests and pathogens. *Global Ecology and Biogeography*, *23*(12), pp.1398-1407.doi: 10.1111/geb.12214.

Bello, A.O., Oladipo, O.T. and Saheed, S.A. 2013. Critical discerning characters of Solanum Linn species (Solanaceae). *South African Journal of Botany*, *86*, p.173. https://doi.org/ 10.1016/j.sajb.2013.02.128.

Benfey, P.N. and Chua, N.H. 1990. The Cauliflower Mosaic Virus 35S promoter: combinatorial regulation of transcription in plants. *Science*, 250(4983), pp.959–966.

Benfey, P.N., Ren, L. and Chua, N.H. 1989. The CaMV 35S enhancer contains at least two domains which can confer different developmental and tissue-specific expression patterns. *The EMBO journal*, *8*(8), pp.2195-2202.

Bilas, R., Szafran, K., Hnatuszko-Konka, K. and Kononowicz, A.K. 2016. Cis-regulatory elements used to control gene expression in plants. *Plant Cell, Tissue and Organ Culture (PCTOC)*, *127*(2), pp.269-287.doi: 10.1007/s11240- 016-1057-7.

Bleve-Zacheo, T., Bongiovanni, M., Melillo, M.T. and Castagnone-Sereno, P. 1998. The pepper resistance genes Me1 and Me3 induce differential penetration rates and temporal sequences of root cell ultrastructural changes upon nematode infection. *Plant Science*, *133*(1), pp.79-90.

Blok, V.C., Tylka, G.L., Smiley, R.W., Jong, W.D. and Daub, M. 2018. Resistance breeding. In *Cyst nematodes* (pp. 174-214). Wallingford UK: CAB International.

Böckenhoff, A. and Grundler, F.M.W. 1994. Studies on the nutrient uptake by the beet cyst nematode Heterodera schachtii by in situ microinjection of fluorescent probes into the feeding structures in Arabidopsis thaliana. *Parasitology*, *109*(2), pp.249-255.

Bohlmann, H. and Sobczak, M. 2014. *The plant cell wall in the feeding sites of cyst nematodes.* Frontiers in Plant Science, 5, p.89. Available at: https://doi.org/10.3389/fpls.2014.00089.

Bradshaw, C.J., Leroy, B., Bellard, C., Roiz, D., Albert, C., Fournier, A., Barbet-Massin, M., Salles, J.M., Simard, F. and Courchamp, F. 2016. Massive yet grossly underestimated global costs of invasive insects. *Nature communications*, *7*(1), p.12986.doi:10.1038/ncomms12986.

Bryan, G., McLean, K., Bradshaw, J., De Jong, W., Phillips, M., Castelli, L. and Waugh, R. 2002. Mapping QTLs for resistance to the cyst nematode Globodera pallida derived from the wild potato species Solanum vernei. *Theoretical and Applied Genetics*, *105*, pp.68-77. https://doi.org/10.1007/s00122-002-0873-9.

CABI. 2022a. *Globodera pallida* (white potato cyst nematode). CABI International. https://doi.org/10.1079/cabicompendium.27033.

CABI. 2022b. *Globodera rostochiensis* (yellow potato cyst nematode). CABI International. https://doi.org/10.1079/cabicompendium.27034.

Cabrera, J., Díaz-Manzano, F.E., Barcala, M., Arganda-Carreras, I., de Almeida-Engler, J., Engler, G., Fenoll, C. and Escobar, C. 2015. Phenotyping nematode feeding sites: three-dimensional reconstruction and volumetric measurements of giant cells induced by root-knot nematodes in Arabidopsis. *New Phytologist*, *206*(2), pp.868-880. doi: 10.1111/nph.13249.

Caillaud, M.C., Abad, P. and Favery, B. 2008. Cytoskeleton reorganization: a key process in root-knot nematode-induced giant cell ontogenesis. *Plant Signaling and Behavior*, 3(10), pp.816- 818.

Campbell, C. 2024. *The power of potatoes*. [online] The James Hutton Institute. Available at: https://www.hutton.ac.uk/news/power-potatoes [Accessed 7 June 2025].

Casadaban, M.J., Chou, J. and Cohen, S.N. 1980. In vitro gene fusions that join an enzymatically active beta-galactosidase segment to amino-terminal fragments of exogenous proteins: Escherichia coli plasmid vectors for the detection and cloning of translational initiation signals. *Journal of bacteriology*, *143*(2), pp.971-980.

Castelli, L., Bryan, G., Blok, V.C., Ramsay, G. and Phillips, M.S. 2005. Investigation of resistance specificity amongst fifteen wild *Solanum* species to a range of *Globodera pallida* and *G. rostochiensis* populations. *Nematology*, 7 (5), pp.689-699.

Castelli, L., Ramsay, G., Bryan, G., Neilson, S.J. and Phillips, M.S. 2003. New sources of resistance to the potato cyst nematodes *Globodera pallida* and *G. rostochiensis* in the Commonwealth Potato Collection. *Euphytica*, *129*(3), pp.377-386.

Castillo, P., Vovlas, N., Subbotin, S. and Troccoli, A. 2003. A new root-knot nematode, *Meloidogyne baetica* n. sp.(Nematoda: Heteroderidae), parasitizing wild olive in Southern Spain. *Phytopathology*, *93*(9), pp.1093-1102. doi: 10.1094/PHYTO.2003.93.9.1093.

Chalfie, M., 1995. Green fluorescent protein. *Photochemistry and photobiology*, *62*(4), pp.651-656.

Chalfie, M., Tu, Y., Euskirchen, G., Ward, W.W. and Prasher, D.C. 1994. Green fluorescent protein as a marker for gene expression. *Science*, *263*(5148), pp.802-805.

Chamnongpol, S., Willekens, H., Moeder, W., Langebartels, C., Sandermann Jr, H., Van Montagu, M., Inzé, D. and Van Camp, W. 1998. Defense activation and enhanced pathogen tolerance induced by H2O2 in transgenic tobacco. *Proceedings of the National Academy of Sciences*, *95*(10), pp.5818-5823.

Chen, J., Luo, M., Hands, P., Rolland, V., Zhang, J., Li, Z., Outram, M., Dodds, P. and Ayliffe, M. 2023. A split GAL4 RUBY assay for visual in planta detection of protein–protein interactions. *The Plant Journal*, *114*(6), pp.1209-1226.

Chen, S., Mitchum, M.G. and Wang, X. 2022. Characterization and response of two potato receptor-like kinases to cyst nematode infection. *Plant Signaling & Behavior*, *17*(1), p.2148372. DOI: 10.1080/15592324.2022.2148372.

Chen, X., Li, S., Zhao, X., Zhu, X., Wang, Y., Xuan, Y., Liu, X., Fan, H., Chen, L. and Duan, Y. 2020. Modulation of (homo) glutathione metabolism and H2O2 accumulation during soybean cyst nematode infections in susceptible and resistant soybean cultivars. *International Journal of Molecular Sciences*, *21*(2), p.388. doi:10.3390/ijms21020388.

Chen, Y., Moore, K.L., Miller, A.J., McGrath, S.P., Ma, J.F. and Zhao, F.J. 2015. The role of nodes in arsenic storage and distribution in rice. *Journal of Experimental Botany*, *66*(13), pp.3717-3724.

Choi, H.W. and Klessig, D.F. 2016. DAMPs, MAMPs, and NAMPs in plant innate immunity. *BMC plant biology*, *16*(1), p.232. doi: 10.1186/s12870- 016-0921-2.

Concibido, V.C., Diers, B.W. and Arelli, P.R. 2004. A decade of QTL mapping for cyst nematode resistance in soybean. *Crop science*, *44*(4), pp.1121-1131. doi: 10.2135/cropsci2004.1121.

Contag, C.H. and Bachmann, M.H. 2002. Advances in in vivo bioluminescence imaging of gene expression. *Annual review of biomedical engineering*, *4*(1), pp.235-260.

Corbesier, L., Vincent, C., Jang, S., Fornara, F., Fan, Q., Searle, I., Giakountis, A., Farrona, S., Gissot, L., Turnbull, C. and Coupland, G. 2007. FT protein movement contributes to long-distance signaling in floral induction of Arabidopsis. *science*, *316*(5827), pp.1030-1033.

Dalamu, B.V., Umamaheshwari, R., Shrama, R., Kaushik, S.K., Joseph, T.A., Singh, B.P., Gebhardt, C. 2012. Potato cyst nematode (PCN) resistance: genes, genotypes and markers – an update. *SABRAO J Breed Genet*, 44, pp.202–228.

Dandurand, L.M. and Knudsen, G.R. 2016. Effect of the trap crop *Solanum sisymbriifolium* and two biocontrol fungi on reproduction of the potato cyst nematode, *Globodera pallida*. *Annals of Applied Biology*, *169*(2), pp.180-189.

Das, S., DeMason, D.A., Ehlers, J.D., Close, T.J. and Roberts, P.A. 2008. Histological characterization of root-knot nematode resistance in cowpea and its relation to reactive oxygen species modulation. *Journal of Experimental Botany*, *59*(6), pp.1305-1313. doi:10.1093/jxb/ern036.

Davies, L.J. and Elling, A.A. 2015. Resistance genes against plant-parasitic nematodes: a durable control strategy?. *Nematology*, 17 (3), pp.249-263.

De Kock, K., Matthys, J. and Kyndt, T. 2024. ROS Detection and Quantification in Plant–Nematode Interactions. In *Plant-Nematode Interactions* (pp. 305-316). New York, NY: Springer US.

De Ruijter, F.J. and Haverkort, A.J. 1999. Effects of potato-cyst nematodes (Globodera pallida) and soil pH on root growth, nutrient uptake and crop growth of potato. *European Journal of Plant Pathology*, *105*(1), pp.61-76.

Decraemer, W. and Hunt, D.J. 2006. Structure and classification. In: Plant Nematology (R.N. Perry and M. Moens, eds), pp. 3– 32. Wallingford, Oxfordshire: CAB International.

Di Vito, M. and Greco, N. 1986. The pea cyst nematode. In: Lamberti, F. and Taylor, C. E. (eds.) Cyst nematodes. Series A: Life science. New York: Plenum Press.

Doyle, E.A. and Lambert, K.N. 2003. Meloidogyne javanica chorismate mutase 1 alters plant cell development. *Molecular Plant-Microbe Interactions*, 16(2), pp.123-131.

Dutta, T.K., Ray, S. and Phani, V. 2023. The status of the CRISPR/Cas9 research in plant–nematode interactions. Planta. https://doi.org/10.1007/s00425-023-04259-0.

Ehsanpour, A.A. and Jones, M.G.K. 1996. Glucuronidase expression in transgenic tobacco roots with a Parasponia promoter on infection with Meloidogyne javanica. *Journal of Nematology*, *28*(4), p.407.

Ellenby, C. 1952. Resistance to the potato root eelworm, *Heterodera rostochiensis* Wollenweber. *Nature*, *170*(4337), pp.1016-1016.Fenwick, D.W., 1940. Methods for the recovery and counting of cysts of *Heterodera schachtii* from soil. *Journal of helminthology*, *18*(4), pp.155-172.

Ellis, P.R. and Maxon Smith, J.W. 1971. Inheritance of resistance to potato cyst-eelworm (*Heterodera rostochiensis* Woll.) in the genus Lycopersicon. *Euphytica*, *20*(1), pp.93-101.

Ernst, K., Kumar, A., Kriseleit, D., Kloos, D.U., Phillips, M.S. and Ganal, M.W. 2002. The broad-spectrum potato cyst nematode resistance gene (Hero) from tomato is the only member of a large gene family of NBS-LRR genes with an unusual amino acid repeat in the LRR region. *The Plant Journal*, *31*(2), pp.127-136.

Escobar, C., Barcala, M., Portillo, M., Almoguera, C., Jordano, J. and Fenoll, C. 2003. Induction of the Hahsp17. 7G4 promoter by root-knot nematodes: involvement of heat-shock elements in promoter activity in giant cells. *Molecular plant-microbe interactions*, *16*(12), pp.1062-1068. https://doi.org/10.1094/MPMI.2003.16.12.1062.

Escobar, C., De Meutter, J., Aristizábal, F.A., Sanz-Alférez, S., del Campo, F.F., Barthels, N., Van der Eycken, W., Seurinck, J., Van Montagu, M., Gheysen, G. and Fenoll, C. 1999. Isolation of the LEMMI9 gene and promoter analysis during a compatible plant-nematode interaction. *Molecular plant-microbe interactions*, *12*(5), pp.440-449.

European and Mediterranean Plant Protection Organization (EPPO). 2024. EPPO Global Database. https://gd.eppo.int.

Evans, K. and Stone, A. R. 1977. A review of the distribution and biology of the potato cyst-nematodes *Globodera rostochiensis* and *G. pallida*. Proceedings of the National Academy of Sciences of the United States of America, 23(2), pp.178–189. https://doi.org/10.1080/09670877709412426.

Eves-van den Akker, S., Lilley, C.J., Jones, J.T. and Urwin, P.E. 2015. Plant-parasitic nematode feeding tubes and plugs: new perspectives on function. *Nematology*, *17*(1), pp.1-9.

Faggian, R., Powell, A., and Slater, A.T. 2012. Screening for resistance to potato cyst nematode in Australian potato cultivars and alternative solanaceous hosts. Australasian *Plant Pathology*, 41(5), pp.453–461. https://doi.org/10.1007/s13313-011-0098-y.

Fenwick, D.W. 1940. Methods for the recovery and counting of cysts of *Heterodera schachtii* from soil. *Journal of helminthology*, *18*(4), pp.155-172.

Flor, H.H. 1971. Current status of the gene-for-gene concept. *Annual Review of Phytopathology*, 9 (1), pp.275-296.

Food and Agriculture Organization (FAO). 2022. FAOSTAT statistical database. https://www.fao.org/faostat/en/#data/QCL.

Forte, C.T., Nunes, U.R., Filho, A.C., Galon, L., Chechi, L., Roso, R., Menegat, A.D., Rossetto, E.R.O. and Franceschetti, M.B. 2019. Chemical and environmental factors driving germination of *Solanum americanum* seeds. *Weed Biology and Management*, 19(4), pp.113-120.

Fosu-Nyarko, J. and Jones, M.G. 2016. Advances in understanding the molecular mechanisms of root lesion nematode host interactions. *Annual Review of Phytopathology*, 54 (1), pp.253-278.

Fuller, V.L., Lilley, C.J., Atkinson, H.J. and Urwin, P.E. 2007. Differential gene expression in Arabidopsis following infection by plant-parasitic nematodes *Meloidogyne incognita* and *Heterodera schachtii*. *Molecular Plant Pathology*, *8*(5), pp.595-609. DOI: 10.1111/J.1364-3703.2007.00416.X.

Galek, R., Rurek, M., De Jong, W.S., Pietkiewicz, G., Augustyniak, H., and Sawicka-Sienkiewicz, E. 2011. Application of DNA markers linked to the potato H1 gene conferring resistance to

pathotype Ro1 of *Globodera rostochiensis*. *Journal of Applied Genetics*, 52(4), pp.407–411. https://doi.org/10.1007/s13353-011-0056-y.

Ganal, M.W., Simon, R., Brommonschenkel, S., Arndt, M., Phillips, M.S., Tanksley, S.D. and Kumar, A. 1995. Genetic mapping of a wide spectrum nematode resistance gene (Hero) against *Globodera rostochiensis* in tomato. *Molecular Plant-Microbe Interaction*, 8, pp.886-891.

Gao, S., Su, L., Jia, H.G., Guo, H.N., Tian, Y.C., Fang, R.X. and Chen, X.Y. 2007. Construction of selectable marker-removable plant expression vectors. *Sheng wu Gong Cheng xue bao= Chinese Journal of Biotechnology*, *23*(1), pp.157-160.

García-Caparrós, P., De Filippis, L., Gul, A., Hasanuzzaman, M., Ozturk, M., Altay, V. and Lao, M.T. 2021. Oxidative stress and antioxidant metabolism under adverse environmental conditions: a review. *The Botanical Review*, *87*, pp.421-466.

Gartner, U., Armstrong, M.R., Sharma, S.K., Jones, J.T., Blok, V.C., Hein, I. and Bryan, G.J. 2024. Characterisation and mapping of a *Globodera pallida* resistance derived from the wild potato species *Solanum spegazzinii*. *Theoretical and Applied Genetics*, *137*(5), p.106.

Gartner, U., Hein, I., Brown, L.H., Chen, X., Mantelin, S., Sharma, S.K., Dandurand, L.M., Kuhl, J.C., Jones, J.T., Bryan, G.J. and Blok, V.C. 2021. Resisting potato cyst nematodes with resistance. *Frontiers in Plant Science*, 12, p.483. https://doi.org/10.3389/fpls.2021.661194.

Ge, X., Wang, P., Wang, Y., Wei, X., Chen, Y. and Li, F. 2022. Development of an eco-friendly pink cotton germplasm by engineering betalain biosynthesis pathway. *Plant Biotechnology Journal*, *21*(4), p.674. https:// doi.org/10.1111/pbi.13987.

Gengatharan, A., Dykes, G.A. and Choo, W.S. 2015. Betalains: Natural plant pigments with potential application in functional foods. *LWT-Food Science and Technology*, *64*(2), pp.645-649.

Gheysen, G. and Mitchum, M. 2019. Phytoparasitic nematode control of plant hormone pathways. Plant Physiology, 179 (4), pp.1213-1226. DOI:10.1104/pp.18.01067.

Gheysen, G., Van der Eycken, W., Barthels, N., Karimi, M. and Van Montagu, M. 1996. The exploitation of nematode-responsive plant genes in novel nematode control methods. *Pesticide Science*, *47*(1), pp.95-101.

Ghim, C.M., Lee, S.K., Takayama, S. and Mitchell, R.J. 2010. The art of reporter proteins in science: past, present and future applications.

Goddijn, O.J., Lindsey, K., van der Lee, F.M., Klap, J.C. and Sijmons, P.C. 1993. Differential gene expression in nematode-induced feeding structures of transgenic plants harbouring promoter—gusA fusion constructs. *The Plant Journal*, *4*(5), pp.863-873.

Gold, D.A., Gates, R.D. and Jacobs, D.K. 2014. The early expansion and evolutionary dynamics of POU class genes. *Molecular Biology and Evolution* 31(12), pp.3136-47.

Goldstein, B. 1927. The X-bodies in the cells of Dahlia plants affected with mosaic disease and dwarf. *Bulletin of the Torrey Botanical Club*, pp.285-293. https://doi.org/10.1016/0042-6822(68)90127-X.

Golinowski, W., Grundler, F.M.W. and Sobczak, M. 1996. Changes in the structure of Arabidopsis thaliana during female development of the plant parasitic nematode *Heterodera schachtii.* Protoplasma. 194, pp.103-116.

Goodell, P. and H. Ferris. 1989. Influence of environmental factors on the hatch and survival of Meloidogyne incognita. Journal of Nematology, 21(3), p328.

Goverse, A., Biesheuvel, J., Wijers, G.J., Gommers, F.J., Bakker, J., Schots, A. and Helder, J. 1998. In planta monitoring of the activity of two constitutive promoters, CaMV 35S and TR2', in developing feeding cells induced by *Globodera rostochiensis* using green fluorescent protein in combination with confocal laser scanning microscopy. *Physiological and Molecular Plant Pathology*, *52*(4), pp.275-284.

Goverse, A., Overmars, H., Engelbertink, J., Schots, A., Bakker, J. and Helder, J. 2000. Both induction and morphogenesis of cyst nematode feeding cells are mediated by auxin. *Molecular Plant-Microbe Interactions*, 13, pp.1121–1129.

Greenhood, N.C. et al. 2022. The potential of *Solanum Americanum* to act as a source of novel resistance to the potato cyst nematode *Globerdera pallida*. Lab report, P.E. Urwin Lab, University of Leeds, UK. Unpublished.

Grundler, F., Betka, M. and Wyss, U. 1991. Influence of changes in the nurse cell system (syncytium) on sex determination and development of the cyst nematode *Heterodera schachtii* - total amounts of proteins and amino acids. *Phytopathology*, 81(1), pp.70-74.

Grunewald, W., Karimi, M., Wieczorek, K., Van de Cappelle, E., Wischnitzki, E., Grundler, F., Inzé, D., Beeckman, T. and Gheysen, G. 2008. A role for AtWRKY23 in feeding site establishment of plant-parasitic nematodes. *Plant Physiology* 148:358-68. doi: 10.1104/pp.108.119131.

Grymaszewska, G. and Golinowski, W. 1998. Structure of syncytia induced by *Heterodera schachtii Schmidt* in roots of susceptible and resistant radish (*Raphanus sativus* L., var. oleiformis). *Acta societatis botanicorum Poloniae*, *67*(3-4), pp.207-216.

Guo, X., Wang, J., Gardner, M., Fukuda, H., Kondo, Y., Etchells, J.P., Wang, X. and Mitchum, M.G. 2017. Identification of cyst nematode B-type CLE peptides and modulation of the vascular stem cell pathway for feeding cell formation. *PLoS Pathogens*, *13*(2), p.e1006142.

Gupta, R., Mfarrej, M.F.B., Elnour, R.O., Hashem, M. and Ahmad, F. 2023. Defence response of host plants for cyst nematode: A review on parasitism and defence. *Journal of King Saud University-Science*, 35(7), p.102829.

Hai, G., Jia, Z., Xu, W., Wang, C., Cao, S., Liu, J. and Cheng, Y. 2016. Characterization of the Populus PtrCesA4 promoter in transgenic *Populus alba*× *P. glandulosa*. *Plant Cell, Tissue and Organ Culture (PCTOC)*, *124*(3), pp.495-505. DOI 10.1007/s11240-015-0909-x.

Hajare, S.T., Chauhan, N.M. and Kassa, G. 2021. Effect of growth regulators on in vitro micropropagation of potato (*Solanum tuberosum* L.) Gudiene and Belete varieties from Ethiopia. The Scientific World Journal, 2021(1), p.5928769. https://doi.org/10.1155/2021/5928769.

Handoo, Z.A., Carta, L.K., Skantar, A.M. and Chitwood, D.J. 2012. Description of Globodera ellingtonae n. sp.(Nematoda: Heteroderidae) from Oregon. *Journal of Nematology*, *44*(1), p.40.

Hansen, E., Harper, G. and McPherson, M.J. 1996. Differential expression patterns of the wound-inducible transgenewun1-uidAin potato roots following infection with either cyst or root knot nematodes. *Physiological and Molecular Plant Pathology*, *48*(3), pp.161-170. https://doi. org/10.1006/pmpp.1996.0014.

Haque, S.M., Halder, T. and Ghosh, B. 2018. In vitro completion of sexual life cycle—Production of next sporophytic generation through in vitro flowering and fruiting in Solanum

americanum and Solanum villosum. *South African Journal of Botany*, *118*, pp.112-119. https://doi.org/10.1016/j.sajb.2018.07.007.

Hasan, M.S. 2019. *The role of Rboh-mediated ROS and glutathione in plant-nematode interaction*. Doctoral dissertation. Rheinische Friedrich-Wilhelms-Universität Bonn.

Hasan, M.S., Lin, C.J., Marhavy, P., Kyndt, T. and Siddique, S. 2024. Redox signalling in plant–nematode interactions: Insights into molecular crosstalk and defense mechanisms. *Plant, Cell & Environment*, *47*(8), pp.2811-2820. https://doi.org/10.1111/pce.14925.

Hashmi, S., Abu Hatab, M.A. and Gaugler, R.R., 1997. GFP: green fluorescent protein a versatile gene marker for entomopathogenic nematodes. *Fundamental and applied nematology*, *20*(4), pp.323-328.

Hayes, A. 2022. The influence of cyst nematodes in the plant secretory pathway. PhD thesis. School of Biology, University of Leeds, UK.

He, Y., Zhang, T., Sun, H., Zhan, H. and Zhao, Y. 2020. A reporter for noninvasively monitoring gene expression and plant transformation. Horticulture research, 7. https://doi.org/10.1038/s41438-020-00390-1.

Heim, R. 1995. Improved green fluorescence. Nature, 373, pp.663-664.

Hernandez-Garcia, C.M. and Finer, J.J. 2014. Identification and validation of promoters and cis-acting regulatory elements. *Plant Science*, *217*, pp.109-119.

Hillocks, R.J. 2012. Farming with fewer pesticides: EU pesticide review and resulting challenges for UK agriculture. *Crop Protection*, *31*(1), pp.85-93.

Hockland, S., Niere, B., Grenier, E., Blok, V., Phillips, M., Den Nijs, L., Anthoine, G., Pickup, J. and Viaene, N. 2012. An evaluation of the implications of virulence in non-European populations of *Globodera pallida* and *G. rostochiensis* for potato cultivation in Europe. *Nematology*, *14*(1), pp.1-13. https://doi.org/10.1163/13885 5411X587112.

Hodda, M. 2022. Phylum Nematoda: a classification, catalogue and index of valid genera, with a census of valid species. Zootaxa, 5114, pp.1-289.

Hodda, M. and Khudhir, M. 2022 Species richness of marine free-living nematodes in eastern Australia. *Hydrobiologia*, [in press].

Hodda, M., Peters, L. and Traunspurger, W. 2009. Nematode diversity in terrestrial, freshwater aquatic and marine systems. Nematodes as environmental indicators. CABI Wallingford UK, pp.45-93.

Hol, W.G. and Cook, R. 2005. An overview of arbuscular mycorrhizal fungi–nematode interactions. *Basic and Applied Ecology*, *6*(6), pp.489-503.

Holbein, J., Franke, R.B., Marhavý, P., Fujita, S., Górecka, M., Sobczak, M., Geldner, N., Schreiber, L., Grundler, F.M. and Siddique, S. 2019. Root endodermal barrier system contributes to defence against plant-parasitic cyst and root-knot nematodes. *The Plant Journal*, *100*(2), pp.221-236.

Holtmann, B., Kleine, M. and Grundler, F.M.W. 2000. Ultrastructure and anatomy of nematode-induced syncytia in roots of susceptible and resistant sugar beet. *Protoplasma*, *211*(1), pp.39-50.

Hoth, S., Stadler, R., Sauer, N. and Hammes, U.Z. 2008. Differential vascularization of nematode-induced feeding sites. *Proceedings of the National Academy of Sciences*, *105*(34), pp.12617-12622.

Hu, Z., Shen, S. and Zhang, X. 2025. Unlocking the Potential of the RUBY Reporter System: How to Address Its Challenges in Plant-Environment Interaction Research?. *Plant, Cell & Environment*, *48*(7), pp.5250-5253.

Huang, X., Springer, P.S. and Kaloshian, I. 2003. Expression of the Arabidopsis MCM gene PROLIFERA during root-knot and cyst nematode infection. *Phytopathology*, *93*(1), pp.35-41.

Hutangura, P., Mathesius, U., Jones, M.G. and Rolfe, B.G. 1999. Auxin induction is a trigger for root gall formation caused by root-knot nematodes in white clover and is associated with the activation of the flavonoid pathway. *Functional Plant Biology*, *26*(3), pp.221-231. https://doi.org/10.1071/PP98157.

Janssen, R., Bakker, J., and Gommers, F. 1991. Mendelian proof for a gene-for-gene relationship between virulence of *Globodera rostochiensis* and the H. *Rev. nématologie* 14, pp.207–211.

Jasmer, D.P., Goverse, A. and Smant, G. 2003. Parasitic nematode interactions with mammals and plants. Annu Rev Phytopathol. 41, pp.245-270.

Jefferson, R.A. 1989. The GUS reporter gene system. *Nature*, *342*(6251), pp.837-838.https://doi.org/10.1038/342837a0.

Jefferson, R.A., Burgess, S.M. and Hirsh, D. 1986. beta-Glucuronidase from Escherichia coli as a gene-fusion marker. *Proceedings of the National Academy of Sciences*, *83*(22), pp.8447-8451.

Jefferson, R.A., Kavanagh, T.A. and Bevan, M.W. 1987. GUS fusions: beta-glucuronidase as a sensitive and versatile gene fusion marker in higher plants. The EMBO journal, 6(13), pp.3901-3907.

Jeong, J., Harris, J., de Souza, L.L. and Leonelli, L. 2025. Combining the CowPEAsy web application with in planta agroinfiltration for native promoter validation in Vigna unguiculata. *Plant, Cell & Environment*, *48*(6), pp.4301-4311.

Jogam, P., Anumula, V., Sandhya, D., Manokari, M., Venkatapuram, A.K., Achary, V.M.M., Shekhawat, M.S., Peddaboina, V. and Allini, V.R. 2024. Monitoring genetic transformation with RUBY visible reporter in Nicotiana tabaccum L. *Plant Cell, Tissue and Organ Culture (PCTOC)*, *157*(1), p.23. https://doi.org/10.1007/s11240-024-02752-2.

Jones, J.D. and Dangl, J.L. 2006. The plant immune system. *nature*, *444*(7117), pp.323-329.

Jones, J.T., Furlanetto, C., Bakker, E., Banks, B., Blok, V., Chen, Q., Phillips, M. and Prior, A. 2003. Characterization of a chorismate mutase from the potato cyst nematode Globodera pallida. Molecular Plant Pathology, 4(1), pp.43-50.

Jones, J.T., Haegeman, A., Danchin, E.G., Gaur, H.S., Helder, J., Jones, M.G., Kikuchi, T., Manzanilla-López, R., Palomares-Rius, J.E., Wesemael, W.M. and Perry, R.N. 2013. Top 10 plant-parasitic nematodes in molecular plant pathology. Mol Plant Pathol. 14(9), pp.946-961. doi: 10.1111/mpp.12057.

Joshi, I., Kumar, A., Kohli, D., Bhattacharya, R., Sirohi, A., Chaudhury, A., Jain, P.K. 2022. Gall-specific promoter, an alternative to the constitutive CaMV35S promoter, drives host-derived RNA interference targeting Mi-msp2 gene to confer effective nematode resistance. Front. Plant Sci. 13, p.1007322.. https://doi.org/10.3389/ fpls.2022.1007322.

Jupe, F., Rivkin, A.C., Michael, T.P., Zander, M., Motley, S.T., Sandoval, J.P., Slotkin, R.K., Chen, H., Castanon, R., Nery, J.R. and Ecker, J.R. 2019. The complex architecture and epigenomic impact of plant T-DNA insertions. *PLoS genetics*, *15*(1), p.e1007819.

Kakrana, A., Kumar, A., Satheesh, V., Abdin, M.Z., Subramaniam, K., Bhattacharya, R.C., Srinivasan, R., Sirohi, A. and Jain, P.K. 2017. Identification, validation and utilization of novel nematode-responsive root-specific promoters in Arabidopsis for inducing host-delivered RNAi mediated root-knot nematode resistance. *Frontiers in Plant Science*, *8*, p.2049. https://doi.org/10.3389/fpls.2017.02049.

Kaloshian, I. and Teixeira, M. 2019. Advances in plant– nematode interactions with emphasis on the notorious nematode genus Meloidogyne. *Phytopathology*, *109*(12), pp.1988-1996.https://doi.org/10.1094/PHYTO-05- 19-0163-IA.

Kammerhofer, N., Egger, B., Dobrev, P., Vankova, R., Hofmann, J., Schausberger, P. and Wieczorek, K. 2015. Systemic above-and belowground cross talk: hormone-based responses triggered by Heterodera schachtii and shoot herbivores in Arabidopsis thaliana. *Journal of Experimental Botany*, *66*(22), pp.7005-7017. doi: 10.1093/jxb/erv398.

Karcher, S. J. 2002. Blue plants: Transgenic plants with the GUS reporter gene. Pages 29-42, in Tested studies for laboratory teaching, Volume 23 (M. A. O'Donnell, Editor). Proceedings of the 23rd Workshop/Conference of the Association for Biology Laboratory Education (ABLE), 392 pages.

Karczmarek, A., Fudali, S., Lichocka, M., Sobczak, M., Kurek, W., Janakowski, S., Roosien, J., Golinowski, W., Bakker, J., Goverse, A. and Helder, J. 2008. Expression of two functionally distinct plant endo-β-1, 4-glucanases is essential for the compatible interaction between potato cyst nematode and its hosts. Molecular plant-microbe interactions, 21(6), pp.791-798.

Karimi, M., de Oliveira Manes, C.L., Van Montagu, M. and Gheysen, G. 2002. Activation of a pollenin promoter upon nematode infection. *Journal of nematology*, *34*(2), p.75.

Kaul, R., Thangaraj, A., Sharda, S. and Kaul, T. 2025. Optimization of tissue culture and Cas9 transgene expression in tomato: A step towards CRISPR/Cas9-based genetic improvement. *Plant Science*, *352*, p.112324. https://doi.org/10.1016/j.plantsci.2024.112324.

Kaur, M., Manchanda, P., Kalia, A., Ahmed, F.K., Nepovimova, E., Kuca, K. and Abd-Elsalam, K.A. 2021. Agroinfiltration mediated scalable transient gene expression in genome edited crop plants. *International journal of molecular sciences*, *22*(19), p.10882. https://doi.org/ 10.3390/ijms221910882.

Kaur, S., Thakur, N. and Jhamta, S. 2024. *Plant parasitic nematodes: Habitat, diversity and nature of damage*. In: *Exploring Innovations in Agricultural, Biological, Chemical, Environmental and Forensic Sciences*. Cognizance Publications, pp.1–121. Available at: https://www.researchgate.net/publication/382179366 [Accessed 4 Aug. 2025].

Khakhar, A., Starker, C.G., Chamness, J.C., Lee, N., Stokke, S., Wang, C., Swanson, R., Rizvi, F., Imaizumi, T. and Voytas, D.F. 2020. Building customizable auto-luminescent luciferase-based reporters in plants. *Elife*, *9*, p.e52786.

Khidr, Y.A., Flachowsky, H., Haselmair-Gosch, C., Thill, J., Miosic, S., Hanke, M.V., Stich, K. and Halbwirth, H. 2017. Evaluation of a MdMYB10/GFP43 fusion gene for its suitability to act as reporter gene in promoter studies in Fragaria vesca L.'Rügen'. *Plant Cell, Tissue and Organ Culture (PCTOC)*, *130*(2), pp.345-356. https://doi.org/10.1007/ s11240-017-1229-0.

Kim, Y. and Choi, J. 2019. Early life exposure of a biocide, CMIT/MIT causes metabolic toxicity via the O-GlcNAc transferase pathway in the nematode C. elegans. *Toxicology and Applied Pharmacology*, *376*, pp.1-8.

Kiryushkin, A.S., Ilina, E.L., Guseva, E.D., Pawlowski, K. and Demchenko, K.N. 2021. Hairy CRISPR: genome editing in plants using hairy root transformation. *Plants*, *11*(1), p.51.

Kooliyottil, R., Dandurand, L.M., Kuhl, J.C., Caplan, A., Xiao, F., Mimee, B. and Lafond-Lapalme, J. 2019. Transcriptome analysis of *Globodera pallida* from the susceptible host *Solanum tuberosum* or the resistant plant *Solanum sisymbriifolium*. *Scientific reports*, *9*(1), p.13256.

Koropacka, K.B. 2010. *Molecular contest between potato and the potato cyst nematode Globodera pallida: Modulation of Gpa2-mediated resistance*. PhD thesis, Wageningen University.

Kumar, A., Harloff, H., Melzer, S., Leineweber, J., Defant, B., Jung, C. 2021. A rhomboid-like protease gene from an interspecies translocation confers resistance to cyst nematodes. *New Phytologist*, *231*(2), pp.801-813. https://doi.org/10.1111/nph.17394.

Kumar, A., Miyara, S.B. 2022. The Use of the Root-knot Nematodes, Meloidogyne spp., for Studying Biotrophic Parasitic Interactions. In: Nematodes as Model Organisms. CABI, GB, pp. 58–81.

Kumar, S., Prakash, S., Kumari, P. and Sanan-Mishra, N. 2025. A robust in-vitro and ex-vitro Agrobacterium rhizogenes-mediated hairy root transformation system in mungbean for efficient visual screening of transformants using the RUBY reporter. *BMC Plant Biology*, *25*(1), p.724. https://doi.org/10.1186/s12870-025-06718-0.

Kumar, V., Khan, M.R., Walia, R.K. 2020. Crop loss estimations due to plant-parasitic nematodes in major crops in India. *National Academy Science Letters*, *43*(5), pp.409-412. https://doi. org/10.1007/s40009-020-00895-2.

Kummari, D., Palakolanu, S.R., Kishor, P.K., Bhatnagar-Mathur, P., Singam, P., Vadez, V. and Sharma, K.K. 2020. An update and perspectives on the use of promoters in plant genetic engineering. *Journal of biosciences*, *45*(1), p.119. doi: 10.1038/318579a0.

Kyndt, T., Goverse, A., Haegeman, A., Warmerdam, S., Wanjau, C., Jahani, M., Engler, G., de Almeida Engler, J. and Gheysen, G. 2016. Redirection of auxin flow in Arabidopsis thaliana roots after infection by root-knot nematodes. Journal of Experimental Botany, 67(15), pp.4559-4570.

Lambshead, P.J.D. 1993. Recent developments in marine benthic biodiversity research. *Recent Developments in Benthology*, 19, pp.5–24.

Lambshead, P.J.D. 2004. Marine nematode biodiversity. In: Chen, Z.X., Chen, S.Y. and Dickson, D.W., eds. *Nematology: Advances and Perspectives. Volume 1: Nematode Morphology, Physiology and Ecology*. Wallingford: CABI, pp.438–468. https://doi.org/10.1079/9780851996455.0438.

Lee, H. A., Lee, H. Y., Seo, E., Lee, J., Kim, S. B., Oh, S., et al. 2017. Current understandings of plant nonhost resistance. Mol. Plant Microbe Interact. 30, 5–15. doi: 10.1094/MPMI-10-16-0213-CR.

Lee, K., Kang, M., Ji, Q., Grosic, S. and Wang, K. 2023. New T-DNA binary vectors with NptII selection and RUBY reporter for efficient maize transformation and targeted mutagenesis. *Plant Physiology*, *192*(4), pp.2598-2603. https://doi.org/10.1093/plphys/kiad231.

Leonetti, P. and Molinari, S. 2020. Epigenetic and metabolic changes in root-knot nematode-plant interactions. *International Journal of Molecular Sciences*, *21*(20), p.7759.

Li, L.L., Cheng, H., Yuan, H.H., Xu, F., Cheng, S.Y. and Cao, F.L. 2014. Functional characterization of the Ginkgo biloba chalcone synthase gene promoter in transgenic tobacco. *Genet Mol Res*, *13*(2), pp.3446-3460. DOI:http://dx.doi.org/10.4238/2014.

Li, P., Chen, B., Zhang, G., Chen, L., Dong, Q., Wen, J., Mysore, K.S. and Zhao, J. 2016. Regulation of anthocyanin and proanthocyanidin biosynthesis by *Medicago truncatula* b HLH transcription factor M t TT 8. *New Phytologist*, *210*(3), pp.905-921.

Li, X.Q., Wei, J.Z., Tan, A. and Aroian, R.V. 2007. Resistance to root-knot nematode in tomato roots expressing a nematicidal *Bacillus thuringiensis* crystal protein. *Plant biotechnology journal*, *5*(4), pp.455-464.

Lilley, C.J., Atkinson, H.J. and Urwin, P.E. 2005. Molecular aspects of cyst nematodes. *Molecular Plant Pathology*, *6*(6), pp.577-588.

Lilley, C.J., Urwin, P.E., Johnston, K.A. and Atkinson, H.J. 2004. Preferential expression of a plant cystatin at nematode feeding sites confers resistance to Meloidogyne incognita and *Globodera pallida*. *Plant biotechnology journal*, *2*(1), pp.3-12. Doi: 10.1046/j.1467-7652.2003.00037.x.

Lin, X., Jia, Y., Heal, R., Prokchorchik, M., Sindalovskaya, M., Olave-Achury, A., Makechemu, M., Fairhead, S., Noureen, A., Heo, J. and Witek, K. 2023. *Solanum americanum* genome-assisted discovery of immune receptors that detect potato late blight pathogen

effectors. *Nature genetics*, *55*(9), pp.1579-1588. https://doi.org/10.1038/s41588-023-01486-9.

Liu, H., Zhu, K., Tan, C., Zhang, J., Zhou, J., Jin, L., Ma, G. and Zou, Q. 2019. Identification and characterization of PsDREB2 promoter involved in tissue-specific expression and abiotic stress response from Paeonia suffruticosa. *PeerJ*, *7*, p.e7052. doi: 10.7717/peerj.7052. eCollection 2019.

Liu, J., Li, H., Hong, C., Lu, W., Zhang, W. and Gao, H. 2024. *Quantitative RUBY reporter assay for gene regulation analysis*, 47(10), pp. 3701-3711.

Lolle, S., Stevens, D. and Coaker, G. 2020. Plant NLR-triggered immunity: from receptor activation to downstream signaling. *Current opinion in immunology*, *62*, pp.99-105.

Lozano-Torres, J.L., Wilbers, R.H., Gawronski, P., Boshoven, J.C., Finkers-Tomczak, A., Cordewener, J.H., America, A.H., Overmars, H.A., Van't Klooster, J.W., Baranowski, L. and Sobczak, M. 2012. Dual disease resistance mediated by the immune receptor Cf-2 in tomato requires a common virulence target of a fungus and a nematode. Proceedings of the National Academy of Sciences, 109(25), pp.10119-10124.

Ma, J.F., Yamaji, N., Mitani, N., Tamai, K., Konishi, S., Fujiwara, T., Katsuhara, M. and Yano, M. 2007. An efflux transporter of silicon in rice. *Nature*, *448*(7150), pp.209-212.

Marshallsay, C., Connelly, S. and Filipowicz, W. 1992. Characterization of the U3 and U6 snRNA genes from wheat: U3 snRNA genes in monocot plants are transcribed by RNA polymerase III. *Plant molecular biology*, *19*(6), pp.973-983.

Matuszkiewicz, M., Sobczak, M. 2023. Syncytium induced by plant-parasitic nematodes. Syncytia: Origin, Structure, and Functions, pp. 371–403.

Maurel, C., Reizer, J., Schroeder, J.I. and Chrispeels, M.J. 1993. The vacuolar membrane protein gamma-TIP creates water specific channels in Xenopus oocytes. *The EMBO journal*, *12*(6), pp.2241-2247.

Mazarei, M., Lennon, K.A., Puthoff, D.P., Rodermel, S.R. and Baum, T.J. 2003. Expression of an Arabidopsis phosphoglycerate mutase homologue is localized to apical meristems, regulated by hormones, and induced by sedentary plant-parasitic nematodes. *Plant Molecular Biology*, *53*(4), pp.513-530.

Mejias, J., Margets, A., Bredow, M., Foster, J., Khwanbua, E., Goshon, J., Maier, T.R., Whitham, S.A., Innes, R.W. and Baum, T.J. 2025. A novel toolbox of GATEWAY-compatible vectors for rapid functional gene analysis in soybean composite plants. *Plant Cell Reports*, *44*(4), pp.1-19. doi: https://doi.org/10.1101/2024.10.12.617978.

Melillo, M.T., Leonetti, P., Bongiovanni, M., Castagnone-Sereno, P. and Bleve-Zacheo, T. 2006. Modulation of reactive oxygen species activities and H2O2 accumulation during compatible and incompatible tomato–root-knot nematode interactions. *New Phytologist*, *170*(3), pp.501-512.

Milczarek, D., Tatarowska, B., Plich, J., Podlewska-Przetakiewicz, A. and Flis, B. 2020. Solanum gourlayi—a source of cyst nematode resistance in potato breeding. *Potato Research*, *63*(4), pp.589-595.

Minnis, S.T., Haydock, P.P.J., Ibrahim, S.K., Grove, I.G., Evans, K. and Russell, M.D. 2002. Potato cyst nematodes in England and Wales-occurrence and distribution. *Annals of Applied Biology*, *140*(2), pp.187-195. https://doi.org/ 10.1111/j.1744-7348.2002.tb00172.x.

Misyura, M., Colasanti, J. and Rothstein, S.J. 2013. Physiological and genetic analysis of Arabidopsis thaliana anthocyanin biosynthesis mutants under chronic adverse environmental conditions. Journal of experimental botany, 64(1), pp.229-240.

Mlotshwa, S., Pruss, G.J., Gao, Z., Mgutshini, N.L., Li, J., Chen, X., Bowman, L.H. and Vance, V. 2010. Transcriptional silencing induced by Arabidopsis T-DNA mutants is associated with 35S promoter siRNAs and requires genes involved in siRNA-mediated chromatin silencing. *The Plant Journal*, *64*(4), pp.699-704.

Moens, M., Perry, R.N. and Starr, J.L. 2009. Meloidogyne species–a diverse group of novel and important plant parasites. Root-knot nematodes, 1, p.483.

Møller, S.G., Urwin, P.E., Atkinson, H.J. and McPherson, M.J. 1998. Nematode-induced expression ofatao1, a gene encoding an extracellular diamine oxidase associated with developing vascular tissue. *Physiological and molecular plant pathology*, *53*(2), pp.73-79. https://doi. org/10.1006/pmpp.1998.0155.

Morel, J.B. and Dangl, J.L. 1997. The hypersensitive response and the induction of cell death in plants. *Cell Death & Differentiation*, *4*(8), pp.671-683.

Niebel, A., de Almeida Engler, J., Tire, C., Engler, G., Van Montagu, M. and Gheysen, G. 1993. Induction patterns of an extensin gene in tobacco upon nematode infection. *The Plant Cell*, *5*(12), pp.1697-1710.

Odell, J.T., Nagy, F. and Chua, N.H. 1985. Identification of DNA sequences required for activity of the cauliflower mosaic virus 35S promoter. *Nature*, *313*(6005), pp.810-812. https://doi.org/10.1038/313810a0.

Ogg Jr, A.G., Rogers, B.S. and Schilling, E.E. 1981. Characterization of black nightshade (*Solanum nigrum*) and related species in the United States. *Weed Science*, *29*(1), pp.27-32.

Opperman, C.H., Taylor, C.G. and Conkling, M.A. 1994. Root-knot nematode—directed expression of a plant root—specific gene. *Science*, *263*(5144), pp.221-223. DOI: 10.1126/science.263.5144.221.

Oriol, G., Geml, J., P´erez-Haase, A., Ninot, J.M. and Penuelas, J. 2017. Abrupt changes in the composition and function of fungal communities along an environmental gradient in the high Arctic. Mol. Ecol. 26 (18), 4798–4810.

Orlando, V. and Boa, E. 2023. Potato cyst nematodes: A persistent and fearsome foe. *Plant Pathology*, *72*(9), pp.1541-1556. DOI: 10.1111/ppa.13779.

Ow, D.W., Wood, K.V., DeLuca, M., De Wet, J.R., Helinski, D.R. and Howell, S.H. 1986. Transient and stable expression of the firefly luciferase gene in plant cells and transgenic plants. *Science*, *234*(4778), pp.856-859.

Palomares-Rius, J.E., Escobar, C., Cabrera, J., Vovlas, A. and Castillo, P. 2017. Anatomical alterations in plant tissues induced by plant-parasitic nematodes. *Frontiers in plant science*, *8*, p.1987.

Papadopoulou, J. and Traintaphyllou, A.C. 1982. Sex differentiation in Meloidogyne incognita and anatomical evidence of sex reversal. Journal of Nematology, 14(4), p.549.

Pape, S., Thurow, C. and Gatz, C. 2010. The Arabidopsis PR-1 promoter contains multiple integration sites for the coactivator NPR1 and the repressor SNI1. *Plant physiology*, *154*(4), pp.1805-1818.

Patel, N., Hamamouch, N., Li, C., Hewezi, T., Hussey, R.S., Baum, T.J., Mitchum, M.G. and Davis, E.L. 2010. A nematode effector protein similar to annexins in host plants. Journal of experimental botany, 61(1), pp.235-248.

Paulson, R.E. and Webster, J.M. 1972. Ultrastructure of the hypersensitive reaction in roots of tomato, *Lycopersicon esculentum* L., to infection by the root-knot nematode, *Meloidogyne incognita*. *Physiological Plant Pathology*, *2*(3), pp.227-234.

Perry, R.N., Moens, M. and Jones, J.T. eds. 2018. *Cyst nematodes*. CABI.

Phillips, M.S. and Trudgill, D.L. 1998. Variation of virulence, in terms of quantitative reproduction of Globodera pallida populations, from Europe and South America, in relation to resistance from *Solanum vernei* and *S. tuberosum ssp. andigena* CPC 2802.

Polturak, G. and Aharoni, A. 2018. "La Vie en Rose": biosynthesis, sources, and applications of betalain pigments. *Molecular plant*, *11*(1), pp.7-22.

Polturak, G., Grossman, N., Vela-Corcia, D., Dong, Y., Nudel, A., Pliner, M., Levy, M., Rogachev, I. and Aharoni, A. 2017. Engineered gray mold resistance, antioxidant capacity, and pigmentation in betalain-producing crops and ornamentals. *Proceedings of the National Academy of Sciences*, *114*(34), pp.9062-9067.

Porto, M.S., Pinheiro, M.P.N., Batista, V.G.L., dos Santos, R.C., de Albuquerque Melo Filho, P. and de Lima, L.M. 2014. Plant promoters: an approach of structure and function. *Molecular biotechnology*, *56*(1), pp.38-49.

Potenza, C., Aleman, L. and Sengupta-Gopalan, C. 2004. Targeting transgene expression in research, agricultural, and environmental applications: promoters used in plant transformation. *In Vitro Cellular & Developmental Biology-Plant*, *40*(1), pp.1-22.

Pradhan, P., Naresh, P., Barik, S., Acharya, G.C., Bastia, R., Adamala, A.K. and Das, M.P. 2023. Breeding for root-knot nematode resistance in fruiting Solanaceous vegetable crops: a review. *Euphytica*, 219(71). https://doi.org/10.1007/s10681-023-03204-2.

Price, J. A., Coyne, D., Blok, V. C., and Jones, J. T. 2021. Potato cyst nematodes *Globodera rostochiensis* and *G. pallida*. Molecular Plant Pathology, 22(5), 495–507. https://doi.org/10.1111/mpp.13047.

Price, J., Preedy, K., Young, V., Todd, D. and Blok, V. C. 2024. Stacking host resistance genes to control *Globodera pallida* populations with different virulence. European Journal of Plant Pathology, 168, 373– 381. https://doi.org/10.1007/s10658-023-02761-5.

Puzio, P.S., Lausen, J., Heinen, P. and Grundler, F.M. 2000. Promoter analysis of pyk20, a gene from *Arabidopsis thaliana*. *Plant Science*, *157*(2), pp.245-255. https://doi.org/10.1016/S0168-9452(00)00287-9.

Rakosy-Tican, E., Thieme, R., König, J., Nachtigall, M., Hammann, T., Denes, T.E., Kruppa, K. and Molnár-Láng, M. 2020. Introgression of two broad-spectrum late blight resistance genes, Rpi-Blb1 and Rpi-Blb3, from *Solanum bulbocastanum* Dun plus race-specific R genes into potato pre-breeding lines. *Frontiers in Plant Science*, *11*, p.699.

Ramar, K., Ayyadurai, V. and Arulprakash, T. 2014. In vitro shoot multiplication and plant regeneration of *Physalis peruviana* L. An important medicinal plant. *Int. J. Curr. Microbiol. App. Sci*, *3*(3), pp.456-464.

Rasmann, S., Ali, J.G., Helder, J. and van der Putten, W.H. 2012. Ecology and evolution of soil nematode chemotaxis. Journal of chemical ecology, 38(6), pp.615-628.

Razak, A.R. and Evans, A.A.F. 1976. An intracellular tube associated with feeding by *Rotylenchulus reniformis* on cowpea root.

Rehman, S., Gupta, V.K. and Goyal, A.K. 2016. Identification and functional analysis of secreted effectors from phytoparasitic nematodes. *BMC microbiology*, *16*(1), p.48.

Rice, S.L., Leadbeater, B.S.C. and Stone, A.R. 1985. Changes in cell structure in roots of resistant potatoes parasitized by potato cyst-nematodes. I. Potatoes with resistance gene H1 derived from *Solanum tuberosum ssp. andigena*. *Physiological Plant Pathology*, *27*(2), pp.219-234.

Rodriguez, E.A., Campbell, R.E., Lin, J.Y., Lin, M.Z., Miyawaki, A., Palmer, A.E., Shu, X., Zhang, J. and Tsien, R.Y. 2017. The growing and glowing toolbox of fluorescent and photoactive proteins. *Trends in biochemical sciences*, *42*(2), pp.111-129.

Rønn, R., Vestergård, M. and Ekelund, F. 2012. Interactions between bacteria, protozoa and nematodes in soil. *Acta Protozoologica*, *51*(3).

Rousselle-Bourgeois, F. and Mugniery, D. 1995. Screening tuber-bearing *Solanum spp.* for resistance to *Globodera rostochiensis* Ro1 Woll. and G. pallida Pa2/3 stone. *Potato research*, *38*(3), pp.241-249.

Ruiz de Galarreta, J.I., Carrasco, A., Salazar, A., Barrena, I., Iturritxa, E., Marquinez, R., Legorburu, F.J. and Ritter, E. 1998. WildSolanum species as resistance sources against different pathogens of potato. *Potato research*, *41*(1), pp.57-68.

Sadoine, M., Ishikawa, Y., Kleist, T.J., Wudick, M.M., Nakamura, M., Grossmann, G., Frommer, W.B. and Ho, C.H. 2021. Designs, applications, and limitations of genetically encoded fluorescent sensors to explore plant biology. *Plant Physiology*, *187*(2), pp.485-503.

Sadowska-Bartosz, I. and Bartosz, G. 2021. Biological properties and applications of betalains. *Molecules*, *26*(9), p.2520.

Santino, A., Taurino, M., De Domenico, S., Bonsegna, S., Poltronieri, P., Pastor, V. and Flors, V. 2013. Jasmonate signaling in plant development and defense response to multiple (a) biotic stresses. *Plant cell reports*, *32*(7), pp.1085-1098.

Sasanelli, N., Konrat, A., Migunova, V., Toderas, I., Iurcu-Straistaru, E., Rusu, S., Bivol, A., Andoni, C. and Veronico, P. 2021. *Review on control methods against plant-parasitic nematodes applied in southern member states (C Zone) of the European Union*. Agriculture, 11(7), p.602.

Sasser, J. 1980. Root-Knot Nematodes: A Globe. Plant Disease, 64(1), p.37.

Schmitz, R.J., Grotewold, E. and Stam, M. 2022. Cis-regulatory sequences in plants: their importance, discovery, and future challenges. *The plant cell*, *34*(2), pp.718-741. https://doi.org/10.1093/plcell/koab281.

Scholte, K. and Vos, J. 2000. Effects of potential trap crops and planting date on soil infestation with potato cyst nematodes and root-knot nematodes. *Annals of Applied Biology*, *137*(2), pp.153-164.

Schouteden, N., De Waele, D., Panis, B. and Vos, C.M. 2015. Arbuscular mycorrhizal fungi for the biocontrol of plant-parasitic nematodes: a review of the mechanisms involved. *Frontiers in microbiology*, *6*, p.1280.

Schultz, L., Cogan, N. O. I., Mclean, K., Dale, M. F. B., Bryan, G. J., Forster, J. W., and Slater, A. T. 2012. Evaluation and implementation of a potential diagnostic molecular marker for H1-conferred potato cyst nematode resistance in potato (*Solanum tuberosum* L.). Plant Breeding, 131(2), pp.315–321. https://doi.org/10.1111/j.1439- 0523.2012.01949.x.

Sevin-Pujol, A., Sicard, M., Rosenberg, C., Auriac, M.C., Lepage, A., Niebel, A., Gough, C. and Bensmihen, S. 2017. Development of a GAL4-VP16/UAS trans-activation system for tissue specific expression in *Medicago truncatula*. *PLoS One*, *12*(11), p.e0188923.

Seyfferth, C. and Tsuda, K. 2014. Salicylic acid signal transduction: the initiation of biosynthesis, perception and transcriptional reprogramming. *Frontiers in plant science*, *5*, p.697. https://doi.org/10.3389/fpls.2014.00697.

Sharifova, S., Prasad, K.V., Cheema, A. and Reddy, A.S. 2025. Genetically encoded betalain-based RUBY visual reporters: noninvasive monitoring of biological processes. *Trends in Plant Science*.

Shatilovich, A., Gade, V. R., Pippel, M., Hoffmeyer, T. T., Tchesunov, A. V., Stevens, L., Winkler, S., Hughes, G. M., Traikov, S., Hiller, M., Rivkina, E., Schiffer, P. H., Myers, E. W. and Kurzchalia, T. V. 2023. A novel nematode species from the Siberian permafrost shares adaptive mechanisms for cryptobiotic survival with *C. elegans* dauer larva. *PLoS genetics*, *19*(7), p.e1010798.

Shen, W.J. and Forde, B.G. 1989. Efficient transformation of *Agrobacterium spp*. by high voltage electroporation. *Nucleic Acids Research*, *17*(20), p.8385.

Shepherd, R.J., Wakeman, R.J. and Romanko, R.R. 1968. DNA in cauliflower mosaic virus. https://doi.org/10.1016/0042-6822(68)90127-X.

Siddique, S., Matera, C., Radakovic, Z.S., Shamim Hasan, M., Gutbrod, P., Rozanska, E., Sobczak, M., Torres, M.A. and Grundler, F.M. 2014. Parasitic worms stimulate host NADPH oxidases to produce reactive oxygen species that limit plant cell death and promote infection. *Science signaling*, *7*(320), pp.ra33-ra33.

Siddique, S., Wieczorek, K., Szakasits, D., Kreil, D.P. and Bohlmann, H. 2011. The promoter of a plant defensin gene directs specific expression in nematode-induced syncytia in Arabidopsis roots. *Plant physiology and biochemistry*, *49*(10), pp.1100-1107.

Sijmons, P. C. 1993. Plant-nematode interactions. *Plant Molecular Biology*, 23(5), pp.917-931.

Sijmons, P.C., Grundler, F.M., von Mende, N., Burrows, P.R. and Wyss, U. 1991. *Arabidopsis thaliana* as a new model host for plant-parasitic nematodes. The Plant Journal, 1(2), pp.245-254.

Singh, A.K., Joshi, I., Kumar, A., Dinkar, V., Kohli, D., Koulagi, R., Kumar, A., Jain, P.K. and Sirohi, A. 2025. Harnessing nematode-responsive promoters: A promising solution for plant parasitic nematodes management. *Plant Stress*, p.100835. https://doi.org/10.1016/j.stress.2025.100835.

Singh, A.K., Kumar, A., Joshi, I., Thorat, Y.E., Jain, P.K. and Sirohi, A. 2017. Evaluation of southern root-knot nematode responsive promoter against other important plant nematodes. *Indian Journal of Nematology*, *47*(1), pp.115-120. https://doi.org/ 10.1126/science.263.5144.221.

Singh, R.R., Verstraeten, B., Siddique, S., Tegene, A.M., Tenhaken, R., Frei, M., Haeck, A., Demeestere, K., Pokhare, S., Gheysen, G. and Kyndt, T. 2020. Ascorbate oxidation activates systemic defence against root-knot nematode *Meloidogyne graminicola* in rice. *Journal of experimental botany*, *71*(14), pp.4271-4284.

Singh, S., Singh, B. and Singh, A.P. 2015. Nematodes: a threat to sustainability of agriculture. *Procedia Environmental Sciences*, *29*, pp.215-216. doi: 10.1016/j.proenv.2015. 07.270.

Slotkin, R.K. and Martienssen, R. 2007. Transposable elements and the epigenetic regulation of the genome. *Nature reviews genetics*, *8*(4), pp.272-285.

Smale, S.T. and Kadonaga, J.T. 2003. The RNA polymerase II core promoter. *Annual review of biochemistry*, *72*(1), pp.449-479.

Smant, G., Helder, J. and Goverse, A. 2018. Parallel adaptations and common host cell responses enabling feeding of obligate and facultative plant parasitic nematodes. *The Plant Journal*, *93*(4), pp.686-702.

Smirnoff, N. 2018. Ascorbic acid metabolism and functions: A comparison of plants and mammals. *Free radical biology and medicine*, *122*, pp.116-129.

Sobczak, M., Avrova, A.O., Jupowicz, J., Phillips, M.S., Ernst, K. and Kumar, A. 2005. *Characterization of susceptibility and resistance responses to potato cyst nematode (Globodera spp.) infection of tomato lines in the absence and presence of the broad-spectrum nematode resistance Hero gene*. Molecular Plant-Microbe Interactions, 18(2), pp.158–168.

Sobczak, M., Golinowski, W. and Grundler, F.M.W. 1997. Changes in the structure of *Arabidopsis thaliana* roots induced during development of males of the plant parasitic nematode *Heterodera schachtii*. *European Journal of Plant Pathology*, 103(2), pp.113-124.

Spychalla, P. and De Jong, W.S. 2024. Breeding for potato cyst nematode resistance in *Solanum tuberosum*. *Crop Science*, *64*(3), pp.1167-1182. DOI: 10.1002/csc2.21244.

Stam, M., Mol, J.N. and Kooter, J.M. 1997. The silence of genes in transgenic plants. *Annals of botany*, *79*(1), pp.3-12.

Strachan, S.M., Armstrong, M.R., Kaur, A., Wright, K.M., Lim, T.Y., Baker, K., Jones, J., Bryan, G., Blok, V. and Hein, I. 2019. Mapping the H2 resistance effective against Globodera pallida pathotype Pa1 in tetraploid potato. *Theoretical and Applied Genetics*, *132*(4), pp.1283-1294.

Strack, D., Vogt, T. and Schliemann, W. 2003. Recent advances in betalain research. Phytochemistry, 62(3), pp.247-269.

Subbotin, S. A., Franco, J., Knoetze, R., Roubtsova, T. V., Bostock, R. M., and Cid Del Prado Vera, I. I. 2020. DNA barcoding, phylogeny and phylogeography of the cyst nematode species from the genus *Globodera* (Tylenchida: Heteroderidae). Nematology, 22(3), pp.269–297. https://doi.org/10.1163/15685411-00003305.

Sultana, M.S., Mazarei, M., Millwood, R.J., Liu, W., Hewezi, T. and Stewart Jr, C.N. 2022. Functional analysis of soybean cyst nematode-inducible synthetic promoters and their regulation by biotic and abiotic stimuli in transgenic soybean (*Glycine max*). *Frontiers in Plant Science*, *13*, p.988048.

Sun, H., Wang, S., Yang, K., Zhu, C., Liu, Y. and Gao, Z. 2023. Development of dual-visible reporter assays to determine the DNA–protein interaction. *The Plant Journal*, *113*(5), pp.1095-1101.

Thorat, Y.E., Dutta, T.K., Jain, P.K., Subramaniam, K. and Sirohi, A. 2024. A nematode-inducible promoter can effectively drives RNAi construct to confer Meloidogyne incognita resistance in tomato. *Plant Cell Reports*, *43*(1), p.3.https://doi.org/10.1007/ s00299-023-03114-6.

Thorpe, P., Mantelin, S., Cock, P.J., Blok, V.C., Coke, M.C., Eves-van den Akker, S., Guzeeva, E., Lilley, C.J., Smant, G., Reid, A.J. and Wright, K.M. 2014. Genomic characterisation of the effector complement of the potato cyst nematode *Globodera pallida*. BMC genomics, 15(1), pp.1-15.

Thurau, T., Kifle, S., Jung, C. and Cai, D. 2003. The promoter of the nematode resistance gene Hs1pro− 1 activates a nematode-responsive and feeding site-specific gene expression in sugar beet (*Beta vulgaris L.*) and *Arabidopsis thaliana*. *Plant Molecular Biology*, *52*(3), pp.643-660. 10.1023/a:1024887516581.

Thwe, A., Valan Arasu, M., Li, X., Park, C.H., Kim, S.J., Al-Dhabi, N.A. and Park, S.U. 2016. Effect of different *Agrobacterium rhizogenes* strains on hairy root induction and phenylpropanoid biosynthesis in tartary buckwheat (*Fagopyrum tataricum Gaertn*). *Frontiers in microbiology*, *7*, p.318.

Timko, M.P., Kausch, A.P., Castresana, C., Fassler, J., Herrera-Estrella, L., Van den Broeck, G., Van Montagu, M., Schell, J. and Cashmore, A.R. 1985. Light regulation of plant gene expression by an upstream enhancer-like element. *Nature*, *318*(6046), pp.579-582.

Timmermans, B.G.H. 2005. *Solanum sisymbriifolium* (Lam.): a trap crop for potato cyst nematodes. PhD Thesis. The Netherlands: University of Wageningen.

Timmermans, B.G.H., Vos, J., Stomph, T.J., Van Nieuwburg, J. and Van der Putten, P.E.L. 2006. Growth duration and root length density of *Solanum sisymbriifolium* (Lam.) as determinants of hatching of *Globodera pallida* (Stone). *Annals of Applied Biology*, 148, pp.213–222.

Timoneda, A., Yunusov, T., Quan, C., Gavrin, A., Brockington, S.F. and Schornack, S. 2021. MycoRed: Betalain pigments enable in vivo real-time visualisation of arbuscular mycorrhizal colonisation. *PLoS Biology*, *19*(7), p.e3001326.

Torres, M.A., Jones, J.D. and Dangl, J.L. 2006. Reactive oxygen species signaling in response to pathogens. *Plant physiology*, *141*(2), pp.373-378. https://doi.org/10.1104/pp.106.079467

Triantaphyllou, A.C. and Riggs, R.D. 1979. Polyploidy in an amphimictic population of *Heterodera glycines*. Journal of Nematology, 11(4), pp.371-376.

Tse, S.W., Annese, D., Romani, F., Guzman-Chavez, F., Bonter, I., Forestier, E., Frangedakis, E. and Haseloff, J. 2024. Optimizing promoters and subcellular localization for constitutive transgene expression in *Marchantia polymorpha*. *Plant and Cell Physiology*, *65*(8), pp.1298-1309.

Turner, S. J. 1996. Population decline of potato cyst nematodes (*Globodera rostochiensis, G. pallida*) in field soils in Northern Ireland. Annals of Applied Biology, 129(2), 315–322. https://doi.org/10.1111/ j.1744-7348.1996.tb05754.x.

Tyagi, A.K. 2001. Plant genes and their expression. *Current science*, pp.161-169.

Tyagi, A.K., Mohanty, A., Bajaj, S., Chaudhury, A. and Maheshwari, S.C. 1999. Transgenic rice: A valuable monocot system for crop improvement and gene research. *Critical reviews in biotechnology*, *19*(1), pp.41-79. doi: 10.1080/0738-859991229198.

Ud-din, A.M., DIN KHAN, Z.U., Ahmad, M., AKRAM KASHMIRI, M.U.H.A.M.M.A.D., Yasmin, S. and Mazhar, H. 2009. Chemotaxonomic significance of flavonoids in the *Solanum nigrum* complex. Journal of the Chilean Chemical Society, *54*(4), pp.486-490.

Urwin, P.E., Lilley, C.J., McPherson, M.J. and Atkinson, H.J. 1997b. Resistance to both cyst and root-knot nematodes conferred by transgenic Arabidopsis expressing a modified plant cystatin. *The Plant Journal*, *12*(2), pp.455-461. DOI: 10.1046/j.1365-313X.1997.12020455.x.

Urwin, P.E., McPherson, M.J. and Atkinson, H.J. 1998. Enhanced transgenic plant resistance to nematodes by dual proteinase inhibitor constructs. *Planta*, *204*(4), pp.472-479.

Urwin, P.E., Møller, S.G., Lilley, C.J., McPherson, M.J. and Atkinson, H.J. 1997a. Continual green-fluorescent protein monitoring of cauliflower mosaic virus 35S promoter activity in nematode-induced feeding cells in *Arabidopsis thaliana*. *Molecular Plant-Microbe Interactions*, *10*(3), pp.394-400.

Urwin, P.E., Troth, K.M., Zubko, E.I. and Atkinson, H.J. 2001. Effective transgenic resistance to *Globodera pallida* in potato field trials. *Molecular Breeding*, *8*(1), pp.95-101.

van Arensbergen, J., van Steensel, B. and Bussemaker, H.J. 2014. In search of the determinants of enhancer–promoter interaction specificity. *Trends in cell biology*, *24*(11), pp.695-702.

Van Der Biezen, E.A. and Jones, J.D. 1998. Plant disease-resistance proteins and the gene-for-gene concept. Trends in biochemical sciences, 23(12), pp.454-45.

van der Fits, L., Deakin, E.A., Hoge, J.H.C. and Memelink, J. 2000. The ternary transformation system: constitutive virG on a compatible plasmid dramatically increases Agrobacterium-mediated plant transformation. *Plant molecular biology*, *43*(4), pp.495-502. doi: 10.1023/a:1006440221718.

van der Voort, J.R., Kanyuka, K., van der Vossen, E., Bendahmane, A., Mooijman, P., Klein-Lankhorst, R., Stiekema, W., Baulcombe, D. and Bakker, J. 1999. Tight physical linkage of the nematode resistance gene Gpa2 and the virus resistance gene Rx on a single segment introgressed from the wild species Solanum tuberosum subsp. andigena CPC 1673 into cultivated potato. *Molecular Plant-Microbe Interactions*, *12*(3), pp.197-206.

Van Poucke, K., Karimi, M. and Gheysen, G. 2001. Analysis of nematode-responsive promoters in sugar beet hairy roots. *Mededelingen (Rijksuniversiteit te Gent. Fakulteit van de Landbouwkundige en Toegepaste Biologische Wetenschappen)*, *66*(2b), pp.591-598.

Varandas, R., Barroso, C., Conceição, I.L. and Egas, C. 2024. Molecular insights into *Solanum sisymbriifolium*'s resistance against *Globodera pallida* via RNA-seq. *BMC Plant Biology*, *24*(1), p.1005. https://doi.org/10.1186/s12870-024-05694-1.

Vieira, P. and Gleason, C. 2019. Plant-parasitic nematode effectors—insights into their diversity and new tools for their identification. *Current opinion in plant biology*, *50*, pp.37-43.

Vierheilig, H., Coughlan, A.P., Wyss, U.R.S. and Piché, Y. 1998. Ink and vinegar, a simple staining technique for arbuscular-mycorrhizal fungi. *Applied and environmental microbiology*, *64*(12), pp.5004-5007.

Walter, A.J., Willforss, J., Lenman, M., Alexandersson, E. and Andreasson, E. 2018. RNA seq analysis of potato cyst nematode interactions with resistant and susceptible potato roots. *European journal of plant pathology*, *152*(2), pp.531-539.

Wang, C., Bruening, G. and Williamson, V.M. 2009. Determination of preferred pH for root-knot nematode aggregation using pluronic F-127 gel. Journal of Chemical Ecology, 35(10), pp.1242-1251.

Wang, C., Gao, G., Cao, S., Xie, Q. and Qi, H. 2019. Isolation and functional validation of the CmLOX08 promoter associated with signalling molecule and abiotic stress responses in oriental melon, *Cucumis melo* var. makuwa Makino. *BMC plant biology*, *19*(1), p.75. doi: 10.1186/s12870-019-1678-1.

Wang, D., Zhong, Y., Feng, B., Qi, X., Yan, T., Liu, J., Guo, S., Wang, Y., Liu, Z., Cheng, D. and Zhang, Y. 2023a. The RUBY reporter enables efficient haploid identification in maize and tomato. *Plant Biotechnology Journal*, *21*(8), pp.1707-1715.

Wang, G., Hu, C., Zhou, J., Liu, Y., Cai, J., Pan, C., Wang, Y., Wu, X., Shi, K., Xia, X. and Zhou, Y. 2019. Systemic root-shoot signaling drives jasmonate-based root defense against nematodes. *Current Biology*, *29*(20), pp.3430-3438. https://doi.org/10.1016/j.cub.2019.08.049.

Wang, M., Da, Y. and Tian, Y. 2023. Fluorescent proteins and genetically encoded biosensors. *Chemical Society Reviews*, *52*(4), pp.1189-1214.

Wang, Y., Brown, L.H., Adams, T.M., Cheung, Y.W., Li, J., Young, V., Todd, D.T., Armstrong, M.R., Neugebauer, K., Kaur, A. and Harrower, B. 2023b. SMRT–AgRenSeq-d in potato (*Solanum tuberosum*) as a method to identify candidates for the nematode resistance Gpa5. *Horticulture Research*, *10*(11), p.uhad211. https://doi.org/10.1093/hr/uhad211.

Wesemael, W., Perry, R. and Moens, M. 2006. The influence of root diffusate and host age on hatching of the root-knot nematodes, *Meloidogyne chitwoodi* and *M. fallax*. Nematology, 8(6), pp.895-902.

Wharton, C., Beacham, A., Gifford, M.L. and Monaghan, J. 2025. Rootrainertrons: a novel root phenotyping method used to identify genotypic variation in lettuce rooting. *Plant Methods*, *21*(1), p.29.

Whitworth, J.L., Novy, R.G., Zasada, I.A., Wang, X., Dandurand, L.M. and Kuhl, J.C. 2018. Resistance of potato breeding clones and cultivars to three species of potato cyst nematode. *Plant disease*, *102*(11), pp.2120-2128.

Wieczorek, K., Golecki, B., Gerdes, L., Heinen, P., Szakasits, D., Durachko, D.M., Cosgrove, D.J., Kreil, D.P., Puzio, P.S., Bohlmann, H. and Grundler, F.M. 2006. Expansins are involved in the formation of nematode-induced syncytia in roots of *Arabidopsis thaliana*. The Plant Journal, 48(1), pp.98-112.

Williamson, V. M. and Kumar, A. 2006. *Nematode resistance in plants: The battle underground*. Trends in Genetics, 22(7), pp.396–403. https://doi.org/10.1016/j.tig.2006.05.003.

Wilschut, R.A. and Geisen, S. 2021. Nematodes as drivers of plant performance in natural systems. *Trends in Plant Science*, *26*(3), pp.237-247.

Wiśniewska, A., Dąbrowska-Bronk, J., Szafrański, K., Fudali, S., Święcicka, M., Czarny, M., Wilkowska, A., Morgiewicz, K., Matusiak, J., Sobczak, M. and Filipecki, M. 2013. Analysis of tomato gene promoters activated in syncytia induced in tomato and potato hairy roots by *Globodera rostochiensis*. *Transgenic research*, *22*(3), pp.557-569. https:// doi.org/10.1007/s11248-012-9665-4.

Witek, K., Lin, X., Karki, H.S., Jupe, F., Witek, A.I., Steuernagel, B., Stam, R., Van Oosterhout, C., Fairhead, S., Heal, R. and Cocker, J.M. 2021. A complex resistance locus in *Solanum americanum* recognizes a conserved *Phytophthora* effector. *Nature Plants*, *7*(2), pp.198-208. DOI: 10.1038/s41477-021-00854-9.

Wixom, A.Q., Casavant, N.C., Sonnen, T.J., Kuhl, J.C., Xiao, F., Dandurand, L.M. and Caplan, A.B. 2020. Initial responses of the trap-crop, *Solanum sisymbriifolium*, to *Globodera pallida* invasions. *The plant genome*, *13*(2), p.e20016.

Wondafrash, M., Van Dam, N.M. and Tytgat, T.O. 2013. Plant systemic induced responses mediate interactions between root parasitic nematodes and aboveground herbivorous insects. *Frontiers in plant science*, *4*, p.87.

Wood, K.V. 1995. Marker proteins for gene expression. *Current opinion in biotechnology*, *6*(1), pp.50-58.

Wu, B., Qi, F. and Liang, Y. 2023. Fuels for ROS signaling in plant immunity. *Trends in plant science*, *28*(10), pp.1124-1131.

Wu, C.H., Abd-El-Haliem, A., Bozkurt, T.O., Belhaj, K., Terauchi, R., Vossen, J.H. and Kamoun, S. 2017. NLR network mediates immunity to diverse plant pathogens. *Proceedings of the National Academy of Sciences*, *114*(30), pp.8113-8118.

Wyss, U. and Grundler, F.M.W. 1992. Feeding behaviour of sedentary plant parasitic nematodes. *Netherlands Journal of Plant Pathology*, 98, pp.165-173.

Wyss, U., Stender, C., and Lehmann, H. 1984. Ultrastructure of feeding sites of the cyst nematode *Heterodera schachtii Schmidt* in roots of susceptible and resistant *Raphanus sativus L. var. oleiformis* Pers. cultivars. *Physiological Plant Pathology*, *25*(1), pp.21-37.

Xu, J.J., Fang, X., Li, C.Y., Yang, L. and Chen, X.Y. 2020. General and specialized tyrosine metabolism pathways in plants. Abiotech, 1(2), pp.97-105.

Xu, R. and Qingshun, L.Q. 2008. Protocol: Streamline cloning of genes into binary vectors in Agrobacterium via the Gateway® TOPO vector system. *Plant methods*, *4*(1), p.4.

Yamaguchi-Shinozaki, K. and Shinozaki, K. 1993. Characterization of the expression of a desiccation-responsive RD29 gene of Arabidopsis thaliana and analysis of its promoter in transgenic plants. Molecular & General Genetics 236(2-3): 331-340.

Yang, H., Zhang, Y., Fu, Q., Jia, X., Zhao, T., Xu, X., Jiang, J. and Li, J. 2023. The DR5 and E8 reporters are suitable systems for studying the application of the RUBY reporter gene in tomato. Vegetable Research, 3(1), p.12. https://doi.org/10.48130/VR-2023-0012.

Yang, T.H., Lenglet-Hilfiker, A., Stolz, S., Glauser, G. and Farmer, E.E. 2020. Jasmonate precursor biosynthetic enzymes LOX3 and LOX4 control wound-response growth restriction. *Plant physiology*, *184*(2), pp.1172-1180.

Yeates, G.W., Bongers, T., Degoede, R.G.M., Freckman, D.W., Georgieva, S.S. 1993. Feeding habits in soil nematode families and genera – an outline for soil ecologists. *Journal of Nematology*, 25 (3), pp.315–331.

Yeates, G.W., Ferris, H., Moens, T. and van der Putten, W. 2009. The role of nematodes in ecosystems. In: Wilson, M. and Kakouli Duarte, T., eds. *Nematodes as Environmental Indicators*. Wallingford, UK: CABI, pp.1–44. https://doi.org/10.1079/9781845933852.0000.

Yu, J., Deng, S., Huang, H., Mo, J., Xu, Z.F. and Wang, Y. 2023. Exploring the potential applications of the noninvasive reporter gene RUBY in plant genetic transformation. *Forests*, *14*(3), p.637. https://doi.org/10.3390/f14030637.

Yusuf, A.G. and Bello, T.T. 2025. Cellular plasticity and transcriptional reprogramming in plant-nematode interactions: insights into feeding site formation and plant defense. *Crop Health*, *3*(1), p.16. https://doi.org/10.1007/s44297-025-00056-1.

Zasada, I.A., Ingham, R.E., Baker, H. and Phillips, W.S. 2019. Impact of *Globodera ellingtonae* on yield of potato (*Solanum tuberosum*). *Journal of Nematology*, *51*, pp.e2019-73.

Zhang, W., Thieme, C.J., Kollwig, G., Apelt, F., Yang, L., Winter, N., Andresen, N., Walther, D. and Kragler, F. 2016. tRNA-related sequences trigger systemic mRNA transport in plants. *The Plant Cell*, *28*(6), pp.1237-1249.

Zhang, X., Li, S., Li, X., Song, M., Ma, S., Tian, Y. and Gao, L. 2023. Peat-based hairy root transformation using Rhizobium rhizogenes as a rapid and efficient tool for easily exploring potential genes related to root-knot nematode parasitism and host response. *Plant Methods*, *19*(1), p.22.

Zhang, Y., Ji, L. and Yang, L. 2021. Abundance and diversity of soil nematode community at different altitudes in cold-temperate montane forests in northeast China. Global Ecology and Conservation 29: 1-12. https://doi.org/10.1016/j.gecco.2021.e01717.

Zheng, Q., Putker, V. and Goverse, A. 2021. Molecular and cellular mechanisms involved in host-specific resistance to cyst nematodes in crops. *Frontiers in Plant Science*, *12*, p.641582. doi: 10.3389/fpls.2021.641582.

Zhou, D.D. and Yu, J.N. 2013. The Progress of establishing transient expression system in plant cell. *Chinese Agricultural Science Bulletin*, *29*(24), pp.151-156.